THE UNIVERSITY
of EDINBURGH

Investigating the Expression and Function of DAZL and BOLL during Human Oogenesis

Jing He

BSc, Nanjing University

MSc, University of Edinburgh

Centre for Reproductive Health

Queen's Medical Research Institute

47 Little France Crescent

Edinburgh EH16 4TJ

Thesis submitted for the Degree of Doctor of Philosophy

The University of Edinburgh

2016

DECLARATION

The studies undertaken in the thesis were the sole work of the author, except where acknowledgement is made by reference. The work described in this thesis has not been previously accepted for, or is currently being submitted for another degree or qualification at the University of Edinburgh or any other institution.

Jing He

February, 2016

ACKNOWLEDGEMENTS

Without the help and support received from a lot of people, it would be impossible to produce this thesis.

First I would like to thank my supervisors, Dr Andrew Childs and Prof Richard Anderson, for the incredible large amount of help I received from them. As an international student who use English as a second language, I started my very first MSc project in UK with them five years ago and was not daring to speak at the beginning, but during such a long time they always show great patience and encouragement when communicate with me, and are never tired of helping me with my writing. They even show a lot of concern on my health and safety as well, which really helped me to adapt to life and research in UK. Their help on science is even greater – I can always go to their office to discuss the results and ideas, and can always get support from their abundant knowledge if I have any queries about the project. At the end of my PhD, I realised that I already learnt a lot about necessary skills such as lab techniques and data analysing, but most important, learnt about how to think like a scientist. All my improvement during my PhD should first credit to my excellent supervisors.

I also would like to thank the other members of Anderson lab who helped me during my PhD. Dr Rosey Bayne had gave me a lot of excellent suggestions on molecular experiments, and Hazel Kinnell is the absolutely skilled one who taught me immunohistochemistry, which is one of the most important technique I used during my PhD. I also would like to express my appreciation to research nurses Anne Saunderson and Joan Creiger, who collected the human tissues for our research – my project would not exist without them. A special thank would go to my excellent honoured student Kayleigh Stewart, who performed very nice immunos on mouse tissue and contributed to both this thesis and the publication related to it. I also would like to thank Roseanne Rosario, for our inspiring communication on the future work, and Jieqian Zhou as well for her support on immnos.

There are also a lot of people out of the Anderson lab I would like to express my thanks to. Prof Philippa Saunders with my supervisors helped me with applying the

Charles Darwin Scholarship of University of Edinburgh, which is a really great support for finishing my PhD. Dr Joao Pedro Sousa Martins from Dr Nicola Gray's lab kindly lent me the human *DAZL* construct he generated, which is almost the basis of my mRNA target work; other staff from Gray's lab are also very supportive. All staff in SuRF@QMRI had given me great help, but I particularly want to thank Mike Miller for the support on immunos, Aranzta Esnal and Sheila MacPherson for teaching me confocal-microscoping and Dr Pam Brown for the measurement of luciferase activity. I also would like to thank Shonna Johnston and Fiona Rossi from Centre for Inflammation Research, for their help on my FACS setting up and operation.

Finally I'd like to thank my family, without their finance support I would not be able to be here, and their love is always the greatest backup and driving force when I was about to give up. This thesis is for all the people who helped me during these years.

ABSTRACT

Fetal germ cell development is a key stage of female reproductive life. The DAZ family proteins (DAZ, DAZL and BOLL) are RNA-binding proteins with critical roles in murine germ cell development but their expression and potential targets in the human are largely unknown. The studies in this Thesis investigated the expression and function of DAZL and BOLL in human fetal ovary.

Both DAZL and BOLL mRNA are increased dramatically at the time of entry into meiosis. Immunohistochemical analysis with specific meiotic markers suggested that DAZL and BOLL have distinct spatial-temporal expression patterns, with minimal co-expression – BOLL expression was transient prior to follicle formation. This pattern was shown not to be present in the mouse fetal ovary, where Dazl and Boll are co-expressed, indicating a limitation of the mouse for exploring the function of Boll.

Two human cell lines, embryonic kidney derived HEK293 cells and germ cell tumour derived TCam-2 cells were used as models to identify the mRNA targets of *DAZL* and *BOLL* after transfection of DAZL or *BOLL* vectors. In HEK293 cells, *TEX19* and *TEX14* were confirmed as potential targets of both DAZL and BOLL, and *CDC25A* as a potential DAZL target. Further experiments indicated that DAZL and BOLL did not increase target mRNA transcription but increased stabilisation. A *DAZL/GFP* co-transfection-FACS system for TCam-2 cells was established as this cell line has very low transfection efficiency. *TEX14* and *SYCP3* significantly increased in GFP^{+ve}-$DAZL^{+ve}$ cells when compare to the GFP^{-ve}-$DAZL^{-ve}$ cells, whilst *SOX17* and *DNMT3L* significantly decreased in the GFP^{+ve}-$DAZL^{+ve}$ cells. A 3'-UTR luciferase assay confirmed regulation of *TEX14* and *SOX17* by DAZL through their 3'-UTR. RNA immunoprecipitation further demonstrated direct binding between human *TEX14*, *TEX19*, *SYCP3*, *SOX17* mRNA and DAZL protein, and that *TEX14* binding is through its 3'-UTR. Dual fluorescence immunohistochemistry showed that *SOX17* and *DMNT3L* are expressed in early germ cells with DAZL, and are later down-regulated co-incident with that of DAZL, consistent with the novel repressive effect of human DAZL on these two potential targets.

These studies indicate that DAZL and BOLL are associated with different key meiotic stages of germ cell development in human fetal ovary. Several potential mRNA targets of DAZL and BOLL, and a novel repression function of human DAZL on its mRNA targets were identified giving further insight into the role of these factors in human ovarian development.

Lay Summary of Thesis

THE UNIVERSITY of EDINBURGH

The lay summary is a brief summary intended to facilitate knowledge transfer and enhance accessibility, therefore the language used should be non-technical and suitable for a general audience. (See the Degree Regulations and Programmes of Study, General Postgraduate Degree Programme Regulations. These regulations are available via: http://www.drps.ed.ac.uk/.)

Name of student:	Jing He	UUN	S0948828
University email:	S0948828@sms.ed.ac.uk		
Degree sought:	PhD	No. of words in the main text of thesis:	61,900
Title of thesis:	Investigating the Expression and Function of DAZL and BOLL during Human Oogenesis		

Sperm, eggs and their precursors are called germ cells. During the germ cell development, a critical process called meiosis happens, which allows the genetic materials to be reduced to half in the mature sperm and egg. Therefore, once fertilisation happens the offspring will have normal amount of genetic materials and the abnormal of meiosis leads to reproductive diseases.

In this study, we investigated the functions of two proteins called DAZL and BOLL which are important for meiosis in human fetal ovary. DAZL and BOLL bind to and regulate RNA targets, however, none of their definitive targets have been identified in humans. So this study aimed to find out whether DAZL and BOLL are expressed in human fetal ovary, and what their targets are.

We first looked at their expression in human fetal ovary by staining DAZL and BOLL proteins in ovary sections. We found that they were expressed in different cell types. DAZL was mostly distributed in less mature germ cells before and just after meiosis started, while BOLL was in more mature ones. Furthermore, BOLL was only expressed in a very short period and DAZL was then re-expressed.

We identified from previous studies some potential Dazl/Boll targets that had been identified in mouse, and investigated them further in human samples. DAZL or BOLL were over-expressed in human cells to see whether the expression of these targets had been changed. Indeed we found that the levels of 3 genes called *TEX14*, *TEX19*, *and SYCP3* were increased by DAZL. Surprisingly, other genes (*SOX17* and *DNMT3L)* decreased, indicating a possible novel repression function of human DAZL. We also did experiments that showed that DAZL could directly bind to these targets.

After identified the potential targets, we tested whether DAZL could regulate them in human fetal ovary. These studies showed that DAZL and DNMT3L/SOX17 were present in the same germ cells in the ovary. In addition, most more mature $DAZL^{+ve}$ germ cells did not express DNMT3L or SOX17, implying that the expression of these two targets could be repressed by DAZL, which was consistent with our previous results.

In conclusion, the expression pattern of DAZL and BOLL suggested that DAZL might be important before and at meiosis initiation, in contrast BOLL was potentially necessary for later stage of meiosis. The putative human DAZL targets we identified, namely *TEX14*, *TEX19*, *SOX17* and *DNMT3L* are all involved with different aspects of the germ cell development. Therefore this study sheds light on the understanding how DAZL/BOLL regulates the production of eggs, and which may have implications for some causes of infertility.

PRESENTATIONS RELATING TO THIS THESIS

Oral Presentation

Post-transcriptional regulation of endogenous target mRNA levels by human DAZL and BOULE

Society for Reproduction and Fertility Annual Meeting 2011

DAZL and BOULE differentially associate with markers of meiosis during human fetal oogenesis

Munro Kerr Society Meeting 2012

A novel repression function of DAZL on the translation of SOX17 mRNA during human fetal oogenesis

Society for Reproduction and Fertility Annual Meeting 2014

Poster Presentation

DAZL and BOULE display distinct spatio-temporal patterns of expression during human ovarian germ cell development and regulate TEX14 and TEX19 in vitro

Reproductive Function and Dysfunction 2011

DAZL and BOULE mark distinct populations of germ cells and differentially associate with markers of meiosis during human fetal oogenesis

Cold Spring Harbour Laboratories Germ Cell 2012

DAZL and BOULE differentially associate with markers of meiosis during human fetal oogenesis

Society for Reproduction and Fertility Annual Meeting 2012

Identification of novel mRNA targets of DAZL in the human germ cell line TCam-2

Society for Reproduction and Fertility Annual Meeting 2013

PUBLICATIONS RELATING TO THIS THESIS

He J, Stewart K, Kinnell HL, Anderson RA, Childs AJ. A Developmental Stage-Specific Switch from DAZL to BOLL Occurs during Fetal Oogenesis in Humans, but Not Mice. *PLoS ONE*. **2013**;**8**:e73996.

TABLE OF CONTENTS

LIST OF FIGURES

LIST OF TABLES

Commonly Used Abbreviations

ActD	Actinomycin D
3'-UTR	3'-Untranslated Region
ACR	Acrosin
Aldh1a	Aldehyde dehydrogenase 1 family member A
ALP	Alkaline Phosphatase
AMH	Anti-Müllerian hormone
ATM	Ataxia Telangiectasia Mutated
AZF	Azoospermia Factor
Bad	BCL2-associated agonist of cell death
BAX	Bcl-2 Associated X Protein
Bcl-2	B-cell leukemia/lymphoma-2
Blimp1	B lymphocyte-induced maturation protein
BMP	Bone Morphogenic Protein
bol	boule
BOLL	BOULE-LIKE
bp	Base Pair
BSA	Bovine Serum Albumin
C. elegans	*Caenorhabditis elegans*
cDNA	Complementary DNA
CDY1	Chromodomain protein, Y-linked 1
c-Kit	Kit Ligand Receptor
CPEB	Cytoplasmic Polyadenylation Element Binding Protein
CTNNB1	Cadherin-associated protein beta 1
DAB	3,3'-Diaminobenzidine
DAPI	4',6-diamidino-2-phenylindole
DAZ	Deleted in Azoospermia
DAZAP	DAZ-Associated Proteins
DAZH	DAZ Homologue
DAZL	Deleted in Azoospermia-Like
DBS	Dazl-binding site
DDX4	DEAD box polypeptide 4
dH_2O	Distilled Water
Dlc	Light Chain of Dynein
DMC1	DNA meiotic recombinase 1
DNA	Deoxyribonucleic Acid
DNase	Deoxyribonuclease
dpc	Days post Coitum
Drosophila	*Drosophila melanogaster*
DSB	DNA undergoes double strand breaks
DTT	Dithiothreitol

e	Embryonic Day
E. coli	Escherichia coli
EBs	embryoid bodies
EDTA	Ethylenediaminetetra-acetic Acid
eIF	Eukaryotic translation initiation factor
ES	Embryonic Stem
ESCs	embryonic stem cells
FAB	Fragment Antigen-Binding
FACS	Fluorescence-Activated Cell Sorting
FGSCs	Female germline stem cells
Figα/Figla	Factor in the germline alpha
FMRP	Fragile X mental retardation protein
FSH	Follicle-Stimulating Hormone
FXR	Fragile X mental retardation
GDF9	Growth Differentiation Factor 9
GFP	Green Fluorescent Protein
Grsf1	G-rich RNA sequence binding factor 1
GV	Germinal Vesicle
h	Hour(s)
H2AX	Histone H2A X
H2O	Water
H47	Histocompatability antigen precursor 47
HRP	Horse radish peroxidase
Hu	Hu antigen proteins
ICM	Inner Cell Mass
IGF2BP1	Insulin-like growth factor 2 mRNA binding protein 1
IHC	Immunohistochemistry
iPSCs	Induced Pluripotent Stem Cells
IVF	*in vitro* Fertilisation
kb	Kilobase Pairs of DNA
kDA	KiloDaltons
l	Liter
LB	Luria Bertani
Macbol	Macrostomum lignano boll
Mcl-1	Myeloid cell leukemia 1
mGSCs	male germ stem cells
MII	Metaphase II
Min	Minutes
ml	Milliliter
MLH	MutL homolog
mRNA	Messenger RNA
Msh	Muscle segment homeobox

Msx	Msh homeobox
Mvh	Mouse VASA Homologue
NRF-1	Nuclear respiratory factor 1
NZ	Normozoospermia
OAT	Oligoasthenoteratozoo-spermic
Oct	Octamer-binding transcription factor
PABP	Poly-A Binding Protein
Pam	Peptidylglycine alpha-amidating monooxygenase
p-ATM	Phospho-ATM
PBS(-T)	Phosphate Buffered Saline (plus 1% or 0.05% w/v Tween-20)
PCR	Polymerase Chain Reaction
PGC	primordial germ cell
PI3K	Phosphatidylinositol 3 kinase
Prdm1	Positive regulatory domain containing 1
PTEN	Phosphatase and tensin homolog deleted on chromosome ten
PUM2	PUMILIO-2
Pα7/C8	proteosomeα7/C8 subunit
qPCR	Quantitative PCR
RA	Retinoic Acid
RAR	Retinoic Acid Receptor
RARE	RA-regulatory elements
REC	Recombination
RIP	RNA Immunopricipitation
RM	Repeated-measures
RNA	Ribonucleic Acid
RNAi	RNA Interference
RNase	Ribonuclease
RNP	Ribonucleoprotein
RPA	Replication protein A
rpm	Revolutions per Minute
RT	Reverse Transcriptase
RXR	Retinoid Reporters
s	Seconds
Sall4	Sal-like 4
SC	Synaptonemal Complex
SDA1	Severe Depolymerization of Actin 1
SDAD	SDA1 Domain containing
Sdf1	Stromal cell-derived factor 1
SDS	Sodium Dodecyl Sulfate
shRNA	Small Hairpin RNA
siRNA	Small Interfering RNA
Smad	Small/mothers against decapentaplegic

SMC	Structural maintenance of chromosome
SNP	Single Nucleotide Polymorphism
SOX	SRY-box containing gene
Sp1	Specificity protein 1
Spo	Sporulation-deficient recessive mutant
STAG	Stromal antigen
StRA8	Stimulated by Retinoic Acid 8
Suz12	Suppressor of zeste 12 homolog
SYCP	Synaptonemal Complex Protein
TAE	Tris-Acetate-EDTA
TBS	Tris-Buffered Saline
Tdrd7	Tudor domain-containing protein 7
TE	Trophectoderm
TEKT1	Tektin1
TEX	Testis Expressed
TGFβ1	Transforming growth factor-β1
Tpx1	Testis specific protein-1
Trf2	Telomeric repeat binding factor 2
Tssk	Testis-specific serine kinase
UTR	Untranslated Region
v/v	Volume by Volume
w/v	Weight by Volume
w/w	Weight by Weight
wk	Week
Wnt5a	Wingless-type MMTV integration site family member 5a
wpf	Week post Fertilisation
X.laevis	*Xenopus.laevis*
Xdazl	X. laevis Dazl
Zdazl	Zebrafish Dazl
Zfp42	Zinc finger protein 42
Zic3	Zic family member of the cerebellum 3
β-ME	β-Mercaptoethanol

Chapter 1

Literature Review

Chapter 1. Literature Review

1.1 Introduction

Germ cells are gametes and their precursors. In mammals, the primordial germ cells are induced from epiblast cells (Tam and Zhou, 1996), migrate through hindgut and proliferate at the same time, and finally reach the genital ridge to form the fetal gonad (Chiquoine, 1954, Witschi, 1948). Once the primordial germ cells are settled, they will undergo a process called meiosis, during which they will duplicate their DNA once and divide twice to form haploid gametes. In mammalian testis, the germ cells will not enter meiosis until puberty, whilst in female, the meiosis starts during fetal life but will arrest at a specific stage called diplotene before birth, and it will resume at puberty in developing follicles. Disruption of meiosis, for example through knockout of meiosis-specific genes (e.g. *Synaptonemal complex protein 3* (*Sycp3*)) can cause severe phenotypes such as aneuploidy and lead to infertility (Yuan *et al.* , 2002). Therefore, germ cell development during fetal life, especially in the fetal ovary is very important for future reproductive capacity.

The highly conserved Deleted in Azoospermia (DAZ) family proteins (DAZ, DAZL and BOLL) are RNA binding proteins, which bind to and regulate target mRNAs at the post-transcriptional level during germ cell development (Eberhart *et al.* , 1996, Reijo *et al.* , 1995, Reijo *et al.* , 1996). *DAZ* is located on the Y chromosome and thus only expressed in males (Reijo *et al.*, 1995). *DAZL* and *BOLL* are autosomal, and therefore, only DAZL and BOLL may be involved in female germ cell development. Loss of Dazl in mice causes complete loss of germ cells (Ruggiu *et al.* , 1997), and male *Boll*$^{-/-}$ mice are also sterile (VanGompel and Xu, 2010). In humans, mutations of *DAZL* and *BOLL* have been found to be associated with subfertility phenotypes such as azoospermia, early menopause or premature ovarian failure (Tung *et al.* , 2006b, Tung *et al.* , 2006c), however the effect of DAZL and BOLL function at molecular level remains unclear. Previous studies have already revealed the expression pattern of human DAZL and BOLL in human testis, and suggested that DAZL and BOLL proteins are distributed in different groups of germ cells (Luetjens *et al.* , 2004), but their expression patterns are poorly detailed in the fetal ovary. Several Dazl or Boll mRNA targets have been identified in model animals

(Reynolds *et al.* , 2007, Reynolds *et al.* , 2005, Zeng *et al.* , 2008, Zeng *et al.* , 2009), and some potential human mRNA targets have been proposed to be bound by DAZL or BOLL (Fox *et al.* , 2005, Kee *et al.* , 2009), however none of these have been definitely proven in humans as yet.

Therefore, to understand how DAZL and BOLL regulate germ cell development in the human fetal ovary, it is necessary to find out their expression pattern and also identify the potential target mRNAs they regulate. This chapter will review germ cell development, especially the meiotic stages during fetal life of human and mouse, and will also discuss previous research on DAZL and BOLL.

1.2 Fetal ovarian development

1.2.1 Introduction

Reviews in this section will be mainly based on both human and mouse data, as human fetal tissue is difficult to obtain, and therefore it has limited the exploration on human; in contrast, mouse tissue is easier to obtain and handle, and most relevant previous research was performed in mice.

In general, both human and mouse germ cells migrate to the genital ridge, proliferating as they migrate. In females, they then form germ cell nests and enter into meiosis, but later arrest as the nests breakdown to form primordial follicles. Many oocytes will undergo apoptosis, during which up to over 90% germ cells could be lost (Baker, 1963).

However, although the general process is similar, the timing of human and mouse ovarian development is very different. This review will talk about human fetal ovary development using the scale of trimesters and gestational ages, i.e. the pregnancy period will be calculated from the date of last menstrual period, which is about 2 weeks prior to the actual week post fertilisation (wpf). Using this scale, the pregnancy period of human is 40 weeks. Human pregnancy is further divided into three trimesters, which can be subdivided further into first (before 13 week), early second (13-16 week) and late second trimester (17 - 28 week), which are coincident

with some key stages of ovarian germ cell development (Stoop *et al.* , 2005). In mice, pregnancy lasts about 20 days. Moreover, the germ cells in mouse fetal ovary are synchronised, which means they are all at approximate the same stage during development (Borum, 1961); (Pepling and Spradling, 1998), whilst in human fetal ovary, the germ cells are not completely synchronised even in the same nest, and more mature cells are distributed toward the central area of the ovary (Gondos, 1987). Also, in humans, follicle formation and most oocyte apoptosis happens during fetal life (De Pol *et al.* , 1997), but follicle formation happens at or immediately after birth in the mouse (Borum, 1961). The key differences of human and mouse early ovarian development are shown in Figure 1.1 and will be further discussed in following sections.

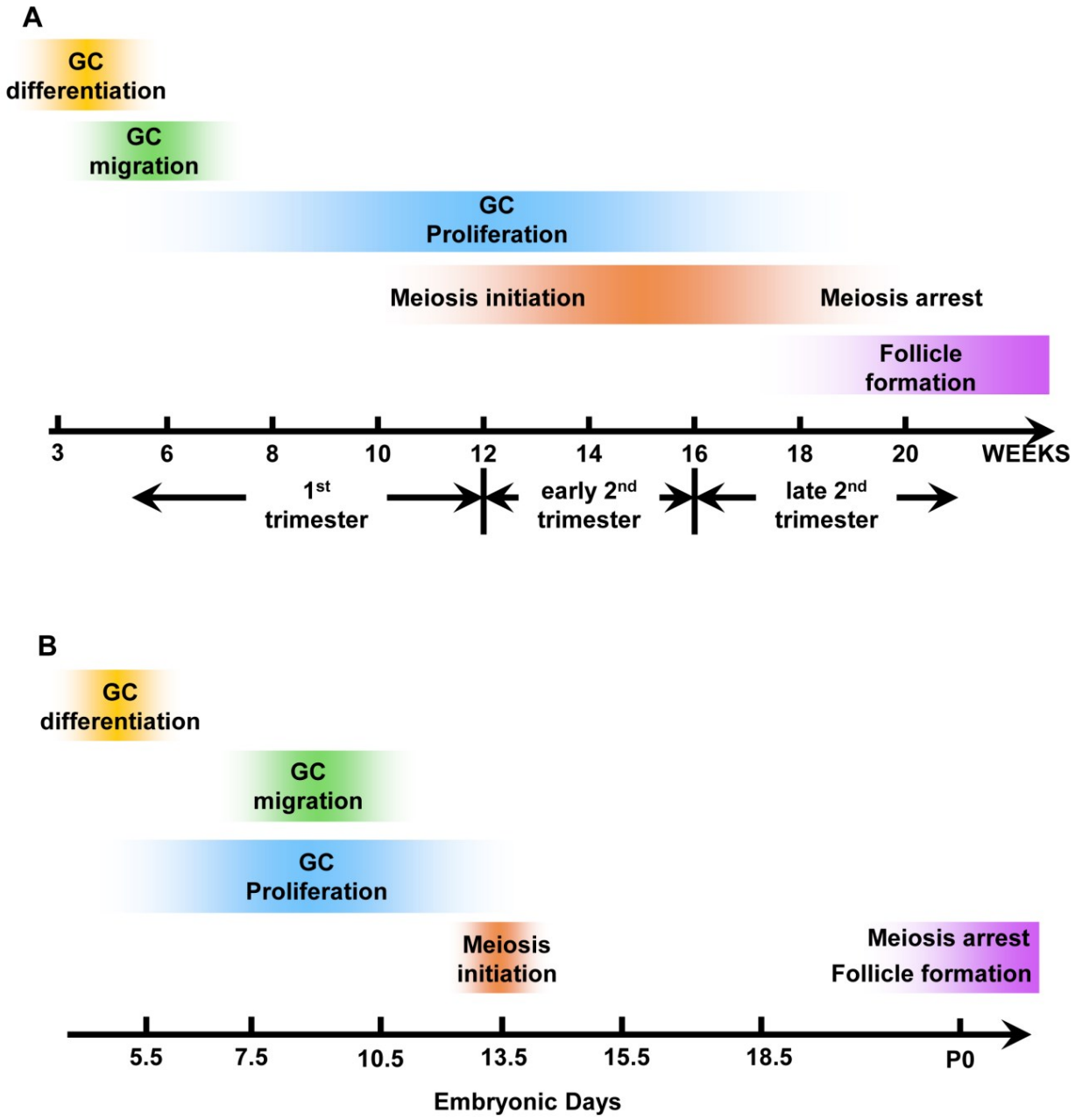

Figure 1. 1 Comparison of key time points of human and mouse fetal ovarian development

A) In human, the primordial germ cells differentiate at ~3 week gestation, then migrate to and settle in the fetal gonad at 6 – 7 week gestation, further differentiating into oogonia. They proliferate during migration and afterwards, and more mature germ cell enter the meiosis at 10 – 12 week gestation (at the beginning of the early second trimester). Meiosis begins to arrest at late second trimester, from 18 week gestation, accompanied by primordial follicle formation and oocyte apoptosis.

B) In mouse, germ cells differentiate from embryonic day (e) 5.5 and are detectable from e7.0; they then migrate, and have mostly settled in fetal gonads by e11.5, proliferating at same time. The mitotic proliferation will arrest at e13.5 and meiosis starts at this time point. Meiosis will begin to arrest, with the follicle formation and oocyte apoptosis around the time of birth.

1.2.2 Germ cell differentiation and migration

Although it is now known that germ cells originate from the proximal epiblast, for a long time it had been believed that primordial germ cells (PGCs) arose at the base of yolk sac. Their extraembryonic appearance in human had been observed as early as in 1910s (Felix, 1912). However, the first detailed description of human germ cell origination and migration is credited to Witschi (1948), whom examined 23 early human embryos from 13 somite stage (3-4 wpf) to 8mm (5-6 wpf), and suggested that the PGCs appear at the base of yolk sac, near the developing allantois and then migrate through the hind gut, enter the mesentery and finally reach the genital ridges. During migration, germ cells proliferate by mitosis, and it seems that those germ cells are guided by some chemicals from gonadal region (Witschi, 1948). However, Witschi mistakenly assumed that these PGCs were originated from common endoderm or early "endoderm" (prospective yolk sac or hind gut) based on his observation that those germ cells seemed to first appear at the base of yolk sac. In 1954, Chiquoine developed the technique of staining PGCs with alkaline phosphatase (ALP) in mouse embryos, and also for the first time demonstrated that mouse germ cells occur as early as E8.5 around the yolk sac, and migrate through a similar pathway as in human to the genital ridge. Using the same technique, Ginsburg *et al.* (1990) demonstrated that the PGCs originate from the proximal epiblast at e7.25 in mouse embryos. Later research suggested that these cells may occur at e7.0 (Saitou *et al.* , 2002) and their precursors are from distal epiblast cells at e6.5 (Tam and Zhou, 1996). In 1999, Lawson *et al*. reported that the epiblast cells may be induced to form germ cells by Bmp4 (bone morphogenetic protein 4) as early as e5.5 in mouse embryo.

BMP signalling is essential for the induction of PGCs. Bmp2, Bmp4 and Bmp8b are all key factors for the germ cell differentiation (Lawson *et al.*, 1999, Ying *et al.* , 2000, Ying and Zhao, 2001). The *Bmp4*-null phenotype is lethal and completely lacking germ cells, whilst heterozygotes survive but have reduced germ cell number. The lower germ cell number is due to the reduced number of precursor cells formed at e7.25 (Lawson *et al.*, 1999). The phenotype of *Bmp8b* mutations in C75BL/6 mice is similar to these of Bmp4 (Ying *et al.*, 2000). Bmp4 and Bmp8b are produced by the extraembryonic ectoderm (Ying *et al.*, 2000). Bmp2, is secreted by proximal

anterior visceral endoderm and its null mutation leads to reduced but not complete loss of germ cells on C75BL/6 mice (Madabhushi and Lacy, 2011, Ying and Zhao, 2001).

The BMPs bind to and stimulate the interaction of its type I and II receptors, and these receptors again send the signals to downstream to regulate transcription (Wieser *et al.* , 1995), by phosphorylating the Small/mothers against decapentaplegic (Smad) family proteins, which are important transducers of this signalling pathway (reviewed by Kretzschmar *et al.*, 1997). Among this family, Smad1 and Smad5, which mainly mediate the signals from BMP2 and 4, are directly phosphorylated and thus activated by the BMP receptor I, migrate to the nucleus and regulate the transcription (Kretzschmar *et al.*, 1997). Loss of Smad1 in mouse causes impaired development of extraembryonic tissues and reduced number of PGCs, but the overall embryo development is relatively normal when compared to BMP-deficient phenotypes (Tremblay *et al.* , 2001). Smad5, which is a very similar homologue of Smad1 and involved in Bmp4 signalling together with Smad4 (Pellegrini *et al.* , 2003), is also necessary for the PGC differentiation, and Smad5 mutation causes a phenotype of reduced germ cell number (Chang and Matzuk, 2001). B lymphocyte-induced maturation protein (Blimp1, or Positive regulatory domain containing 1, Prdm1), which is regulated by Bmp signalling, is also necessary for the germ cell differentiation (Ohinata *et al.* , 2005). The Blimp1^{+ve} cells in the epiblast will develop into PGCs and deficiency of this gene will cause both loss and abnormal behaviour of germ cells (Ohinata *et al.*, 2005).

After formation, germ cells migrate to the fetal gonads (Witschi, 1948). The initiation of germ cell migration starts in mouse at e7.5, moving from the streak to the definitive endoderm (Anderson *et al.* , 2000), just after these cells could first be detected using the ALP staining at e7.25 (Ginsburg *et al.*, 1990). Molyneaux *et al.* (2001) extended the research to e9.0 - e12.5, suggested that the part of the endoderm (hindgut pocket) which contains germ cells will later develop into the hindgut by e9.0, and although germ cells are already motile before this stage, they will only move out of the hindgut and invade into the dorsal body wall between e9.0 and e9.5. By e9.5, the movement appears quite random and not toward genital ridge, however

the germ cells will soon find their target by e10.5 and most are settled into the fetal gonad at e11.5.

The mechanism of germ cell migration is still largely unknown. Most research has focused on two main aspects: how do the germ cells gain their motile ability, and how do they home to the genital ridge? The movement of germ cells is amoeboid-style (Blandau *et al.* , 1963), and stimulation of this ability is thought to associate with the somatic steel/c-kit expression (Runyan *et al.* , 2006) (Gu *et al.* , 2009). c-kit is the tyrosine-kinase receptor for the Steel ligand, whilst Steel is a glycoprotein with two isoforms (reviewed by Loveland and Schlatt, 1997) . Both the ligand and receptor are expressed during the germ cell migration in pre-hindgut (Motro *et al.* , 1991) and also on the route of later migration (Keshet *et al.* , 1991). Expression of W^e, a mutation of c-Kit caused delayed germ cell migration but the cells still localised into genital ridge successfully (Buehr *et al.* , 1993), and the $Steel^{-/-}$ phenotype suggested that this gene is necessary for germ cell motility from early on when the germ cells were still in the allantois, until after their entry into the hindgut (Gu *et al.*, 2009).

It has been thought for a long time that germ cells are at least partly attracted by some factors released by the genital ridge, and some strong evidence was provided by Rogulska *et al.* in 1971, who found mouse germ cells could travel toward the chick gonad in transplantation. Later studies suggested that Stromal cell-derived factor 1 (Sdf1) and its receptor Cxcr4 are expressed by the dorsal body wall and PGCs respectively, and are involved in chemotaxis (Molyneaux *et al.* , 2003), as *in vitro* studies demonstrated that germ cell migration was disrupted when culture media contained Sdf1 and that germ cells could also be attracted by Sdf1-coated beads. Furthermore, loss of Cxcr4 in germ cells decreases the number of germ cells that colonise the genital ridges, but this activity is only necessary for the migration after they moved into hindgut. Beside Sdf1/Cxcr4, Wingless-type MMTV integration site family member 5a (Wnt5a) and Transforming growth factor-β1 (TGFβ1) are also thought to be associated with the signals sent from genital ridge (Chawengsaksophak *et al.* , 2012, Godin and Wylie, 1991). Notably, germ cells form a network after leaving the hindgut (Gomperts *et al.* , 1994) and disruption of this network by

blocking E-Cadherin function leads to failed colonisation of germ cells in the genital ridge (Bendel-Stenzel *et al.* , 2000).

1.2.3 Germ cell colonization and formation of nests

Upon their arrival at the genital ridge, germ cells quickly lose motility and their shape becomes rounded (Donovan *et al.* , 1986), although a few germ cells in mouse ovary still maintain motility even after entry of meiosis whilst all the germ cells in testis are quiescent as soon as the seminiferous tubules form (Blandau *et al.*, 1963). Germ cells still undergo mitosis and apoptosis in the fetal ovary as they did during migration (Blandau *et al.*, 1963), however their gene expression pattern begins to change, with the re-activation of the silenced X chromosome (Monk and McLaren, 1981) and the loss of some early PGC markers like Nanos3 (Tsuda *et al.* , 2003). However, the expression of pluripotency markers Nanog and Octamer-binding transcription factor (Oct)4 is maintained (Anderson *et al.* , 2007, Pesce *et al.* , 1998, Yamaguchi *et al.* , 2005) until the germ cells enter meiosis. Some later germ cell specific markers, such as DAZL and VASA (also known as Ddx4, DEAD box polypeptide 4) begin to be expressed in these germ cells as well (Anderson *et al.*, 2007). The differentiated germ cells in ovary are now called oogonia, which could be visually distinguished from PGCs by their shape (Gondos, 1987). Oogonia further differentiate and enter meiosis during the second trimester, whereupon they become oocytes (Gondos, 1987, Gondos *et al.* , 1986). Meiosis in the fetal ovary will be discussed in detail in Section 1.3.

Another significant change during the transition from PGCs to oogonia is the formation of intercellular bridges. The existence of intercellular bridges in mammals was first found in cat testis, and then was described in the ovary of many species (reviewed by Ruby *et al.*, 1969). As mentioned in Section 1.2.1, the PGCs are connected and form a network during migration, however this connection is lost after reaching the genital ridge by e11.5 (Gomperts *et al.*, 1994) and instead germ cells are connected between each other by intercellular bridges from this stage on (Pepling and Spradling, 1998). In humans, the intercellular bridges were also only found during oogonial stages but not in PGCs, and persisted during meiosis until follicle

formation occurs (Gondos, 1987). The clusters of germ cells connected by these bridges are termed germ cell cysts or nests (Pepling and Spradling, 1998).

The formation of intercellular bridges between germ cells is believed to be due to incomplete cytokinesis during mitotic proliferation (Zamboni and Gondos, 1968). This phenomenon was first described by LaValette St. George in 19th Century as connected testicular germ cells after division *in vitro* (reviewed by Dym & Fawcett, 1971), and was finally confirmed by Weber and Russell (1987)'s work on rat spermatogenesis. The process of cytokinesis is quite complicated, including site selection, furrow ingression, and midbody abscission; the midbody is a temporal structure formed at late cytokinesis, connecting two daughter cells and similar to inter cellular bridges; the proper germ cell intercellular bridges are formed after the breakdown of midbody and therefore it is the late cytokinesis which is most important for this process (reviewed by Greenbaum *et al.*, 2011). One of the key factors involved in the formation of intercellular bridge is *Tex14* (Testis-expressed gene 14; Greenbaum *et al.*, 2007). This study showed that during late cytokinesis, the Tex14 protein localised to the inner side of the dividing site, forms a ring and later expands and merges with an outside centralspindlin ring (a protein complex, the division remnants of spindle with a ring-like structure) (Mishima *et al.* , 2002) and the size of the mature ring canal increases during development. The intercellular bridge cannot form without Tex14, and beside its structural function, other factors recruited by Tex14 also seem to be necessary to prevent the complete abscission of midbody and to stabilise the intercellular bridges (Greenbaum *et al.* , 2007).

Ultrastructural studies suggest that intercellular bridges contain microtubules and organelles (Gondos, 1987, Pepling and Spradling, 1998, Ruby *et al.*, 1969). Therefore, it is believed that these bridges are involved in the synchronized development of germ cells and also the nursing behaviour between oocytes in mammals (Ruby *et al.*, 1969, Zamboni and Gondos, 1968). As Tex14 is necessary for the formation of intercellular bridges, loss of Tex14 could partly reveal their functions. *Tex14*$^{-/-}$ mice have no intercellular bridges and display infertility phenotypes, including decreased testes weight and meiosis defects, i.e. lacking of germ cells from late pachytene stage (Greenbaum *et al.* , 2006). However, it seems

that the development of PGCs and spermatogonia/oogonia is not affected, and infertility phenotype of *Tex14*$^{-/-}$ is restricted to male mice (Greenbaum *et al.* , 2009). Although loss of intercellular bridges also occurs in *Tex14*$^{-/-}$ females and they have fewer oocytes at birth, these mice are still fertile and their folliculogenesis is unaffected in relatively long-term (Greenbaum *et al.*, 2009). Interestingly, the existence of intercellular bridges is conserved from insects to human, but these bridges are required for the *Drosophila* gametogenesis in both male and female, and mutations of several key factors could disrupt oogenesis (reviewed by Greenbaum *et al.*, 2011), which implies some non-conserved functions of intercellular bridge between species and sexes.

1.2.4 Primordial follicle formation and germ cell apoptosis

At later stages of ovarian germ cell development, the pregranulosa cells will invade the germ cell nest and surround single germ cells to form primordial follicles (Gondos, 1987). In mouse, this happens at or just after birth (Borum, 1961) whilst in human, it begins during fetal life, from 18 weeks gestation onwards (De Pol *et al.*, 1997, reviewed by Mahishwari and Fowler, 2008). Not all the germ cells in the ovary form primordial follicles; some early research indicated that total germ cell loss could exceed 90% by birth (Baker, 1963), but recent studies showed that through primordial follicle assembly and nest breakdown, up to one third to two thirds germ cells are lost (reviewed by Tingen *et al.*, 2009).

The arrest of meiosis at diplotene (see Section 1.3) seems to be required for the breakdown of germ cell nests. Studies in rats suggested that meiotic arrest occurs before primordial follicle formation (Beaumont and Mandl, 1962) and loss of synaptonemal complex protein 1 (Sycp1), an important factor for recombination during meiosis, leads to both earlier meiotic arrest and nest breakdown (Paredes *et al.* , 2005).

A lot of other factors associated with this process have been identified as well. Factor in the germline alpha (Figα, subsequently termed Figla) is a transcription factor expressed from meiosis initiation in females (Soyal *et al.*, 2000). Mutation of *Figα*

causes female-specific infertility, due to the absence of primordial follicles without disruption of meiosis, and these mice suffer complete germ cell loss after birth (Soyal *et al.* , 2000). Another gene called *Nobox* is also necessary for follicle formation, as loss of this gene will cause delayed nest breakdown and fewer primordial follicles at postnatal day 7; even these very rare follicles will all undergo degeneration and lead to sterility whilst males are still fertile (Rajkovic *et al.* , 2004). The members of the TGFβ superfamily of genes such as Growth differentiation factor 9 (GDF9) also join this process. *In vitro* studies suggest that Gdf9 is necessary for primordial follicle formation in hamster, as the formation of pregranulosa cells seems to be blocked by silencing *Gdf9* with siRNA in cultured hamster ovary (Wang and Roy, 2006), which might also represent its function during human folliculogenesis as it is also expressed in human fetal ovary before follicle formation (data generated by our lab).

Soon after primordial follicle formation, it is believed that the process of continuous follicle activation and growth (initial recruitment) begins; the follicles will grow through primary, secondary and early antral stages; these follicles will all undergo atresia until ovulation occurs from the time of puberty (McGee and Hsueh, 2000). At puberty, under the stimulation of circulating FSH, some of the activated antral follicles will be able to grow further and escape from the fate of atresia during each menstrual cycle (called cyclic recruitment) (McGee and Hsueh, 2000). Follicle activation includes the growth of oocyte, as well as the differentiation and proliferation of granulosa cells – the flattened pregranulosa cells will become cuboidal-shaped and steroidogenic (reviewed by Wandji *et al.* , 1996). Factors which are known to be involved in the maintenance of arrest and activation of primordial follicles including Phosphatase and tensin homolog deleted on chromosome Ten (PTEN), Kit ligand and its receptor c-Kit, GDF9, Anti-Müllerian hormone (AMH) and more (reviewed by Adhikari and Liu, 2009). The Phosphatidylinositol 3 kinase (PI3K) pathway is crucial for the activation of primordial follicles before they are able to response to FSH directly (Liu *et al.* , 2006). This pathway can be supressed by PTEN, as deletion of this gene in oocytes causes global premature follicle activation (Reddy *et al.* , 2008). AMH is also a suppression factor of initial recruitment but it is undetectable in primordial follicles; it can be produced by

primary or later follicles and therefore repress the activation of their adjacent follicles, acting as a paracrine factor (reviewed by Adhikari and Liu, 2009). In contrast, GDF9 is not only important for the formation of primary follicles but also play a role in promoting their activation in human, as more primordial follicles started growth when cultured with GDF9 (Hreinsson *et al.* , 2002).

Germ cell loss is due to programmed apoptosis (De Pol *et al.*, 1997). Several hypotheses were developed to explain the significance of germ cell apoptosis during follicle formation. For example, it might due to the quality control mechanism, such that germ cells with chromosome aneuploidy (e.g. Tuner's Syndrome) show much higher apoptosis ratio (Modi *et al.* , 2003). In addition, it seems that the germ cells "nursing" others through the intercellular bridges also will undergo apoptosis; the intercellular bridge is sufficient for the transfer of mitochondria (see Section 1.2.2) and injection of mitochondria into mouse oocyte could significantly rescue the germ cells from apoptosis (Perez *et al.* , 2000). This phenomenon is similar to the case in *Drosophila*, as during its oogenesis only one oocyte out of 16 connected ones in a cyst will survive, and mitochondria, proteins and mRNAs are all enriched in this particular oocyte (reviewed by Huynh and St Johnston, 2004).

The molecular basis of germ cell apoptosis remains largely unknown, but it is associated with several different protein families, such as B-cell leukemia/lymphoma-2 (Bcl-2) and TGFβ. The most important factors of general programmed cell apoptosis might be the Bcl-2 family of proteins, which contain pro- and anti-apoptosis members (reviewed by Morita & Tilly, 1999). Bcl-2 itself belongs to the anti-apoptotic group and therefore is a negative regulator of apoptosis; in contrast, another member of this family, the Bcl-2 associated X protein (Bax) belongs to pro-apoptotic group and can suppress the Bcl-2 function by directly interacting with it, subsequently promoting cell death (Oltvai *et al.*, 1993; reviewed by Tilly, 2001). *Bax*$^{-/-}$ female mice have more primordial follicles than the WT, and this effect is maintained during their adulthood (Perez *et al.* , 1999). In addition, two other members of this family, Myeloid cell leukemia 1 (Mcl-1) and BCL2-associated agonist of cell death (Bad) play similar roles to Bcl-2 and Bax respectively; like Bcl-2, Mcl-1 could also maintain the viability of cells (Kozopas *et al.* , 1993).

Although Bad can also interact with Bcl-2, its binding to Bcl-x_L, another anti-apoptosis member of Bcl-2 family is stronger, and also promotes cell death (Yang *et al.* , 1995). In the human fetal ovary, BCL-2 and BAD expression is restricted to somatic cells through first to late second trimester, whilst MCL-1 is only expressed in germ cells (Hartley *et al.* , 2002). The pro-apoptosis protein BAX is widely expressed in both germ and somatic cells, and it seems that its protein is more concentrated in germ cells around the edge of the ovary between 14-17 weeks gestation, prior to primordial follicle formation (Hartley *et al.*, 2002).

A TGFβ family member, activin is also associated with germ cell survival. Both *in vivo* studies in mouse and *in vitro* studies in human suggested that treating neonatal female mouse or human fetal ovary fragments (second trimester) with recombination human Activin A could increase number of primordial follicles (Bristol-Gould *et al.* , 2006, Martins da Silva *et al.* , 2004). Activin is expressed in germ cells and might act as a suppressor of kit ligand expression in somatic cells (Childs and Anderson, 2009), as its subunit activin βA is mainly expressed in the oocytes before follicle formation and its expression pattern is inversely coincident with the dynamic changes of c-kit during fetal ovary development (Coutts *et al.* , 2008).

Although it was believed for over fifty years that the number of oocytes does not increase after birth and therefore the female reproductive capacity cannot be restored (reviewed by Kuo and Yang, 2008), the effort of looking for germ stem cells in the adult ovary has never ceased. Over the recent decade, the aforementioned theory has been challenged. One of the most remarkable finding is the proposed existence of new-formed germ cells which express early meiotic markers in adult mouse ovary, as well ongoing folliculogenesis (Yuan *et al.* , 1998). Work by another research group isolated female germline stem cells (FGSCs) from adult mouse ovary using flow cytometry (with germ cell marker Mvh) and demonstrated their self-renewal ability, with the further potential of producing offspring (Moses, 1958). Similar putative germ stem cells have also found in human ovary (White *et al.* , 2012). While these are undoubtedly important findings, much further work will be required to investigate their potential contribution to ovarian physiology.

1.3 Meiosis in fetal ovary

1.3.1 Introduction

Meiosis, which was historically named "reduction division" by A. Weismann and firstly termed as "maiosis" (Farmer and Moore, 1905), is what its obsolete name indicates; the process by which diploid germ cells replicate their DNA once and divide twice to form haploid gametes. The general process of meiosis includes two stages, i.e. meiosis I and meiosis II, and each stage is further divided to four phases, namely prophase, metaphase, anaphase and telophase. In meiosis I, the DNA replicates, then homologous chromosomes pair allowing crossover between them and the exchange of genetic material (i.e. recombination). Homologous chromosomes then separate when the germ cell divides into two daughter cells, leaving each cell with half a set of chromosomes, but each chromosome has a pair of chromatids. During meiosis II the daughter cells divide again to separate the sister chromatids and form the haploid gametes. The pairing of homologous chromosomes during meiosis I is termed synapsis by Moore (1895); the special structure formed by paired chromosomes during meiosis is called bivalent or tetrad.

The prophase of meiosis I can be further divided into four stages, i.e. leptotene, zygotene, pachytene and diplotene. Leptotene, pachytene and diplotene were defined and termed by H. von Winiwarter (1900) and zygotene by V. Gregoire (1907) (reviewed by Agar, 1911, Manton, 1939). During leptotene, the chromosomes are long and thin; during zygotene, the homologue chromosomes begin to pair, they then become shorter, condensed, and entirely pair at pachytene; synapsis and crossover also happen at this stage. During diplotene, the chromosomes further thicken and show a very clear structures of crossover and recombination called chiasmata, a morphology very unique to meiosis.

Early at the end of 19th Century, the core of meiosis theory, i.e. the halving of chromosome number in germ cells by two divisions during gametogenesis was already established. Scientists (T. Boveri and O. Hertwig) began to realise that the general process of meiosis is strikingly similar between two sexes, and they also found that one primary spermatocyte will first divide into two secondary spermatocytes and finally form four sperms, whilst in female the primary oocyte will

first divide into a secondary oocyte and a first polar body. The first polar body usually degenerates before the second meiotic division in mammals, but can persist, in which case the first polar body and secondary oocyte together will finally form one egg and three second polar bodies (reviewed by Baxter & Farley, 1979).

In mammals, meiosis initiates in the ovary during fetal life, whilst in male it only begins at puberty. During oocyte development in the fetal ovary, meiosis arrests at diplotene of prophase I, and resumes when ovulation occurs (i.e. from puberty (reviewed by Baillet & Mandon-Pepin, 2012)) as it is triggered by the mid-cycle LH surge. Despite all stages of meiosis being important for the adult reproductive capacity, this review will only focus on the meiosis prophase I which occurs during fetal ovary development.

1.3.2 Entry of meiosis

Meiosis initiates in the mouse fetal ovary at e13.5 (Borum, 1961, Monk and McLaren, 1981), and in human at 10-12 weeks gestation (Gondos *et al.*, 1986). In the mouse fetal ovary, the germ cells are roughly synchronised and entering meiosis in an anterior-to-posterior wave (Menke *et al.* , 2003). In the human fetal ovary, germ cell development is very asynchronous – the germ cells toward the periphery are still in mitosis, whilst those in central area are more mature and entering meiosis (Gondos, 1987). Therefore, germ cells of different maturation stages, from oogonia to primordial follicles can all exist in the same human fetal ovary.

In mouse, the different timing of meiosis entry between male and female is very likely due to the action of retinoic acid (RA) in the ovary, and the expression of the retinoic acid metabolising enzyme Cyp26b1 in the testis (Bowles *et al.* , 2006, Koubova *et al.* , 2006).

CYP26B1 is a cytochrome P450 enzyme expressed in gonadal somatic cells of both sexes (Bowles *et al.*, 2006). It was firstly identified and termed as “P450RAI-2” by White *et al.* (2000) in human brain; this study also showed that CYP26B1 is specifically involved in the metabolism of all-trans-RA, one of the retinoids, and acts to metabolise this molecule. In mouse fetal gonads, *Cyp26b1* is expressed in both

males and females at e11.5 when germ cells settle in the genital ridge, but is only detectable in males after e13.5 (Bowles *et al.*, 2006), which is coincident with the timing of meiosis initiation in the fetal mouse ovary. Adding the P450 enzyme inhibitor ketoconazole to cultured gonads at e11.5 led to increased expression of meiosis markers in male gonad, and meiotic cells were found as well (Bowles *et al.*, 2006), demonstrating that a P450 enzyme must be involved in inhibiting meiosis in the fetal testis. A similar effect was shown in *Cyp26b1*-null testes, and germ cells in the ovaries of *Cyp26b1*-null mice enter meiosis slightly earlier than in those in wild type mice (Bowles *et al.*, 2006). Further examination of their testes indicated that meiosis occurs prematurely at e13.5 of fetal life but only reaches pachytene stage, accompanied by increased germ cell apoptosis, whilst germ cells in the ovary are normal (MacLean *et al.* , 2007). The high expression of *Cyp26b1* at e12.5-e13.5 in male gonad and prior to meiosis initiation in female gonad (Bowles *et al.*, 2006), indicates that this gene may act as the proposed meiosis inhibiting factor in the fetal testis (McLaren and Southee, 1997), and also prevents premature meiosis initiation in the fetal ovary (Bowles *et al.*, 2006).

Adding Cyp26-resistant synthetic retinoid to cultured *Cyp26b1*-deficient male gonad also induces meiosis, further providing evidence about the role of direct regulation on meiosis by RA itself, rather than its metabolites generated by Cyp26b1 (MacLean *et al.*, 2007). There is extensive expression of RA signalling pathways during fetal development. This molecule acts through RA receptors (RAR), including RARα, β and γ, which can form heterodimers with retinoid reporters (RXR) α, β and γ, then the heterodimers bind to the RA-regulatory elements (RARE) of their target genes to modulate their expression (reviewed by Bowles and Koopman, 2007). Both RARs and RXRs are expressed in germ cells (Koubova *et al.*, 2006), and they are responsive to RA at e12.5-14.5 as shown by studies using a *LacZ*-reporter gene controlled by a RARE that is expressed during this period in mesonephros of both sexes and ovary (Bowles *et al.*, 2006). The possible source of RA in mouse is the mesonephros, because Aldehyde dehydrogenase 1 family member A (*Aldh1a*)*2* (also known as *Raldh2*), the main gene relating to RA synthesis, is strictly expressed in the fetal mouse mesonephros but not in fetal mouse gonads (Bowles *et al.*, 2006).

RA was first found to accelerate entry of oogonia into meiosis whilst reducing the number of oogonia in cultured rat ovary, and this effect is similar to that induced by RARα agonist in culture (Livera *et al.* , 2000). Several subsequent studies in mice proved this role of RA, as adding this molecule in culture could increase the expression of meiosis markers and decrease the level of pluripotency markers at the same time; an effect that could be masked by adding RA receptor antagonist (Bowles *et al.*, 2006). Interestingly, RA treatment could prematurely promote meiosis in e11.5 mouse fetal testis, but after e13.5 it seems lose this capacity and instead prevents the mitotic arrest of germ cells in those specimens (Trautmann *et al.* , 2008).

The effect of RA on initiating meiosis is believed to be through *Stimulated by Retinoic Acid 8* (*Stra8*). Mouse *Stra8* was first identified by Bouillet *et al.* (1995) with 11 other novel *Stra* genes, as their expression is promoted by treating mouse embryonic carcinoma cells with RA, and it was further characterised by Oulad-Abdelghani *et al.* (1996), showing that it was not only induced but also phosphorylated by RA signalling. They also found that in adult mouse testis, both *Stra8* mRNA and protein expression only occurred in pre-meiotic germ cells, so the authors assumed that it may associate with pre-meiotic phase of spermatogenesis. This prediction was proved correct and expanded to oogenesis by further investigations (Anderson *et al.* , 2008, Baltus *et al.* , 2006, Menke *et al.*, 2003). In the mouse embryo, *Stra8* has been proven to be an early meiosis marker, expressed specifically in germ cells of female from e12.5 to e14.5, in an anterior-to-posterior wave (Menke *et al.*, 2003). The germ cells of *Stra8*$^{-/-}$ outbred (C57BL/6×129) mice display multiple abnormalities at the entry of meiosis in mouse ovary including defects in DNA replication, chromosome thickening and synapsis/recombination (Baltus *et al.*, 2006). The male mouse of the same strain has meiosis initiation problems as well – their germ cells barely develop beyond the leptotene stage and end up in apoptosis (Baltus *et al.*, 2006). The inbred mouse strain (C57BL/6), derived from the aforementioned outbred mice by backcrossing, also show similar meiotic defects in males when they lose *Stra8*, but their germ cells could successfully replicate their DNA and enter the pre-leptotene stage (Anderson *et al.*, 2008).

It is clear that *Stra8* expression in germ cells is induced by RA signalling. When RA signalling is blocked by a pan-antagonist of Retinoic acid receptor (RAR) receptors, no *Stra8* is expressed in mouse fetal ovary (Koubova *et al.*, 2006). After injection with vitamin A, adult mice previously fed with vitamin A-deficient diet show dramatically increased *Stra8* expression in their testes (Koubova *et al.*, 2006). It seems that all three kinds of RAR receptors (α, β and γ) can induce *Stra8* expression, as adding the specific agonist of any of the receptors could induce *Stra8* in the fetal gonads of both sexes (Koubova *et al.*, 2006). RA signalling directly functions on germ cells rather than through somatic cells, because RA could promote the expression of *Stra8* from isolated germ cells from neonatal testes (Zhou *et al.* , 2008).

Cyp26b1, which metabolises and degrades RA as described before, negatively regulates *Stra8* expression by disrupting the RA signalling. Nonspecific inhibition of CYP family members, results in expression of *Stra8* in cultured mouse fetal testes (Koubova *et al.*, 2006). Blocking RAR receptors in *Cyp26b1*$^{-/-}$ adult male mouse can repress *Stra8* expression (Saba *et al.* , 2014). In *Cyp26b1*/*Stra8* double-knockout mice, although *Cyp26b1* is absent and therefore cannot block RA signalling, the expression of meiosis markers is still almost completely absent without the presence of *Stra8* (Saba *et al.*, 2014). Together with the evidence provided by Bowles *et al.* (2006), who found that *Cyp26b1* is selectively expressed in mouse fetal testis after e13.5, and also demonstrated that inhibiting Cyp26b1 activity promotes the expression of meiosis markers in mouse, it is possible to conclude that Cyp26b1→RA→Stra8 is an important, if not the only pathway to regulate the entry of meiosis in mouse.

However, this theory, although based on and supported by abundant observation and evidence, is challenged. Mark *et al.* (2008), who also established *Stra8*-null mutant mice on an outbred background (C57BL/6×129/sv), found that in this strain, the germ cells of male mice could successfully enter meiosis and express some meiotic markers, but synapsis is abnormal and they cannot reach the stages beyond pachytene. Therefore, the induction of meiosis might not be completely dependent on Stra8. Another study (Kumar *et al.* , 2011) questioned the Stra8 model further. In

Raldh2-null mice, or even *Raldh2/Raldh3* double-knockout mice (which are expressed in mesonephros, which is the main source of RA adjacent to fetal gonad), Stra8 is still expressed normally in fetal ovary at e12.5 and e14.5, and meiosis is initiated at e13.5. *Raldh2*-null mutation is lethal so these embryos were supplied with low dose of RA maternal diet from e6.75 to e9.25; however according to the RARE-*LacZ* reporter, these fetal ovaries did not receive enough RA to trigger signalling (Kumar *et al.*, 2011). They further found that in *Raldh2*$^{-/-}$ fetal testis, adding an inhibitor of Cyp26b1 also induced *Stra8* expression, without the presence of RA or activation of RARE-*LacZ* reporter; and this might due to signalling from mesonephros as once they were removed, the effect disappeared (Kumar *et al.*, 2011). In addition, Trautmann *et al.* (2008) found that treating e13.5 mouse fetal testis with RA induces *Stra8* expression, but unlike in e11.5 tissue, these gonads show no sign of meiotic recombination, suggesting there is another way in relatively more mature fetal testis to prevent the entry of meiosis. Therefore these studies indicate that meiosis initiation might not be completely dependent on *Stra8*, that *Stra8* expression might not be solely induced by RA, and that Cyp26b1 may also inhibit Stra8 expression and meiosis through another pathway other than RA signalling.

Several other genes might be additional candidate regulators of Stra8 expression. Dazl, which will be further discussed later in section 1.4, is essential for the RA-induced *Stra8* expression and meiosis initiation; loss of *Dazl* almost completely ablates Stra8 expression, and also causes severely decreased expression of meiosis markers (Lin *et al.* , 2008). Muscle segment homeobox (Msh) homeobox (Msx) 1 and Msx2, two homebox transcription factors, are also associated with the modulation of *Stra8* expression and meiosis progression in mouse – Stra8 expression is reduced, although still far from completely quenched in the fetal ovary of *Msx1* /*Msx2* double knockout mouse; these mice also have delayed meiosis and much fewer oocytes which reach the end of meiosis prophase I (Le Bouffant *et al.* , 2011).

These challenging lines of evidence may partly explain differences in meiosis initiation-related gene expression in the human fetal ovary compared to the mouse. Childs *et al.* (2011) reported that, unlike the mouse, the human fetal mesonephros

may not be the only source of RA synthetic enzymes, and germ cells in the human fetal testis may not be completely shielded from RA. All three groups of *ALDH1A* genes (1, 2 and 3) are expressed in both the human fetal testis and ovary through the first and second trimesters (Childs *et al.*, 2011). Furthermore, the level of *ALDH1A2* is strikingly higher in the human fetal testis than in either the human fetal ovary or mesonephros at 8-9 week gestation. This finding is consistent with the study of Le Bouffant *et al.* (2010), who found that *ALDH1A1* and *2* are expressed in the human fetal ovary. RA signalling is very likely to be activated in germ cells in both the human fetal testis and ovary, as the RARs and Retinoid X receptors are all expressed in both fetal ovary and testis and localised to the germ cell nuclei (Childs *et al.*, 2011). In human fetal gonads, *CYP26B1* expression is no longer male-specific, and its expression is even higher in fetal ovary at 14-16 weeks gestation (after the initiation of meiosis) than in the testis (Childs *et al.*, 2011). RA, but probably not CYP26B1, regulates meiosis initiation in human female, as exogenous RA promotes meiosis in cultured ovary, and adding the pan-inhibitor of RARs or RA synthetic enzymes inhibits meiosis but adding an inhibitor of CYP26B1 has no effect (Le Bouffant *et al.*, 2010). Interestingly, treating the human fetal testis at second trimester with RA also induces the expression of *STRA8*, but not the synapsis and recombination-associated genes *SYCP3* and *DNA meiotic recombinase 1* (*DMC1*), which is in agreement with the findings of Trautmann *et al.* (2008) on RA treated e13.5 mouse fetal testis. This suggests that although the expression pattern of meiosis-related genes are very different between human and mouse, there might be some conserved mechanisms of meiosis regulation between the two species.

1.3.3 Meiosis prophase I in mammals

The most remarkable meiotic events are synapsis and recombination. As mentioned in Section 1.3.1, during meiosis prophase I the homologous chromosomes pair and align (synapsis), connect with each other, and exchange genetic material (recombination). The word "synapsis" is derived from Greek word "συναψις" (which means "connection") and was first applied by Moore (1895) over a hundred years ago, to describe the chromosomes' behaviour at meiosis prophase I. Although this

phenomenon had been observed before Moore's research, he is the first scientist who realised the importance of synapsis during the reproductive cycles as it is highly conserved between animals and plants (Moore, 1895).

A lot of research has been performed on synapsis and recombination, and several critical steps and molecules are identified. One of the most important event of synapsis is the formation of synaptonemal complex (SC), which contains two axial lateral elements and a central element (Moses, 1958). In addition, cohesins form the cohesion complex which also contributes to this process by helping sister chromatids adhere to each other (Michaelis *et al.* , 1997). One of the major component of lateral elements is SYCP3 (Lammers *et al.* , 1994) (Dobson *et al.* , 1994), which is first expressed at pre-leptotene (Roig *et al.* , 2004). In human pre-leptotene germ cells, SYCP3 protein appears as aggregates, then becomes distributed as thin threads (loaded into chromosomes) and aggregated clusters at leptotene. These SYCP3 threads continue to condense until pachytene, and finally begin to dissolve at diplotene, at which stage the aggregates disappear (Roig *et al.*, 2004). Loss of *Sycp3* in mice causes male infertility due to germ cell apoptosis and arrested meiosis at zygotene; but germ cell development prior to this stage is not affected (Yuan *et al.* , 2000). Further analysis reveals synapsis abnormalities, with less organised foci of recombination and failed formation of SCs (Yuan *et al.*, 2000). In female mice, Sycp3-deficiency does not lead to complete loss of reproductive capacity, but litter sizes are significantly reduced due to increased embryo death, and aging females have further reduced litter sizes, demonstrating a shortened reproductive lifespan (Yuan *et al.*, 2002). These phenotypes are caused by increased numbers of oocytes with aneuploidy due to disrupted formation of SCs and chiasmata, and abnormal recombination (Yuan *et al.*, 2002). In humans, mutations in *SYCP3* are also associated with infertility phenotypes in both sexes. A 1bp deletion of *SYCP3* has been identified in azoospermic men, which causes a truncated SYCP3 protein and reduced ability of SYCP3 molecules to interact with each other to form threads (Miyamoto *et al.* , 2003). Two other mutations have been identified in women with recurrent miscarriages and no liveborn offspring; one mutation is a four nucleotide deletion and the other is a Single nucleotide polymorphism (SNP) (Bolor *et al.* , 2009). The two patients both have reduced *SYCP3* mRNA expression, and these

mutated SYCP3 proteins also show reduced ability of interaction and forming fibres, and therefore could be a potential factor of human infertility (Bolor *et al.*, 2009).

Another SC component, the central element SYCP1 is expressed later in germ cell development than SYCP3; from zygotene to dioplotene (Roig *et al.*, 2004). The assembling of Sycp1 into the SC is partly affected by the loss of Sycp3, as Sycp1 fibres show fragmented morphology in *Sycp3*-deficient mice compared to wild types (Yuan *et al.*, 2000). In contrast, the cohesin proteins, including Recombination (REC)8, Stromal antigen (STAG)3, Structural maintenance of chromosome (SMC)1β and SMC3 are loaded onto chromatin before SYCP3 pre-leptotene in human germ cells, and their expression completely co-localises with SYCP3 on thickening chromosomes during the rest of prophase I (Garcia-Cruz *et al.* , 2010).

During homologous recombination, to exchange genetic material between maternal and paternal chromosomes, DNA undergoes double strand breaks (DSB) and damage repair. A lot of proteins are involved in this process including Sporulation-deficient recessive mutant (Spo)11 homolog and Dmc1 (Barchi *et al.* , 2005), but one of the most important DSB markers is γ-H2AX, which is associated with DNA repair (Rogakou *et al.* , 1998). H2AX is a member of the histone H2A proteins, and γ-H2AX is its phosphorylated form on residue serine 139 which is a rapid response to DSB (Rogakou *et al.*, 1998). $H2AX^{-/-}$ mice show multiple phenotypes associated with genome instability and DNA repair defects, and the males are sterile due to meiosis arrest at pachytene and germ cell apoptosis; the females are fertile but have reduced litter size (Celeste *et al.* , 2002). In male mice, γ-H2AX expression is almost exclusive to testis; strong γ-H2AX expression is found in primary spermatocytes from pre-leptotene to zygotene, then is only detectable on sex vesicle (the hetero-paired XY chromosomes) during pachytene, indicating that it may play a role during meiosis (Hamer *et al.* , 2003, Mahadevaiah *et al.* , 2001). In human males, γ-H2AX is found in leptotene spermatocytes, then it reduces during zygotene and is restricted to the sex vesicle at pachytene, very similarly to the dynamic changes in mouse, and finally becomes barely detectable at late diplotene (Roig *et al.*, 2004). In human females, γ-H2AX expression is similar to that of male at leptotene and zygotene, except that at pachytene the γ-H2AX foci are still detectable, which

indicates that the de-phosphorylation of H2AX, i.e. the early steps of DNA damage repair progresses much more slowly in human female (Roig *et al.*, 2004).

The phosphorylation of H2AX is known to be regulated by Ataxia Telangiectasia Mutated (ATM), which is a serine/threonine protein kinase (Burma *et al.* , 2001, Keegan *et al.* , 1996). ATM is usually distributed in cell nuclei as an inactivated multimer or dimer, and once DSBs occur, it will auto-phosphorylate on serine residue 1981 (phospho-ATM), which causes the dissociation of dimer to gain the kinase activity (Bakkenist and Kastan, 2003). In response to DNA damage, the activity of ATM rapidly increased without significant change of protein levels, and molecules move to the DSB sites, which co-localise with γ-H2AX (Andegeko *et al.* , 2001). In mouse meiotic germ cells, Atm is found distributed along synapsed chromosomes but is absent at asynapsed sites during zygotene and pachytene in both sexes (Keegan *et al.*, 1996). However, cells isolated from *Atm*$^{-/-}$ mice show dramatically reduced phosphorylation of H2AX in response to irradiation induced DSB when compare to wild type, and this can be rescued by introducing ectopic ATM; the phosphorylation activity on H2AX is also confirmed by *in vitro* study using immunoprecipitated ATM protein (Burma *et al.*, 2001).This demonstrates that that phospho-ATM is activated at least prior to leptotene when γ-H2AX occurs. Targeted disruption of *Atm* kinase domain in mouse causes growth defects, as well as infertility in both sexes due to abnormal synapsis, fragmented chromosome damage and meiosis arrest at zygotene/pachytene (Xu *et al.* , 1996).

Another protein that helps to stabilise the genome during recombination is Testis expressed gene (Tex)19.1 (Ollinger *et al.* , 2008). The mouse has two *Tex19* homologues, *Tex19.1* and *19.2*, and the former is more identical to the single human homologue *TEX19* (Kuntz *et al.* , 2008). Both human *TEX19* and mouse *Tex19.1* are detected in adult testis, and in mouse, the Tex19.1 protein is mainly distributed in the cytoplasm of spermatogonia and early spermatocytes which indicates that it is not directly interacting with the meiotic chromosomes in the nucleus (Kuntz *et al.*, 2008, Ollinger *et al.*, 2008). *Tex19.1*$^{-/-}$ male mice show subfertility phenotypes with no or reduced haploid germ cells, whilst females are still fertile and have no significant ovarian abnormality (Ollinger *et al.*, 2008, Tarabay *et al.* , 2013). Further

investigation suggests that loss of *Tex19.1* causes failed synapsis initiation and germ cell apoptosis from pachytene, which is due to abnormal recombination and DSB repair defects. Four-fold increased expression of retrotransposon MMERVK10C is detected in *Tex19.1*$^{-/-}$ mouse testis, and *in situ* hybridisation indicates that it is mainly distributed in meiotic spermatocytes (Ollinger *et al.*, 2008). The activated retrotransposon element may contribute to non-homologous synapsis between chromosomes and meiotic defects (Bourc'his and Bestor, 2004), and therefore Tex19.1 stabilises genome by repressing the retrotransposons and maintains normal recombination. However, no study on the functions of human TEX19 during germ cell development has been performed so far, and its expression in human ovary remains unknown.

1.4 DAZ family proteins

1.4.1 Introduction

The Deleted in Azoospermia (DAZ) family of proteins include DAZ, DAZL and BOLL. As the family name suggests, its first and characteristic member is *DAZ*, which was first identified by Reijo *et al.* (1995), when the researchers were screening for the azoospermia factor (AZF) on a deleted portion of Y chromosome; the deletion was likely to cause azoospermia in their patients. They also pointed out that DAZ might be an RNA-binding protein by analysing its amino acid sequences, and concluded that it contains an identical RNA recognition motif (RRM) to many RNA- or single-stranded DNA-binding proteins.

A year later, another member of the DAZ family, DAZ-Like (*DAZL*, also called *Dazla*, *Daz like, autosomal*) was identified in mouse (Cooke *et al.* , 1996). Although *BOLL* (*BOULE-LIKE)* is the ancestor of *DAZL* and *DAZ*, and was first identified in *Drosophila* (wherein it is called *boule* (*bol*) by Castrillon *et al.*) in 1993, earlier than the other two members, it was the last one to be confirmed to belong to the DAZ family (Eberhart *et al.*, 1996).

The same group which identified *Dazl* also predicted that *DAZ* probably only existed on the Y chromosomes of primates (Cooke *et al.*, 1996). Subsequent studies

confirmed that *DAZ* is only located on the Y chromosomes of humans, primates and old world monkeys (Saxena *et al.* , 1996), whilst DAZL is expressed in vertebrates, and BOLL in metazoans (Xu *et al.* , 2001). Evolutionally, *BOLL* is the ancestor and *DAZL* is derived from *BOLL* by duplication, then *DAZL* duplicated again to form *DAZ* (Haag, 2001). When Boll was identified in mouse, research compared the protein sequence of mouse Dazl, Boll and human DAZ, and concluded that they all have a highly-conserved RRM, plus a copy (or copies) of the characteristic DAZ repeat motif (Figure 1.2). Further investigation on human DAZ, DAZL and BOLL revealed that human DAZL and DAZ are 50% identical overall, with 82% identity between them in the first (N-terminal) two thirds of the protein including the RRM and DAZ repeat; human DAZL and BOLL are only 30% identical and the N-terminal two thirds of the protein is 37% conserved (Collier *et al.* , 2005). Interestingly, human DAZL and mouse Dazl are overall 88% conserved, which is higher than the conservation between human DAZ and DAZL (Collier *et al.*, 2005).

This literature review is focused on fetal ovary development; therefore, the male-specific Y chromosome gene *DAZ* will not be discussed. *DAZL* and *BOLL* are autosomal genes and involved in reproductive capacity, especially meiosis in both sexes, and will be discussed in detail, covering their expression, function and mRNA targets across species and sexes.

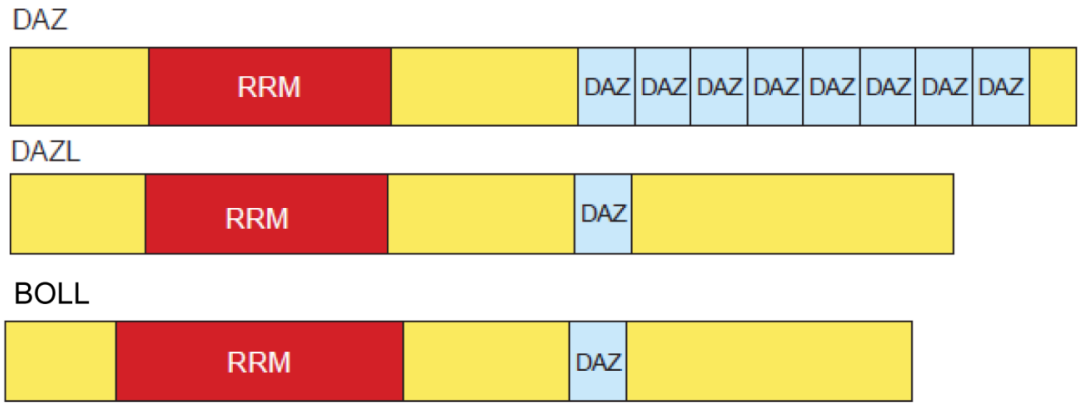

Figure 1. 2 General structures of DAZ family proteins.

All three genes in DAZ family contain an RNA Recognise Motif (RRM), and DAZ repeat. The RRM and DAZ repeat are both highly conserved between the three genes. Both DAZL and BOLL only have a single copy of DAZ repeat, whilst DAZ has 7 to 24 copies (reviewed by Brook *et al.*, 2009).

Image adapted from Brook *et al.*, 2009

1.4.2 Deleted in Azoospermia-Like (DAZL)

1.4.2.1 DAZL functions and co-factors

As an RNA-binding protein, DAZL functions to bind to its mRNA targets and promote their translation, and possibly also increase their stability.

The different functions of DAZL on mRNA regulation are possibly depended on the DAZL co-factors (see Table 1.1). The major co-factors of DAZ family proteins are Poly-A Binding Proteins (PABPs), which exist widely in eukaryotes. As their name suggested, PABPs have RRMs, which bind the 3' poly-A tail of mRNA (Blobel, 1973). Although the functions of PABPs vary, one of their most important roles is to promote translation by recruiting and interacting with translation initiation factors such as Eukaryotic translation initiation factor (eIF)4G (Wells *et al.* , 1998). It is known that the initiation of translation involves both the 5' cap and 3' poly-A tail of mRNA. The formation and degradation of the poly-A tail are called polyadenylation and deadenylation, respectively. Although translation and ribosome binding runs from 5' to 3', a lot of evidence suggests that during translation, mRNA forms a circular structure; the interaction between the 5' cap and 3' poly-A tail (closed-loop model) promotes the translation of mRNA, and PABP/eIF4G interaction is required for this process (reviewed by Kahvejian *et al.*, 2001).

As their name suggests, the binding of PABPs requires a poly-A tail, allowing translation to be activated; however, researchers found that a long poly-A tail is not always necessary for the initiation of translation (Collier *et al.*, 2005). Collier *et al.* (2005) investigated the functions of *Xenopus laevis* (*X. laevis*) *Dazl (Xdazl)*, mouse *Dazl* and human *DAZ*, *DAZL* and *BOLL*, by co-injecting one of these mRNAs which contains *MS2* coding region together with luciferase reporter mRNA which contains MS2 binding sites into *X. laevis* oocytes; all of these co-injections could promote the translation of luciferase, despite variability in their ability to promote translation. They then found that all of the DAZ family proteins tested could interact with PABPs; once the region of Dazl which interacts with PABPs is removed, its ability to stimulate translation is completely lost and therefore PABPs are required for Dazl function (Collier *et al.*, 2005). Further experiments performed with luciferase reporters with or without poly-A tails showed that Dazl could promote the translation

of both reporters, but its effect is much stronger on nonadenylated mRNA (8.5 fold increase) than on adenylated mRNA (2.8 fold) (Collier *et al.*, 2005). Based on these findings, Collier *et al.* (2005) established the classic model of DAZL function (Figure 1.3). In this model, DAZL recognises and binds to its own binding sites in the 3'-Untranslated Region (3'-UTR) of its target mRNA, which have no or only short poly-A tails. DAZL then recruits co-factors such as PABPs, which bind to DAZL rather than the poly-A tail, and promote translation.

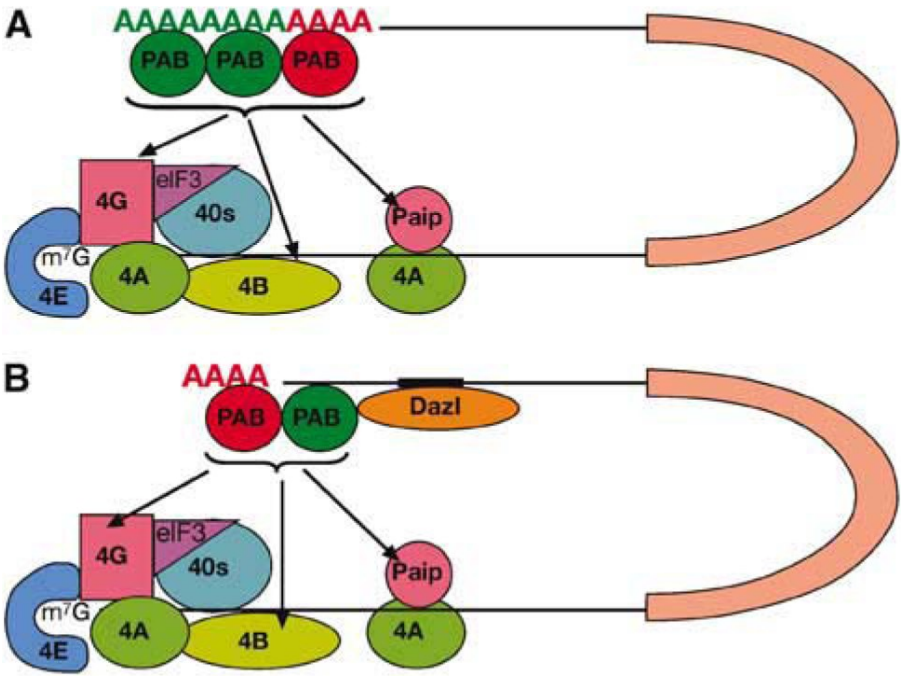

Figure 1. 3 The model of DAZL-PABPs interaction during initiation of mRNA translation.
A) mRNA undergoes 3' polyadenylation and forms a long poly-A tail (Green As) to recruit additional PABPs (Green PAB); (Red PAB) is recruited by short poly-A tail (Red As). PABPs then interacts with its co-factors to form a closed-loop structure to initiate translation. **B)** When DAZL is present, it binds to the 3'-UTR of the mRNA and recruits the additional PABPs (Green PAB) directly; polyadenylation is not necessary and translation is still stimulated. 4A/B/E/G indicate eIF4 factors; 40s, 40s ribosome; Paip, poly-A-binding protein-interacting protein.

Images from Collier *et al.*, 2005

Other DAZL co-factors include DAZ-Associated Proteins (DAZAP1 and DAZAP2). DAZAPs are also RNA-binding proteins but their functions remain unclear (Tsui *et al.* , 2000a). Unlike the binding between DAZL and PABPs through the N-terminal RRM region of DAZL, the interactions between DAZL and DAZAPs are reliant on the DAZ repeat; thus DAZAP can also interact with DAZ (Tsui *et al.*, 2000a). DAZAP1 is mainly expressed in the germ cells of human testis and has two RNA-binding regions which are similar to a protein involved in pre-mRNA processing and nucleus-cytoplasm transport. The authors therefore predicted that DAZAP1 mainly regulates mRNA transport, and together with both DAZL and DAZ it may also regulate translation during spermatogenesis (Tsui *et al.*, 2000a). Later studies suggested that Dazap1 is also expressed in mouse testis, has high sequence identity to its human homologue (over 80%) but is probably not involved in mRNA translation (Dai *et al.* , 2001). In contrast, another group reported that by regulating the phosphorylation of DAZAP, the DAZ-DAZAP complex may be associated with the stability and/or translation of mRNA (Morton *et al.* , 2006).

Another co-factor of DAZL is PUMILIO-2 (PUM2). PUM2 is highly conserved during evolution – the identity between the C-terminal RNA-binding domain of human PUM2 and *Drosophila* pumilio is 80% (Zamore *et al.* , 1997). *Drosophila pumilio* was reported to be required for both embryo and germ cell development (reviewed by Fox *et al.*, 2005). Human PUM2 was found to interact with DAZ, as DAZ could co-precipitate with PUM2 protein when both were expressed in yeast; the interaction between DAZL and PUM2 was confirmed by yeast two-hybrid analysis (Moore *et al.* , 2003). Furthermore, PUM2 is co-expressed with DAZ or DAZL in both human testis and ovary (Moore *et al.*, 2003). Additional evidence was provided by Fox *et al.* (2005), who demonstrated that the binding sites of both DAZL and PUM2 are present on the 3'-UTR of human *Severe Depolymerization of Actin 1* (*SDA1*) *Domain containing* (*SDAD*)*1* mRNA, and therefore *SDAD1* might be regulated by the interaction of DAZL and PUM2. In *Drosophila*, pumilio represses translation by deadenylation (Wreden *et al.* , 1997), and as it is highly conserved with human PUM2, it is possible that the human DAZL/PUM2 interaction also functions as repressing translation.

Table 1. 1 Important DAZL co-factors and their functions

DAZL-interacting protein	Molecular function(s)
PABPs	i) Translation initiation factor ii) mRNA stability and deadenylation iii) Translational repressor iv) Nonsense-mediated mRNA decay
DAZAPs	i) mRNA transport (prediction) ii) Stability and/or translation of mRNA
PUM2	i) Translational repressor of CPE-dependent translation ii) Translational activator of CPE-dependent translation iii) Direct translational repressor

Adapted from Brook *et al.*, 2009

Interestingly, a recent study identified a new splicing isoform of mouse Dazl (Dazl_Δ8), which could repress but not stimulate translation in embryonic stem cells (ESCs) but not germ cells (Xu *et al.* , 2013); the normal form of Dazl also seems to have this effect. Dazl_Δ8 is expressed in both mouse ESCs and germ cells *in vivo* and co-localises with the normal form; after being overexpressed into ESCs, the protein expression of Mouse vasa homolog (Mvh), Oct3/4 and SRY-box containing gene (Sox) 2 all decreased, and luciferase assays with reporter genes carrying the 3'-UTRs of these target genes further confirmed repression of their translation (Xu *et al.*, 2013). This suggests that Dazl may have both stimulatory and repressive effects on translation.

Although the mechanisms remain unclear, there are also studies suggest that zebrafish Dazl (Zdazl) could not only promote the translation of its mRNA targets, but could also increase their stability. Two studies performed on zebrafish revealed such functions on *Tudor domain-containing protein 7* (*Tdrd7*) (Takeda *et al.* , 2009) and *Hu antigen proteins* (*Hu*) *HuB* (Wiszniak *et al.* , 2011). *Tdrd7* is expressed in the germ line of zebrafish and can be degraded by microRNA miR-430 mediated deadenylation, thereby repressing its translation (Mishima *et al.* , 2006). By

co-injecting *Green Fluorescent Protein* (*GFP*) reporter mRNA containing *Tdrd7* 3'-UTR (*Tdrd7-GFP*), negative control reporter mRNA with wild type or mutated *Zdazl* mRNA into one-cell stage zebrafish embryos, it was observed that wild type *Zdazl* specifically increased GFP expression 4.2 fold, and this was also completely repressed by miR-430; once the RRM or DAZ region of *Zdazl* was absent, the enhancement became less significant (Takeda *et al.*, 2009). Further research revealed that Zdazl binding sites indeed existed on the 3'-UTR of *Tdrd7*, and co-injecting *Zdazl* mRNA with A-capped *Tdrd7-GFP* mRNA which could not be translated led to the increased length of poly-A tail, suggesting that Zdazl was promoting polyadenylation without the requirement of translation (Takeda *et al.*, 2009). Furthermore, when the *Tdrd7-GFP* mRNA lacked miR-430 binding site, co-injection of *Zdazl* further increased its poly-A tail (Takeda *et al.*, 2009). Similar experiments were also performed with a *Zdazl-GFP* mRNA reporter, and the study demonstrated that *Zdazl* itself is also a target of miR-430 mediated deadenylation, and it could protect its own mRNA from degradation and increase expression (Takeda *et al.*, 2009). Using the same technique, Wiszniak *et al.* (2011) identified another potential Zdazl target, *HuB*, which is a maternally originated and germ cell specific RNA-binding protein; overexpressing Zdazl could promote the expression of *mCherry* mRNA reporter fused with *HuB* 3'-UTR (*HuB-mCherry*) 3.4 fold compared to expressing the reporter alone, and *in situ* hybridisation indicated that *HuB-mCherry* mRNA was enriched as well (Wiszniak *et al.*, 2011). Although it is still unclear whether Zdazl can promote both the stabilisation and translation of *HuB*, or whether this is also through increased polyadenylation, stabilising its mRNA target seems to be another important function of DAZL and thus it might regulate these targets at post-transcription level rather than only at translation level.

1.4.2.2 DAZL expression and phenotypes in model animals

DAZL expression is mainly detected in the germ lines of vertebrates, and found to play a critical role during meiosis and probably early embryo development. This section will review the expression of Dazl in a wide range of model animals, from

fish, frog to mammals (including mouse, rat, goat, porcine and bovine) and also the phenotypes caused by the mutation/absence of Dazl.

1.4.2.2.1 Fish

In fish, Dazl is detected in many species including zebrafish (Maegawa *et al.* , 1999), medaka (Xu *et al.* , 2007), rainbow trout (Li *et al.* , 2011a) and gibel carp (Peng *et al.* , 2009). Surprisingly, despite zebrafish being widely used as a model animal, *Zdazl* expression during early germ cell development has not been investigated in detail. It is known that *Zdazl* is expressed in the adult gonads of zebrafish in both sexes (Maegawa *et al.*, 1999). *In situ* hybridisation suggests that *Zdazl* transcripts are mainly distributed in the spermatogonia and early spermatocytes in the testis (Maegawa *et al.* , 2002). In stage I oocytes in the ovary, (which are undergoing meiosis before diplotene arrest) (Selman *et al.* , 1993), *Zdazl* is localised near the nucleus; after stage I, meiosis is arrested and *Zdazl* dynamically changes location, moving strictly to the vegetal cortex, (Kosaka *et al.* , 2007). After fertilisation, in early embryogenesis, the maternal *Zdazl* mRNA begins to translocate from vegetal cortex to the embryonic cleavage furrows (Kosaka *et al.*, 2007), and dramatically decreases at late blastula stage (Maegawa *et al.*, 1999).

Studies on rainbow trout (Li *et al.*, 2011a) and medaka (Xu *et al.*, 2007) have provided further detail. In rainbow trout, *Dazl* mRNA is expressed in the gonads of both sexes as well (Li *et al.*, 2011a). In adult trout ovary, *Dazl* expression persists during oogenesis, from undifferentiated oogonia to stage III oocytes, which are just beyond the resumption of meiosis (Selman *et al.*, 1993), and peaks at stage II and III (Li *et al.*, 2011a). In the trout testis, *Dazl* expression is also detectable from the spermatogonial stage, and persists to round spermatids (Li *et al.*, 2011a).

In medaka testis, Dazl expression is detected at both mRNA and protein level in spermatogonia and spermatocytes but in contrast to the rainbow trout, Dazl mRNA is absent from spermatids (Xu *et al.*, 2007). The mRNA expression of *Dazl* in female medaka is more similar to that in rainbow trout – it persists during oogenesis, the highest level is seen in stage II and III oocytes, then deceases at later stages. However, protein expression is slightly different; Dazl protein is more abundant in oogonia and early oocytes (Xu *et al.*, 2007). *Dazl* expression during medaka

embryogenesis has also been investigated by the same group. Similar to zebrafish, maternal *Dazl* expression is detectable from zygote until blastula stage, and interestingly, it also later appears in putative PGCs (Xu *et al.*, 2007).

In gibel carp, Dazl is also expressed by both sexes; Dazl protein is found in PGCs, persists during their proliferation and differentiation, and is continuously expressed in later stages from oogonia to mature oocytes (Peng *et al.*, 2009). As in zebrafish, the translocation of *Dazl* mRNA and protein from adjacent to the nucleus to the vegetal cortex is also observed in later stage I oocytes of gibel carp. After fertilisation, *Dazl* mRNA and protein migrates again to the blastomere, then decreases at early gastrulation (Peng *et al.*, 2009). In males, both *Dazl* mRNA and protein are mainly detected in spermatogonia and spermatocytes, but not in spermatids and spermatozoa (Peng *et al.*, 2009).

Overall, in fish, Dazl shows germ cell/embryogenesis-specific expression. It is inherited maternally from the one-cell embryo stage and persists until gastrulation then decreases; but when putative PGCs differentiate, Dazl is again expressed and continues through the whole of oogenesis but its distribution dynamically changes from perinuclear to vegetal cortex as the oocytes mature. In males, Dazl expression decreases or disappears at the spermatid stage. This suggests that Dazl expression in fish might play important roles during both germ cell development and embryogenesis; the minor inconsistencies between fish species are possibly due to evolution.

1.4.2.2.2 Xenopus

Xdazl was first identified by Houston *et al.* (1998) from a library of *Xenopus* oocytes. Their further investigation reveals that its transcript is firstly detectable in the cytoplasm of oocytes from post-metamorphic froglets; these oocytes are at early diplotene stage, and at later stages *Xdazl* shows a dynamic translocation as seen in the fish as the oocytes mature (see section 1.4.2.2.1), transferred from perinuclear area to the vegetal cortex (Houston *et al.*, 1998). Mita & Yamashita's (2000) showed that Xdazl protein is most abundant in oogonia and very early (pre-vitellogenic, stage

I) oocytes which are undergoing meiosis (Dumont, 1972), but it is not detected (when using immunohistochemistry) in later stage I oocytes, then reappears at stage IV, but it was found to be expressed across all stages of oogenesis by Western blotting (Mita and Yamashita, 2000).

In testis, *Xdazl* is expressed in some spermatogonia but mainly presents in spermatocytes which are undergoing meiosis; spermatids and spermatozoa do not show *Xdazl* expression (Houston *et al.*, 1998). Analysis of Xdazl protein suggests that it is continuously expressed from spermatogonia to spermatids, but undetectable in spermatozoa; secondary spermatogonia and spermatocytes (both primary and secondary) show strong staining (Mita and Yamashita, 2000).

Xdazl mRNA expression is also found in embryos. During embryogenesis, the maternal *Xdazl* localises in germ plasm, which exists in flies, fish and frogs and contains the factors which will pre-determine the germ cells; therefore *Xdazl* expression appears closely related to the formation of putative PGCs, and this is supported by the positive *Xdazl* signals detected in these PGCs (Houston *et al.*, 1998). The Xdazl protein was also found in the germ plasm of embryos from blastulae to early tailbud stage and in PGCs it is only expressed until early tailbud stage and then is soon interrupted afterwards (Houston and King, 2000). Other research, however, suggests that Xdazl protein has an even distribution pattern in the cytoplasm of the early embryo rather than being restricted to the germ plasm, and disappears after gastrulation; it is then re-expressed in post-migration PGCs (Mita and Yamashita, 2000).

By silencing maternal *Xdazl* mRNA (with injected antisense oligodeoxynucleotides), researchers were able to study the function of *Xdazl* during early germ cell development in *Xenopus*. They found that despite the formation of PGCs being normal, the number of PGCs which are located at the dorsal mesentery during migration is largely reduced or completely absent, and two out of three ovaries lacked germ cells (Houston and King, 2000). Further study revealed that the PGCs failed to move from ventral endoderm into the dorsal mesentery; and these phenotypes could be rescued in some cases by injecting extra *Xdazl* mRNA into these embryos (Houston and King, 2000). This suggests that in *Xenopus*, maternal *Xdazl* is

essential for PGC differentiation and migration, but not for the formation of putative PGCs.

1.4.2.2.3 Rodents

Mouse *Dazl*, which is located on chromosome 17, was first identified Cooke *et al*. in 1996. *Dazl* transcripts were examined in a range of different tissues and found to be expressed specifically in the gonads of both sexes; and was undetectable in testes without germ cells, which suggests that expression is germ cell-specific (Cooke *et al.*, 1996, Seligman and Page, 1998). With northern blotting, further investigation suggests that in mouse fetal gonads, *Dazl* transcripts are detectable from e11.5 when germ cells settle in the gonads but prior to sex differentiation (Seligman and Page, 1998). *Dazl* expression then increases at e13.5 and e14.5, which is coincident with the initiation of meiosis in the female (Seligman and Page, 1998). After that *Dazl* expression decreases to half of its peak level at e16.5. In the female, *Dazl* is barely detectable by puberty, probably as a consequence of the loss of oocytes, whilst in the male its expression level is 100-fold higher than that in female (Seligman and Page, 1998).

Studies which generated anti-Dazl antibodies and applied immunohistochemistry to investigate its protein expression further confirmed that mouse Dazl is likely to be exclusively expressed in germ cells (Reijo *et al.* , 2000) .Weak staining in granulosa cells of developing follicles in pre-pubertal ovary has also been reported (Ruggiu *et al.*, 1997); this might be due to cross-reaction as it has not been reported by other studies. In mouse testis, Dazl protein is found in gonocytes, spermatogonia and spermatocytes, and most abundantly in pachytene spermatocytes (Reijo *et al.*, 2000, Ruggiu *et al.*, 1997). In the female, Dazl is detected in the cytoplasm of germ cells in fetal and pre-pubertal ovaries, and also in the peripheral cytoplasmic area of oocytes in follicles of adult mouse (Ruggiu *et al.*, 1997). Before the first division of the 1-cell embryo, Dazl protein expression is up-regulated during the maturation of oocytes until Metaphase II (MII) and the zygote stage, by recruiting the *Dazl* mRNA to polysomes without a change in overall level of transcripts. Strong cytoplasmic Dazl expression is also present in pre-implantation embryos from the 2-cell stage; the

latest known expression period is the blastocyst (Pan *et al.* , 2008). Both the granulosa and embryo Dazl expression challenge the theory of specific Dazl expression in germ cells, however without any additional evidence provided by other studies and methods, it is unclear whether the weak Dazl signal in granulosa cells is genuine or a cross-reaction. Despite *Dazl* being found in pre-implantation embryos, it is possible that this expression is maternal, inherited from egg. Therefore, this thesis will discuss Dazl expression in terms of it being germ cell specific.

The translation of *Dazl* is initially promoted by Cytoplasmic Polyadenylation Element Binding protein (CPEB) which is important for cytoplasmic polyadenylation, but positive feedback is also involved (Chen *et al.* , 2011). Dazl knock down by morpholino oligonucleotides results in delayed resumption of meiosis during oocyte maturation; the phenotypes include fewer oocytes completing meiosis I and defects at MII transition. Both phenotypes could be rescued by injecting human *DAZL* mRNA or protein, but the rescue is only partial for the latter (Chen *et al.*, 2011).

A translocation from nucleus to cytoplasm of Dazl protein during spermatogenesis was reported in male mice. In fetal gonocytes, Dazl shows both nuclear and cytoplasmic expression, then is mainly detected in the nucleus in spermatogonia, and finally becomes cytoplasm specific in spermatocytes, which is consistent with entry into meiosis (Reijo *et al.*, 2000). This translocation is also observed in the testis of primates, including human and marmoset (Reijo *et al.*, 2000, Ruggiu *et al.* , 2000) (See Section 1.4.2.3).

In the rat, Dazl protein is also germ cell-specific, and its most abundant pachytene expression in testis is conserved with that of mouse (Ruggiu *et al.*, 2000); the up-regulated timing at pachytene was demonstrated as well (Rocchietti-March *et al.* , 2000). Interestingly, the nuclear to cytoplasmic translocation of Dazl is not observed in rat; it is consistently localised to the cytoplasm from the gonocyte to the spermatocyte stage (Ruggiu *et al.*, 2000).

Dazl is essential for mouse germ cell development. Indeed, the *Dazl*-deficient phenotype has been investigated in great detail in mouse. Ruggiu *et al.* (1997)

generated the *Dazl*-deficient (*Dazl*$^{Tm1Hgu/Tm1Hgu}$) mouse on an outbred background, and found that these mice were infertile, with severe, almost complete germ cell loss by six to eight weeks after birth in both sexes. This is due to increased germ cell apoptosis which initiates in fetal life, possibly at e19.5. At e15.5 however, the germ cells in fetal gonads are still undistinguishable from those in WT mice, with meiosis initiated and reaching pachytene in ovaries. The heterozygote (*Dazl*$^{Tm1Hug/+}$) mice are fertile, but display a higher ratio of abnormal sperm when compared to the wildtype controls(Ruggiu *et al.*, 1997).

Further investigation based on the same strain of *Dazl*-deficient mice suggests that in the female, germ cell loss actually begins from e17.5 and all the germ cells are depleted by day 4 after birth (Saunders *et al.* , 2003). Interestingly, the heterozygous female mice with reduced *Dazl* expression seemed to have larger litter sizes, possibly resulting from an increased number of antral follicles (McNeilly *et al.* , 2011). Furthermore, these follicles had a larger area of granulosa cells were more sensitive to follicle-stimulating hormone (FSH) (McNeilly *et al.*, 2011). Ovaries with a complete loss of Dazl and follicle structures are still able to produce normal level of estrogen, very likely by the presence of surviving steroidogenic cells, but increased FSH and decreased inhibin levels are detected in plasma of heterozygotes (McNeilly *et al.* , 2000).

In *Dazl*-deficient males, during the first wave of spermatogenesis (day 2 to 19 after birth), germ cell loss begins from day 7 onwards, and they already show abnormalities (such as multinucleated germ cells) as early as at day 2 and 4 (Saunders *et al.*, 2003). The germ cells in the testes of *Dazl*-deficient mice show delayed meiotic entry at day 9 when most in WT are at pre-leptotene, and spermatogenesis in *Dazl*-deficient mice finally arrests when the germ cells enter meiosis, and rarely progresses beyond leptotene (Saunders *et al.*, 2003). Another study suggests that the most advanced germ cell type present in *Dazl*^{Tm1Hgu}/*Dazl*^{Tm1Hgu} mice is pachytene spermatocytes, and most germ cells in the testis of *Dazl*-deficient mice are actively mitotically dividing type A spermatogonia, which display impaired differentiation (Schrans-Stassen *et al.* , 2001). Comparison of the gene expression profile of *Dazl*$^{Tm1Hgu/Tm1Hgu}$ mouse testis to those of wild type

littermates indicated reduced expression of genes involved in germ cell development, including the genes associated with advanced spermatogonial development, entry into meiosis and meiosis prophase I (leptotene to pachytene) (Maratou *et al.* , 2004). Some genes involved in spermatogonia development and embryonic testis are also found strongly associated with ovary development. Although meiosis is initiated in the *Dazl* null mouse, the effect of losing Dazl on gene expression begins as early as day 5 after birth, when the only germ cell type in the testes are type A spermatogonia (Maratou *et al.*, 2004).

By backcrossing the *Dazl*$^{Tm1Hgu/Tm1Hgu}$ mice onto a C57BL/6 mouse strain, Lin & Page (2005) established a strain of inbred *Dazl*-deficient mice on the C57BL/6 genetic background. Instead of maintaining germ cells until after birth, male inbred *Dazl*$^{Tm1Hgu/Tm1Hgu}$ mice were born with almost no germ cells due to increased apoptosis (Lin and Page, 2005). At e13.5, there were no major differences in germ cell number or morphology between WT and *Dazl*$^{Tm1Hgu/Tm1Hgu}$. However from e14.5, more apoptotic germ cells occurred in the inbred *Dazl*$^{Tm1Hgu/Tm1Hgu}$ mice and the surviving germ cells maintained condensed chromatin like those in early e12.5-e13.5 gonads, whilst those of WT testes had a more diffuse appearance (Lin and Page, 2005). Germ cell apoptosis continued at e15.5, and by e17.5 most germ cells in the *Dazl*-null gonads are lost. The gene expression profile revealed by *in situ* hybridisation suggests that the mRNA level of several germ cell-specific genes, such as *Mvh*, *Stella* and *Oct4* are slightly decreased at e13.5, and further reduced at e15.5; Mvh and GCNA protein expression are also decreased at e14.5 and e15.5, respectively (Lin and Page, 2005).

Human *DAZ* and *DAZL* transgenes could partly rescue the *Dazl*$^{Tm1Hgu/Tm1Hgu}$ phenotypes in murine testis (Slee *et al.* , 1999, Vogel *et al.* , 2002). Both transgenes could significantly increase the number of surviving germ cells, and promote the differentiation from spermatogonia to primary spermatocytes (i.e. rescue the dysregulated initiation of meiosis), but this was still not sufficient to restore the fertility of *Dazl*$^{Tm1Hgu/Tm1Hgu}$ mice. The difference is that the human *DAZ* but not the *DAZL* transgene significantly increased the number of spermatocytes that reached pachytene stage, and meiosis in *DAZL* transgene mice still showed

leptotene/zygotene arrest as in *Dazl*$^{Tm1Hgu/Tm1Hgu}$ mice (Slee *et al.*, 1999, Vogel *et al.*, 2002). This reveals the both conservation and differences between mouse Dazl and human DAZ/DAZL. Notably, human *DAZL* transgene did not show any rescue effect on *Dazl* deficient phenotypes in female mice (Vogel *et al.*, 2002), this may imply that even in the same species, Dazl functions may not be completely conserved between male and female during gametogenesis.

Recently, Dazl has been found to be involved in the maintenance or repression of pluripotency in mouse PGC and/or ES cells. In female *Dazl*-deficient mice, expression of the early germ cell markers *Oct3/4*, *Stella* and *c-Kit* is down-regulated, and embryonic germ cell lines (pluripotent derivatives of PGCs) cannot be established using germ cells from *Dazl*-deficient fetal gonads. The efficiency of *in vitro* differentiation from *Dazl*-null ES cells to germ cells is also reduced, and these cells show lower expression of pluripotency markers and higher expression of pro-apoptotic markers when compared with wild type or heterozygotes (Haston *et al.* , 2009). A splicing variant of *Dazl* (*Dazl_Δ8*) seems to repress the translation of *Mvh* and *Oct4* in mouse ES cells but not in germ cells (Xu *et al.*, 2013), implying that Dazl may play different roles in ES and germ cells. A recent paper also suggests that Dazl represses pluripotency in PGC-like cells by suppressing the translation of related genes *Sox2* and *Sal-like 4* (*Sall4*), but in contrast with two previous papers, the expression of Oct4 is unaffected; moreover, Dazl also seems to repress the expression of apoptosis-associated genes *Caspase 2*, *7* and *9* (Chen *et al.* , 2014).

Besides the post-transcriptional regulation of mRNA targets, Dazl may also be associated with transport of mRNA. Lee *et al.* (2006) reported that in male germ cells, Dazl could interact with the light chain of dynein (Dlc), which is part of the dynein-dynactin motor complex. The two proteins could be co-precipitated with each other when using either antibodies. Dazl may gain the ability of moving through microtubule network, allowing it to bind with and transport its mRNA targets, including *Testis specific protein-1* (*Tpx1)*, *Cdc25C* (via 5'-UTR) and *Mvh*. mRNA transportation by Dazl is also relevant to the formation of stress granules, cytoplasmic particles which contain abundant messenger ribonucleoproteins and which cells use to limit their translation by storing RNAs when subjected to cellular

stress. When treated with the toxin arsenite which can induce the stress granule, most Dazl protein translocates into stress granules (Lee *et al.*, 2006). This translocation is confirmed by another study which demonstrated that Dazl was also involved in the formation of stress granules under heat stress in mouse male germ cells. This protects these cells from heat-induced apoptosis by storing specific signalling molecules and blocking the apoptotic pathway (Kim *et al.* , 2012).

To summarise, increased *Dazl* expression at e13.5, most abundant expression at pachytene in both mouse and rat, and meiosis arrest phenotypes in $Dazl^{Tm1Hgu/Tm1Hgu}$ outbred mice indicates that Dazl may play an important role at meiosis entry and prophase I, although its increased expression at e13.5 occurs in both sexes rather than being female specific implies that it may not be completely meiosis associated. In addition, Dazl is also involved in germ cell differentiation and stress protection. Its expression in pre-implantation embryos implies that Dazl may be necessary during the process of early embryo development, and the loss of germ cell phenotypes, especially prior to meiosis in inbred mice, suggests that Dazl is an important contributor to germ cell survival.

However, it is necessary to point out that most of this research was focused on male reproduction. Although Dazl is known to be continuously expressed in the germ cells of mouse ovary from fetal life to adulthood (Ruggiu *et al.*, 1997), where it seems to regulate the maturation of follicles by modulating their sensitivity to FSH (McNeilly *et al.*, 2011), Dazl expression or phenotypes in female mouse are far less clearly described. Therefore, how Dazl regulates mouse oogenesis is yet to be investigated in depth.

1.4.2.3 Human DAZL expression, mutation and phenotypes

The human homologue of *DAZL* was first identified by Saxena *et al.* (1996) from an adult human testis cDNA library, and originally named "*DAZH* (DAZ Homologue)". It is located on chromosome 3 and was confirmed to be expressed at a lower level in adult human ovary than testes, and not expressed in any other tissues examined. *DAZL* expression has been widely investigated and was found in human gonads

(Anderson *et al.*, 2007, Dorfman *et al.* , 1999, Moore *et al.*, 2003, Reijo *et al.*, 2000, Ruggiu *et al.*, 2000, Tung *et al.* , 2006a, Xu *et al.*, 2001), pre-implantation embryos and inner cell mass (ICM) (Cauffman *et al.* , 2005), undifferentiated embryonic stem (ES) cells (Clark *et al.* , 2004), and potentially, in corpus luteum (Pan *et al.* , 2009).

DAZL expression in human testis has been reported in several studies. In the adult, the protein occurs almost through all the stages of spermatogenesis, including spermatogonia, early and late spermatocytes, spermatids and it was also found in mature spermatozoa (Lin *et al.* , 2001, Moore *et al.*, 2003, Reijo *et al.*, 2000, Ruggiu *et al.*, 2000, Tung *et al.*, 2006a, Xu *et al.*, 2001). In fetal testis, DAZL was also expressed at first and second trimester at both mRNA and protein level; its mRNA slightly increased at second trimester, and its protein seemed to be mainly distributed in the nucleus of gonocytes, with no or weak cytoplasmic expression (Anderson *et al.*, 2007, Reijo *et al.*, 2000, Ruggiu *et al.*, 2000). Interestingly, two groups reported at almost the same time that both human and mouse Dazl show a dynamic distribution from nucleus to cytoplasm during differentiation (Reijo *et al.*, 2000, Ruggiu *et al.*, 2000), although their conclusions are slightly different. According to Reijo *et al.* (2000), DAZL is expressed in both nucleus and cytoplasm in gonocytes, then in nucleus and part of cytoplasm in spermatogonia, and finally becomes cytoplasmic-specific in both spermatocytes and spermatids; however Ruggiu *et al.* (2000) reported that DAZL is already completely transferred to the cytoplasm by the spermatogonia stage, and not found in any other germ cell types later than spermatocytes. The former finding is supported by Moore *et al.* (2003) and Xu *et al.* (2001)'s research, which also suggests that human DAZL is expressed in not only spermatogonia and spermatocytes, but also in post-meiotic germ cells in testis, whilst Lin *et al.* (2001) found that DAZL is only expressed in spermatogonia and spermatocytes in adult testes.

In the human ovary, DAZL is also expressed from the fetal period at both mRNA and protein level, and *DAZL* mRNA levels increase significantly (20 fold) in the second trimester when compared to that in the first trimester (Anderson *et al.*, 2007). DAZL protein showed weak staining during first trimester as in fetal testis, but in second trimester, it becomes very clear and is mainly distributed in the cytoplasm of meiotic

germ cells (Anderson *et al.*, 2007, Dorfman *et al.*, 1999). DAZL shows limited co-localisation with OCT4, and partly co-localises with VASA. In addition, after measuring the nuclear diameters, an indicator of germ cell maturation, Anderson *et al.* (2007) found that DAZL/VASA co-expressed germ cells have bigger nuclei than DAZL single-positive cells, but they are smaller than VASA single-positive cells, implying that DAZL might be absent in more mature germ cells in human fetal ovary. Dorfman *et al.* (1999) looked at the DAZL protein expression in 19 week gestation fetus and adult (37 and 44 years old) ovaries, and found that expression occurred in oogonia, primary and secondary follicles, and is most intense in the cytoplasm of developing oocytes; consistently, Moore *et al.* (2003) also found that DAZL is expressed in the cytoplasm of oocytes in adult ovary. Furthermore, *DAZL* transcript expression in mature (from Germinal Vesicle (GV) to MII) oocytes is reported by Cauffman *et al.* (2005). The nuclear to cytoplasmic translocation of DAZL in female has not been reported by these previous researches due to the lacking of studies on human fetal ovaries, however it is possible that this transfer is conserved between male and female in both primates and mouse.

Although DAZL expression is believed to be germ cell-specific, it also appears in several other kinds of tissues/cells. As it is expressed in oocytes, it is not a surprise that DAZL also appears in zygotes and early embryos. Cauffman *et al.* (2005) investigated *DAZL* mRNA expression in human oocytes, zygotes and pre-implantation embryos, and found that *DAZL* transcripts are detectable in almost all oocytes, zygotes and 4-cell embryos they examined with only one exception. Surprisingly, although *DAZL* is expressed by only about 52% of 5-8 cell embryos, it soon recovered to its previous level (100% of embryos) in 9-13 cell embryos, implying a transition from maternal to embryonic expression (Cauffman *et al.*, 2005). The same research group also found that *DAZL* expression seems to be associated with the quality of embryos; all the *DAZL* negative blastocysts were marked as not suitable for transfer during *in vitro* fertilisation (IVF), and the *DAZL* mRNA levels between suitable and unsuitable embryo groups show significant differences (Cauffman *et al.*, 2005). In separated ICM and trophectoderm (TE) from blastocysts using mechanical techniques, *DAZL* is detectable in both kinds of embryos which are marked as best quality (Cauffman *et al.*, 2005). Interestingly,

DAZL was undetectable in most ICM cells when separated by immunosurgery (Clark *et al.*, 2004). In addition, *DAZL* mRNA is also found endogenously in several human ES cell lines (both XX and XY) and their spontaneous early-differentiated colonies as well as embryoid bodies (EBs) (Cauffman *et al.*, 2005, Clark *et al.*, 2004). Together, embryonic *DAZL* expression may imply that it plays a role in differentiation in early embryos.

Other research has reported that DAZL protein is expressed in the human corpus luteum and interacts with CDC25A as a transcription factor (Pan *et al.*, 2009). However, these observations are only based on the co-immunoprecipitation with anti-CDC25A or DAZL antibodies using human corpus samples, without applying any RT-PCR or immunostaining against DAZL. Therefore, this claim still needs more evidence to support it.

In humans, the relationship between DAZL expression/mutations and reproductive capacity has been investigated. A study based on a male population in Taiwan found that *DAZL* mRNA levels were lower (but not significantly so) in patients with hypospermatogenesis compared with patients with normal spermatogenesis, although the protein was still expressed in spermatogonia and spermatocytes (Lin *et al.*, 2001). These data do not however clarify the relationship between DAZL and normal spermatogenesis. Based on the same population, Teng *et al.* (2012) identified three SNPs in the *DAZL* promoter, and one of them (-792G→A) seemed to affect the binding of transcription factor Nuclear respiratory factor 1 (NRF-1) and interrupt interactions with other transcriptional factors such as SP1. Importantly, this SNP was negatively associated with sperm quality, including concentration and motility. As the methylation of the *Dazl* promoter has been reported to be a negative regulator of its expression in pigs, possibly by affecting Specificity protein 1 (Sp1) binding (Linher *et al.* , 2009), it might be that the -792G→A base change involves a similar pathway. The abnormal methylation of *DAZL* promoter and associated phenotypes have also been reported by two other studies (Li *et al.* , 2013a, Navarro-Costa *et al.* , 2010). Moderate or severe hypermethylation is only detected in patients with spermatogenic defects (Li *et al.*, 2013a). Using similar methods, Navarro-Costa *et al.* (2010) compared the *DAZL* methylation between the sperm of normozoospermic

(NZ) and oligoasthenoteratozoospermic (OAT) men. They found that the frequency of non-methylation was lower in defective sperm from NZ men, and was decreased in those with OAT. Therefore, it is clear that abnormal high *DAZL* methylation in human sperm is associated with spermatogenesis defects.

Mutations of *DAZL* have also been identified and associated with human reproductive parameters (Tung *et al.*, 2006b, Tung *et al.*, 2006c). Seven SNPs, one of which located on exon 2 whilst others are on the DAZL 3'-UTR, are found associated with different reproductive phenotypes (Tung *et al.*, 2006b). Interestingly, all seven SNPs seem to be associated with male reproductive capacity by increasing both the total sperm count and total motile count, however three of them are negatively associated with female parameters, including earlier age of ovarian failure/menopause and promoting premature ovarian failure. This may indicate important roles in the establishment of the primordial follicle pool. This also implies complex DAZL functions in both sexes, and according to the authors, this may due to either *DAZL* mRNA stabilisation/translation by different factors, or the differences in translation initiation complexes involving DAZL between male and female (Tung *et al.*, 2006b). In addition, four missense *DAZL* mutations are also identified; their positions and relative phenotypes are listed in Table 1.2 (Tung *et al.*, 2006c). None of these mutations were found in fertile controls, which strongly suggests that they are associated with subfertility phenotypes.

Table 1. 2 Human DAZL polymorphisms and phenotypes

Exon	Change		Occurrence	
		Sex	Genotype	Phenotype
2	Pro6→His6	Female	Heterozygous	Spontaneous early menopause at age 45. 3 children previously
2	Asn10→Cys10	Male	Homozygous	Azoospermia
		Female	Heterozygous	Familial early menopause at age 44. 4 children previously
2	Ile37→Ala37	Female	Heterozygous	Spontaneous early menopause at age 43. 1 child previously.
5	Arg115→Gly115	Female	Homozygous	Spontaneous premature ovarian failure at age 34. 0 children previously.

Adapted from Tung et al., 2006c

Beside *in vivo* research, *in vitro* experiments also reveal the key DAZL function of promoting germ cell differentiation. DAZL is expressed in undifferentiated human ES cells at both mRNA and protein levels along with several other pre-meiotic germ cell markers, this may indicate either a similar molecular programme between germ and ES cells, or that ES cells spontaneously tend to differentiate into germ cells (Clark *et al.*, 2004). Under differentiation conditions, DAZL expression decreases and ES cells begin to express the germ cell marker *VASA* and meiosis marker *SYCP1;* however they also express both post-meiotic marker *GDF9* (female-specific) and *Tektin1* (*TEKT1*) (male-specific), no matter whether they are originally XX or XY (Clark *et al.*, 2004). A later attempt at deriving human germ cells from ES cells was performed by Medrano *et al.* (2012), who overexpressed *VASA* and/or *DAZL* in human ES or induced pluripotent stem cells (iPSCs), and found that although VASA alone could promote germline formation and meiosis progression, the best efficiency for driving meiosis occurred following *DAZL* overexpression, (based on detection of the morphology of SYCP3 staining (elongated) and the number of haploid cells), whilst the combination of *VASA* and *DAZL* overexpression slightly decreased this effect. The function of DAZL in promoting primordial germ cell differentiation and meiosis from human ES cells was further confirmed by Kee *et al.* (2009). Again they induced primordial germ cells from ES cells using *VASA-GFP* overexpression, and then silenced *DAZL* expression with short hairpin RNA (shRNA) in these cells. The number of VASA-GFP positive cells dramatically decreased to about 50% after the silencing of *DAZL*, and this could be rescued by overexpressing *DAZL*. By observing the elongation of SYCP3, they also found that DAZL and BOLL show similar ability of promoting meiosis in XX cell lines, but DAZ is also necessary for the same progress in XY cell lines. By overexpressing DAZL, BOLL and DAZ together, haploid cells are also formed from 2% of these ES cells, and they express mature

sperm marker Acrosin (ACR). Together, these results suggest that DAZL functions to both promote germ cell differentiation and meiotic progression.

To summarise here, DAZL expression is found in both human germ cells and early embryos, and it is associated with both male and female subfertility phenotypes. It may function in two aspects, i.e. regulating pluripotency/differentiation, and promoting meiosis progression. However, the mechanism underlying these modulations remains largely unknown, and one of the keys of understanding DAZL function is to identify its mRNA targets.

1.4.2.4 RNA binding capacity and potential targets of DAZL

Although DAZL shows multiple functions during germ cell and early embryonic development, the number of potential DAZL mRNA targets identified so far is very limited.

The basis of identifying DAZL target mRNAs is to investigate its binding sites, by testing the binding specificity between DAZL protein/RRM with particular RNA sequences. Houston *et al.* (1998) first characterised the binding motif of potential Xdazl targets using homopolymeric RNA, and demonstrated that Xdazl tends to recognise poly-U and poly-G RNA and therefore is likely to bind U or G rich sequences *in vivo*. This finding was extended by Tsui *et al.* (2000b), who first tested the binding capacity of human/mouse Dazl and human DAZ to RNA, and found that their binding to poly-U is more stable than to poly-G; further investigation using partly deleted DAZL protein constructs suggests that the RRM is the key region to recognise the poly-U motif whilst the DAZ repeat may be relevant to poly G binding, and therefore the RRM is mainly responsible for RNA binding. The study further looked at the subcellular distribution of Dazl *in vivo*; after separating an extract of

mouse testis into nuclear, mitochondrial and postmitochondrial fractions, Dazl mainly occurred in the postmitochondrial supernatant (over 75%), most of which co-migrated with the polysomes; RNase treatment disassociated these polysomes and significantly reduced the Dazl component in the postmitochondrial supernatant (Tsui *et al.*, 2000b). Together with the detection of Dazl in endogenous poly-A ribonucleoprotein (RNP) particles, the evidence pointed to the conclusion that Dazl is associated with activated translational regulation through poly-U binding (Tsui *et al.*, 2000b). Further advances were made by Jiao *et al.* (2002), who first screened the common recognition motif of Dazl and clearly identified several potential targets. By co-precipitating RNP with Dazl from mouse testis extract, they identified *Tpx1*, *Peptidylglycine alpha-amidating monooxygenase* (*Pam*), *Telomeric repeat binding factor 2* (*Trf2*), G-rich RNA sequence binding factor 1 (*Grsf1*), *Proteosomeα7/C8 subunit* (*Pα7/C8*) and *Histocompatability antigen precursor 47* (*H47*) as potential targets and found they all share a 26-nucleotide region in their 3'-UTRs (as follows):

$$\begin{matrix} UA & & C & & U & & & & & & & & G & & U & G \\ AG & UU & U & AGUA & A & AANAACUUU & & & & & GAA & A & U & A & A \end{matrix}$$

Each single nucleotide in this sequence appears at least four times in the aforementioned target genes and two nucleotides which share a common position appears at least three times. N means any nucleotide.

This 26-nucleotide sequence was named the Dazl-binding site (DBS) and was further confirmed by generating appropriate oligonucleotides and binding them with Dazl (Jiao *et al.*, 2002). In addition, this research also found that *Cdc25A*, a homologue of the fly bol target *twine* could bind Dazl as well, but its homologue gene *Cdc25C* could not (Jiao *et al.*, 2002). However, other research reached the opposite conclusion - Venables *et al.* (2001) identified *Cdc25C* as a potential Dazl target by *in*

vitro binding assay, and binding was abolished when four mutations were introduced into the Dazl RRM. Interestingly, although Dazl is believed to regulate its mRNA targets through the 3'-UTR, the Dazl binding sites of *Cdc25C* are located on the 5'-UTR (Venables *et al.*, 2001). A more precise Dazl binding motif was described by this research as well; compared to Tsui *et al.* (2000b)'s broad poly-U and poly-G rich theory, the range was further narrowed down to extreme U-rich sequences interrupted by G, with binding slightly weakened when G is replaced by C, or was further weakened but still not completely quenched if replaced by A. Therefore, the Dazl binding motif is most likely to be $(G/CU_n)_n$ (Venables *et al.*, 2001).

A year later, the recognition motif of Zdazl was also reported, although different from that of mammals; the common binding sequence of Zdazl is GUUC (Maegawa *et al.*, 2002). The sufficiency of recognising GUUC by Zdazl was confirmed by binding assays performed using mutated RNA probes (Maegawa *et al.*, 2002). The GUUC motif is also found on the 3'-UTR of fly *twine*, and when it was conjugated with luciferase vector and co-transfected with *Zdazl* in monkey kidney cell CV1, luciferase activity was increased but this effect would disappear once GUUC motifs were removed (Maegawa *et al.*, 2002). In addition, GUUC was also identified in the 3'-UTR of *Zdazl* mRNA itself, thus *Zdazl* mRNA translation is enhanced by its own protein (Maegawa *et al.*, 2002).Auto-regulation of *Dazl* mRNA translation by Dazl protein was later found to occur in mouse as well (Chen *et al.*, 2011). Further investigation indicated that multiple binding sites are also important for enhanced translation, as one or two copies of GUUC on an artificial 3'-UTR was not sufficient to stimulate significantly increased luciferase activity (Maegawa *et al.*, 2002). The importance of the RRM domain of Zdazl was also investigated: by introducing a F91A mutation into the RRM, the RNA binding capacity of Zdazl was completely lost, whilst it was unaffected if the DAZ motif was deleted (Maegawa *et al.*, 2002). Therefore in Zdazl, as with mouse Dazl, RNA recognition and binding is through the

RRM, and the DAZ repeat is thought to be required for translation activation via polysome binding (Maegawa *et al.*, 2002).

Beside *Zdazl* itself, two additional Zdazl targets were also identified in zebrafish. *Tdrd7*, (which is expressed in zebrafish PGCs) is down-regulated by microRNA miR-430, (Takeda *et al.*, 2009), and Zdazl inhibits the microRNA-mediated repression and activate the expression of *Tdrd7* by stabilising its mRNA, possibly by inducing polyadenylation at the same time, which is consistent with Collier *et al.* (2005). Both the GUUC and GUUA elements were found on the 3'-UTR of *Tdrd7*, and when mutated (GU→CA) in the 3'-UTR attached to a GFP reporter gene, the stimulation effect is lost (Takeda *et al.*, 2009). *Zdazl* is also a target of miR-430, and can protect its own mRNA from degradation and stimulate protein expression (Takeda *et al.*, 2009). A similar protective effect of Zdazl on *HuB*, another germ cell-specific maker that is expressed maternally, was also investigated (Wiszniak *et al.*, 2011). 3'-UTR-mediated degradation of *HuB* was detected in differentiated somatic cells during embryo development, however both the mRNA and protein levels of an mCherry reporter fused to the *HuB* 3'-UTR were increased in somatic cells overexpressing Zdazl (Wiszniak *et al.*, 2011). The F91A mutation of Dazl (Maegawa *et al.*, 2002), which leads to loss of RNA-binding capacity, prevented this effect (Wiszniak *et al.*, 2011). Therefore, Zdazl may function to both stabilise *HuB* and/or stimulate its translation. In contrast to *Tdrd7*, the defined GUUC motif is not found on the 3'-UTR of *HuB*, instead a 30-nucleotide sequence may act as the Zdazl recognition site (Wiszniak *et al.*, 2011).

In mammals however, the sequence $(G/CU_n)_n$ has been confirmed as a DAZL binding site by several studies, and a lot of potential mRNA targets have been identified, mostly in rodents. Reynolds *et al.* (2005) isolated several potential Dazl mRNA targets in both rat and mouse using co-immunoprecipitation and microarrays,

and identified the *Mvh* as a definitive Dazl target. Almost all the potential Dazl targets contain the $(G/CU_n)_n$ motif, or be more accurate, U(2-10)[G/C]U(2-10), and five putative binding sites were found in the 3'-UTR of *Mvh* (Reynolds *et al.*, 2005). Binding of Dazl to the *Mvh* 3'-UTR was completely abolished when all the five sites were mutated (Reynolds *et al.*, 2005). Injecting *Xenopus* oocytes with *Dazl*-encoding RNA, followed by injection of RNA encoding a luciferase reporter gene fused to the *Mvh* 3'-UTR confirmed that Dazl enhances *Mvh* translation (Reynolds *et al.*, 2005). In addition, the similar phenotypes (meiosis arrest around leptotene/zygotene) observed between *Dazl* and *Mvh* null mice, and the low level of Mvh protein in the testes of Dazl-deficient mice, also provide further evidence that *Mvh* translation is stimulated by Dazl (Reynolds *et al.*, 2005).

Sycp3 was also identified as a Dazl target (Reynolds *et al.*, 2007). Both mouse and rat *Sycp3* contain the U(2-10)[G/C]U(2-10) motif in their 3'-UTRs, and direct binding of Dazl RRM to mouse *Sycp3* 3'-UTR was confirmed (Reynolds *et al.*, 2007). Furthermore, Dazl could also stimulate the translation of luciferase reporter conjugated to the *Sycp3* 3'-UTR, and mutation of the binding sequence ablated the increase in luciferase activity (Reynolds *et al.*, 2007). The relationship between Dazl and *Sycp3* was also investigated *in vivo*; by crossing C57BL/6 *Dazl* heterozygote mice to CD1 $Dazl^{+/+}$ mice and then intercrossing the offspring, to recapitulate the original *Dazl*-deficient mice that were generated on an outbred background (Reynolds *et al.*, 2007, Ruggiu *et al.*, 1997). The male mice displayed meiosis arrest at leptotene/zygotene at 7 days after birth, and the protein level of Sycp3 decreased to between 11 and 55 percent of that in wild type mice, suggesting that Dazl stimulates, but is not essential for, the translation of *Sycp3 in vivo* (Reynolds *et al.*, 2007). In addition, Dazl is also necessary for RA-induced *Stra8* expression, and other meiosis markers *Dmc1*, *Spo11*, *Sycp3* and *Rec8* all decreased in Dazl knockout mice (Lin *et al.*, 2008), although a direct RNA-protein interaction for these mRNAs has

not been proven (except for *Sycp3*). Although not investigated in the same depth as *Mvh* and *Sycp3*, mouse *Tex19.1*, *Testis-specific serine kinase* (*Tssk*)*1*, *2* and *4* are also reported to be potential mRNA targets of Dazl (Zeng *et al.*, 2008, Zeng *et al.*, 2009). These mRNAs all contain the U(2-10)[G/C]U(2-10) binding sites on their 3'-UTR and are found to be bound directly by Dazl. Surprisingly, the translation of *Tex19.1* seems to be repressed, rather than increased, by Dazl when *Dazl* and luciferase reporter fused with *Tex19.1* 3'-UTR are co-injected into zebrafish embryo (Zeng *et al.*, 2009).

Beside *Tex19.1*, a repression function of Dazl on its mRNA targets has recently been reported in mouse by several groups, and is mainly related to roles in stem cell pluripotency and/or differentiation (Chen *et al.*, 2014, Xu *et al.*, 2013). As discussed in Section 1.4.2.1 and 1.4.2.2.3, one study identified a new mouse Dazl variant Dazl_Δ8, and suggests that it down regulates the translation of *Mvh*, *Oct3/4* and *Sox2* in mouse embryonic stem cells (Xu *et al.*, 2013). This research is extended by a recent report, which investigated Dazl function in both ES cell- derived PGC-like cells and PGCs *in vivo* (Chen *et al.*, 2014). During the differentiation of ES cells, Dazl expression initially declines, but then increases again at later stages, accompanied with dynamic expression changes of stage-specific germ cell markers, and is consistent with the gene expression pattern during germ cell development *in vivo* (Chen *et al.*, 2014). Cytoplasmic granular Dazl expression was also observed, which is consistent with Xu *et al.* (2013)'s study as well (Chen *et al.*, 2014).

Several new co-factors of Dazl, i.e. Insulin-like growth factor 2 mRNA binding protein 1 (IGF2BP1), Fragile X mental retardation protein (FMRP), Fragile X mental retardation (FXR)1 and 2) were identified and co-localised with Dazl granules, and FMRP is known as a translation inhibitor (Chen *et al.*, 2014). Using RIP and microarrays, 120 potential Dazl targets with proper Dazl binding sites were

identified, among which *Sox2*, *Sall4*, *Suppressor of zeste 12 homolog* (*Suz12*), *Zinc finger protein 42* (*Zfp42*) and *Zic family member of the cerebellum 3* (*Zic3*) are involved in the maintenance of pluripotency, and Sox2, Sall4 and Suz12 proteins are expressed in the gonads of Dazl-deficient mice whilst they are absent in wild type mice, consistent with a failure of these germ cells to differentiate. In addition, the translation of apoptosis-associate genes *Caspase2*, *7* and *9* are also down-regulated by Dazl in fetal mice gonads, suggesting that Dazl may also act to prevent apoptosis (Chen *et al.*, 2014). However, the function of Dazl in limiting pluripotency is partly challenged by another report, which indicated that loss of Dazl in fetal male gonads resulted in reduced expression of pluripotency markers such as *Nanos2* and *3*, *Pum2*, *Stella* and *Oct4* whereas the opposite was true in females (Haston *et al.*, 2009). The reportedly reduced *Sycp3* expression is consistent with previous study however, and Sycp3 protein alignment, i.e. proper loading on chromosomes, is also affected by *Dazl* knockout (Haston *et al.*, 2009).

Another candidate Dazl target is *Tpx2*, identified by Chen *et al.* (2011). It contains multiple Dazl binding sites and co-precipitated with Dazl protein from oocyte lysate. When Dazl is knocked down in oocytes, the activity of luciferase reporter fused with 3'-UTR of *Tpx2* also significantly decreased, suggesting that *Tpx2* translation is directly up-regulated by Dazl binding to its 3'-UTR (Chen *et al.*, 2011).

Far fewer potential DAZL target mRNAs have been identified in humans, but the regulation of *VASA* and *SYCP3* by DAZL seems to be conserved between humans and mice (Kee *et al.*, 2009), although more evidence is needed. In differentiating human ES cells, the percentage of VASA-positive cells is significantly reduced when *DAZL* is silenced by shRNA, and could be rescued by overexpressing *DAZL*. The percentage of cells showing properly-elongated SYCP3 is also increased by overexpressed DAZL in both XX and XY ES cells, suggesting that SYCP3 could be

a human DAZL target as well (Kee *et al.*, 2009). However, direct binding between these two targets and human DAZL has not been confirmed so far. Using yeast three-hybrid assay, *SDAD1* was shown to be bounds by with DAZL and its co-factor PUM2 through its 3'-UTR, but the effect of DAZL on *SDAD1* mRNA translation remains unknown (Fox *et al.*, 2005). Similarly, human *TSSK1*, *2*, *4* and *5* are also reported to be bound by DAZL through their 3'-UTRs but no further investigation was performed so far (Zeng *et al.*, 2008).

The binding site of DAZL was also investigated on molecular basis by studying the crystal structure of RRM from Dazl, the GUU triplet were reported as the sufficient RNA recognise motif, and again the RRM of DAZL alone is confirmed to be responsible for RNA-binding by kinked and extended β strands (Jenkins *et al.* , 2011). This study also provided the molecular explanation of the aforementioned Arg115→Gly115 mutation in humans which is associated with premature ovarian failure and sterility (Tung *et al.*, 2006c), as the Arg115 directly contacts with the U_3 in GUU triplet and therefore the mutation leads to severe 50-fold weaker RNA-protein interaction when compared to wild type. It also confirmed direct binding between Dazl and *Mvh* or *Sycp3*, and pointed out that multiple Dazl molecules could bind to several copies of GUU in a single RNA (Jenkins *et al.*, 2011).

In conclusion, DAZL mRNA targets are identified in a range of species, and cover both germ cell development and differentiation. DAZL not only stimulates translation, but also could increase mRNA stability or repress translation. However, only *Mvh* and *Sycp3* have been confirmed to be Dazl targets *in vivo* so far with sufficient evidence, and all the other targets identified so far, especially those in human, are still putative. Furthermore, the novel repression and mRNA stabilisation functions of Dazl have only been identified in mouse and zebrafish respectively, and

are yet to be confirmed with more evidence and expanded to more species. It is also worth pointing out that most of this work has only been performed in males, and despite Dazl-deficient female animals and humans displaying various subfertility phenotypes, little is known about Dazl's role(s) during oogenesis. Therefore, to understand how DAZL functions during germ cell development, it is important to identify human DAZL targets, especially in females, and find out how they are modulated as well.

1.4.3 BOLL

1.4.3.1 BOLL functions and Co-factors

Despite being the ancestor and the first member identified in DAZ family, studies on BOLL are very limited when compared with DAZL.

Like DAZL, BOLL also interacts with proteins from PABP family, although this interaction was only confirmed by yeast two-hybrid assay using the C-terminus of PABP1 (Collier *et al.*, 2005). The stimulation of translation by human BOLL was also confirmed by tethered luciferase assay (Collier *et al.*, 2005). Another common co-factor of DAZL and BOLL is PUM2, which can interact with BOLL homodimers in a two-hybrid yeast assay (Urano *et al.* , 2005). However, the mechanism of BOLL-PUM2 interaction seems to be different from the DAZL-PUM2, and BOLL-PUM2 cannot bind with the 3'-UTR of *SDAD1*, which is a potential mRNA target of DAZL-PUM2 complex (Urano *et al.*, 2005).

In *C. elegans*, cpb-3 was identified as a co-factor of boll *in vivo* as well, because they are partly co-expressed in the gonads, and can be co-precipitated with each other from worm extracts when performing immunoprecipitation using antibodies to either protein (Hasegawa *et al.* , 2006).

Because of the lack of research, the mode of BOLL action is still unknown; however, as it also interacts with PABP1 and stimulates translation, it is possible that BOLL functions through a similar pathway as DAZL (See section 1.4.1 and Figure 1.3).

1.4.3.2 BOLL expression, functions and phenotypes in model animals

Although not as widely investigated as DAZL, BOLL expression has been described in various model animals including *Drosophila*, worms, fish, mouse, goats and cows.

The association between *bol* and infertility was first identified in *Drosophila* in 1993, by globally generating and screening gene mutations which cause male sterility (Castrillon *et al.*, 1993). The genes identified were associated with defects of different stages during germ cell development, and *bol* was categorised as a meiotic entry defect, as meiosis did not occur and germ cells formed abnormal multi-nucleated cells, or contained various sizes of nuclei (Castrillon *et al.*, 1993). The nebenkern, a special mitochondrial structure in insect male germ cells also became abnormally large, which all pointed to abnormal nuclear division accompanied by lack of cytokinesis (Castrillon *et al.*, 1993). Therefore, *bol* seems to be necessary for spermatogenesis in *Drosophila*. Further investigation revealed that *bol* is only expressed in the germ cells of male flies, and indeed, bol-deficient females are still fertile (Eberhart *et al.*, 1996). Despite their spermatocytes being normal, flies with either decreased *bol* expression or truncated *bol* transcripts (3.0kb to 1.1kb) display similar spermatogenesis defects, including no entry of meiosis, arrest at meiotic prophase or completely loss of germ cells (Eberhart *et al.*, 1996), and this could be partially rescued (increased meiotic and post-meiotic germ cells) by germline transformation with a human *BOLL* expression vector (Xu *et al.* , 2003). The meiosis defects are caused by abnormal behaviour of a cell cycle-related protein Cyclin A, which is degraded in the nuclei of wild type germ cells soon after the

G2/M transition, but persists in those of *bol* mutants. Subsequently, the centrosomes failed to reach the poles, and both separation of chromosomes and nuclear division stopped, causing meiosis arrest before metaphase (Eberhart *et al.*, 1996). With 42% conservation, the human *BOLL* transgene could also partly rescue the phenotypes of *Drosophila bol* mutation, and the morphology of germ cells is undisguisable with that of germ cells rescued with fly *bol*; however, neither of the transgenes successfully restored fertility. Further analysis suggests that 11 genes which show reduced expression in *bol* mutants are restored by both transgenes, including the potential bol target *twine* (Xu *et al.*, 2003) (see Section 1.4.3.4).

In contrast to the exclusive expression in germline of other animals, *Drosophila bol* was also found expressed endogenously in neurons during metamorphosis, and seems to act as a negative factor of axon pruning. However, this was only observed when *bol* is overexpressed in neurons, and loss of *bol* did not show any obvious effect and therefore it might be redundant rather than necessary during this process (Hoopfer *et al.* , 2008).

boll null-mutation in *C. elegans* also shows a sex-biased phenotype but only in hermaphrodites rather than in males, and the sperm produced by hermaphrodites is not affected. No oocytes were found in the gonads of *boll*-deficient hermaphrodites, therefore, boll in *C. elegans* is crucial for oogenesis (Karashima *et al.* , 2000). Further examination suggests that pre-meiotic mitosis is normal, but meiosis is arrested at pachytene in female germ cells in *boll* mutant worms, with mitotic-like small nuclei, and cell death by apoptosis (Karashima *et al.*, 2000). The defects seen in *boll* mutants partially overlap with those caused by *cpb-3* mutation, which includes deficient oogenesis and pachytene arrest, and as they show partial co-localisation *in vivo*, the two proteins may share similar functions or act together at specific stages of oogenesis (Hasegawa *et al.*, 2006). The female-specific function of

worm *boll* was confirmed using mutant feminised or masculinised hermaphrodites; loss of *boll* resulted in no mature oocytes being formed but normal spermatogenesis in these two mutants respectively (Karashima *et al.*, 2000). Consistent with its pachytene arrest phenotype, *C.elegans boll* transcripts show dynamic expression changes during germ cell development; expression commences prior to meiosis, accumulates at the mitosis to meiosis transition and is most abundant at pachytene, before being dramatically down-regulated in mature oocytes (Karashima *et al.*, 2000).

boll expression and phenotypes were also investigated in flatworm (*Macrostomum lignano*), a less popular model animal (Kuales *et al.* , 2011). Three different splice variants (*Macrostomum lignano boll* (*Macbol*) *1*, *2* and *3*) were identified, all containing a conserved RRM and a DAZ repeat. Both *Macbol1* and *2* are expressed in the male germline, in primary spermatocytes or secondary spermatocytes/spermatids respectively (Kuales *et al.*, 2011). Knockdown of *Macbol1* with RNAi caused increased size of the testes but an absence of mature sperm, due to degenerated primary spermatocytes at later stages (Kuales *et al.*, 2011). Oogenesis and the morphology of spermatogonia and early spermatocytes are unaffected (Kuales *et al.*, 2011). Knockdown of *Macbol2* had no effect on gametogenesis. Interestingly, like human and *Drosophila boll*, *Macbol1* could also partially rescue the *boll*-mutant phenotypes in flies, although the rescued animals are still sterile and produce sperm with abnormally-shaped nuclei (Kuales *et al.*, 2011). *Macbol3* is expressed in oocytes and developing eggs, but not in oogonia or early oocytes. Knockdown of *Macbol3* resulted in disrupted egg maturation and sterility, but early oogenesis, including meiosis seemed to be unaffected (Kuales *et al.*, 2011). This is distinct from the *Macbol1* phenotypes in male germline and meiosis arrest phenotypes in flies and *C.elegans*.

boll expression has also been described in fish, namely rainbow trout and medaka (Li *et al.*, 2011a, Xu *et al.* , 2009). In rainbow trout, *boll* is expressed in the germ cells of both sexes. In female, it is expressed by differentiating oogonia just prior to meiosis, increases at meiosis and then decreases (Li *et al.*, 2011a). It also shows dynamic distribution at different stages of oogenesis (Li *et al.*, 2011a). In oogonia, it forms small particles around the nucleus, then is distributed evenly in small oocytes, but forms condensed patches later and re-disperses again shortly afterwards (Li *et al.*, 2011a). In contrast, during spermatogenesis *boll* expression peaks at the spermatogonia stage and is barely detectable in spermatids (Li *et al.*, 2011a). Notably, although *boll* is co-expressed with *dazl* in same oocyte, they are distributed in different regions, which is consistent with Xu *et al.* (2009)'s finding in medaka. In males, *dazl* and *boll* mRNA show different expression patterns – *boll* is distributed evenly whilst *dazl* forms speckles (Xu *et al.*, 2009). In medaka, *boll* is also expressed in both sexes (Xu *et al.*, 2009) . However, unlike the male rainbow trout, *boll* expression is most abundant in meiotic spermatocytes, and it shows a distinct spatial-temporal distribution compared to *dazl*, which is most abundant in spermatogonia, decreases in spermatocytes and is undetectable in spermatids (Xu *et al.*, 2009). In female medaka, *boll* expression persists from pre-meiotic stage, is weak in oogonia and peaks at early meiosis, and is distributed differently from *dazl* transcripts as described before (Xu *et al.*, 2009). In addition, *boll* is also detectable in early medaka embryos, which implies maternal origin and later becomes exclusively expressed in migrating and post-migrat ory PGCs (Xu *et al.*, 2009). However, the phenotypes associated with *boll*-deficiency have not been investigated in fish so far; therefore its relationship with *dazl* and functions during germ cell development remain unknown.

In the mouse, *Boll* is highly expressed in adult testis but not in ovary, although low levels of transcript are detectable in fetal ovaries (Shah *et al.* , 2010), and Xu *et al.*

(2001) predicted that it is probably not expressed at protein level in the ovary. Boll protein is undetectable in PGCs or spermatogonia, but occurs in the cytoplasm of spermatocytes and is expressed through meiosis, most abundantly at late pachytene or diplotene and persists until the spermatid stage (Xu *et al.*, 2001). A *Boll*-mutant (lacking the RRM) outbred mice strain was generated to study its function, and it again shows a sex-specific phenotype - only the *Boll* mutant male mice are sterile, whilst female are fertile with no significant difference of litter size with wild type or heterozygotes (VanGompel and Xu, 2010). The male mice do not produce elongating spermatids or mature sperm, and this seems to result from a block during spermatogenesis, which is comparable with the *Drosophila bol* phenotype (Shah *et al.*, 2010). However, in-depth studies reveal that the block does not occur at meiosis but is post-meiotic (VanGompel and Xu, 2010). Meiosis progresses normally in the *Boll*-mutant mouse testis when checked with either morphology of germ cells or meiosis markers (Sycp3, Replication protein A (RPA) and MutL homolog (MLH)) staining, and the abnormality happens at the round spermatid stage (VanGompel and Xu, 2010). Most round spermatids do not mature but form multinuclear giant cells (cysts) and then enter apoptosis (VanGompel and Xu, 2010). This phenotype is not associated with any significant expression change of known spermatogenesis factors and therefore may indicate that Boll is regulating the maturation of round spermatids through a novel, unknown pathway (VanGompel and Xu, 2010).

Finally, Boll expression has also been studied in large mammals such as goat and cow (Li *et al.* , 2013b, Zhang *et al.* , 2009). In goat, *Boll* is detected at a very low level before and during puberty, and is highly expressed in germ cells of adult testis at both mRNA and protein levels (Li *et al.*, 2013b). It also shows low or no expression in the testes of animals with azoospermia (Li *et al.*, 2013b). Although the *Boll*-null phenotype has not been investigated in goat, overexpression of *Boll* in male germ stem cells (mGSCs) leads to increased expression of several germ cell or

meiosis markers, including *Stra8*, *Sycp3*, *Cdc25a*, *Cdc2* and *Vasa*, suggesting that Boll may promote meiosis in male goats (Li *et al.*, 2013b). Similarly, bovine *Boll* is also highly expressed in the adult testis, and is low or undetectable in testis with spermatogenesis defects such as in cattle-yaks (Zhang *et al.*, 2009).

To conclude, Boll expression and phenotypes strongly indicate that it is associated with germ cell development, but is sex-biased and related to different stages of gametogenesis depending on species.

1.4.3.3 BOLL expression and human subfertility

The expression pattern of BOLL in human gonads and its relationship with subfertility phenotypes have been widely studied, but almost only in males.

Xu *et al.* (2001) first investigated human *BOLL* in detail, and found that it is located on Chromosome 2. In human testis, BOLL is expressed at both mRNA and protein levels, and seems to be undetectable in ovary using Northern blotting (Xu *et al.*, 2001). An anti-BOLL antibody was also generated, and it reveals that BOLL protein is expressed from the pachytene spermatocyte stage, peaks at late pachytene and persists during meiosis until the early spermatid stage in human adult testis, similar to the pattern seen in mice (Xu *et al.*, 2001). However, another study suggests that BOLL protein is expressed from leptotene, peaks at pachytene and begins to reduce at diplotene, finally disappearing in round and elongating spermatids (Luetjens *et al.*, 2004). Consistent with this study, research on human and primates testes suggests that BOLL protein expression is restricted to the germ cells at first meiotic division, begins at zygotene and peaks at pachytene; but this pattern varies in five primate species, from restricted pachytene expression to persistent post-meiotic expression in round spermatids (Tung *et al.*, 2006a). Again, this is confirmed by Kostova *et al.*

(2007)'s study, which suggests that BOLL protein is only expressed during meiosis I and is most abundant at pachytene. This expression pattern is different from that of DAZ or DAZL, which are abundant in both the nuclei and cytoplasm of spermatogonia, as well as in the cytoplasm of meiotic spermatocytes (Xu *et al.*, 2001).

As in flatworms, three kinds of *BOLL* variants namely *B1*, *B2* and *B3* are also identified in human due to different splicing of exon 1, and are expressed in the normal testes roughly at the relative ratio of 80:220:1 (Kostova *et al.*, 2007). The levels of all three in patients with meiosis arrest show a shifted ratio of *B1:B2:B3* to 209:190:1, in another word, increased *B1* ratio is negatively related with successful meiosis; therefore *B2* may be most important whilst *B1* may have negative regulatory functions in spermatogenesis (Kostova *et al.*, 2007). Several other studies also correlated BOLL expression to male reproductive phenotypes. Luetjens *et al.* (2004) found that *BOLL* mRNA is completely missing in the testes of 18 patients with complete meiosis arrest despite spermatocytes being present, and decreased *BOLL* expression is found in twelve patients with mixed atrophy (display variable levels of spermatogenic damage in tubules). Although three additional patients had germ cells more advanced than spermatocytes, *BOLL* expression was still absent in their testes (Luetjens *et al.*, 2004). In two other studies, *BOLL* expression has been tested for predicting the success of sperm retrieval in patients with spermatogenic failure using testicular sperm extraction (Lin *et al.* , 2005) (Kleiman *et al.* , 2011). One of the studies suggests that the threshold level of *BOLL* to distinguish the success or failure of sperm retrieval is 0.5 relative to *GAPDH* with a 100% specificity and sensitivity, and it may also represent the lowest level of *BOLL* required for the completion of meiosis (Lin *et al.*, 2005). Other research investigated the potential of both *BOLL* and *Chromodomain protein, Y-linked 1* (*CDY1*) for prediction of the retrieval of sperm. Despite the increased level of *BOLL* transcripts again are found to be an

effective measure of whether sperm retrieval will be successful, it is less sensitive when compared with *CDY1*, and the latter alone is sufficient for prediction (Kleiman *et al.*, 2011).

In conclusion, human BOLL is expressed mainly during the first division of meiosis and most abundant at pachytene, and its transcription level is positively correlated with the production of mature sperm. Although the mechanism is unknown, based on its expression period and ability of promoting G2/M transition in *bol*-mutant flies (Xu *et al.*, 2003), human BOLL is most likely to be crucial for spermatogenesis and play a role during meiosis prophase I, especially at G2/M transition and pachytene. However, although Shah *et al.* (2010) reported that *Boll* mRNA is expressed in mouse ovary, all the research has been based on the male, which is probably due to the prediction that it is not translated in the ovary (Xu *et al.*, 2001). Indeed, BOLL shows sex-biased expression and phenotypes in model animals. Therefore considering its comparable expression between human and mouse, it is still possible that human *BOLL* mRNA is expressed during fetal life in the ovary as well.

1.4.3.4 Potential targets of BOLL

The recognition motif of BOLL has not been investigated so far, and therefore it is difficult to identify its potential mRNA targets. However, when investigating the DAZL binding motif, Jenkins *et al.* (2011) mentioned that despite BOLL not being able to absolutely recognise the GUU triplet sequence in mRNAs that DAZL does, the conservation of β strand structures may indicated that the mode of RNA recognition is conserved between DAZ family proteins. A study on zebrafish also suggests that the Zdazl could bind to the potential boll target *twine* (see below), and the Zdazl binding motif GUUC is also found on the 3'-UTR of *twine* (Maegawa *et*

al., 2002). This possibly indicates that DAZL and BOLL share some common recognition sequences, and therefore possibly share mRNA targets.

As early as the *Drosophila bol* phenotypes were defined in 1996, Eberhart *et al.* (1996) already realised that these phenotypes are identical to those of *twine* mutations, a homologue of mammal *CDC25* phosphatase which is required for meiosis initiation. Disruption of *twine* causes failure of entry into meiosis (Castrillon *et al.*, 1993), and a single nucleotide mutated *twine* allele twe^{Z0758} leads to arrest after the first meiosis division in male *Drosophila* (Maines and Wasserman, 1999). The phenotype of the latter mutation was caused by reduced transcription of *twine*, and homozygous twe^{Z0758} flies with only one copy of *bol* failed to enter meiosis, identical to flies with complete loss of *bol* or *twine* (Maines and Wasserman, 1999). It was possible therefore that *twine* was regulated by bol. Consistent with this, the expression of a *twine* reporter gene was found to be decreased in *bol* mutant flies, and *twine* expression independent of bol was sufficient to rescue the meiosis initiation phenotype in *bol*-mutant *Drosophila*, both further suggest that bol regulates the translation of *twine* (Maines and Wasserman, 1999).

In humans, *CDC25A* has been reported to be regulated by BOLL (Lin *et al.* , 2009). *CDC25A* mRNA is co-precipitated using anti-BOLL antibodies from extracts of BOLL transfected HeLa cells (Lin *et al.*, 2009), and it is detected using RT-PCR with primers against 3'-UTR of *CDC25A*, which suggests that BOLL directly binds with the 3'-UTR of *CDC25A* (Lin *et al.*, 2009). A 21-nucleotide sequence (AGGUGUAGGUGGGUUUUUCUU), which is conserved among vertebrates, appears responsible for the RNA recognition by BOLL, as it alone is sufficient to form a RNA-protein complex with BOLL (Lin *et al.*, 2009). Mutation of this motif from UUUUU to CCCCC reduces the binding efficiency, suggesting that the U-rich region is necessary for BOLL recognition and binding (Lin *et al.*, 2009). Whilst

co-transfecting *BOLL* with luciferase reporter fused with *CDC25A* 3'-UTR in HeLa cells results in increased luciferase activity (indicating increased translation of the reporter mRNA), the *CDC25A* mRNA level is unaffected after BOLL transfection (Lin *et al.*, 2009). This effect disappears if the 21-nucleotide recognition sequence is absent in the reporter mRNA, suggests that BOLL is stimulating the translation of *CDC25A* through its 3'-UTR (Lin *et al.*, 2009). *In vivo*, CDC25A is first expressed in the cytoplasm just prior to metaphase of meiosis I and persists until spermatid elongation, which partly overlaps with BOLL expression (Lin *et al.*, 2009). In patients with spermatogenic failure, both BOLL and CDC25A protein levels are decreased, due to reduced number of spermatocytes (Lin *et al.*, 2009). CDC25A protein is also undetectable in men with complete meiosis arrest accompanied by absence of BOLL (Luetjens *et al.*, 2004), suggesting that *CDC25A* is possibly regulated by BOLL in human testes.

Besides *CDC25A*, *Stra8* has also been identified as a potential Boll target mRNA in goat (Li *et al.*, 2013b). Both mRNA and protein levels of a luciferase reporter conjugated with goat *Stra8* 3'-UTR are up-regulated after co-transfected with *Boll* in goat mGSCs, and this is likely a direct regulation (Li *et al.*, 2013b). In addition, both Boll and Stra8 protein expression could be promoted by RA treatment in *Boll*-transfected goat mGSCs (Li *et al.*, 2013b), again implying that Boll is functionally-associated with meiosis.

Finally, although it remains unclear whether BOLL is expressed in the human ovary, it is worth mentioning that BOLL can regulate VASA expression in human XX but not XY ES-derived PCG-like cells (Kee *et al.*, 2009). Silencing of *BOLL* does not significantly decrease the number of VASA-GFP positive cells, but overexpressing *BOLL* strongly promoted the number of these cells (Kee *et al.*, 2009). Similarly, BOLL could also promote the elongation of SYCP3 during synaptonemal complex

formation in germ cells derived from both XX and XY cells (Kee *et al.*, 2009). Therefore, *VASA* and *SYCP3* also could be regulated by BOLL, and BOLL might have distinct functions and be important during human oogenesis as well as spermatogenesis. In this case, it is necessary to find whether BOLL is expressed during oogenesis in the human ovary, especially during fetal life, and investigate how it regulates meiosis by looking for its potential mRNA targets.

1.5 Aims of PhD

The critical stages of human oogenesis - germ cell differentiation and entry of meiosis - occur during fetal life. Compared to the extensive studies performed on human testis, knowledge of how this process is regulated in the ovary remains limited.

The DAZ family RNA-binding proteins (DAZ, DAZL and BOLL) are crucial regulators of germ cell development and meiosis. As *DAZ* is Y-linked, only DAZL and BOLL may play a role during human oogenesis. Although DAZL is known to be expressed in the human fetal ovary, whether BOLL is expressed is unclear. DAZL mutations are associated with subfertility phenotypes and reproductive parameters in both sexes, including premature ovarian failure, early menopause, azoospermia and (motile) sperm count, although the mechanisms underlying these are unknown. Our understanding of DAZL and BOLL functions is restricted by the lack of identified human DAZL/BOLL mRNA targets, although some have been identified in mice and other model organisms. Therefore, to understand how DAZL and BOLL regulate germ cell development in the human fetal ovary, it is necessary to determine their expression patterns, and identify the target mRNAs they regulate.

Based on the information above, I propose the following hypotheses:

1. DAZL and BOLL show different expression patterns during human oogenesis, and these expression patterns may reflect distinct roles for these proteins in regulating this process.
2. DAZL plays a critical role in regulating human oogenesis by controlling the translation of mRNAs encoding key proteins involved in germ cell development.

The work in this thesis aimed to test these hypotheses, by addressing the following specific research questions:

1. **Where and when are DAZL and BOLL expressed in the human fetal ovary, and what is the relationship between their expression patterns?**

As BOLL protein expression in the testis peaks at pachytene, it is likely to appear in the fetal ovary during the early stages of meiosis prophase I if it is expressed in the females, but little is known about its expression in the female fetus. DAZL is known be to expressed in the human fetal ovary, but the relationship between DAZL expression, BOLL expression, and germ cell development remains unclear. Thus, the first aim of this thesis is to address hypothesis 1 above, by to establishing a detailed expression profile for DAZL and BOLL in the human fetal ovary to reveal their possible functions during oogenesis.

2. **What are the mRNA targets of human DAZL and BOLL?**

DAZL and BOLL are RNA-binding proteins, which modulate germ cell development by regulating the translation, and potentially the stability of their mRNA targets. Therefore, to understand the functions of DAZL and BOLL, identifying their mRNA targets is essential. Although some mRNA targets have been identified in model organisms, and *Dazl* and *Boll* mutant phenotypes likely arise from dysregulated target

mRNA expression/translation, no definitive mRNA targets have been identified in humans except *CDC25A*. Thus, the second aim of this thesis is to address hypothesis 2 above, by establishing whether putative mRNA targets of DAZL and BOLL that have previously been identified in mice are regulated by human DAZL or BOLL, and to determine whether they are subjected to translational regulation by these proteins.

Chapter 2

General Materials and Methods

Chapter 2 General Materials and Methods

2.1 Cloning and transformation

2.1.1 Preparation of LB agar dishes and broth

Luria Bertani (LB) agar plates were prepared by dissolving one pack of LB Agar EZMix Powder (Sigma-Aldrich, Dorset, UK) in 500ml dH_2O, and autoclaving. Autoclaved agar was melted in a microwave oven, and allowed to cool to 55°C before the addition of antibiotics (ampicillin (Sigma-Aldrich; final concentration of 100μg/ml) or kanamycin (Sigma-Aldrich; final concentration of 25μg/ml – both from 1000× stocks diluted in dH_2O and filter sterilized using 0.22μm membrane filter (Millipore, Watford, UK) and stored at -20°C)). To prepare LB agar plates, LB agar containing antibiotics was poured into 10cm dishes (about 20-25ml per dish (Greiner-BioOne)), left for 5-10min to solidify, then stored upside down at 4°C for up to 1 month. Before culture, the dishes were warmed at 37°C, with lids opened upside down for 30min to remove excess water.

LB broth was made from the LB Broth powder (Sigma-Aldrich) by dissolving 20g LB Broth powder in 1L dH_2O which was then sterilized by autoclaving. Antibiotics were added as required at the concentrations detailed above.

2.1.2 Transformation of competent *E.coli*

To amplify vectors, DH5α *Escherichia coli* (*E. coli;* Library Efficiency DH5α Competent Cells (Invitrogen, Paisley, UK) or NEB 5-α Competent *E. coli* (High Efficiency; New England Biolabs, Herts, UK) were used for transformation. 10ng plasmid DNA was mixed with 50μl competent *E. coli* and incubated on ice for 30min, followed by heat shock at 37°C for 1min, or at 42°C for 40 seconds (s). The *E. coli* were then incubated on ice for 2min, mixed with LB broth (no antibiotics) to achieve final volume of 1ml and cultured at 37°C, 200 revolutions per minute (rpm) in a 1.5ml eppendorf tube. After 45min, 100μl of the culture was spread onto a 10cm LB agar plate, and the remaining 900μl centrifuged at 5000rpm for 3min, the supernatant discarded and the pellet resuspended in 100μl LB broth and spread onto a 10cm LB agar plate (to achieve final seeding densities of $1/10^{th}$ and $9/10^{th}$). Both plates were

stood face up for 5min to allow the liquid to be absorbed before being incubated at 37°C overnight inverted.

2.2 Plasmid DNA Extraction

2.2.1 Mini-preparation of plasmid DNA from bacteria (mini-prep)

Individual *E. coli* colonies were picked and inoculated into 5ml LB broth containing antibiotics in a 50ml polypropylene tube (Greiner Bio-One, Stonehouse, UK), and incubated at 37°C, with shaking at 220rpm overnight. For mini-preps, the High Pure Plasmid Isolation Kit (Roche Applied Sciences, West Sussex, UK) was used as per the manufacturer's instructions. 3-5ml of the bacterial culture was centrifuged at 5000rpm for 3min, the supernatant discarded, and the pellet resuspended in 250µl Suspension Buffer (2.5mg RNase A added into 25ml buffer and stored at 4°C before use). 1 volume of Lysis Buffer was added and mixed gently by pipetting. After 5min incubation at room temperature, 350µl ice-cold Binding Buffer was added to the lysate and mixed vigorously by shaking, followed by 5min incubation on ice. The lysate was then centrifuged at maximum speed for 10min and the supernatant transferred to a High Pure filter tube. The column was then centrifuged at maximum speed for 1min to remove the excess liquid, and then washed by adding 700µl Wash Buffer II to the column and spinning at 13000g for 1min. The column was finally placed in a nuclease-free 1.5ml eppendorf tube, and the plasmid DNA eluted by adding 100µl dH_2O to the column and centrifuging at 13000*g* for 1min.

2.2.2 Maxi-preparation of plasmid DNA from bacteria (Maxi-Prep)

Individual *E. coli* colonies were picked and inoculated into 5ml LB broth containing antibiotics in a 50ml polypropylene tube (Greiner Bio-One), incubated at 37°C , 220rpm for 8 hours, and then added to added to 400ml LB broth (containing antibiotics) and cultured at 37°C, 220rpm overnight. For maxi-preps, the NucleoBond Xtra Maxi Plus kit (Machery-Nagel, Düren, Germany) was used according to the manufacturer's instructions. 200-400ml *E. coli* were centrifuged at 4700rpm at 4°C for 15min in SIGMA 6K15 high capacity centrifuge (Sigma Laborzentrifugen, Osterode am Harz, Germany). The pellets were resuspended in

12ml Buffer RES (10mg RNase A added to 150ml buffer and stored at 4°C before use) and transferred to a 50ml polypropylene tube (Greiner Bio-One). Bacteria were lysed by adding 12ml Buffer LYS, inverting for 5 times to mix, and incubating at room temperature for 5min. At the same time, a NucleoBond Xtra column was equilibrated by applying 25ml Buffer EQU to the rim of filter and allowing the column empty by gravity flow. The bacterial lysis was stopped by neutralization with 12ml ice-cold Buffer NEU, and the tube inverted for 10-15 times to mix. The suspension was immediately applied to the filter of equilibrated NucleoBond Xtra column. When the column had emptied, the filter was washed by adding 15ml Buffer EQU and the flow-through discarded. The column was then washed again using 25ml of Buffer WASH (flow through discarded) and the plasmid DNA was eluted by applying 15ml of Buffer ELU to the column, and the flow-through/eluate collected. To concentrate the plasmid, 10.5ml isopropanol was added to the 15ml eluate and mixed well by vortexing. After 2min incubation at room temperature, the mixture was loaded into a 30ml syringe, and pressed slowly through the NucleoBond Finalizer. The precipitate on the NucleoBond Finalizer was then washed by pressing 5ml 70% ethanol (prepared from absolute ethanol (VWR, Lutterworth, UK) and MilliQ-filtered dH_2O) through the Finalizer, and finally dried by pressing air through the Finalizer for at least 6 times. To elute the purified plasmid DNA, 1ml Buffer TRIS was pressed through the NucleoBond Finalizer using 1ml syringe, the flow-through collected and used to repeat the process.

After elution, the concentration of plasmid from both mini- and maxi-prep was determined using NanoDrop 1000 Spectrophotometer (NanoDrop, Wilmington, USA), and the quality of plasmid was determined by 0.8% (w/v) agarose gel electrophoresis (see Section 2.5 above for the methods).

2.2.3 Preparation of glycerol stocks of bacteria

If necessary, 0.5ml transformed *E.coli* were mixed with 1 volume of sterilised glycerol for long-term storage at -80°C.

2.3 RNA extraction and cDNA synthesis

2.3.1 RNA micro-prep

For small-scale isolation of total RNA from cells and tissues, the RNeasy Micro-prep kit (QIAGEN, Crawley, UK) was used. Tissue or cells were first lysed in 350µl Buffer RLT (containing 1% (v/v) β-mercaptoethanol (β-ME; Sigma-Aldrich) and homogenized well using a hand-held pellet-pestle homogenizer and centrifuged in a benchtop microcentrifuge at 10000g for 2min. Lysates were stored at -20°C (short term) or -80°C (long term) or processed immediately by adding 1 volume of 70% (v/v) ethanol to lysate and mixing by pipetting. The mixture was loaded onto an RNeasy MinElute spin column and centrifuged at 10000g for 30s and the flow-through discarded. 350µl Buffer RW1 was added to the column and spun at 10000g for 30s again to wash the precipitate, and the flow-through discarded. 10µl DNase I was diluted in 70µl Buffer RDD and applied to the membrane of the column to remove contaminating genomic or plasmid DNA for 15min at room temperature. The DNase was removed by adding 350µl Buffer RW1 to the column and spinning at 10000g for 30s, and the collection tube and flow through discarded. The column was placed in a new collection tube, and the membrane washed by adding 350µl Buffer RPE and centrifuging at 10000*g* for 30s, followed by adding 500µl (v/v) 80% ethanol to the column and centrifuging at 10000*g* for 2min. The collection tube was replaced again, and the membrane was dried by spinning at max speed for 5min with the column lid open. The RNA was eluted by adding 14µl dH_2O directly onto the membrane and spinning at max speed for 1min, and this step was repeated once using the flow-through to increase the yield.

2.3.2 RNA mini-prep

mRNA from cells grown in 10cm dishes or 6-well plates were extracted using the RNeasy Mini-prep kit (QIAGEN) and NucleoSpin RNA II kit (Machery-Nagel).

For the RNeasy kit, cells were lysed by 600µl Buffer RLT (containing 1% (v/v) β-ME) and the lysate homogenized for 30s using a hand-held pellet pestle homogenizer. 1 volume of 70% (v/v) ethanol was added to the lysate, mixed by pipetting and the mixture transferred to an RNeasy column which was then centrifuged at 10000g for 30s, and the flow-through discarded. The column was

washed by adding 350µl Buffer RLT and spinning at 10000g for 30s, and the flow-through again discarded. 10µl DNase I was mixed with 80µl Buffer RDD, and directly applied on the membrane of column for 20min at room temperature to digest the DNA. The DNase I was removed by adding 350µl Buffer RW1 to the column and spinning at 10000*g* for 30s. The collection tube was replaced after this step, and the membrane washed by adding 500µl Buffer RPE and spinning at 10000g for 30s, and this step was repeated a second time, with the centrifugation time extended to 2min. To elute the RNA, columns were placed in a nuclease-free 1.5ml eppendorf tube and 30-50µl nuclease-free dH_2O was added to each column, and the columns were centrifuged at max speed 1min. This step was repeated using the flow-through to increase the RNA yield.

When using the NucleoSpin kit, cells were lysed in 350µl Buffer RA1 containing 1% β-ME. The lysate was cleared by loading onto a NucleoSpin Filter and centrifuging at 11000g for 1min. 1 volume of 70% ethanol was added to the flow-through, and mixed well by pipetting. The samples were then loaded onto the NucleoSpin RNA II column, and spun at 11000*g* for 30s. The collection tube was replaced and the membrane of column was desalted by adding 350µl Buffer MDB to the column and centrifuging at 11000g for 1min, and the flow-through discarded. Contaminating DNA was digested by adding 95µl Reaction Buffer (containing 9.5µl rDNase I) to the membrane and incubating at room temperature for 15min. To stop the reaction, 200µl Buffer RA2 was loaded to the column and spun at 11000g for 30s. The collection tube was replaced again, and the membrane was washed again by adding 600µl Buffer RA3 to the column and centrifuging at 11000g for 30s, then adding 250µl Buffer RA3 and centrifuging at 11000g for 2min. To elute the RNA, the column was placed in a nuclease-free 1.5ml eppendorf tube. 30-50µl of nuclease-free dH_2O was added to each column, and the column centrifuged at 11000g for 1min. This step was repeated using the flow-through to increase the RNA yield.

2.3.3 cDNA synthesis

Before cDNA synthesis, the concentration of mRNA was determined by NanoDrop, and mRNA was diluted in dH_2O (Ambion, Austin, USA) to a volume of 16µl. This was divided in two, and half of the mRNA (8µl, 500 or 1000ng) was used for +

reverse transcriptase (RT) reactions whilst the other half was for negative -RT reactions.

The SuperScript VILO cDNA Synthesis Kit (Invitrogen) or the Maxima Universal First Strand cDNA Synthesis Kit (Thermo Scientific, Waltham, USA) were used for cDNA synthesis, and the components of the reaction mix was similar for each. For the +RT reaction, each reaction mix contained 8µl diluted mRNA, 4µl 5×RT mix, 6µl dH_2O and 2µl Enzyme mix (final volume 20 µl). The reaction mix of –RT was similar to the +RT, but the Enzyme mix was replaced by dH_2O.

The reaction mix was then loaded on the PTC-100 Thermo Cycler (MJ Research Inc, Reno, USA), and run on the following programmes:

VILO: 25°C for 10min, 42°C for 60min, 85°C for 5min.

Maxima: 25°C for 10min, 50°C for 15min, 85°C for 5min.

The same kit was used throughout an experiment, with no mixing/comparison of samples prepared using kits from different manufacturers.

2.4 Reversed transcription polymerase chain reaction (RT-PCR)

2.4.1 Design and preparation of oligonucleotide primers for PCR

First introduced by Mullis and Faloona (1987), PCR has become one of the most widely used molecular techniques in modern medical research. PCR enables the amplification of a specific region of double-stranded DNA using two oligonucleotide primers, and a thermostable DNA polymerase enzyme. For RT-PCR, primers were designed to cross exon-exon junctions (except the primers for *luciferase* vectors as the sequence does not contain an intron) to prevent amplification from contaminating genomic DNA. Exon sequences of target genes were found using Ensembl Genome Browser (http://www.ensembl.org/index.html), by searching the gene by name or GenBank ID. Primers were designed using online primer design software Primer3 v. 0.4.0 (http://bioinfo.ut.ee/primer3-0.4.0/primer3). Square brackets were added to the input sequence to designate the sequence which should be included in the PCR product and to make sure the primers were across exon-exon junctions; if the target

gene had different splicing then the common part of mRNA variants was selected. The general settings of the software were as default, except 2 options as follows:

Product Size Ranges: 150-300, Max Self Complementarity: 3.00 or 5.00

These settings were to make sure the primers had approximate equal GC contents and melting temperature, appropriate product size for qRT-PCR and lowest self-complementarity or 3' self-complementarity to reduce the possibility of forming primer-dimer.

Primer pairs selected by the software were checked using the nucleotide blast function on the Basic Local Alignment Search Tool (BLAST) website (http://blast.ncbi.nlm.nih.gov/Blast.cgi) against the human Reference RNA Sequence (refseq_rna).

Lyophilized primers (Integrated DNA Technologies, Leuven, Belgium or Invitrogen) were dissolved in dH_2O to make the 100μM solutions for long-term stock, and 25μM working solutions were made from the stocks by dilution with dH_2O.

2.4.2 RT-PCR (end-point)

RT-PCR was performed using either the ImmoMix Red Mix or MyTaq HS Red Mix (BIOLINE), with the same reaction setup for both kits. cDNA reactions were used undiluted, or diluted (with dH_2O) at 1/2 or 1/5 (v/v). Each reaction mix contained 0.5μl forward/reverse primers (0.625μM each primer), 10μl 2×ImmoMix Red or 2×MyTaq HS Red mix, 8μl dH_2O (Ambion) and 1μl cDNA template. For each gene, both RT+ and RT- cDNA reactions were used (to indicate whether DNA contamination had occurred). Samples were run on a PTC-100 Thermo Cycler (MJ Research Inc) with the following programmes:

ImmoMix Red: 95°C for 10min, (95°C for 30s, 58 or 60°C for 30s, 72°C for 45s)×30-35 cycles, 72°C for 10min

MyTaq HS: 95°C for 1min, (95°C for 15s, 60°C for 15s, 72°C for 10s)×30-35 cycles

The products of RT-PCR were analysed using agarose gel electrophoresis (Section 2.5 below).

2.4.3 RT-qPCR (quantitative PCR)

By adding fluorescent dyes which specifically bind to double-stranded DNA, it is possible to quantify the production of PCR products by measuring the amount of fluorescence in a PCR reaction at the end of each PCR cycle (Higuchi *et al.* , 1992). In this study, RT-qPCR was performed using the SYBR Green PCR Master mix (Applied Biosystems, Warrington, UK) and Brilliant III Ultra-Fast SYBR Green QPCR Master Mix (Agilent Technologies, Wokingham, UK). cDNA reactions were usually diluted in dH_2O at 1/10 for quantification, and for cDNA reactions from Actinomycin D (ActD) treatment, RNA immunoprecipitation or to detect genes expressed at a low level (*TEX19* and *TSSK2*) the dilution could be up to 1/2 or 1/5. To make the standard curves, the cDNA reactions were diluted 1/10, 1/25, 1/100, 1/250, 1/1000, 1/2500, 1/10000.

Reactions containing the SYBR Green PCR Master mix were prepared using 0.2µl each of the forward and reverse primers (0.5µM each primer), 5µl 2×SYBR Green mix, 3.6µl dH_2O and 1µl diluted cDNA. When using the Brilliant III kit, each reaction contained 0.2µl each of the forward and reverse primers (0.5µM each primer), 5µl 2×SYBR Green mix, 3.45µl dH_2O, 0.15µl 1/50 diluted Reference Dye in dH_2O and 1µl diluted cDNA. Each +RT cDNA sample was performed in duplicate (two wells) and –RT reactions done once.

qPCR reactions were run on ABI 7900HT machines (Applied Biosystems), using the SDS 2.4 software (Applied Biosystems). The Detector was set to be SYBR and Quencher was Non-Fluorescence. For regular quantification, the task of samples was set to be UNKNOWN or the NTC; when running standard curves, the task of samples was set to be Standard or NTC and the values of dilutions of cDNA were entered as decimals (e.g. a 1/10 dilution becomes 0.1).

The setup of PCR programmes was as follows:

For the ABI kit setup:

2-Steps qPCR: 50°C for 2min, 95°C for 10min, (95°C for 15s, 60°C for 1min)×40 cycles

3-Steps qPCR: : 50°C for 2min, 95°C for 10min, (95°C for 15s, 58°C for 15s and 72°C for 45s)×40 cycles (for *RPL32* (as internal control), *TEX14*, *TEX19* and *GRSF1*)

For the Brilliant III kit setup:

95°C for 3min, (95°C for 5s, 60°C for 15s)×40 cycles

All the PCR programmes were followed by an additional dissociation (melt curve) stage which was 95°C for 15s, 60°C for 15s and 95°C for 15s again to check the specificity of PCR products. This was determined by the presence of a single overlapping peak in all samples (Ririe *et al.* , 1997).

After the PCR programme finished, the standard curves were automatically generated by the software (by plotting C_T value against relative cDNA concentration) after the PCR programme was finished. Ct values from regular quantifications were exported as text file by SDS 2.4. Averaged Ct values (difference ≤1.5 cycles between replicates) of +RT cDNA duplicated wells were taken as the final Ct values.

In qPCR, the standard curve programme gave the slope value for each pair of primers to indicate the amplifying efficiency (E) of the reactions. When E=2, which was the ideal situation indicating target DNA perfectly duplicated after each cycle, the slope value=-3.32 based on the equation $E=10^{(-1/slope)}$. Slope value <-3.32 suggesting low efficiency, whilst >-3.32 meaning efficiency was too high and unspecific PCR products (e.g. primer-dimer) were formed. An R^2 value was also obtained along with the slope value which was indicating the correlation coefficient of the standard curve, and only slope value with the $R^2 \geq 0.98$ was accepted for qPCR analysis. The expression level of each gene was analysed using the formula Relative Amount=$10^{(Ct/slope)}$, and then compared to the level of *RPL32* as relative expression using Microsoft Excel 2003 or 2010.

Table 2. 1 Primer List

Gene	Forward (5'→3')	Reverse (5'→3')	Product Size
BOLL	TATAAGGATAAGAAGCTGAACATTGGT	CGAAGTTACCTCTGGAGTATGAAAATA	171bp
CDC25A	AGATAGCAGTGAACCAGG	TGCATCGGTTGTCAAGG	202bp
CRISP2	CAAAGGTGGGCAAACAAGTG	GCAATTCCACAGCCTACCTG	245bp
CTNNB1	TGCAGTTCGCCTTCACTATG	ACTAGTCGTGGAATGGCATC	142bp
DAZL	GAAGGCAAAATCATGCCAAACAC	CTTCTGCACATCCACGTCATTA	186bp
*DNMT3L**	GCAGCAGCCCTCATCCCCATG	TGCAATAAGATCTCTGCCTGTCC	135bp
ERCC1	CCTCAAGGAGCTGGCTAAGA	AATGTGGTCAGGAGGGTCTG	228bp
GAPDH	GAACGGGAAGCTCACTGGCAT	GTCCACCACCCTGTTGCTGTAG	306bp
GRSF1	AAGGCATCCACATCTTCATTG	CCTGGTCATGCACTATGGAA	232bp
Luciferase	GGCTTCTTCAGCAACGCTAT	GCAGCAGGGTGTCTATCCAT	211bp
RPL32	CATCTCCTTCTCGGCATCA	AACCCTGTTGTCAATGCCTC	153bp
SOX17	AGCAGAATCCAGACCTGCAC	CTTCAGCCGCTTCACCTG	185bp
SRY	ACAGTAAAGGCAACGTCCAG	ATCTGCGGGAAGCAAACTGC	300bp
SYCP3	AGCCGTCTGTGGAAGATCAG	CAACTCCAACTCCTTCCAGC	197bp
TERF2	AAGCAGTGGTCGAATCCAGT	GCATCTTCTGCTGGAAGGTC	225bp
TEX14	CGGTCATTGGAGAAAAGGAA	GGAGAGACACACAGCCATCA	248bp
TEX19	GAAGACAACTGGGACCCTGA	CCTCCTGAGGCCATAGTTCA	220bp
TSSK2	CCTCTGACGGACGGATCTAC	GCTTGGAGAAGCCAAAGTCA	237bp
VASA	AAGAGAGGCGGCTATCGAGATGGA	CGTTCACTTCCACTGCCACTTCTG	238bp

***DNMT3L* primers were from Gokul *et al.* (2007) *Epigenetics* 2:2, 80-90.**

2.5 Agarose gel electrophoresis

Agarose (BIOLINE, London, UK) was added to 50 or 100ml 1×Tris-acetate-EDTA (TAE) buffer (containing 0.04M Tris-acetate, 0.01M Ethylenediaminetetraacetic Acid (EDTA), pH8.0; prepared by diluting 50×TAE buffer (484g Trizma Base (Sigma-Aldrich), 114.2g glacial acetic acid and 100ml 0.5M EDTA diluted in distilled water (dH_2O) to make the final volume of 2l) with water and microwaved until completely dissolved. GelRed (Biotium, Hayward, USA) was added to the solution (1/10000, volume by volume (v/v) to enable visualization of nucleic acids under ultraviolet (UV) light.

Gels were run in 1×TAE buffer (sufficient to cover the gel) in either Mini-Sub Cell GT or Wide Mini-Sub Cell GT gel tanks (Bio-Rad, Hemel Hempstead, UK). For PCR products (in which the loading dye was incorporated into the master mix (as described above in Section 2.4), 10µl samples were directly loaded onto 2% (weight by volume (w/v) gels. For plasmids, 6×Loading Buffer (Promega, Southampton, UK) was added to DNA solution containing 500ng DNA (Promega) before loading onto 0.8% gels (w/v). 500ng, 100bp or 1kb DNA ladders (Promega or BIOLINE) were also added to the gel to enable determination of DNA fragment size. Gels were run at 80-100V for 45-90 minutes (min). Gel images were taken under UV light using a GeneFlash Transilluminator (Syngene, Cambridge, UK) and Video Copy Processor Model P91 (Mitsubishi, Herts, UK).

2.6 Cell culture

To thaw frozen cells (stored at -80°C in Bambanker (ANACHEM, Luton, Bedfordshire, UK)), the tube containing frozen cells was warmed in 37°C water bath until a small piece of was ice left. 1ml warm fresh media (see below) was then added to the cells slowly, and the mix was transferred to 15ml polypropylene tube (Greiner Bio-One), following by adding 10ml warm fresh media to the tube. The cells were centrifuged at 300g for 5min, and resuspended in 10ml fresh media gently by pipetting. The cells were then transferred to a $25cm^2$ flask (Corning, Tewksbury, USA) for culture.

HEK293 cells were cultured in Modified Eagle's Medium (MEM) +GlutaMAX (Gibco, Paisley, UK) supplemented with 10% (v/v) Fetal Bovine Serum (FBS; Gibco). TCam-2 cells (obtained from Professor Leendert Loijenga) were cultured in RPMI1640 (Gibco) containing 10% (v/v) FBS and 2mM L-Glutamine (Gibco) in a humified incubator (37°C, 5% CO_2.)

At 70-90% confluency, cells were passaged 1:4 to 1:8 to new flasks. The media was aspirated, and cells washed twice with Ca^{2+}-free phosphate buffered saline (PBS; Gibco), then incubated with 1.5ml 0.05% (v/v) Typsin/EDTA (Gibco) at 37°C for 2-3min. The trypsinization was stopped by adding 8.5ml complete media (as above) and 1.25ml (1/8 passage) or 2.5ml (1/4 passage) cell suspension was added to 20ml media in new 75cm^2 flasks (Corning).

2.7 Transfection and following treatment

For transfection, HEK293 or TCam-2 cells were trypsinzed, added to fresh media of appropriate volume in the plates/dishes 24 hours prior transfection to achieve 70-80% (HEK293) or 80-100% (TCam-2) confluence at the time of transfection (for plating density and media volume see Table 2.2). Plasmid DNA and transfection reagent TansIT-LT1 (Mirus, Madison, USA) were mixed at a ratio of 1:3 (µg:µl) in serum-free OPTI-MEM (Gibco) and incubated at room temperature for 20-30min. The culture media was changed before the transfection mixture was added onto the cells. The volume of culture media and transfection mix was described below in Table 2.2. After 24h, the media was changed again and cells were harvested 48h after transfection for further analysis if no following treatment required.

Table 2. 2 Volume of Media and Transfection Mix

Dish/Plate size	Culture Media Volume	Number of cells (HEK293)	Number of cells (TCam-2)	OPTI-MEM (Serum Free) Volume	Vector Amount (μg)	TransIT-LT1 Reagent (μl)
10cm Dish	12ml	2.5×10^6	1×10^6	1.5ml	15μg	45μl
6-well plate	2ml	3×10^5	1.5×10^5	250μl	2.5μg	7.5μl
12-well plate	1ml	1.2×10^5	6×10^4	100μl	1μg	3μl
24-well plate	0.5ml	6×10^4	3×10^4	50μl	0.5μg	1.5μl
96-well plate	100μl	2×10^4	1.2×10^4	9μl	0.1μg	0.3μl

2.7.1 Establishment of stably-transfected TCam-2 Cells

To establish a stable cell line, TCam-2 cells were plated in 10cm dishes and transfected with *pCMV6-Entry*, *-DAZL* or *-BOLL* vectors (ORIGENE, Rockville, USA) according to the amounts detailed in Table 2.2, and cultured in media contained 300μg/ml G418 (100mg/ml stock, Invivogen, Toulouse, France) after 48 hour transfection. Cells were split regularly afterwards, and were harvest after 1 month for further analysis.

2.7.2 mRNA stabilisation assay

HEK293 cells were first plated in 12-well plates and transfected with either *pCMV6-Entry* or *–DAZL* vectors for 48h, and then the cells were further cultured in media containing 5μg/ml Actinomycin D (ActD; Sigma-Aldrich, diluted 5mg/ml in Dimethyl Sulphoxide (DMSO; Sigma-Aldrich) and stored at -20°C) or DMSO alone (as vehicle control) for 24h. The cells were lysed in Buffer RLT at time 0 and 24h after ActD treatment for mRNA extraction.

2.7.3 Time course of exogenous DAZL and BOLL expression

HEK293 cells were first plated in 6-well plates and transfected with *pCMV6-DAZL* or *BOLL* vectors, and were lysed using 100μl RIPA (Radioactive ImmunoPrecipiation Assay, 50mM Tris-HCl pH7.0, 1% (v/v) IGEPAL CA-630, 0.5% (w/v) Na-deoxycholate, 0.1% (w/v) Sodium dodecyl sulfate (SDS), 150mM NaCl, 2mM EDTA, all from Sigma-Aldrich, except HCl from Fisher Scientific) buffer per well at time 12h, 24h, 36h, 48h, 60h, 72h after transfection for Western blotting and semi-quantification (for the methods refer to Section 2.13 below). Untrasfected cells were lysed at time 0 as a negative control.

2.8 Fluorescence-activated cell sorting (FACS)

Cells can be labelled with fluorescent markers which can be charged with different electrostatic signals and then further separated by flow cytometry (Bonner *et al.* , 1972). To prepare the cells for FACS, TCam-2 cells were first plated in 10cm dishes

and co-transfected with both *Enhanced Green Fluorescence Protein* (*EGFP*) vectors and *pCMV-DAZL* vectors (1:1, w/w), or single transfected with same amount of *EGFP* vectors. Mock transfections (cells treated with only Transfection reagent TransIT-LT1 (Mirus)) were also set up as negative control. After 48h, the cells were trypsinized and filtered with 40μm cell strainer (BD Biosciences, Oxford, UK) to remove big clumps, then washed in PBS for twice and finally resuspended in 800μl to 1.2ml PBS containing ≤1% (v/v) FBS to achieve a cell density of 1-2 million/ml.

The cells were then sent to the FACS lab in CIR (MRC Centre for Inflammation Research) for FACS, using the BD FACSAria II System (BD Biosciences). Before sorting, 1μl 4',6-diamidino-2-phenylindole (DAPI; Sigma-Aldrich) were added to the cells to stain the nucleus of dead cells and to separate the live and dead cells during the FACS. The mock transfected cells were used as standard to set up the gating. Singlets of cells were determined by FSC (Forward SCatter detector) and SSC (Side SCatter detector), which could represent the cell size and cell granularity/internal complexity, respectively; the area beside the diagonal between FSC-A (area) and FSC-H (height) was indicating the singlets, and the living cells were preliminarily isolated as dead cells had lower FSC-A and higher SSC-A. The GFP gate (emission B 525/50-A) and DAPI gate (emission UV 450/50-A) was then set up using the mock transfected sample as it was GFP^- and so could be the control to determine the threshold of GFP gate. Generally the cells had UV 450/50-A values ≤$1.2\text{-}1.3\times10^2$ (low or no DAPI staining) were considered as living cells, and the B 525/50-A boundary between GFP^+ and GFP^- was at $1.2\text{-}1.4\times10^2$. The DAZL/GFP co-transfected cells were then loaded on the machine and pre-test was performed before the sorting to slightly adjust and confirm the settings.

RPMI1640+L-GlutaMAX containing 20% (v/v) FBS was used as collection media of sorted cells, and only live GPF^+ and GFP^- cells were collected. The parameters of collected cells were briefly checked on the machine using all the gates described before. The cells were then either washed twice with PBS and lysed in 15 to 45μl (depending on the cell numbers) RIPA buffer for Western blotting (see Section 2.13), or centrifuged and lysed in 350μl Buffer RLT for mRNA extraction (micro-prep).

2.9 RNA-immunoprecipitation (RIP)

2.9.1 Preparation of RIP samples

RIP was first developed by modifying chromatin immunoprecipitation to study protein-RNA interactions (Gilbert *et al.* , 2004). For the RIP, cells were plated in 10cm dishes to achieve appropriate confluency and transfected with *pCMV6-Entry* or *pCMV-DAZL* vectors (TCam-2), or co-transfected with *pCMV6-Entry* or *pCMV-DAZL* vectors combined with luciferase vectors with either *GAPDH* or *TEX14* 3'-UTR (HEK293). After 48h transfection, cells were trypsinized and washed with ice-cold PBS for twice, and then lysed in 1 volume of lysis buffer (containing 10mM HEPES pH7.0, 100mM KCl, 5mM $MgCl_2$, 0.5% IGPAL CA-630, 1mM dithiothreitol (DTT), 0.25% (v/v) RNase Inhibitor and 0.5% (v/v) Proteinase Inhibitor. All chemicals from Sigma-Aldrich and diluted with dH_2O, except the RNase/Protein inhibitors which were from the RIP kit (Millipore) and added to the buffer just before use). The lysate was incubated on ice for 5min and centrifuged at 10000g for 15min at 4°C. The supernatant was stored at -80°C as 100µl aliquots if not be used immediately.

2.9.2 Immunoprecipitation of DAZL protein

Before RIP, the potential RNase contamination from the environment was removed by wiping all the surface of bench and equipment using the RNaseZAP (Ambion). The Magna RIP RNA-Binding Protein Immunoprecipitation Kit (Millipore) was used for RIP. To prepare the magnet agarose beads, 50µl beads per reaction was taken from the kit, washed with 500µl Wash Buffer twice and resuspended in 100µl Wash Buffer, incubated with Rabbit anti-DAZL antibody (Cell Signaling, Hitchin, UK) 1/40 at room temperature for at least 30min. After incubation, the beads were washed 3 times with 500µl Wash Buffer, and resuspended in 900µl RIP buffer containing 860µl Wash Buffer, 35µl EDTA and 5µl RNase Inhibitor per reaction. 100-120µl cell lysate was then added to the beads, and incubated at 4°C, rotating for at least 4h.

2.9.3 Isolation of DAZL co-precipitated RNA

After the incubation, the beads were washed with Wash Buffer for 6 times, and then digested in 150µl Proteinase K buffer containing 117µl Wash Buffer, 18µl Proteinase K and 15µl 10% (w/v) SDS at 55°C for 30min.

After digestion, the beads were discarded, and 50µl dH_2O was added to the 150µl supernatant of each sample to make up the volume of 200µl. 700µl Buffer RLT, followed by 500µl absolute ethanol was added to the diluted supernatant and mixed well by pipetting. The mixture was then loaded onto the RNeasy MinElute spin columns (QIAGEN) and the flow-through was discarded after spinning at 10000g for 30s. The precipitate was then washed by adding 500µl Buffer RPE and spinning at 10000g for 30s, followed by adding 500µl 80% (v/v) ethanol and spinning at 10000g for 2min. The collection tube was replaced after washing, and the membrane of the column was dried by spinning at maximum speed with lid open for 5min. The column was then placed in a nuclease-free 1.5ml eppendorf tube, and the RNA was eluted by adding 14µl dH_2O to the membrane of column and spinning at maximum speed for 1min, and this step was repeated using the flow-through to increase the yield. The concentration of eluted RNA was determined using the NanoDrop, and afterwards the RNA was converted to cDNA for both + and –RT using the Maxima kit as described in Section 2.3.3.

2.10 Luciferase 3'-UTR assay

2.10.1 Experimental procedure of 3'-UTR assay

The principle of luciferase 3'-UTR assay is shown in Figure 2.1. Cells are transfected with luciferase vectors conjugated with the 3'-UTR of the target gene. The substrate is catalysed by *Renilla* luciferase, which is produced by the transfected cells with the generation of luminescence. The amount of luminescence will be altered if the expression of luciferase is modulated through the 3'-UTR by other added factors such as DAZL. Therefore, by detecting the change in luminescence, it is possible to investigate how the expression of luciferase is modulated by the regulators and whether it is through 3'-UTR.

HEK293 or TCam-2 Cells were plated in white 96-well plates with clear base (Thermo Scientific) to achieve appropriate confluence 16-24h prior transfection and then cells were co-transfected with *pCMV-DAZL* or *pCMV6-Entry* vectors plus LightSwitch *RenSP Luciferase* vectors (SWITCHGEAR GENOMICS, Menlo Park, USA) which were conjugated with no-, *GAPDH* or *TEX14* 3'-UTR (1:1, w/w). Each combination of vectors was repeated in triplicate and the culture media was replaced by 100µl fresh regular media per well after 24h.

After 48h transfection, the luciferase assay was performed using LightSwitch Luciferase Assay kit (SWITCHGEAR GENOMICS). Before performing the assay, the solid Assay Substrate was reconstituted in 100uL Substrate Sovlent and stored as 20 µl or 30µl aliquots at -20°C for up to 1 month. The Assay Buffer was warmed at 37°C for at least 1h (hour), and then the substrate was diluted 1/100 (v/v) in the Buffer. 100µl diluted substrate per well was then added directly to the 100µl culture media and mixed by shaking the plate on plate shaker for 15s. The plate was then incubated at room temperature for 30min, protected from light.

To read the strength of luminescence, the plate was loaded on FLUOstar OPTIMA (BMG LABTECH, Bucks, UK) using OPTIMAR software, read under luminescence/end-point mode, 2s for each well and the gain was set to 4059. The data was exported using OPTIMAR-Data Analysis as an .xls file.

To analyse the data, Microsoft Office Excel 2010 was used. The readings of triple wells were averaged, and the luminescence values was normalised using those values from cell transfected by Empty and *GAPDH* vectors following the manufacturer's instructions to minimise the affection between different conditions. Briefly, the average signal for each construct (Empty or *GAPDH*) under different conditions were calculated, then the ratio of each treatment's luminescence value to the average was calculated. Then the ratios from different constructs (Empty and *GAPDH*) but same treatment was averaged, and the original luminescence values were divided by these averaged ratios to normalise. Finally the normalised data was analysed using GraphPad Prism to find out the significance between each treatment.

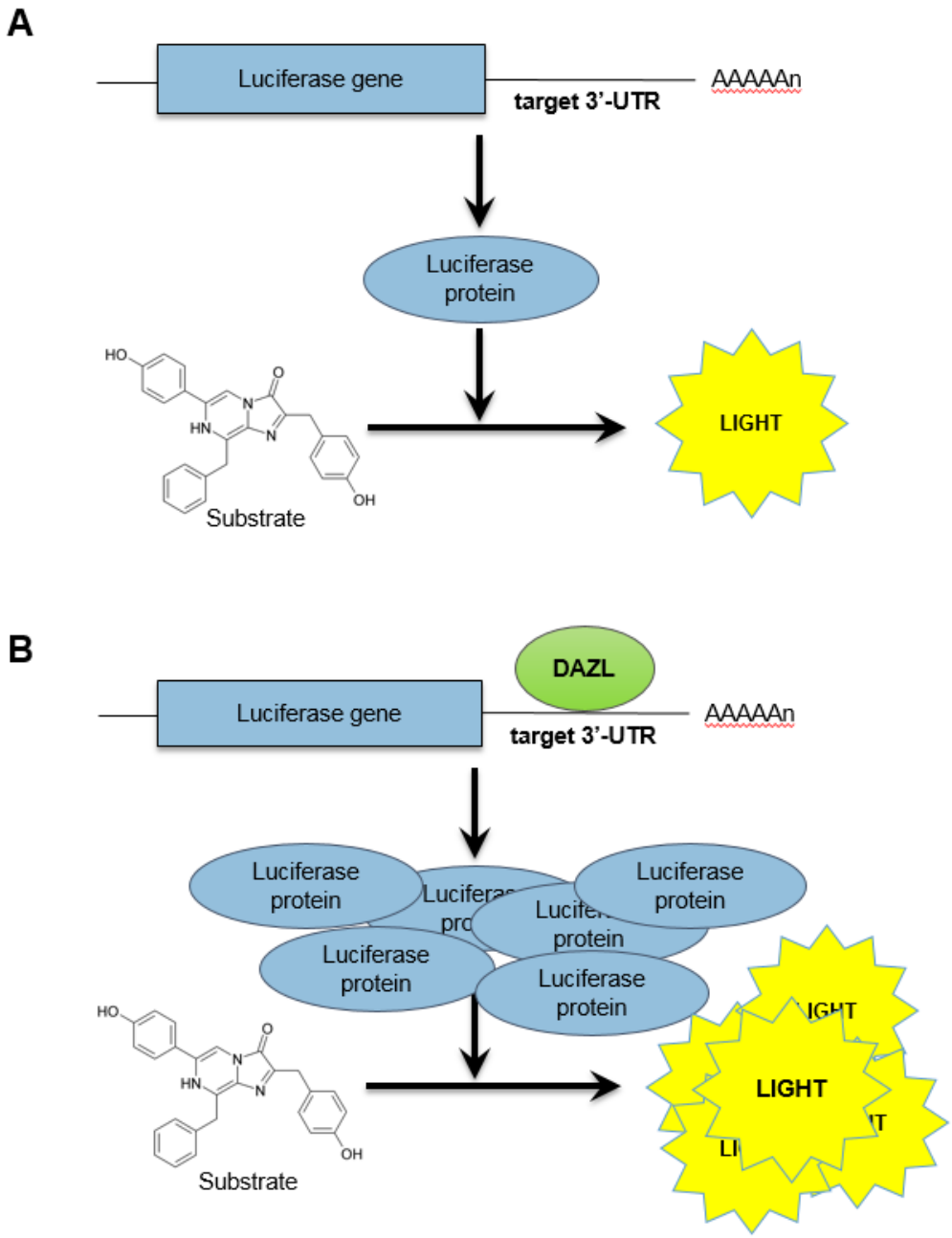

Figure 2.1 Diagram of 3'-UTR luciferase assay.

A) The assay system without DAZL. The luciferase gene is translated into luciferase protein, and when substrate is added, this protein will catalyse the substrate and stimulate luminescence. **B)** The assay system with DAZL. DAZL protein could bind to the 3'-UTR of the target gene, which is conjugated with luciferase gene, and then promote the translation. This will lead to the production of more luciferase protein in the system and enhanced catalytic ability; therefore once the substrate is added, the luminescence will be stronger.

Figure by Dr Andrew Childs

2.10.2 Data normalisation for luciferase 3'-UTR assay

The data normalisation of the data generated by luciferase 3'-UTR assay was performed following the instructions from the manufacturer's website (http://switchgeargenomics.com/sites/default/files/pdf/LightSwitch_3UTRnorm.pdf). The whole process will be explained quoting part of the original protocol, with sample data as below.

In this study, there was two experimental conditions (co-transfection with *DAZL* or empty vector), and *luciferase* vectors no 3'UTR or conjugated to the *GAPDH* 3'-UTR were used as controls for normalisation. It was assumed that the data obtained in one experiment was shown in Table 2.3, and the average signal of controls under the two conditions were calculated (19.3 and 66.4 for empty or *GAPDH*, respectively).

Table 2. 3

	Experimental 3'-UTR	Controls	
	3'-UTR	EMPTY	*GAPDH*
Condition 1	46.6	20.5	68.6
Condition 2	13.3	18.1	64.1
Controls Average		**19.3**	**66.4**

The next step was to calculate the ratio of each control's luminescence to the average, as shown in Table 2.4.

Table 2. 4

	Controls	
	EMPTY	GAPDH
Condition 1/Average	20.5/19.3	68.6/66.4
Condition 1 Ratio	**=1.06**	**=1.03**
Condition 2/Average	18.6/19.3	64.1/66.4
Condition 2 Ratio	**=0.94**	**=0.97**

And then the ratios under each condition were averaged as shown in Table 2.5.

Table 2. 5

	Controls		Control Average
	EMPTY	GAPDH	
Condition 1 Ratio	1.06	1.03	**1.045**
Condition 2 Ratio	0.94	0.97	**0.955**

And finally, the raw data was divided by the average control ratios obtained in Table 2.5 for normalisation, and these values (bold numbers in Table 2.6) were used for further analysis.

Table 2. 6

	Experimental 3'-UTR	Controls	
	3'-UTR	EMPTY	GAPDH
Condition 1/Average Ratio	46.6/1.045	20.5/1.045	68.6/1.045
Condition 1 Normalised	**=44.59**	**=19.62**	**=65.65**
Condition2/Average Ratio	13.3/0.955	18.1/0.955	64.1/0.955
Condition 2 Normalised	**=13.93**	**=18.95**	**=67.12**

2.11 Human dissection and tissue collection

The human fetuses (8-20 week gestation) were obtained from termination of pregnancy, and the ethical approval was obtained from Lothian Research Ethics Committee (study code LREC 08/S1101/1). The donation of human tissue was agreed by informed written consent from all the patients following national guidelines (http://www.hta.gov.uk/legislationpoliciesandcodesofpractice/codesofpractice/code1consent.cfm?FaArea1=customwidgets.content_view_1&cit_id=665&cit_parent_cit_id=652). Most abortions were performed using medicine methods but the termination of pregnancy at 10-14 week gestation (not include 14 week) were performed by surgical methods (vacuum aspiration after administration of misoprostol 200mg/vagina).

All the fetuses used in this study were morphologically normal. The gestational age was determined using ultrasound before termination, and was then further confirmed by measuring crown-rump length of the first trimester fetuses or the foot length of the second trimester fetuses. The gender of first trimester fetuses was determined by PCR for the *SYR* gene and following agarose gel electrophoresis (see Section 2.12), and the one of second trimester fetuses was determined by the morphology of external genitalia and gonads.

The fetal gonads were then removed from the fetuses using sterilised tools and rest in PBS before next step. For RNA extraction or Western blotting, the extra-ovarian tissue was removed using sterilised syringe needles and the ovaries were either lysed in Buffer RLT (for RNA extraction, see Section 2.3) or RIPA buffer (for Western blotting, see Section 2.13), or immediately frozen on dry ice and stored at -80°C for long-term storage. For tissue processing for immunohistochemistry, see Section 2.15.1.

2.12 Mouse dissection and tissue collection

Mouse fetal gonads were obtained from C57BL6 mouse embryos. The mice were

kept on a 12h light/dark cycle from 7am each day at 19-21°C and fed *ad libitum*, according to UK Home Office and local University of Edinburgh ethical standards. The appearance of a vaginal plug was designated as e0.5.

The pregnant mice were killed by cervical dislocation and the uteri were isolated and stored in PBS on ice while dissecting other fetuses. The fetal gonads were isolated at day e13.5, e15.5 and e18.5, and the gonads of the neonatal mice were also isolated, both under dissecting microscope and using sterilised tools. The gender of fetuses was determined by the location and morphology of gonads. For the tissue processing of immunohistochemistry see Section 2.15.1.

2.13 SRY genotyping

The PCR for the *SRY* gene was performed to determine the gender of human first trimester specimens. Tissue (hand or foot) was digested in 100µl 25mM NaOH/0.2mM EDTA at 95°C for 20min, and then neutralised using 100µl 40mM Tris on ice. The lysate was then mixed vigorously by vortex, and spun briefly.

Each PCR reaction contained 5µl supernatant from the tissue lysate, 12.5µl 2×ImmoMix Red, 0.5µl *SRY* forward/reverse primer (see Table 2.1 primer list for the sequence of *SRY* primers and product size) and 6.5µl water, and an extra reaction containing human male genome DNA was also set up as positive control. The PCR programme was 95°C for 10min, (95°C for 30s, 58 or 60°C for 30s, 72°C for 45s)×30-35 cycles, 72°C for 10min. The PCR product was analysed by agarose gel electrophoresis (for the methods refer to Section 2.5 on agarose gel electrophoresis above). The appearance of band indicated male and absence of band indicated female.

It is necessary to mention that although the positive control was performed using the *SRY* primers and human male genomic DNA, we could not exclude the possibility of false positive results, especially if the tissue was collected and/or the genotyping was performed by male staff. Therefore, in future, female genomic DNA should also be

included as a negative control to ensure no contamination occurred in the experiments.

2.14 Protein extraction and western blotting

2.14.1 Preparation of protein and determination of concentration

RIPA buffer containing 50mM Tris-HCl pH7.0, 150mM NaCl, 1% (v/v) IGPAL CA-630 and 0.25% (w/v) Na-Deoxycholate (all from Sigma-Aldrich except HCl from Fisher Scientific, Loughborough, UK) was used to lyse the cells. One Complete Protease Inhibitor Cocktail Tablet (Roche Applied Sciences) was added to 10ml RIPA buffer before use and the buffer was stored at 4°C up to 1 month afterwards. Tissue or cells were washed with PBS twice, and then lysed by directly adding RIPA buffer to them; tissue suspension was homogenized. The lysate was centrifuged at 13000g for 3min at 4°C and the supernatant contained protein. The protein was stored at -20°C for short-term or at -80°C for long-term storage, and thawed slowly on ice before use.

The concentration of protein was detected using the DC Protein Assay kit (Bio-Rad). Before the assay, standard BSA samples (0.125, 0.25, 0.5, 1.0μg/μl) were prepared by diluting Bovine Serum Albumin (BSA) Standards (2mg/ml, Thermo Scientific) in RIPA buffer, and Reagent S was added to Reagent A 1/50 to make Reagent A'. Standard or protein samples were loaded to 96-well microplate as duplicates 5μl per well, followed by adding 25μl Reagent A' and 200μl Reagent B each well. The samples were mixed on a plate shaker briefly, and incubated at room temperature for 15min, protected from light. The plate was finally scanned on Multiskan EX microplate (MTX LAB SYSTEMS, Vienna, USA) reader at 620nm. The concentration of each sample was calculated by comparing the absorption with the standard curve generated from BSA samples on the same plate, using Microsoft Excel 2003 or 2010.

2.14.2 Sodium dodecyl sulfate- polyacrylamide gel electrophoresis (SDS-PAGE)

Protein samples (from Section 2.14.1 above) were mixed with 4×SDS gel-loading buffer (625mM Tris-HCl pH6.8, 5% (v/v) glycerol, 2% (w/v) SDS, 0.0025% (w/v) Bromophenol Blue, 10% (v/v) β-ME (all from Sigma-Aldrich, except HCl from Fisher Scientific) and boiled for 6min to denature, cooled on ice for 2min and centrifuged. Up to 30µg or 30µl of protein was loaded per well onto pre-cast gels (12% or 4-20% 12-well Precise Tris-HEPES gels (Thermo Scientific) or 12% 10-well Mini-PROTEAN TGX Precast Gel (Bio-Rad). 6µl SeeBlue Plus2 (Life Technologies, Paisley, UK) or PageRuler Plus (Thermo Scientific, Waltham, USA) pre-stained protein standards were also run to enable approximate determination of protein sizes. Precise Tris-HEPES gels were run in 1×Tris-HEPES Running Buffer (prepared by diluting 20×Tris-HEPES Running Buffer (Thermo Scientific) with dH_2O) in an XCell SureLock Mini-Cell tank (Invitrogen) at 120V for 1-1.5 hours. Mini-PROTEAN TGX Precast Gels were run in 1×Tris-Glycine running buffer (prepared by diluting a 10×stock (129g Trizma Base, 144g glycine, 100ml 10% (w/v) SDS (all from Sigma-Aldrich) in a final volume of 1L) with dH_2O) in a Mini-PROTEAN Tetra Cell (Bio-Rad) tank at 200V for about 1 hour.

2.14.3 Western blotting

The technique of transferring electrophoretically separated proteins from gel to a membrane (originally nitrocellulose membrane) and detecting them with antibodies was developed by Towbin *et al.* (1979). Following PAGE, protein gels were washed in dH_2O (2×5min), and incubated in 1×transfer buffer (prepared by diluting 10×Pierce Fast Semi-Dry Transfer Buffer (Thermo Scientific) with dH_2O) for 10min on a rocker with gentle agitation. Immobilon-FL PVDF membrane (Millipore) was cut into 7×9cm squares (equivalent to one mini-gel), activated by soaking in methanol (Fisher Scientific) for 1min, washed in dH_2O for 1min and also incubated in transfer buffer for 10min. 2 pieces of western blotting filter paper (Thermo Scientific) were cut to the same size as the PVDF membrane and soaked in transfer buffer for at least 3min before transfer. These were then assembled into a blot sandwich (order from bottom: 1 layer of filter paper, PVDF membrane, protein gel

and finally 1 layer of filter paper) and loaded onto a Fast Semi Dry Blotter (Thermo Scientific). The transfer was run at 25V for 7-9min.

After transfer, the membrane was stained using Ponceau S Solution (Sigma-Aldrich) and washed with dH_2O until water was not pink to check the quality of transfer, and then blocked in blocking buffer (Bløk - FL Fluorescent Blocker (Millipore) mixed 1:1 (v/v) with 1% (v/v) PBS-T (Tween) for at least 1h. The membrane was then incubated in 1ml or 5ml primary antibody diluted in blocking buffer at 4°C overnight. The information and concentration of antibodies used in Western blotting was described below in Table 2.7. PBS was made from 10×PBS stock (100 Phosphate buffered saline tablets (Sigma-Aldrich) dissolved in 2L dH_2O), and 1ml Tween-20 (Sigma-Aldrich) was added to 1L 1×PBS diluted from the stock to make the 1% PBS-T.

Table 2. 7 Antibodies used for Western Blotting

Primary Antibody	Manufacturer	Species Raised	Dilution
DAZL	Abcam	Mouse	1/200
DAZL	Cell Signalling	Rabbit	1/1000
BOLL	Abcam	Mouse	1/100
FLAG	Sigma	Mouse	1/500
Myc	Stanta Cruz	Mouse	1/200
α-tubulin	Sigma	Mouse	1/5000

On day2, The membrane was washed in 0.05% (w/v) PBS-T for 15min once, then washed again for 5min for 4 times, and incubated with 5-10ml 1/10000 diluted fluorescence-conjugated secondary antibody (Donkey anti-IgG of the species of primary antibody, all from Invitrogen) for 1h at room temperature. The membrane was then washed in 0.05% PBS-T for 5min twice and in PBS for 5min once, and stored in PBS at 4°C before scanning.

2.14.4 Semi-quantification of Western blotting

Membranes were scanned on the Odyssey Infrared Imaging System and the Odyssey software (Li-Cor Biosciences, Cambridge, UK).To quantify the strength of bands, rectangles of same size were added to the image of blots using the Odyssey software; each rectangle completely covered a single band and did not overlap each other. The colour intensity was measured automatically and the report was exported as text file by the software. The intensity of band was calculated as the average intensity subtracted the background intensity, and the intensity of target bands were standardized by dividing the values of the bands of α-tubulin in corresponding lanes using Microsoft 2003 or 2010.

2.15 Immunohistochemistry (IHC)

2.15.1 Tissue fixation, processing and slide prep

Most immunohistochemistry experiments were performed by myself, except the work on mouse were performed by honoured student Kayleigh Stewart under my supervision.

Before immunohistochemistry, the human fetal ovaries were fixed in Bouin's Fluid (Clin-Tech, Guildford, UK) overnight or 4% Neutral Buffered Formalin (NBF, Clin-Tech) for 2-3 hours, whilst the dissected mouse gonads were fixed in 4% NBF for 3-4 hours, and then transferred to 70% ethanol for temporal storage.

The tissue was then sent to the SuRF @ QMRI (Queen's Medical Research Institute Shared University Research Facilities) in CRH (The University of Edinburgh/MRC Centre for Reproductive Health) to be finally embedded as paraffin blocks using HistoStar Embedding Workstation (Therom Scientific).

The paraffin embedded tissue blocks were cut as 5μm sections using a Leica RM2125 microtome (Leica). The fresh cut sections were floated into a 37°C water bath to smooth and then mounted onto electrostatically charged glass slides (Leica). The slides were incubated at 50°C overnight to dry and finally stored in dry place at room temperature.

2.15.2 Tissue dewax and rehydration

To dewax, the paraffin-embedded sections on glass slides were immersed in xylene (VWR) for 5min twice, and then rehydrated by immersing in 100% (v/v) ethanol twice for 20s, and then in 90%, 80%, 70% (v/v) ethanol once each for 20s. The slides were then rinsed in tap water to remove the excessed ethanol and stored in tap water until being progressed to the next step.

2.15.3 Haematoxylin and eosin (H&E) staining

Slides were taken from newly prepared sections every 10 slides to check the quality of specimen. The rehydrated slides were first incubated in haematoxylin (Leica) for 5min to stain the nucleus (blue) and then rinsed in tap water and the staining was checked under microscope. This step might be repeated until the staining was

sufficient. Then the slides were washed in acid alcohol (70% (v/v) ethanol with 1% (v/v) 37.5% (w/v) HCl) for 5s to remove the excessed background staining and rinsed again in tap water, then the colour was developed by incubating in Scott's Tap Water Substitute (CellPath, Powys, UK) for 30s. The slides were then rinsed again in tap water and finally immersed in eosin (Leica) for 20s to stain the cytoplasm (pink) and rinsed in tap water.

2.15.4 Antigen retrieval

The rehydrated slides were antigen retrieved in 250ml 0.01M citrate buffer pH6.0 (made from 10×citrate buffer stock; 1L stock was made from 820ml 0.1M sodium citrate (Sigma-Aldrich) and 180ml 0.1M citric acid (Sigma-Aldrich), and the pH was adjusted to 6 using 5M NaOH (VWR) in a water bath in a Decloaking Chamber (Biocare Medical, Concord, USA). The programme was 125°C for 30s and then slowly cooled to 90°C for 10s. The slides were then rinsed in tap water and rested in water before next step.

2.15.5 Non-specific blocking

The slides were rinsed 3 times in dH_2O, and then incubated at room temperature in either 3% (v/v) hydrogen peroxidase (30% (v/v) stocks, Fisher Scientific) diluted in methanol (Fisher Scientific) for 30min on rocker, or Peroxidase Blocking Reagent (Dako, Cambridge, UK) was added to the sections 100µl per slide and incubated for 10min to block the action of endogenous peroxidase. After that, the slides were rinsed in dH_2O 3 times again and then washed in Tris-Buffered Saline (TBS, for 3,3'-Diaminobenzidine (DAB) immuno) or in PBS (for fluorescence immuno) for 5min twice. Both TBS and PBS were made from 10×stocks; for TBS, 121.1g Trizma Base (Sigma-Aldrich) and 170g NaCl (Sigma-Aldrich) was dissolved in 2L dH_2O and the pH was adjusted to 7.4 using 37.5% (w/v) HCl (Fisher Scientific) to make the 10×stock. For PBS, see Section 2.13.3 above for the methods of making 10×stock.

The slides were then blocked by the serum block at room temperature for 30min. The block containing 20% (v/v) normal animal serum (Biosera, Uckfield, UK) and 5% (w/v) BSA (Sigma-Aldrich) diluted in PBS, and the species of serum were the same

species in which the secondary antibody was raised in. For mouse tissue, if the primary antibody was also raised in mouse, then the Rodent Block Buffer from Mouse on Mouse Polymer IHC Kit (Abcam, Cambridge, UK) was applied on the tissue instead of regular serum block. After the serum blocking, the slides were washed again in PBS or TBS for 5min twice, and the slides for DAB immunos were further blocked by avidin and biotin blocks (VECTOR LABORATORIES, Peterborough, UK), each for 15min followed by 5min TBS wash×2 afterwards.

2.15.6 Primary antibody incubation

The primary antibody was diluted in serum block and applied 100µl per slide to the sections. The appropriate concentration of primary antibody was determined by applying different ranges of dilution of antibody on the sections and processing the whole work flow, until find out the best primary antibody concentration which could generate sufficient staining with lowest background. 100µl serum block without any antibody was applied on one slide as negative control. The slides were then covered by small pieces of parafilm to protect the sections from drying out, and incubated at either 4°C overnight or room temperature for 1h. The information and concentration of antibodies used in immunos was described below in Table 2.8.

Table 2. 8 Antibodies used for Immunohistochemistry/Immunocytochemistry

Primary Antibody	Manufacturer	Species Raised	Dilution	Secondary Antibody	Manufacturer	Visualisation Methods
DAZL	Abd Serotec	Mouse	1/200	Goat anti-Mouse Alexa 488	Molecular Probes	Directly Conjugated Fluorescence
			1/500	Goat anti-Mouse peroxidase fab	Abcam	TSA Fluorescence
DAZL	Cell Signaling	Rabbit	1/100	Goat anti-Rabbit biotinylated	Vector	DAB
			1/500 (tissue) or 1/2000 (cells)	Goat anti-Rabbit peroxidase fab	Abcam	TSA Fluorescence
BOLL	Abcam	Mouse	1/50 (old) or 1/200 (new)	Goat anti-Mouse peroxidase fab	Abcam	TSA Fluorescence
			1/50	Mouse-on-Mouse HRP polymer	Abcam	DAB
			1/200	Mouse-on-Mouse HRP polymer	Abcam	TSA Fluorescence
SYCP3	Abcam	Rabbit	1/50000	Goat anti-Rabbit peroxidase fab	Abcam	TSA Fluorescence
Phospho-ATM	Rockland	Mouse	1/200	Rabbit anti-Mouse peroxidase	Vector	TSA Fluorescence
SOX17	R&D Systems	Goat	1/500	Horse anti-Goat peroxidase	Vector	TSA Fluorescence
DNMT3L	Abcam	Rabbit	1/5000	Goat anti-Rabbit peroxidase fab	Abcam	TSA Fluorescence
LIN28	Abcam	Rabbit	1/500	Goat anti-Rabbit biotinylated	Vector	Streptavidin-Conjugated Fluorescence

2.15.7 Secondary antibody incubation

On day2, the slides were washed in PBS or TBS for 5min twice, and the secondary antibody was diluted in serum block at 1/200-1/500. 100µl antibody was applied on the sections per slide and incubated at room temperature. The incubating time was depending on the variations of antibodies. The biotinylated antibodies or antibodies conjugated with peroxidase were incubated for 30min, and the fluorophore conjugated antibodies were incubated for 1h. For the mouse tissue sections with primary antibody raised in mouse, Mouse on Mouse HRP Polymer from Mouse on Mouse Polymer IHC Kit was applied 1 drop per slide instead of regular secondary antibody, and incubated at room temperature for 30min as well.

2.15.8 DAB staining and streptavidin- conjugated fluorescence staining

For the slides incubated with biotinylated secondary antibody, Streptavidin HRP (Horse Radish Peroxidase, VECTOR LABORATORIES, Peterborough, UK) diluted 1/1000 in PBS (for DAB staining), or Streptavidin-conjugated fluorophore (Molecular Probes, Invitrogen) diluted 1/200 in PBS (for Streptavidin-conjugated fluorescence staining) was applied 100µl per slide to the sections and incubated at room temperature for 30min or 1h respectively, protected from light. The slides were then washed with TBS for 5min twice. No further step was required for Streptavidin-conjugated fluorescence staining afterwards.

For the slides incubated with Mouse on Mouse HRP Polymer, the DAB staining was directly processed after the step of secondary antibody, without incubation of HRP.

For the DAB staining, the Liquid DAB+Substrate Chromogen System (Dako) was used. Before the staining, 1 drop DAB+Chromogen solution was added to 1ml Substrate Buffer and mixed well by vortex to make the work solution. The DAB work solution was then immediately added to the sections (100µl per slide) and the colour development was observed under microscope one by one. Once the staining was sufficient, the slides were immersed in TBS to stop the reaction. The slide of negative control was incubated with DAB for 5min to ensure the sufficient developing time.

2.15.9 Tyramide staining

For the Tyramide staining, the TSA (Tyramide Signal Amplification) Plus Cyanine 3 (Red), Cyanine 5 (Blue) or Fluorescein (Green) System (PerkinElmer, Cambridge, UK) was applied. Before use, the solid Fluorophore Amplification Reagent was reconstituted in 150µl DMSO to make the Fluorophore Amplification Reagent Stock Solution and the solution was stored at 4°C for up to 3 month. To make the working solution, the stock solution was diluted 1/50 in the 1×Plus Amplification Diluent, protected from light.

The working solution was then added directly on the sections which were incubated with peroxidase conjugated secondary antibody or Mouse on Mouse HRP Polymer, 50µl per slide and protected from light. After 10min, the slides were immersed in PBS to stop the reaction and washed in PBS for 5min twice.

2.15.10 Double or triple fluorescence staining

The double staining was only applied to the slides which were previously stained with Tyramide, as the protocol would remove all the antibodies applied to the tissue during previous staining, and all the washing steps after the incubation of primary antibody were changed to wash with 0.05% (v/v) PBS-T for 5min plus PBS for 5min to decrease the background staining.

After the Tyramide staining and following washes, slides were microwaved in boiling 0.01M citrate buffer for 2.5min before resting in the buffer at room temperature for 40min to cool. This step was to remove both the primary and secondary antibodies. The slides were then rinsed in PBS, and processed to non-specific blocking and its following steps as described before in Section 2.14.5.

For triple staining, the two previous staining also needed to be both done with Tyramide, and the slides were again microwaved in citrate buffer as described in this section and then the staining steps were repeated from non-specific blocking.

2.15.11 Counter stain, tissue dehydration and mounting

The work flow of counter staining with DAB slides was similar to the H&E staining, but without Eosin staining.

To gradiently dehydrate the tissue, slides were immersed in 70%, 80%, 95% (v/v) ethanol for 20s once each, and then in 100% ethanol for 20s twice, and finally incubated in xylene for 5min for twice. The slides were then immersed in fresh xylene and directly mounted with Pertex (Histolab, Gothenburg, Sweden) and Premier Cover Glass (Leica), and the bubbles on sections were removed by applying pressure using forceps. The slides were then left on ventilated downdraft table to dry and stored in dry place at room temperature.

To counter stain fluorescence sections, DAPI diluted 1/500 or 1/1000 in PBS were applied to the sections, 100µl per slide and incubated at room temperature for at least 15min, protect from light. The slides were then washed with PBS for 5min twice, and mounted with Permaflur Aqueous Mounting Medium (Thermo Scientific) and Premier Cover Glasses (Leica) were directly applied without dehydration, and the slides were stored at 4°C, protected from light after drying.

2.16 Fluorescence immunocytochemistry

To prepare the slides, cells were first plated in 4-well or 8-well chamber slides (Millipore or Nalge Nunc International, Thermo Scientific). After required treatment, the cells were washed with ice-cold PBS, and fixed in ice-cold methanol (Fisher Scientific) for 20min on ice. The cells were then washed again with ice-cold PBS for twice, and stored at 4°C resting in PBS for up to 1 month.

For immunocytochemistry, the cells were washed in PBS at room temperature for 5min, and then blocked and also permeabilised by adding permeabilisation to the cells and incubating at room temperature for 20min. The component of permeabilisation was similar to serum block (refer to Section 2.14.5 above for the recipe) but containing 0.2% (v/v) IGEPAL CA-630 (Sigma-Aldrich).

The cells were then stained as described above from Section 2.14.6, but the volume of diluted antibodies and Tyramide varied from 25 to 50µl per chamber depending on the size of chambers. After the counter stain, the chambers were removed following manufacturer's instruction, and the slides were mounted with Permaflur Aqueous

Mounting Medium (Thermo Scientific) and Premier Cover Glass (Leica), then stored at 4°C, protected from light after dried.

2.17 Nuclear diameter measurement and cell counting

It had been demonstrated that the nuclear diameter of germ cells increases during development (Hilscher *et al.* , 1974). Correlation of this parameter with the germ cell development has been confirmed in the human fetal ovary (Anderson *et al.*, 2007, Martins da Silva *et al.*, 2004), indicating that it can be used as a marker of development. Therefore, nuclear diameter measurement was used in this study to indicate the germ cell maturation.

The images of fluorescence stained whole sections were taken using LSM 710 Confocal Microscope (Carl Zeiss, Oberkochen, Germany) and Zen 2009 or 2011 software (Carl Zeiss).

For nuclear diameter measurement, 10 random pictures with scale bars were picked manually from each image, containing both the edge and central area. The pictures were then moved to Seterology System (Carl Zeiss), and each nucleus was measured at pixels on two axial directions (longest and shortest) using the measure function of Image-Pro Plus software (Media Cybernetics, Rockville, USA). The average of two numbers was calculated as the final diameter. By relative to the scale bars, the original pixel unit was transferred to μm unit.

To count the cells, the image of whole section or 2-6 random pictures picked manually from images were used depending on the size of sections. To count the cells, plugin Cell Counter of ImageJ (NIH) was used. Cells were sorted to different groups by the pattern of co-localisation, and the number of cells in each group was counted manually by selecting the cell types and clicking cells of corresponding group once per cell. The numbers of clicks were automatically recorded as cell numbers by the plugin, and the results were finally exported as Microsoft Excel files using ImageJ.

The data were analysed using Microsoft Excel 2003 or 2010 and GraphPad Prism 5 software. The normality of data was analysed by D'Agostino & Pearson omnibus normality test. As the results showed that these were not normally distributed, the significance were analysed with a non-parametric Mann Whitney test instead of a parametric unpaired t-test.

Chapter 3

Validation of

Novel Methodologies

Chapter 3. Validation of Novel Methodologies

3.1 Introduction

The previous chapter describes in detail the methods applied in my research Most of these were developed based on manufacturer's protocol and/or published works, and thus further discussion of them is not required.

However, in this study, novel primers designed by myself, new antibodies and methods were also utilised. Despite some of them being used in, or reported by other studies, they had not been used in our lab and/or for the same experiments before. Therefore, it is necessary to validate these new materials/methods. In this chapter, I show how I verified these new materials and methods to make sure that the results I generated were robust and reproducible.

3.2 Results

3.2.1 Validating the specificity of PCR primers

Most of the primers used in my experiments were designed by me (for detailed design methods and primer list see Section 2.4.1 and Table 2.1). They were then checked on BLAST website (see Section 2.4.1) in Nucleotide Blast against human reference RNA sequence with default settings except the "Expect threshold" option was adjust to 1000, and only primers with low self-complementarity and high specificity (i.e the first several nucleotides at 5' end were not identical to any other human reference RNA sequence) were selected, to reduce the possibility that non-specific products would be amplified.

The PCR products generated with these primers were not sequenced. Instead, to test them, all primers were initially used in end-point PCR reactions using +RT and –RT human fetal ovary cDNA samples as template, and the products of these were run in agarose electrophoresis with ladders to see whether they were the predicted size (see Sections 2.4 and 2.5). *RPL32* primers were also used as a positive control to detect whether the PCR was working properly and whether there was contamination in the –RT samples. After electrophoresis, all tested primers show a clear single band of the correct predicted size (except a faint band of 150bp appeared in the +RT of *TEX14*), indicating that these are the expected products (Figure 3.1). Although the gel images of four primer pairs are shown here (as examples), this procedure was applied to all the primers used.

For qRT-PCR, the primers were first used to create a standard curve (Figure 3.2) of serially-diluted human fetal ovary cDNA (Section 2.4.3), during which the melt curves that revealed the amplifying efficiency were also recorded (Figure 3.3). Figure 3.2 shows the standard curves (slope value) of selected primer pairs, and when slope=-3.32 the DNA is ideally duplicated during each reaction cycle. The R^2 values that represented the correlation coefficient of these stand curves were also calculated and all were around 0.99. The melt curves of all primer pairs showed only single peak, suggesting that for each primer pair, only a single amplicon was produced in the qRT-PCR reaction include *TEX14*, which showed an unspecific band in end-point PCR. The melt curve peaks of different primer pairs clustered around

79-89ºC, all above the Tm value of primers, indicating that the size of these products is above those of the primers (Figure 3.3). The melt curves were also created during every qRT-PCR performed to make sure that only a single product of consistent melting temperature were amplified with no contamination.

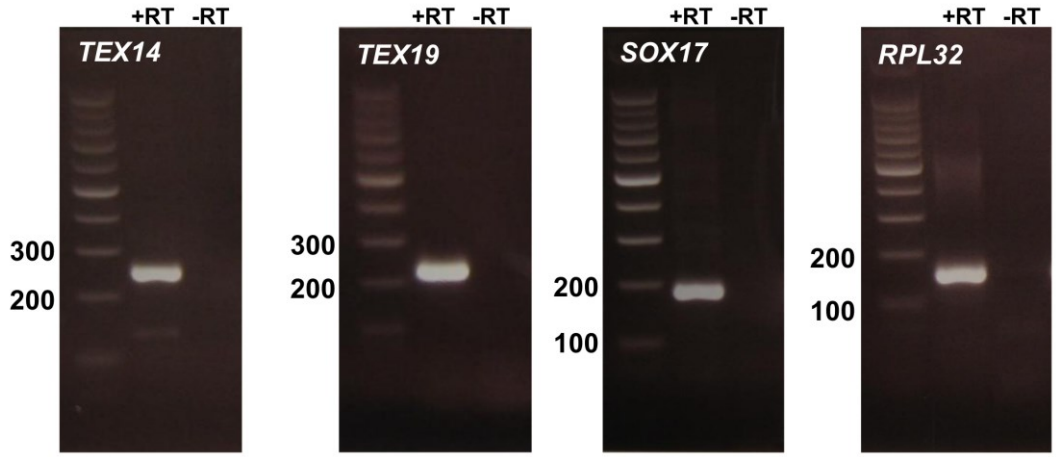

Figure 3. 1 The agarose gel images of PCR products generated from selected primer pairs using human fetal ovary cDNA as template.

TEX14 and *SOX17* primers were designed by me, and *TEX19* and *RPL32* primers were designed by staff of our lab. The predicted size of the products was *TEX14*=248bp, *TEX19*=220bp, *SOX17*=185bp, *RPL32*=153bp. Bands matched the right size when compare with ladders. No bands were detected in the –RT reactions.

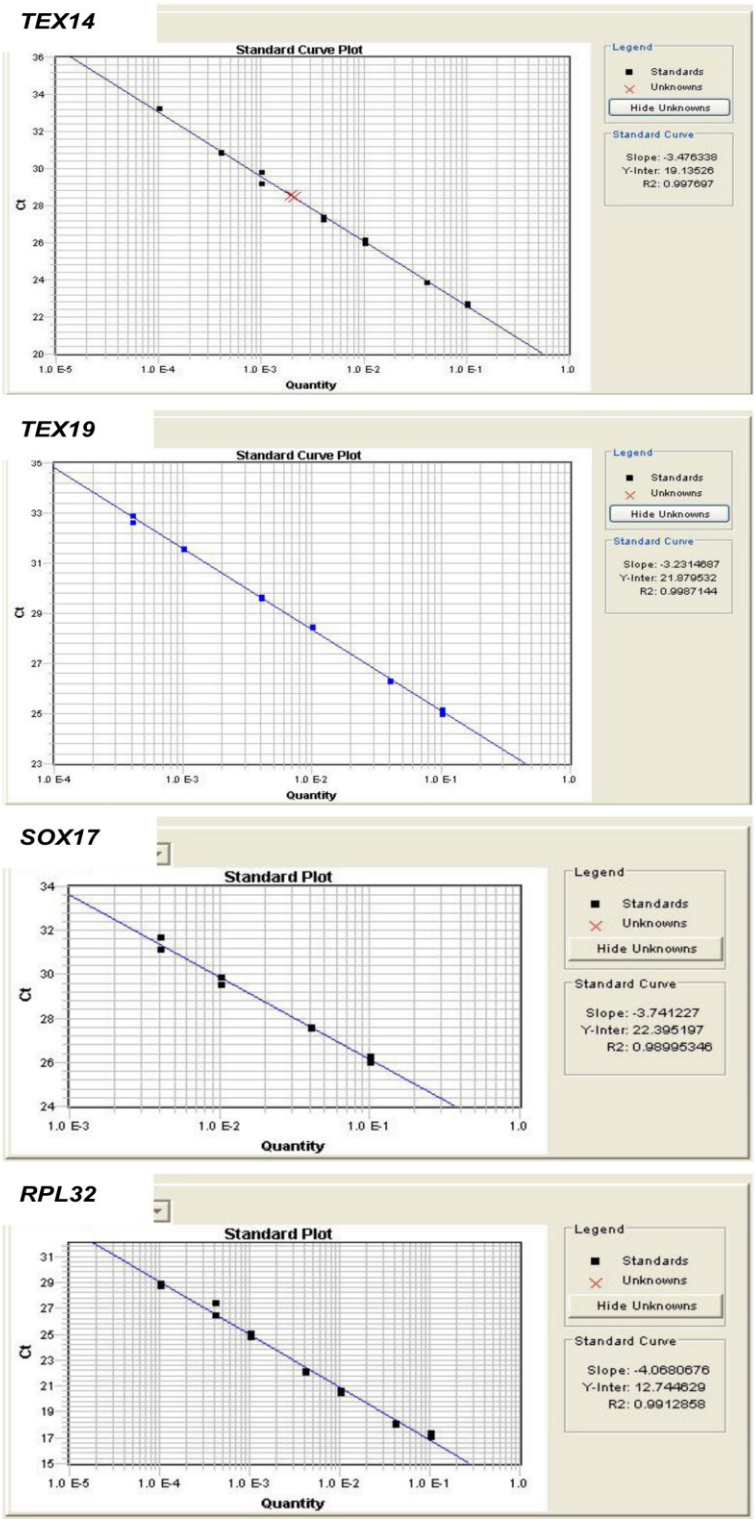

Figure 3. 2 Standard curves of selected primer pairs for qRT-PCR.

The slope values represent the efficiency of qRT-PCR. The slope value of each primer pairs are as follows: *TEX14*=-3.48, *TEX19*=-3.23, *SOX17*=-3.74 and *RPL32*=-4.07. The R^2 values recorded in all my experiments were around 0.99, suggesting that the scattered points in each slope showed a high linear dependence.

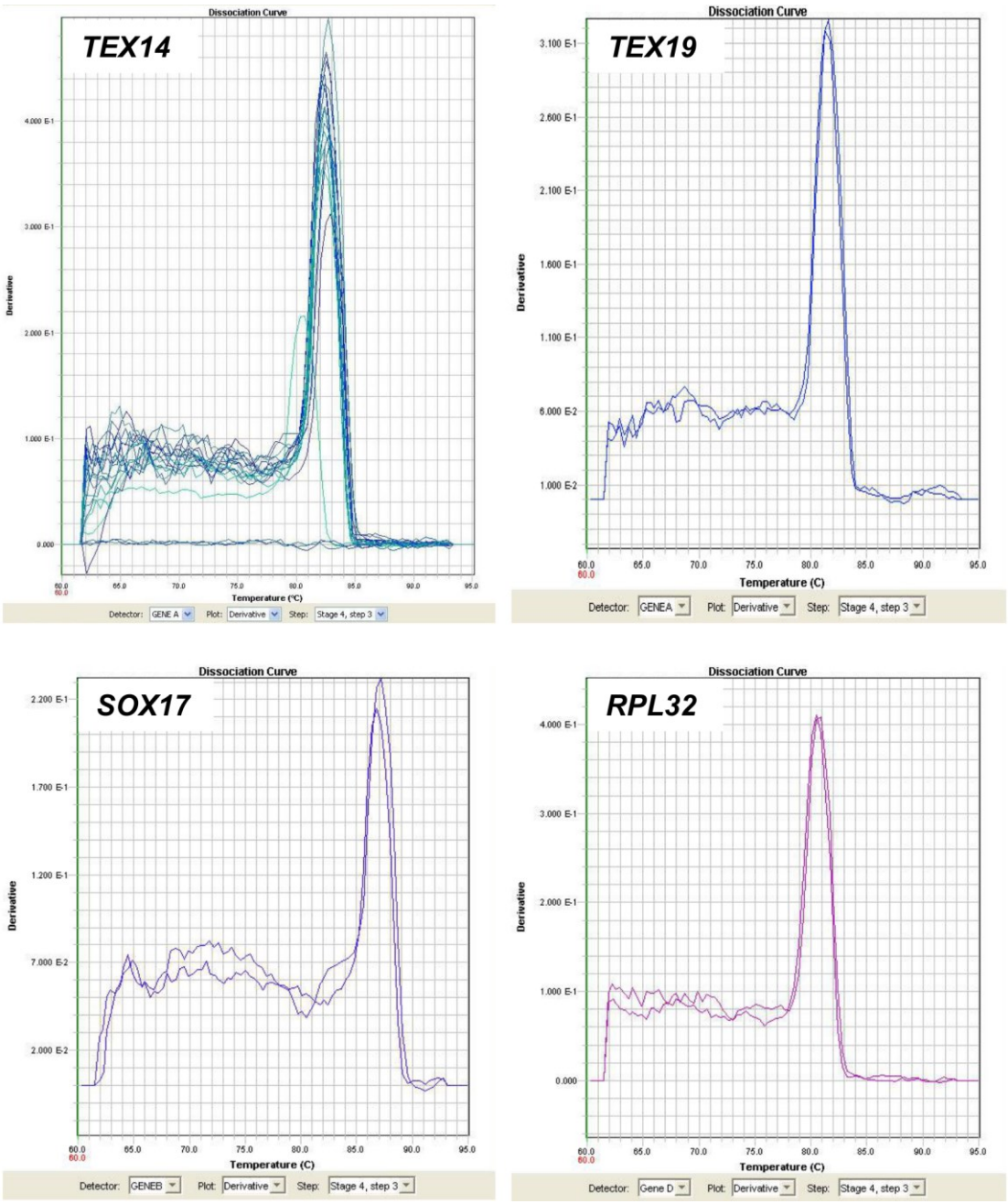

Figure 3. 3 The melt curves of qRT-PCR products using selected primers used during the PhD project.

All the products showed a single, unique peak ranges between 79 to 89ºC, indicating that only a single specific amplicon was generated during the qRT-PCR.

3.2.2 Specificity of the Dazl and Boll antibodies on mouse

To test the antibodies, we first performed DAB immunohistochemistry for Dazl and Boll on sections of adult mouse testis, before performing fluorescence immunohistochemistry, using rabbit anti-Dazl and mouse anti-Boll antibodies (see Section 2.15). No commercial available anti-Boll antibody has been shown to be specific on mouse, therefore we used the mouse anti-Boll antibody which can detect human BOLL. As the tissue is from mouse, and the Boll antibody raised in mouse, the Mouse on Mouse Polymer IHC kit (Abcam) was used for Boll staining. Each experiment was performed on sections from at least two individuals. Figure 3.4 show the images at both 10× and 40× magnification. Dazl is mainly distributed in the cytoplasm of germ cells at earlier stage of development (from spermatogonia to pachytene) across the edge of tubules, and it also show some weak staining in round spermatids (Figure 3.4), which is consistent with published data (Nicholas *et al.* , 2009, Ruggiu *et al.*, 1997). Boll expression is absent from spermatogonia and germ cells at early stage of development but dramatically increases in germ cells at later stages of meiosis prophase I (especially pachytene), and has some strong staining in round spermatids as well (Figure 3.4). This is also consistent with a previous report (VanGompel and Xu, 2010). No signal was detected in the negative control (primary antibody replaced by serum block), and these data suggest that our Dazl and Boll antibodies are both working effectively and specifically on mouse tissue. For a more accurate validation of antibodies, the combination of primary antibodies and the corresponding peptides which were used to raise them is a more robust choice of negative control. However, none of these peptides were commercially available from the manufacturers and therefore serum block was used instead.

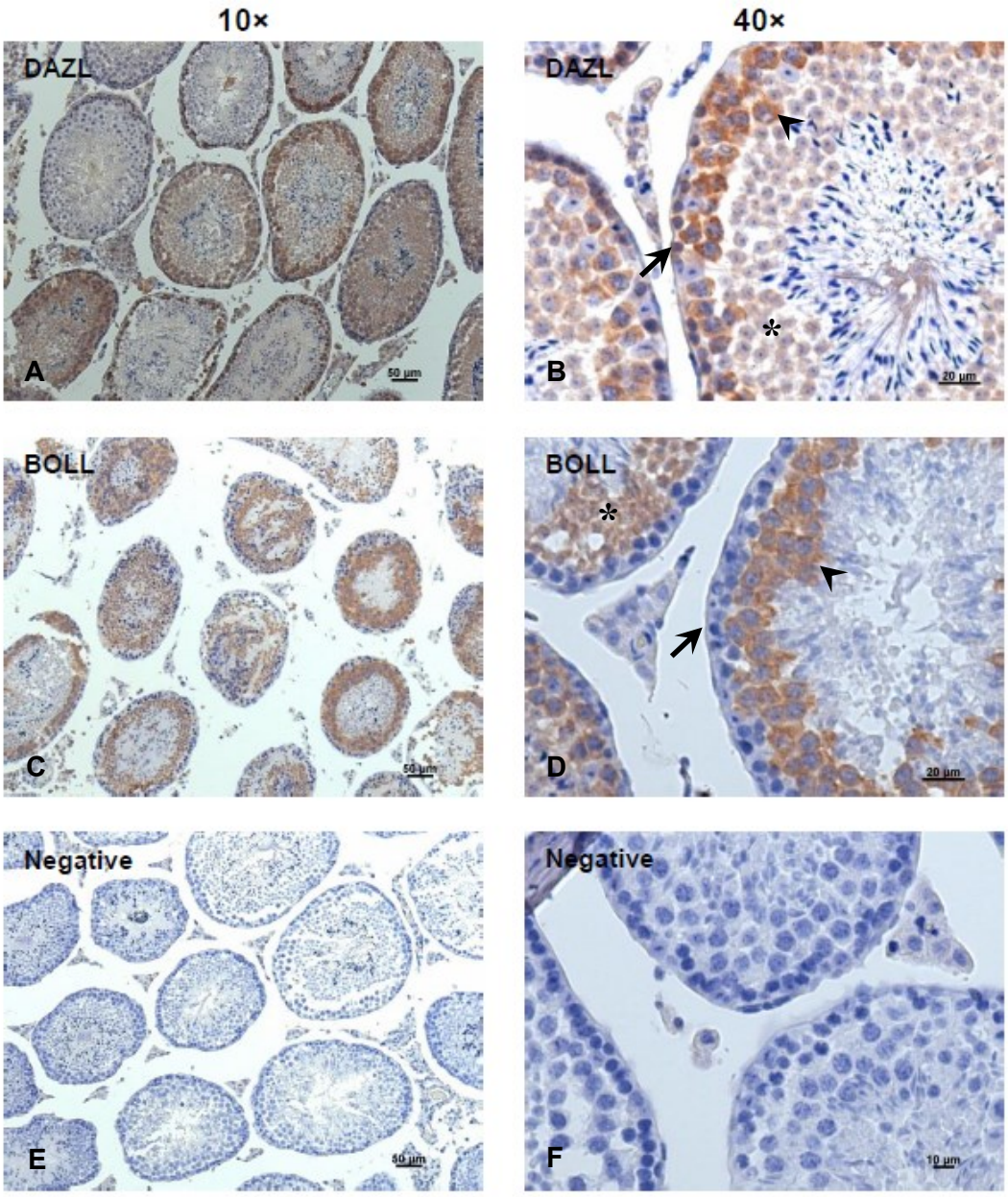

Figure 3. 4 DAB immunohistochemistry performed on adult mouse testis with rabbit anti-Dazl and mouse anti-Boll antibodies.

Left panels (A, C and E) are the 10× low power images to show the general distribution. Both Dazl and Boll are extensively expressed in the tubules. **A)** Dazl is distributed in germ cells at earlier stages which are located at the periphery of tubules whilst Boll is absent in these cells. **C)** Boll is extensively expressed in germ cells at later stage of meiosis prophase I. Right panels (B, D and F) are high resolution 40× images to show the details of the staining. **B and D)** Dazl but no Boll is expressed in the spermatogonia (arrows), and both proteins are expressed in pachytene spermatocytes (arrowheads) and round spermatids (asterisks). **E and F)** No non-specific staining detected in negative controls. Scale bar, left panel=50μm, right panel=10μm

3.2.3 DAZL and BOLL proteins are successfully expressed in HEK293 cells after transfection

To identify potential DAZL/BOLL targets, we transfected human cell lines with plasmid vectors encoding recombinant human *DAZL* or *BOLL* (with FLAG and Myc epitope tags) and compared mRNA target expression with empty vector transfected cells. We first used HEK293 cells to see whether DAZL/BOLL proteins were expressed successfully after transfection. Cells were transfected with either *pCMV6-DAZL*, *pCMV6-BOLL* or *pCMV6-Entry* (the latter being an empty vector, and will be referred to subsequently as the 'Control'). Western blotting was performed to detect protein expression 48h after transfection. As the recombinant DAZL/BOLL proteins are FLAG-tagged, three primary antibodies (anti-DAZL (AbD Serotec), anti-BOLL (Abcam) and anti-FLAG (Sigma-Aldrich)) were used. On each set of blots, containing lysates of each of the empty vector, DAZL, and BOLL transfected cells, bands of the expected size (DAZL=36.8kDa, 33.2kDa of DAZL+3.6kDa of FLAG-Myc tag; BOLL=34.9kDa, 31.3kDa of BOLL+3.6kDA of FLAG-Myc tag) were detected by the appropriate antibodies (Figure 3.5), with no bands of the expected size in the control (empty vector-transfected) lanes, suggesting that the appropriate proteins were expressed, and could be specifically detected by the relevant antibodies without cross-reactivity between DAZL and BOLL.

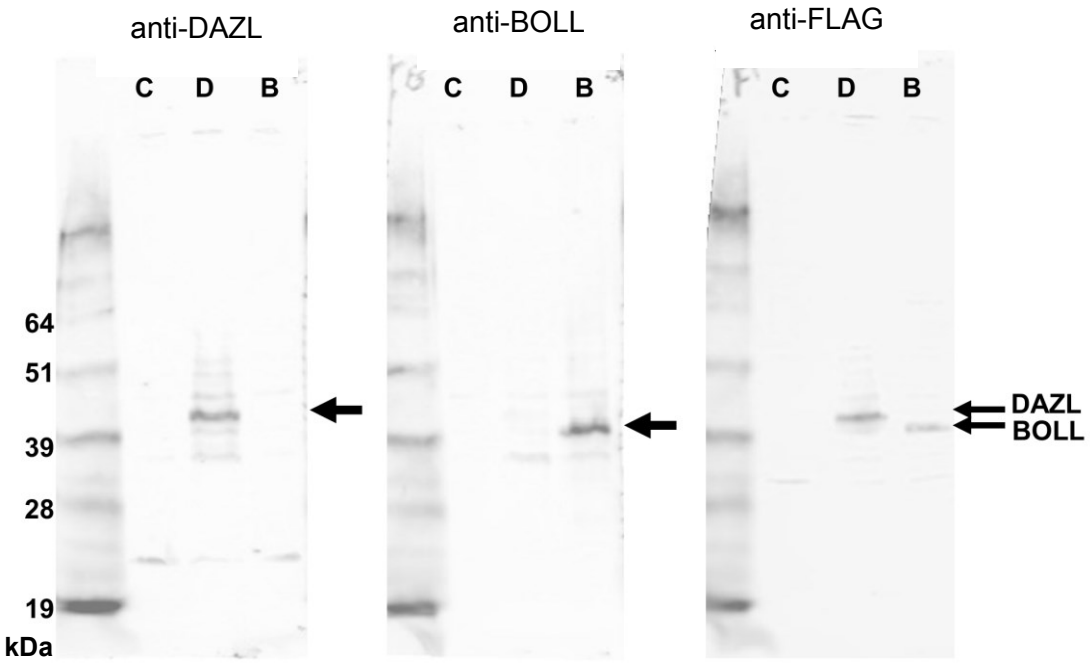

Figure 3. 5 Western blotting for FLAG-tagged DAZL/ BOLL transfected HEK293 cells. DAZL, BOLL and FLAG antibodies were used as the primary antibodies. Each set of blots include proteins isolated from *pCMV6-Entry* (C), *pCMV6-DAZL* (D) or *pCMV6-BOLL* (B) transfected HEK293 cells. DAZL and BOLL antibodies detected a single band in DAZL/BOLL expressing samples, respectively; each band has the same size as the one detected by FLAG antibody in corresponding lanes. No similar signals were found in the empty vector (*pCMV6-Entry*) transfected cells, suggested that the corresponding proteins were only produced by and detected in the transfected cells and therefore the vectors are functional.

3.2.4 Specificity of the DAZL and BOLL antibodies on human

After testing the specificity of these antibodies in western blotting, we next test the specificity of these antibodies (mouse anti-DAZL (AbD Serotec)), mouse anti-BOLL (Abcam) and rabbit anti-DAZL (Cell Signaling Technologies)) for use in fluorescence immunocytochemistry on *pCMV6-DAZL*, *pCMV6-BOLL* or mock transfected HEK293 cells, to some antibodies may only be appropriate for western blotting or had not previously been reported to work in immunocytochemistry. Each antibody was applied to all three types of transfected cells, and as in the western blotting, both the anti-DAZL antibodies detected antigens in only DAZL-transfected cells, whilst the staining in BOLL-transfected cells only appears when using the anti-BOLL antibody (Figure 3.6). In addition, no signal was detected in mock transfected cells, suggesting that all the antibodies are also specific when applied with immunocytochemistry methods.

Together, these results confirm that the anti-DAZL and anti-BOLL antibodies we used could effectively and specifically detect human DAZL or BOLL proteins using both western blotting and immunohistochemistry/immunocytochemistry.

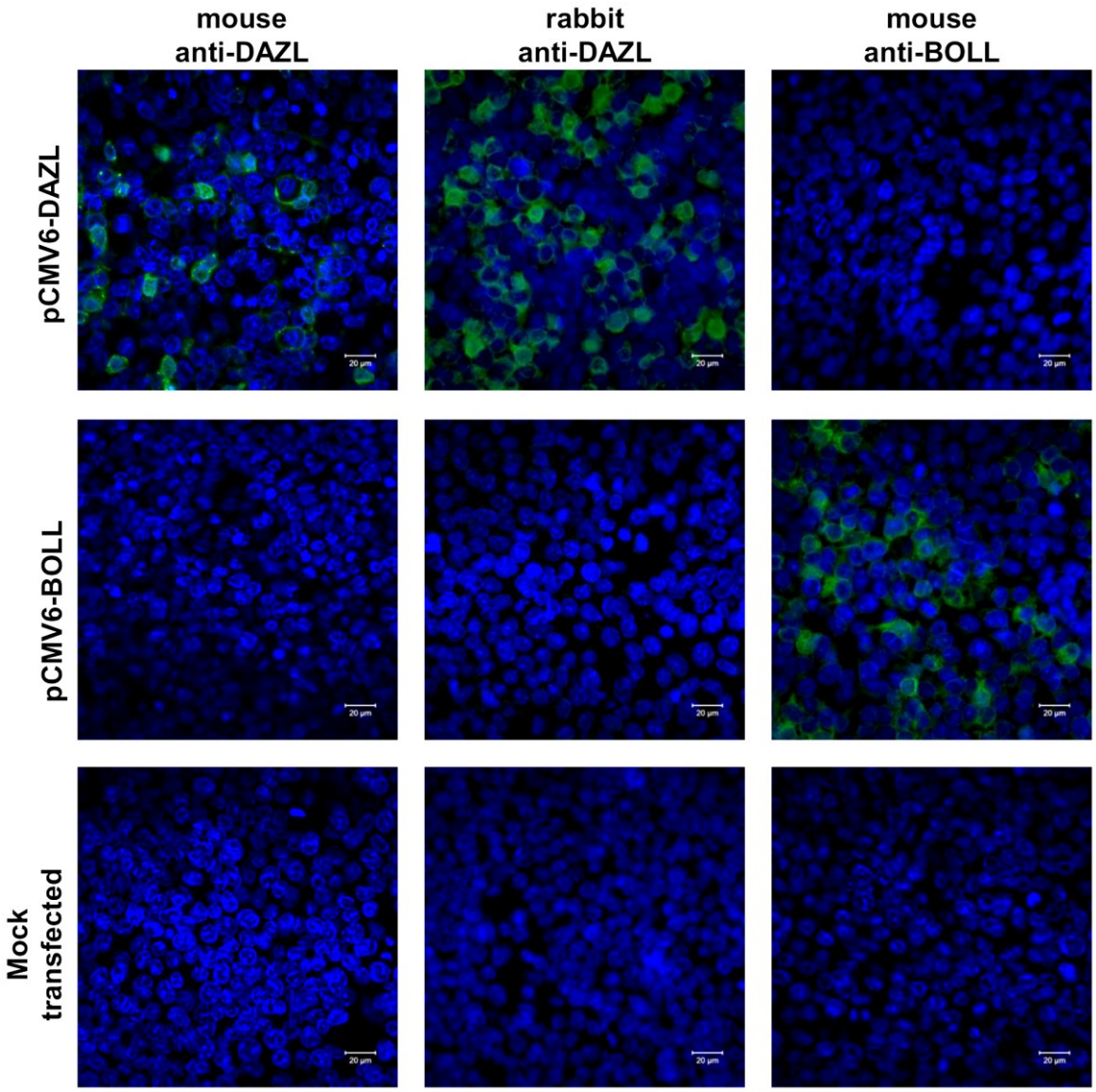

Figure 3. 6 Specificity of DAZL and BOLL antibodies in fluorescence immunocytochemistry. Each image shows the HEK293 cells transfected with *DAZL* or *BOLL* vectors, or mock (only treated by transfection reagent) transfected cells. Both anti-DAZL antibodies detected DAZL^{+ve} cells in only DAZL transfected cells, and similarly the anti-BOLL antibody detected BOLL^{+ve} cells in only BOLL transfected cells. No signal was detected in mock transfected cells. Counter stained with DAPI, Scale bar=20µm

3.2.5 Establishing stably transfected TCam-2 cells expressing DAZL or BOLL

TCam-2 cells are a cell line generated from human germ cell (male) tumor (Mizuno *et al.* , 1993). Previous studies have demonstrated that TCam-2 cells express several germ cell and meiosis markers at both the mRNA and protein levels, (de Jong *et al.* , 2008a, de Jong *et al.* , 2008b, Eckert *et al.* , 2008, Nettersheim *et al.* , 2011) but do not express DAZL or BOLL protein (our unpublished work), and thus they might be a better model to study the functions of DAZL and BOLL than HEK293 cells.

We first tried to transfect the TCam-2 cells with the same transient methods which were applied to HEK293 cells as described in previous sections (See Section 2.7). However, no protein was detected following western blotting (data not shown). This might be due to the low transfection ratio of TCam-2 cells of ~15% (which was confirmed by the experiments of other projects in our lab). Therefore, we decided to establish a stably transfected TCam-2 cell line using G418 selection as the vectors contained a neomycin resistance gene. TCam-2 cells were transfected with either *pCMV6-DAZL*, *pCMV6-BOLL* or *pCMV6-Entry* (empty) vectors and then cultured in media which contained G418 (see Section 2.6). After selection, RT-PCR was performed. Cells transfected with *pCMV6-DAZL* or *pCMV6-BOLL* showed a very strong band when using corresponding primers indicating that the vectors had been stably integrated and were expressing mRNA (Figure 3.7A). However, when we tried to detect the proteins by western blotting with both DAZL and FLAG primary antibodies, no specific bands were detected in the stably transfected samples (Figure 3.7B). A strong band at the predicted size of DAZL appeared in the lanes of transfected HEK293 cells (the positive control) however, suggesting that the western blotting was effective (Figure 3.7B). Similar experiments were performed on the BOLL stably transfected cells and the results were similar (data not shown). Furthermore, we used immunocytochemistry to test the protein expression (Figure 3.7C). However, no cytoplasmic staining was seen in the *pCMV6-DAZL* transfected cells and there was no difference between *pCMV6-DAZL* or empty vector stably transfected TCam-2 cells (Figure 3.7C). In addition, clear cytoplasmic staining occurred in the *pCMV6-DAZL* transfected HEK293 cells, indicated that the immunocytochemical method was also effective (Figure 3.7C), and although the

stably transfected TCam-2 cells were expressing the mRNA, no DAZL or BOLL protein was produced.

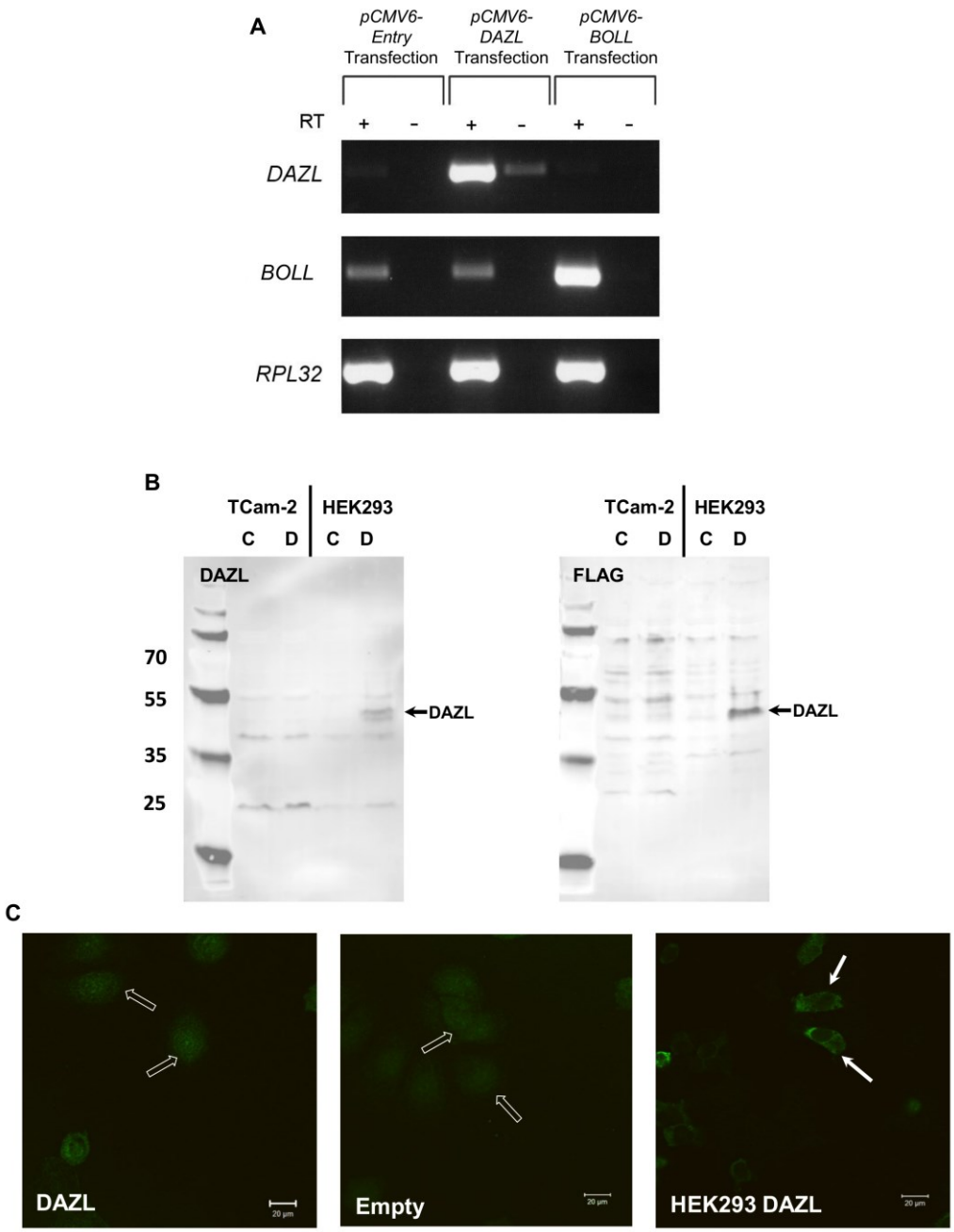

Figure 3. 7 Detection of mRNA and protein for stably transfected TCam-2 cells.

A) RT-PCR for the stably transfected TCam-2 cells. When using the *DAZL* primers, a very strong band appeared in only the +RT of *pCMV6-DAZL* transfected sample, and so did the *BOLL* primers. A faint band occurred in the –RT of *pCMV6-DAZL* samples, possibly caused by residual plasmid contamination. *RPL32* was used as the positive control for RT-PCR. **B)** Western blotting with DAZL or FLAG primary antibodies for stably transfected TCam-2 cells and transiently transfected HEK293 cells. C=Control (empty vector), D=DAZL. No specific band is detected in all the lanes of TCam-2 samples and empty vector transfected HEK293 cells, and strong bands of DAZL appeared in the lanes of DAZL expressing HEK293 samples. **C)** Immunocytochemistry of stably transfected TCam-2 cells and transiently transfected HEK293 cells. The *pCMV6-DAZL* transfected TCam-2 cells only show very weak background nuclear staining and could not be distinguished from the empty vector transfected cells (unfilled arrows). In contrast, the DAZL expressing HEK293 cells (positive control) have very clear cytoplasm staining (arrows). Scale bar=20μm

3.2.6 *pCMV-DAZL* vector is successfully expressed in TCam-2 cells

After the unsuccessful attempt to make stably transfected TCam-2 cells, it appears that the translation of protein of *pCMV6* vectors was blocked in TCam-2 cells, based on the fact that the *pCMV6* vectors produced proteins in HEK293 cells, but only RNA in TCam-2 cells. We then sought other vectors and obtained a *pCMV-DAZL* vector (recombinant human DAZL tagged with T7, provided by Dr. Joao Pedro Sousa Martins from Prof. Nicola Gray's group, MRC CRH).

To test the vector, TCam-2 cells and HEK293 cells were transiently transfected with the *pCMV-DAZL* or *pCMV6-DAZL* vectors, and western blotting or immunocytochemistry with primary antibody against DAZL performed to test protein expression. By western blotting (Figure 3.8), a clear band was detected in the lane of *pCMV-DAZL* transfected TCam-2 cells (~34kDa) and also in the lane of *pCMV6-DAZL* transfected HEK293 cells (i.e. positive control, Figure 3.8A), No bands of the correct size were detected in the lane containing lysates from control vector (*pCMV6-Entry*) transfected TCam-2 cells. The small size difference may due to the different tags on the DAZL protein – the FLAG-Myc tagged DAZL is ~37kDa and the T7 tagged DAZL is 34.3kDa (33.2kDa of DAZL+1.1kDa of T7 tag). Similar results were also obtained by immunocytochemistry. Clear cytoplasmic staining was detected in the *pCMV-DAZL* transfected TCam-2 cells and also *pCMV6-DAZL* transfected HEK293 cells, but no such staining was found in the mock transfected (only treated with transfection reagent TransIT-LT1) TCam-2 cells. These experiments indicate that the *pCMV-DAZL* vector is effective at producing DAZL protein when transfected into TCam-2 cells.

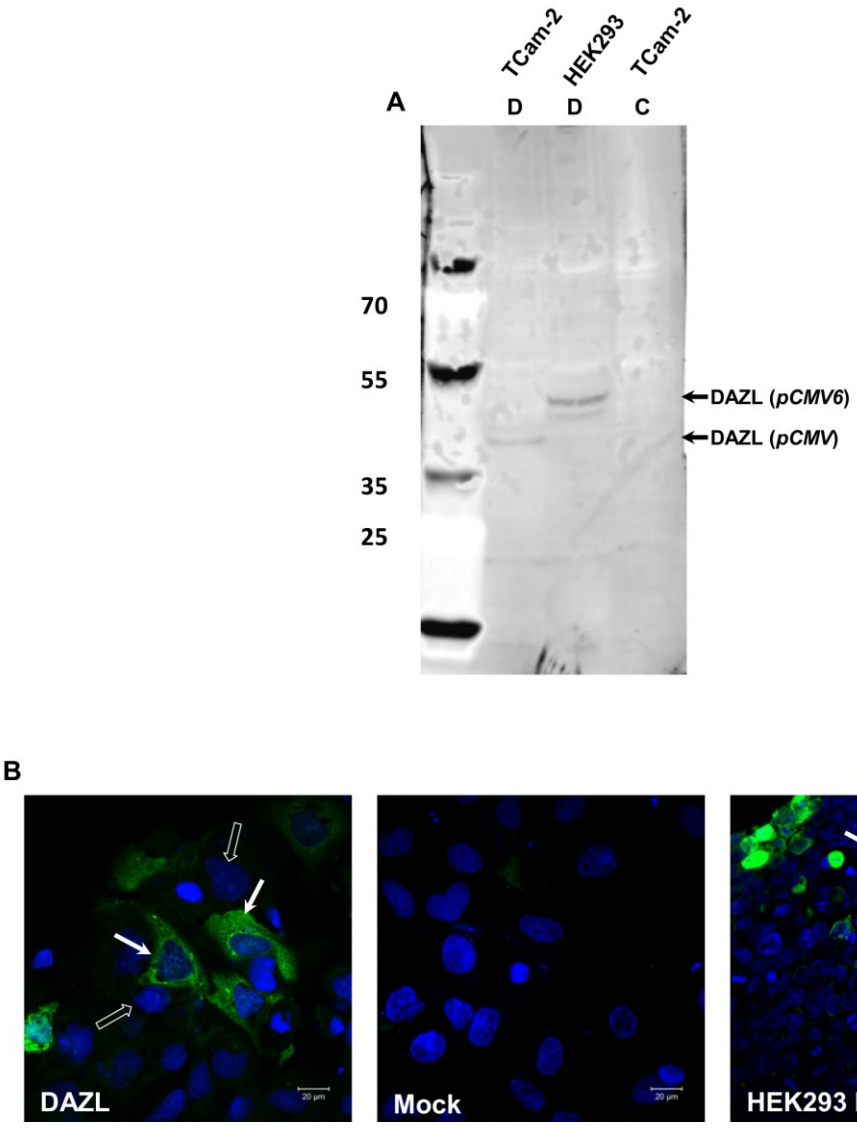

Figure 3. 8 The *pCMV-DAZL* vector is expressed in TCam-2 cells.

TCam-2 cells were transfected with *pCMV-DAZL*, and HEK293 cells transfected with *pCMV6-DAZL* vectors were used as the positive control. **A)** Western blotting for *DAZL* transfected cells. The bands of DAZL protein are detected in both *DAZL* expressing TCam-2 and HEK293 cells (positive control), and no bands at the size of DAZL are detected in empty vector transfected TCam-2 cells. The size difference of the DAZL bands between the TCam-2 and HEK293 is probably due to the different tags on DAZL protein (34kDa in TCam-2 transfected with T7 tagged *pCMV* vectors and 37kDa in HEK293 transfected with FLAG+Myc tagged *pCMV6* vectors. TC=TCam-2, HEK=HEK293, D=DAZL, C=Control (empty vector). **B)** Fluorescence immunocytochemistry for *DAZL* expressing cells. Green DAZL staining (arrows) is seen in both *DAZL* transfected TCam-2 cells (left panel) and HEK293 cells (right panel) with *pCMV* and *pCMV6* vectors respectively, however most TCam-2 cells are still DAZL^{-ve} (unfilled arrows). No green staining is found in mock transfected TCam-2 cells (middle panel), suggesting that the DAZL staining is specific. Counter stained with DAPI, Scale bar=20μm

3.2.7 Establishment of the co-transfection/FACS system for TCam-2 cells

Although we demonstrated that TCam-2 cells could express DAZL protein when transfected with the *pCMV-DAZL* vector, the transfection ratio of these cells was still very low, which made it very difficult to observe effects after transfection. Moreover, it was not possible to make a stable line with this vector as it does not contain an antibiotic resistance marker for selection in eukaryotic cells. To solve this problem, we developed a co-transfection/FACS system with a second, GFP-expressing vector, to separate the transfected/untransfected cells based on previous reports that cells co-transfected with two fluorescent reporters generally express both proteins (Susa *et al.* , 2008). The TCam-2 cells were transfected with both *pCMV-DAZL* and *pEGFP-C1* vectors for 48h. Cells were then harvested and sorted by Fluorescence-Activated Cell Sorting (FACS) detecting the GFP fluorescence. DAPI was also added to mark the dead cells before FACS and the staining was detected by another gate to ensure the cells collected during FACS were live.

To test this system, western blotting was first applied to the sorted cells. Three replicates were performed on different passages of cells. The blots were incubated with anti-DAZL, anti-GFP and anti-α-tubulin primary antibodies. α-tubulin was detected in all the lanes, demonstrating equivalent loading of protein. Bands corresponding to DAZL and GFP were detected in the lanes of transfected cell suspension before FACS (unsorted) and GFP^{+ve} cells. No similar bands were seen in GFP^{-ve} cells. Furthermore, both DAZL and GFP bands were much stronger in the lane of GFP^{+ve} cells compared to the unsorted cells, implying that both GFP and DAZL proteins were enriched in the GFP^{+ve} cells (Figure 3.9A). To semi-quantify the western blotting, the intensity of DAZL and GFP bands relative to α-tubulin was determined. Because of high background, the average value of GFP^{-ve} cells became negative. The data were analysed using paired t-test. When compared to the mock transfection, the intensity of the DAZL band increased 3.66±0.79 fold in GFP^{+ve} cells, and GFP increased for 3.54±0.62 fold, both were significant ($p<0.05$, $n=3$). In contrast, almost no DAZL or GFP protein was found in the GFP^{-ve} samples (Figure 3.9B).

qRT-PCR was also used to compare the mRNA levels of *DAZL* and *GFP* between GFP^{+ve} and GFP^{-ve} cells. The experiments were performed 5 times on different passages of cells and each sample was replicated for twice for qRT-PCR. The average Ct value was calculated and the results were related with *RPL32*. Data were analysed with paired t-test. Both *DAZL* and *GFP* mRNA levels in the GFP^{+ve} cells were significantly higher than those in the GFP^{-ve} cells (Figure 3.9C), suggesting that DAZL was enriched in GFP^{+ve} cells at both mRNA and protein levels, and thus the co-transfection/FACS system effectively separates the $GFP^{+ve}/DAZL^{+ve}$ and $GFP^{-ve}/DAZL^{-ve}$ TCam-2 cells.

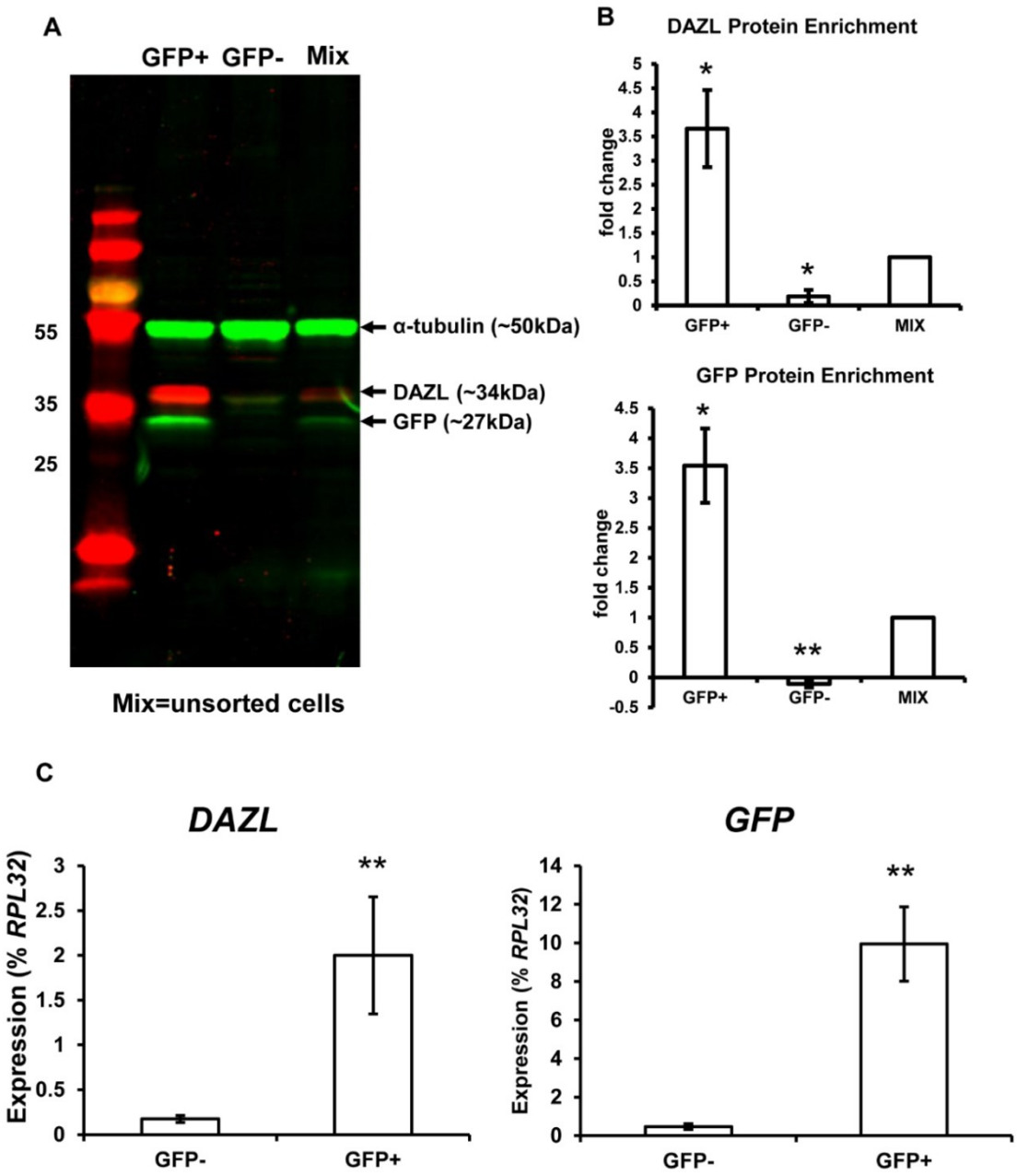

Figure 3. 9 The GFP and DAZL expression in co-transfected TCam-2 cells after FACS at both protein and mRNA levels.

A) Western blotting for GFP^{+ve}, GFP^{-ve} and unsorted TCam-2 cells. Both the GFP^{+ve} and unsorted samples show bands for DAZL and GFP proteins, and no bands at similar sizes are detected in GFP^{-ve} cells. **B)** Quantification of the western blotting. DAZL increases 3.66±0.79 and GFP increases 3.54±0.62 fold after sorting when compared to the unsorted cells, and the amount of DAZL or GFP protein is extremely low in the GFP^{-ve} cells. n=3, *p<0.05, **p<0.01. **C)** qRT-PCR to quantify the mRNA expression of *DAZL* and *GFP* in GFP^{+ve} and GFP^{-ve} TCam-2 cells. Both DAZL and GFP mRNA are expressed significantly higher in GFP^{+ve} cells, all relative to *RPL32*. n=5, **p<0.01

3.2.8 Establishment of RNA immunoprecipitation experiments using human DAZL

To investigate the interaction between DAZL protein and its mRNA targets, we also established RNA immunoprecipitation (RIP) experiments to immunoprecipitate DAZL and then isolate/determine the RNA which was co-precipitated with the DAZL protein. Despite this antibody has not been reported to be used for RIP in other studies, it is stated by the manufacturer that being suitable for RIP and the recommended concentration is given.

HEK293 cells were co-transfected using the combination of Luciferase vectors (see Table 3.1) which were conjugated with *GAPDH* or *TEX14* 3'-UTR, together with *pCMV6-Entry* (empty) or *pCMV6–DAZL* vectors for 48h, and then DAZL protein was immunoprecipitated using the Millipore RIP kit (see Section 2.8). Western blotting was applied on the protein samples before (Input) and after immunoprecipitation (RIP) to find out whether the DAZL was expressed and precipitated successfully. The mouse anti-DAZL, rabbit anti-DAZL and also mouse anti-α-tubulin were used as primary antibodies. Emission spectra 680nm (red channel) anti-rabbit IgG and emission spectra 800nm (green channel) anti-mouse IgG antibodies were used as secondary antibodies.

Table 3. 1 The combination of vectors in the RIP

pCMV6-Entry vec+ Luc-GAPDH 3'-UTR	***pCMV6-Entry vec+ Luc-TEX14 3'-UTR***
pCMV6-DAZL vec+ Luc-GAPDH 3'-UTR	***pCMV6-DAZL vec+ Luc-TEX14 3'-UTR***

Figure 3.10A shows the western blot for Input samples. Two red DAZL bands detected by rabbit anti-DAZL antibody were seen only in the lanes from DAZL co-transfected samples. The mouse anti-DAZL antibody also detected DAZL-sized bands at the same size in these two lanes, suggesting that DAZL was expressed in the DAZL co-transfected cells before RIP. After RIP (Figure 3.10B), the rabbit anti-DAZL antibody detected not only the DAZL bands in DAZL-transfected

samples, but also the antibody heavy chain and light chain in all the lanes, because this antibody was also the one used to precipitate DAZL. In contrast, in channel 800 (Green) only two DAZL bands appeared in the DAZL transfected samples and no band of α-tubulin or heavy/light chain was seen. Both the merged images of INPUT and RIP showed that the red and green bands of DAZL detected by different primary antibodies completely overlapped (yellow), indicating that DAZL is specifically expressed in the DAZL co-transfected cells and successfully precipitated in RIP experiments, without detectable contamination of other proteins such as α-tubulin.

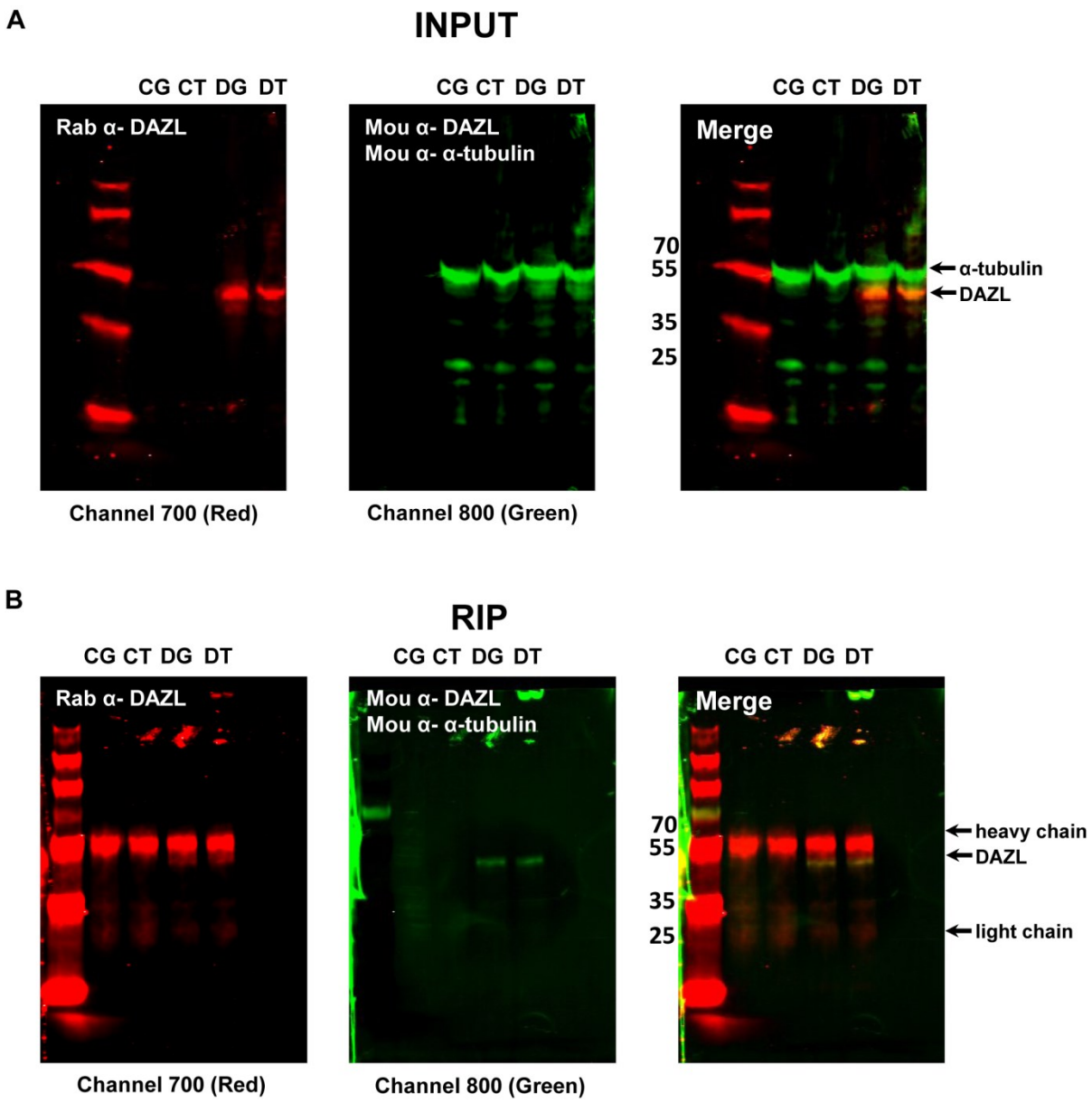

Figure 3. 10 DAZL protein is successfully precipitated in the RIP experiments.

A) The western blotting for INPUT samples before RIP. Both mouse and rabbit anti-DAZL antibodies detect DAZL bands (~37kDa) only in the lanes of DAZL transfected samples, and the mouse anti-α-tubulin (loading control) detects the bands of α-tubulin (~50kDa) at the expected size in all the lanes. **B)** Western blotting for the RIP samples. The rabbit anti-DAZL antibody detects the bands of its own heavy (~50kDa) and light (~25kDa) chain in all the lanes and two DAZL bands in only DAZL transfected samples. The mouse anti-DAZL antibody also detects the same DAZL bands in DAZL transfections, and no α-tubulin is found in these blots, suggesting that DAZL is specifically precipitated in the experiments.

CG=*Entry+GAPDH-Luc*, CT=*Entry+TEX14-Luc*, DG=*DAZL+GAPDH-Luc*, DT=*DAZL+TEX14-Luc*

3.3 Conclusion

In this chapter, the results obtained in validation experiments are shown, to verify the novel materials and methods applied during this PhD project.

For PCR, the quality of primers was strictly controlled from the step of design. The products of all the primers used show a band of predicted size in agarose electrophoresis following end-point PCR, as well as a single peak in melt curve during qRT-PCR, suggests that only single product was created from each primer pair. Therefore, all the primers should be specific. However this procedure could still be improved by cloning and sequencing the PCR products to further confirm the specification.

For the validation of antibodies, the antibodies used are specific for both western blotting and immunohistochemistry on human protein. The mouse anti-DAZL antibody (AbD Serotec) and the mouse anti-BOLL antibody (Abcam) have not been previously reported on mouse tissue. However both Dazl and Boll show identical staining expression comparing to the previous studies (Ruggiu *et al.*, 1997, VanGompel and Xu, 2010). Furthermore, data using the mouse anti-DAZL antibody in immunohistochemistry have been published by both our lab and another lab (Anderson *et al.*, 2007, Conrad *et al.* , 2014).

The novel methods, namely transfection/FACS and RIP, although never been applied by our lab, both work successfully as described in previous sections. In addition, the RIP had been successfully applied by Reynolds *et al.* (2005) and Jiao *et al.* (2002) to identify the mouse Dazl targets, suggested that it is an effective method for this purpose. Overall, the experiments described in this chapter confirmed the efficiency of the new materials and technologies, and these are all necessary for the aims of this thesis and were working properly.

Chapter 4

DAZL and BOLL Expression during Human and Mouse Germ Cell Development in Fetal Ovary

Chapter 4. DAZL and BOLL Expression during Human and Mouse Germ Cell Development in Fetal Ovary

4.1 Introduction

DAZL and BOLL are RNA-binding proteins from the DAZ family, of which all three members (DAZ, DAZL and BOLL) are expressed in germ cells (Eberhart *et al.*, 1996, Reijo *et al.*, 1995, Saxena *et al.*, 1996) and can bind to, and regulate the translation of, their mRNA targets (Collier *et al.*, 2005). DAZL is expressed only in vertebrates, whilst BOLL is expressed in almost all the metazoans. Both DAZL and BOLL are associated with infertility and subfertility phenotypes in both human and model animals (Eberhart *et al.*, 1996, Karashima *et al.*, 2000, Lin *et al.*, 2009, Ruggiu *et al.*, 1997, Tung *et al.*, 2006b, Tung *et al.*, 2006c, VanGompel and Xu, 2010). Dazl-deficiency leads to sterility in both sexes of mice (Ruggiu *et al.*, 1997)In humans, four DAZL mutations and seven SNPs have been identified that are associated with subfertility phenotypes in both sexes, such as azoospermia, sperm count, early menopause and ovarian failure (Tung *et al.*, 2006b, Tung *et al.*, 2006c).

Compared to DAZL, BOLL has not been extensively studied, although several studies have suggested that Boll is required for the germ cell development in various species from flies and worms, to fish and mice (Eberhart *et al.*, 1996, Karashima *et al.*, 2000, VanGompel and Xu, 2010). In mice, *Boll* deficiency leads to infertility in males only, due to post-meiotic spermatogenic defects at elongating spermatid stage, whereas females are fertile (VanGompel and Xu, 2010). A similar sex-biased phenotype of azoospermia also occurs in bol-deficient *Drosophila* (in which *bol* expression is male specific as well) (Eberhart *et al.*, 1996) and *C.elegans* (in which it causes sterility in hermaphrodites, affecting oogenesis) (Karashima *et al.*, 2000), and both organisms show meiosis arrest phenotypes. There are fewer relevant studies on human BOLL compared to model animals. Kostova *et al.* (2006) demonstrated that reduced BOLL expression is associated with human spermatogenic failure, including Sertoli cell only syndrome and meiosis arrest, and higher levels of *BOLL* transcripts were detected in azoospermia patients with successful sperm retrieval when compared to patients in which it failed (Lin *et al.*, 2005). However, no studies have

documented how BOLL functions during human oogenesis. It has been suggested that Boll protein is not produced in the mammalian female germline, (as occurs in *Drosophila*) although low levels of transcripts have been detected in the mouse ovary (Eberhart *et al.*, 1996, Shah *et al.*, 2010, Xu *et al.*, 2001).

The macroscopic phenotypes caused by the loss of DAZL and BOLL reveal their microscopic functions during germ cell development. In *Xenopus*, dazl is necessary for early germ cell migration to the genital ridge and also the maintenance of a normal number of germ cells (Houston and King, 2000). The mouse *Dazl*$^{-/-}$ sterility phenotype arises from a meiotic arrest at early pachytene in females and at leptotene in males in mice with an outbred genetic background (Ruggiu *et al.*, 1997, Saunders *et al.*, 2003). On an inbred background, earlier defects are observed, with germ cell loss in males due to apoptosis by e15.5 (Lin and Page, 2005) and a failure to enter meiosis appropriately in female germ cells (Lin *et al.*, 2008). Dazl is also reported to be required for sexual differentiation (Gill *et al.* , 2011), mRNA transport through interaction with the dynein motor complex in mouse germ cells (Lee *et al.*, 2006), and epigenetic programming and maintaining the pluripotency of mouse PGCs (Haston *et al.*, 2009). In contrast, the functions of BOLL are still unclear. It seems to promote G2/M transition in *Drosophila* meiosis by regulating its target *twine* (Eberhart *et al.*, 1996), and is also has meiotic functions in *C.elegans* oogenesis based on the meiosis arrest phenotype in boll-deficient worms (Karashima *et al.*, 2000). Notably, both DAZL and BOLL are highly functionally conserved between species: human DAZL can partially rescue the mouse *Dazl*$^{-/-}$ phenotype (Vogel *et al.*, 2002), and human BOLL can rescue *Drosophila boll*-deficient phenotypes as well (Xu *et al.*, 2002). This suggests that DAZL or BOLL functions might be highly conserved between human and model animals as well.

Key to understanding the complicated functions of DAZL or BOLL during human germ cell development is establishing the expression period and patterns of DAZL and BOLL at particular stages of development. Several studies have revealed the expression of DAZL and BOLL in human testis (Anderson *et al.*, 2007, Kostova *et al.*, 2007, Lin *et al.*, 2009, Luetjens *et al.*, 2004, Reijo *et al.*, 2000, Ruggiu *et al.*, 2000, Xu *et al.*, 2001). In the testis, DAZL is extensively expressed at several stages

of spermatogenesis including spermatogonia, early and late spermatocytes, and post-meiotic cells (Reijo *et al.*, 2000), whilst BOLL is mainly expressed in pachytene spermatocytes and persists through to germ cells forming early spermatids. The expression of DAZL and BOLL show minimal overlap (Lin *et al.*, 2009, Luetjens *et al.*, 2004, Xu *et al.*, 2001), indicating they may have different functions at different stages of germ cell development (Xu *et al.*, 2001). Furthermore, DAZL shows a dynamic pattern of translocation from nucleus to cytoplasm during human spermatogenesis (Reijo *et al.*, 2000, Ruggiu *et al.*, 2000), which may be an indicator of the activation of its RNA-binding function.

Unlike the male, meiosis starts in human females during fetal life. To study oogenesis in humans, early ovarian development can be divided to three trimesters (see Section 1.2.1 and Figure 1.1). In humans, meiosis initiates at early second trimester and arrests as oocytes form primordial follicles in the late second trimester (Hartshorne *et al.* , 2009). In mice, meiosis initiates at e12.5 and arrests around postnatal day 0 (P0) (Borum, 1961). The figure below shows images of different developmental stages of human and mouse fetal ovaries, which were used in this study (Figure 4.1).

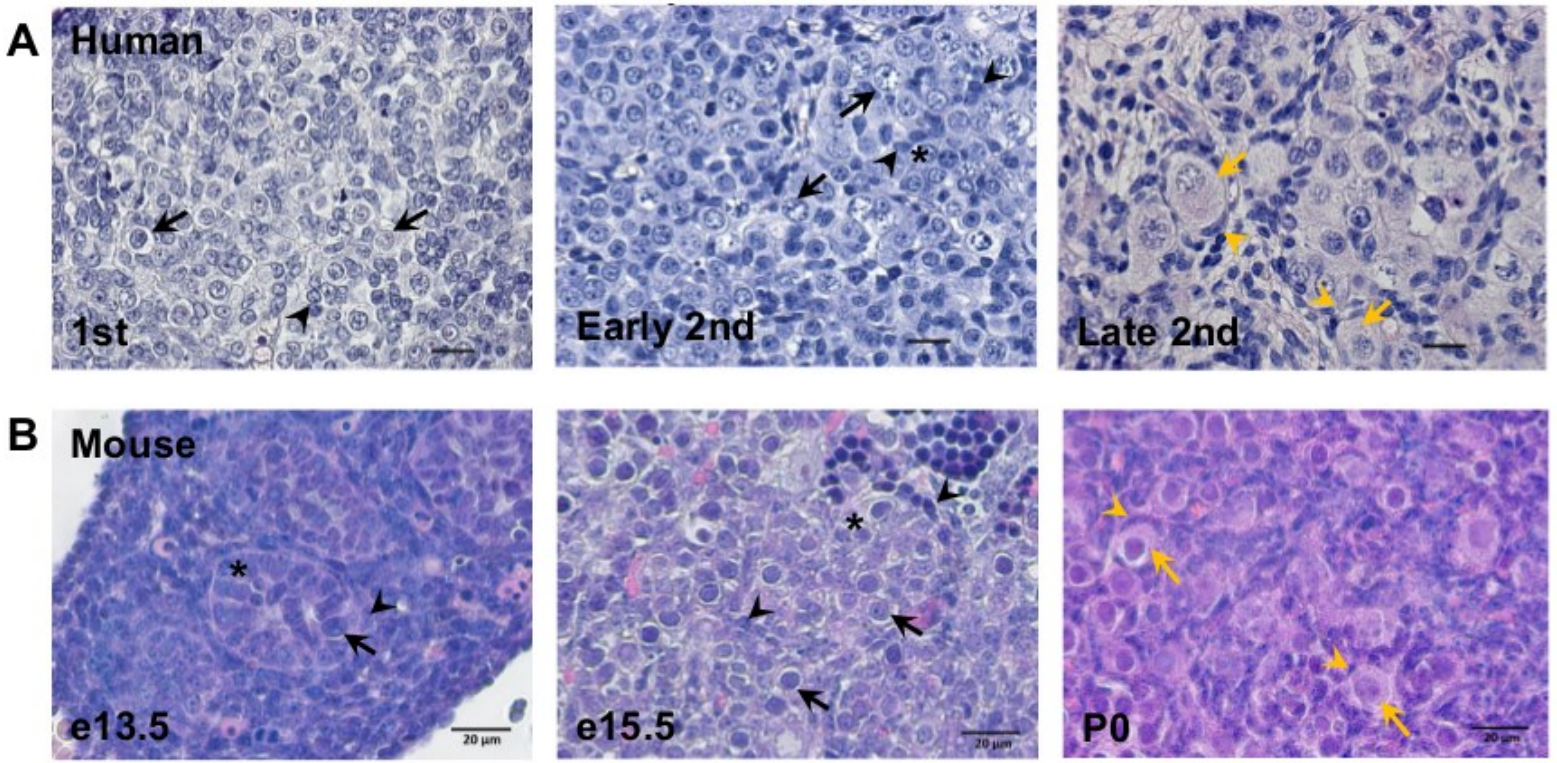

Figure 4. 1 Different stages of human and mouse fetal ovary development.

A) Human fetal ovary development. In the first trimester, the primordial germ cells (arrows) and somatic cells (arrow heads) are not clearly distinguishable but germ cells have bigger, rounded nuclei. In the early second trimester, meiosis begins in the more mature germ cells (arrows) located in central area. The pre-granulosa cells (arrowheads) surround several germ cells to form nests (asterisk). In the late second trimester, nests in central area are broken-down by invading pre-granulosa cells (yellow arrowheads), which surround single growing germ cells (yellow arrows) to form primordial follicles. **B)** Mouse fetal ovary development. Meiosis initiates in mouse ovary at e12.5, therefore at e13.5 nests already formed (asterisk) and germ cells (arrow) are surrounded by pre-granulosa cells (arrowhead). At e15.5 meiosis reaches leptotene/pachytene, the size of germ cells (arrows) increases and they are still surrounded by pre-granulosa cells (arrowheads) in nests (asterisk). At P0 the nests also breakdown like in human, and single germ cells (yellow arrows) are surrounded by pre-granulosa (yellow arrowheads) cells to form the primordial follicles. Scale bar=20µm, human fetal ovary images by Dr Sharon Eddie

Previous work from our lab has demonstrated that the translocation of DAZL protein (as observed in human testis) also occurs during human oogenesis, and *DAZL* mRNA levels increase between the first and second trimester, co-incident with the entry of the first germ cells into meiosis in the human fetal ovary (Anderson *et al.*, 2007). Another study suggested that DAZL is also expressed in the oocytes in human primordial follicles (Dorfman *et al.*, 1999).

Although *Boll* transcripts have been reported in the mammalian fetal ovary (Mandon-Pepin *et al.* , 2003, Shah *et al.*, 2010, Vangompel and Xu, 2011), the existence of Boll protein in mammalian female germ cells has not yet been demonstrated. In this chapter, we will try to explore BOLL expression during human oogenesis, and also extend the existing knowledge on DAZL expression in the developing ovary by correlating it with specific meiotic stages. We will also compare the expression patterns of DAZL and BOLL in the developing ovaries of humans and mice, to find out whether the female mouse is an appropriate model in which to study the function of human BOLL.

4.2 Results

4.2.1 *DAZL* and *BOLL* mRNA are expressed in human fetal ovary

To find out whether DAZL and BOLL are expressed in human fetal ovary and how they associate with germ cell development, we first investigated the expression of *DAZL* and *BOLL* mRNA during human fetal ovary development, using qRT-PCR (Figure 4.2).

Low levels of *DAZL* mRNA were expressed in first trimester ovaries, at 8 to 9 weeks gestation before meiosis when most germ cells are primordial germ cells. *DAZL* expression then increases significantly at 14 to 16 weeks gestation ($p<0.001$), i.e. early second trimester when meiosis starts, and remains at this level remains to late second trimester at 17 to 20 weeks gestation which represents the beginning of follicle formation (Figure 4.2A, n=5-6 samples per gestation group).

There is almost no *BOLL* mRNA expression in first trimester, and its mRNA level also significantly increases at early second trimester ($p<0.001$). However, when compared to the early second trimester, the level of *BOLL* mRNA slightly decreases in late second trimester but not significantly (Figure 4.2B, n=5-6 samples per gestation group). Relative to *RPL23*, expression of *BOLL* was around half that of *DAZL* at 14-16 and 17-20 weeks gestation (0.017+/-0.005 vs 0.010+/-0.001). Both data of DAZL and BOLL were analysed using One-Way ANOVA with Tukey's multiple comparisons test; the normality of data was not able to be analysed due to the small sample number.

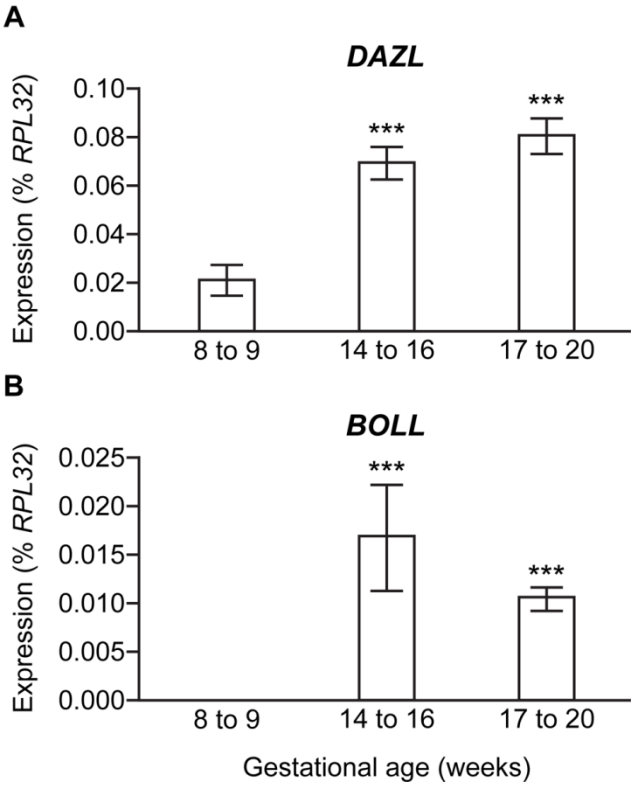

Figure 4. 2 Expression of *DAZL* and *BOLL* mRNA during human ovary development. **A)** *DAZL* significantly increases from 8-9 to 14-16 weeks, with no significant change thereafter. **B)** *BOLL* expression is not detectable at 8-9 weeks and also significantly increases at 14 to 16 weeks. There is no significant change between 14-16 and 17-20 weeks (n=5-6, value=mean±s.e.m. ***p<0.001 vs 8-9 weeks for both *DAZL* and *BOLL*).

4.2.2 DAZL and BOLL proteins show dynamic changes during germ cell development in human fetal ovary

After confirming the specificity of the DAZL and BOLL antibodies (see Section 3.2.4), we used fluorescence immunohistochemistry on human fetal ovary sections to investigate DAZL and BOLL protein expression during germ cell development. All the experiments were performed on at least 2 sections from 2 different individuals.

On day 65, before the germ cells enter into meiosis (Figure 4.1A, first panel), only DAZL was expressed, and was detected in these primordial germ cell nuclei and cytoplasm (Figure 4.3A). BOLL was not detected in either germ cells or somatic cells (Figure 4.3A). However, at 14 weeks of gestation, following the initiation of meiosis (Figure 4.1A, second panel), both DAZL and BOLL were found to be expressed in germ cells. Notably, DAZL translocated from the nucleus to cytoplasm at this stage, and BOLL appeared in a limited number of cells (Figure 4.3B). At 18 weeks gestation, when germ cells began to enter into the later stages of meiosis, DAZL was still expressed extensively and BOLL expression became more abundant (Figure 4.3C). Finally at 19 weeks gestation, when germ cells were forming follicles together with pre-granulosa cells (Figure 4.1A, third panel), DAZL was expressed in the oocytes of primordial follicles whilst BOLL expression became less abundant, with no BOLL protein detectable in primordial follicles (Figure 4.3D). The dynamic changes of DAZL and BOLL protein expression in human fetal ovary are consistent with their mRNA expression described above (Section 4.2.1), i.e. DAZL showed a low expression in first trimester and then increased after meiosis initiation and stays at a high level through later stages, including in primordial follicles. In contrast, BOLL is not expressed in first trimester, increases in the second early trimester but is not detected in primordial follicles.

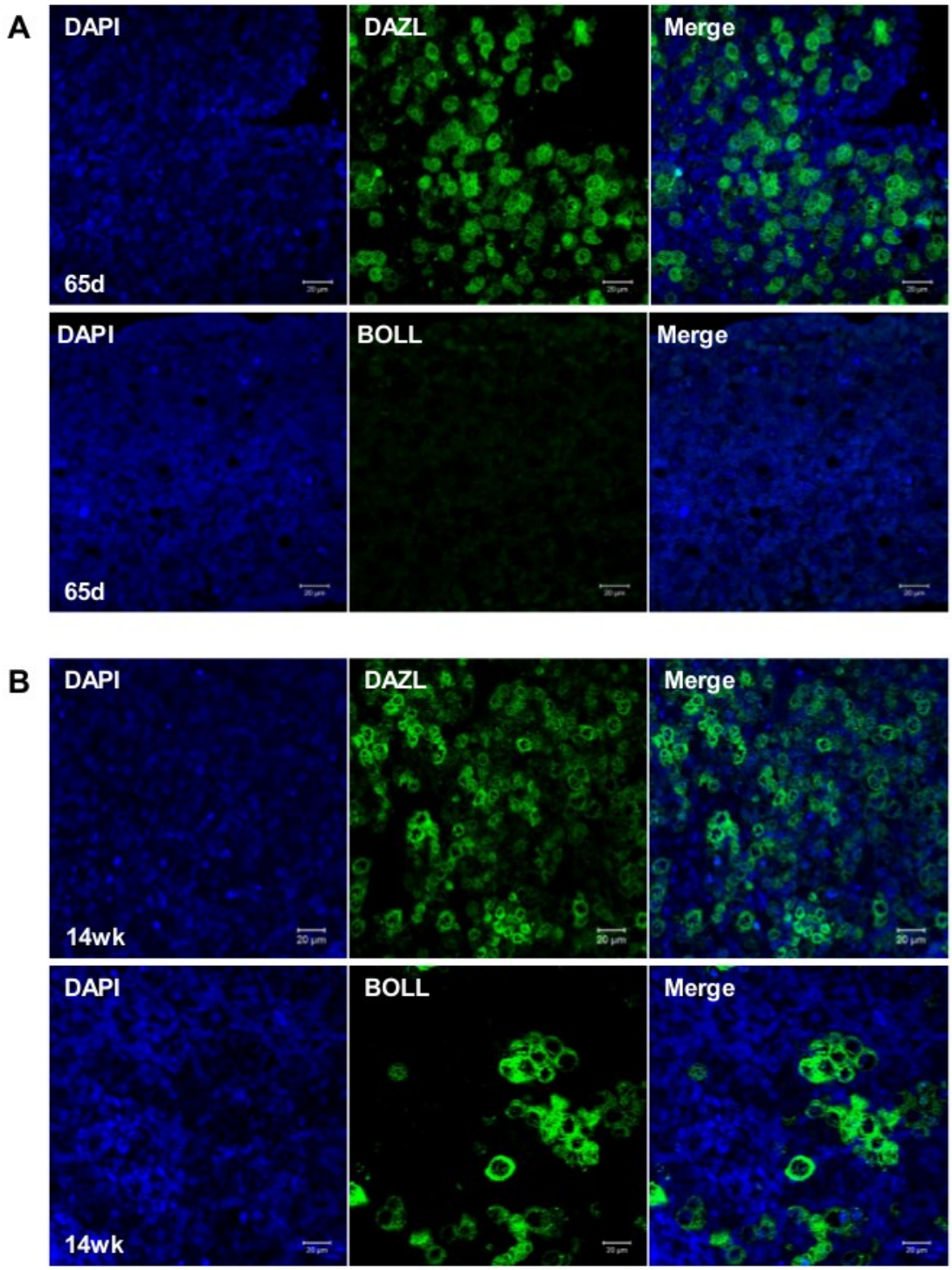

Figure 4. 3 (1/2) Dynamic changes in DAZL and BOLL protein expression during development of the human fetal ovary.

Both proteins (green colouration) are germ cell specific. At 65 days**,** DAZL expression was both nuclear and cytoplasmic, whilst BOLL was not detected **(A)**. At 14 week, both cytoplasmic DAZL and BOLL expression was detected in groups of germ cells, but the number of BOLL^{+ve} was relatively small **(B)**.

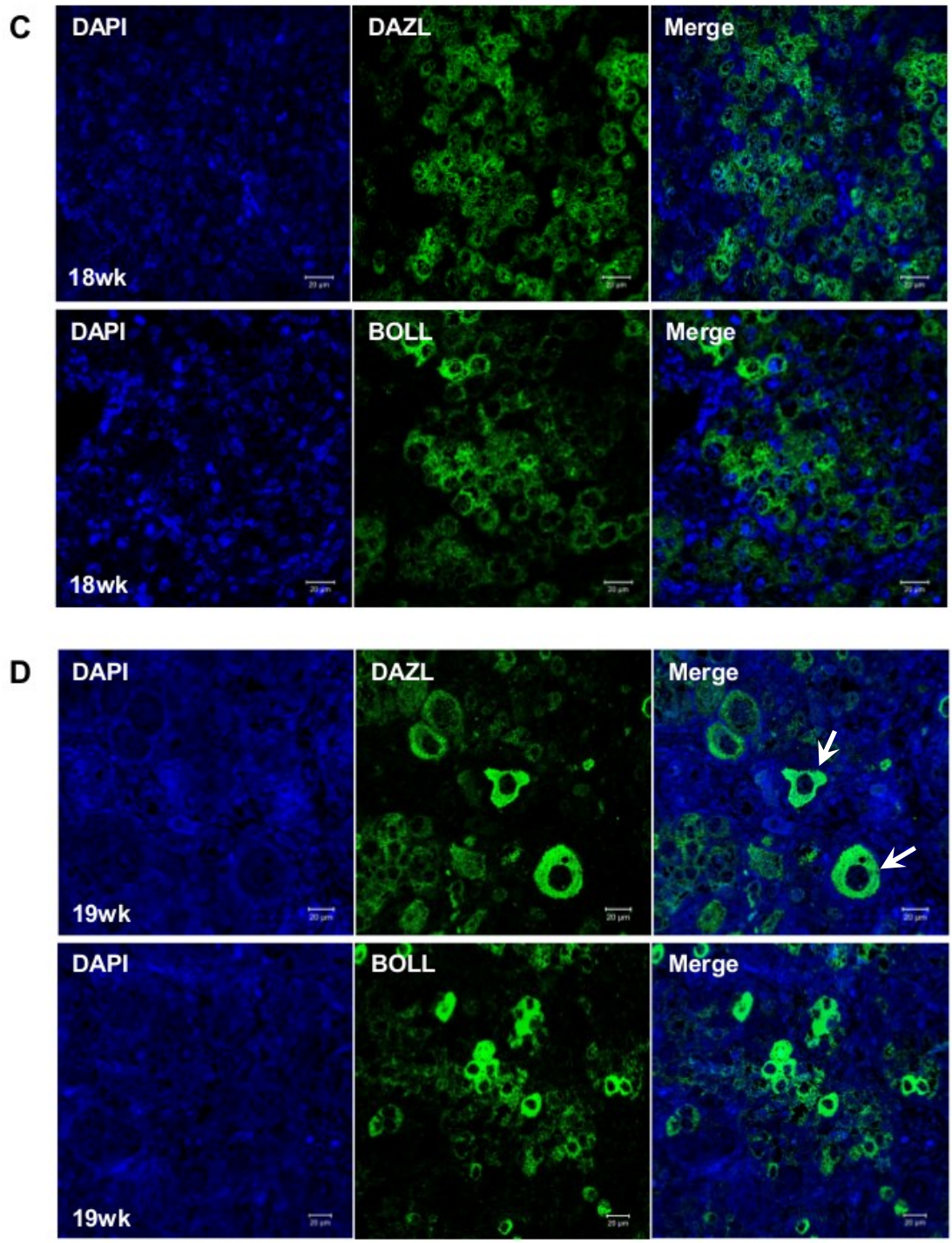

Figure 4. 3 (2/2) Dynamic changes in DAZL and BOLL protein expression during development of the human fetal ovary.

At 18 week, DAZL was still abundantly expressed in germ cells and the abundance of BOLL^{+ve} cells increased **(C)**. At 19 week DAZL expressed in the oocytes within newly-formed primordial follicles (arrows) whilst the number of BOLL^{+ve} cells decreased, and no primordial follicle was found BOLL^{+ve} **(D)**.

Counter stained with DAPI (blue), Scale bar=20μm

4.2.3 DAZL and BOLL expression represents distinct groups of germ cells

As DAZL and BOLL are both expressed in human fetal ovary and display dynamic changes during germ cell development, the next question we asked was whether these changes were associated with their functions, and whether these two proteins from the same family have similar or different functions during this process. To answer these questions, we further investigated the co-expression patterns of DAZL and BOLL using dual fluorescence immunohistochemistry. As BOLL is not expressed in the first trimester human fetal ovary, only early and late second trimester tissues were used.

We first took the tiled images of the tissue to see their broad distribution at the tissue level. The images show that at 14 weeks gestation, DAZL is extensively expressed in both the peripheral and central areas of the ovary, whilst BOLL expression is restricted in small groups of germ cells in the central area (Figure 4.4A). At 18 weeks gestation, most cells that express DAZL are around the periphery of the ovary, with a few $DAZL^{+ve}$ cells localised in the central area. The number of $BOLL^{+ve}$ cells dramatically increased when compared with 14 week and they are all located in the central area (Figure 4.4B). Interestingly, only very few cells expressed both DAZL and BOLL at any gestation.

To further investigate the degree of co-expression, we took high resolution images for DAZL and BOLL dual immunohistochemistry (Figure 4.5). The 14 week tissue has both DAZL and BOLL expression: most cells are $DAZL^{+ve}$, with several $BOLL^{+ve}$ cells. Few cells expressing both DAZL and BOLL are also found in this section. The 18 week tissue clearly shows a higher proportion of $BOLL^{+ve}$ cells, and while DAZL is also expressed in this section, there is little evidence of co-expression between DAZL and BOLL. The 20 week tissue shows two typical primordial follicles which were only $DAZL^{+ve}$. Although BOLL is expressed near the follicles in the medulla of ovary, it appears to be less widely distributed than in the 18 week tissue.

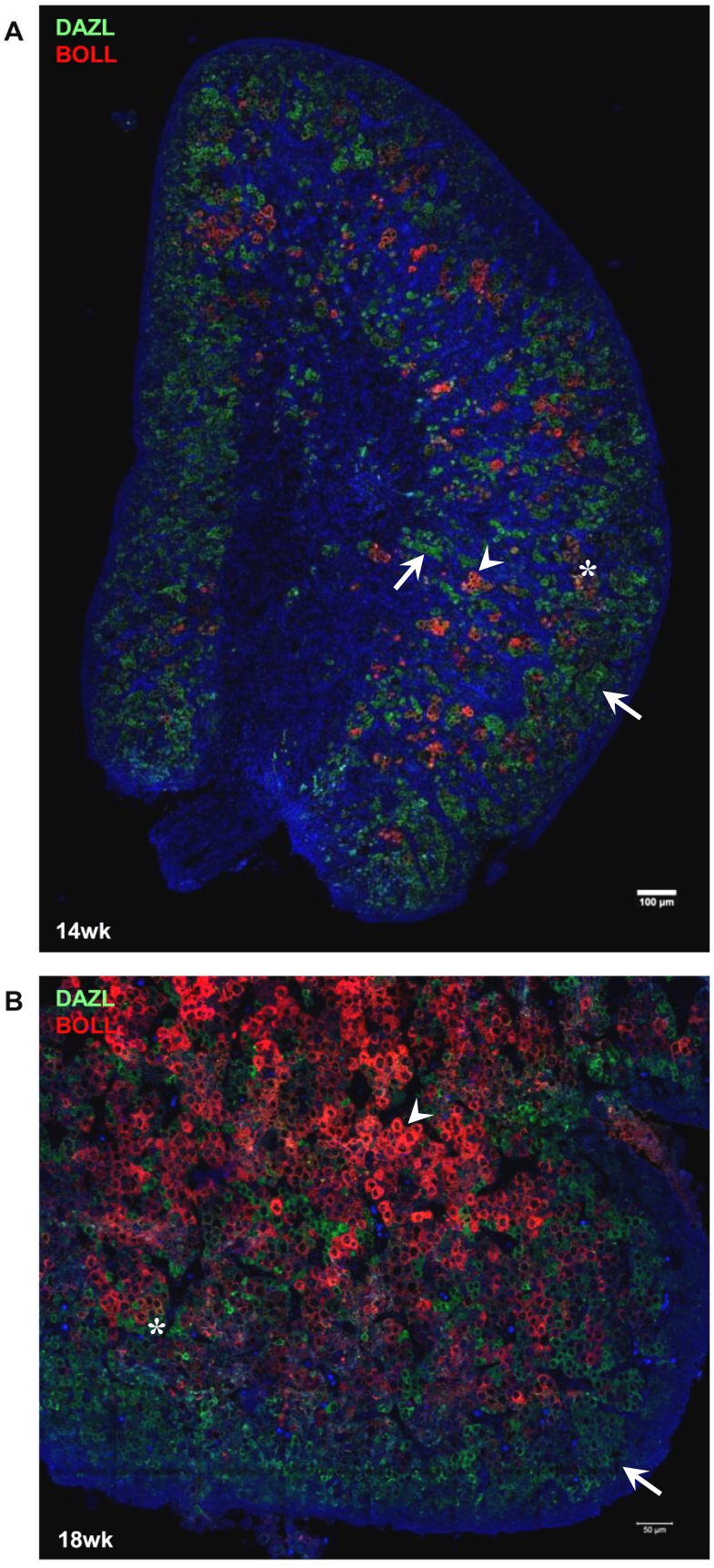

Figure 4. 4 The overview of DAZL and BOLL distribution and co-localisation in human fetal ovary.

A) Tiled image of 14 weeks human fetal ovary. DAZL (green) is extensively expressed in both periphery and medulla areas (arrows) and BOLL (red) is only expressed in medulla of ovary in small groups of germ cells (arrowhead). **B)** Tiled image of 18 weeks ovary. DAZL is expressed in less mature germ cells in a more peripheral localisation (arrow), while BOLL is extensively expressed in more centrally-located germ cells (arrowhead). DAZL and BOLL showed minimal co-localisation in both sections (asterisk).

Counter stained with DAPI (blue), Scale bar **A)**=100µm, **B)**=50µm,

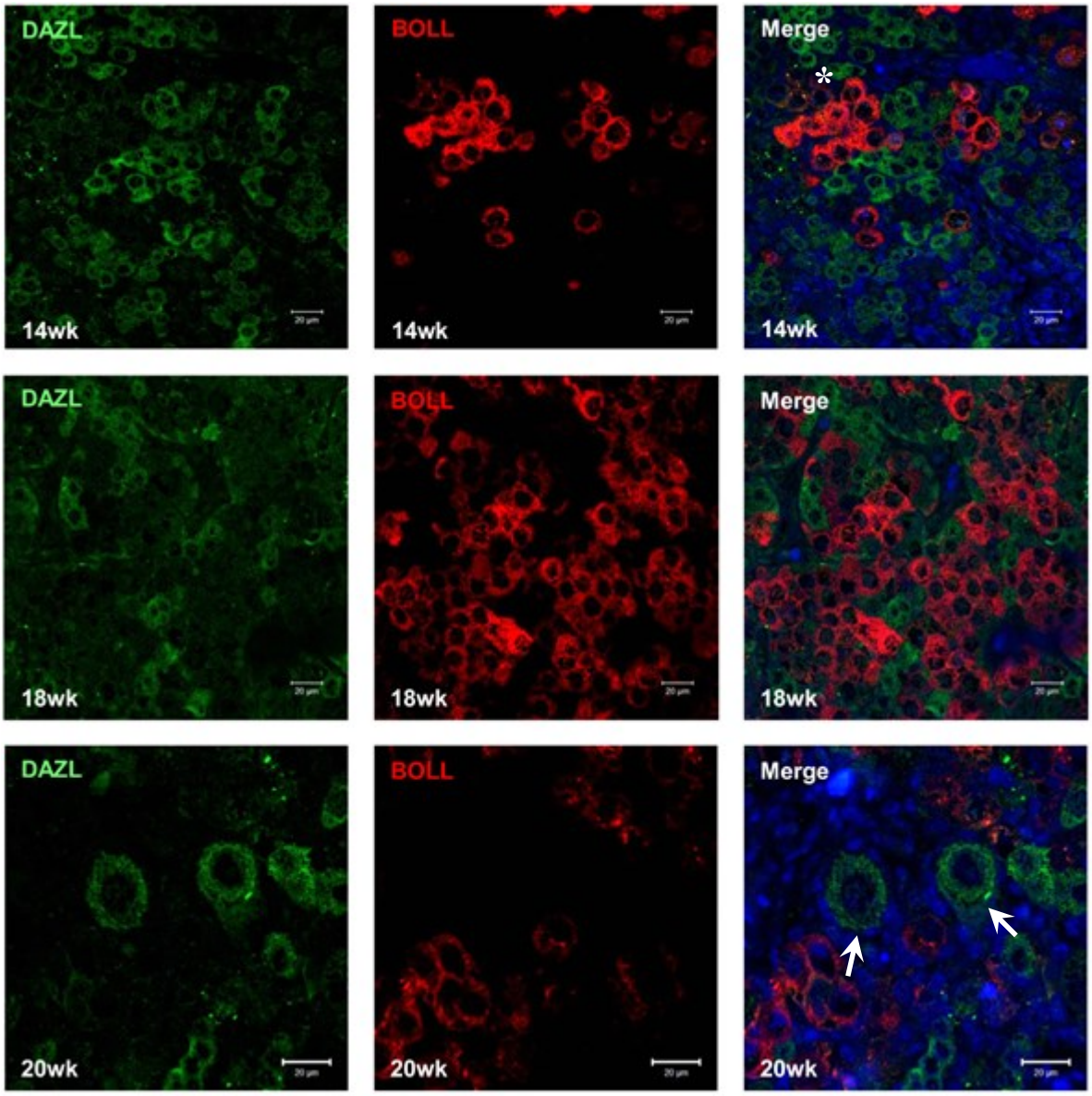

Figure 4. 5 The co-localisation of DAZL and BOLL at different stages of germ cell development in human fetal ovary.

Both proteins are expressed across14 to 20 weeks. To distinguish the different cell types of the ovary, see Figure 4.1A. Similar to the single staining (Figure 4.3), DAZL (green) is stably expressed across 14 to 20 weeks gestation. In contrast, BOLL (red) is detected in a few germ cells at 14weeks, then the number of BOLL^{+ve} cells increases at 18 week, before decreasing at 20 weeks. DAZL, but not BOLL, is expressed in oocytes of primordial follicles (arrows). Rare germ cells expressing both DAZL and BOLL are detectable (asterisk). Counter stained with DAPI (blue), Scale bar=20μm

4.2.4 DAZL and BOLL expression represents distinct groups of germ cells

The above data suggest that BOLL is expressed in germ cells at a later stage of development than DAZL. To further confirm this hypothesis, we measured the nuclear diameter of germ cells which are either $DAZL^{+ve}$ or $BOLL^{+ve}$ using the tiled images of DAZL and BOLL dual immunohistochemistry at both 14 and 18 weeks gestation, as this metric was reported as an indicator of germ cell maturation, increasing as germ cells progress through development (Hartley *et al.*, 2002).

We found that $BOLL^{+ve}$ cells had significantly larger nuclei when compared to $DAZL^{+ve}$ cells at both 14 (6.60+/-0.12μm vs 9.37+/-0.20μm) and 18 weeks gestation 18 (6.87+/-0.12μm vs 9.23+/-0.19μm) (Figure 4.6A, both $p<0.001$, n=108-191 (cell number) per group, each gestation contains one sample). As the data of each group are not normally distributed according to D'Agostino & Pearson omnibus normality test, the significance were analysed with Mann Whitney test instead of unpaired t-test. This suggests that BOLL is mainly expressed in germ cells at later development stages. We also grouped the data by value ranges to show the distribution of $DAZL^{+ve}$ and $BOLL^{+ve}$ cells at both gestations, and found that $DAZL^{+ve}$ and $BOLL^{+ve}$ germ cells display distinct, although overlapping, nuclear diameter frequency distributions (Figure 4.6B & 4.6C). $DAZL^{+ve}$ cells have nuclei which are <4 to 12 μm (primordial follicles are excluded), compared to 4 to >14μm for $BOLL^{+ve}$ cells. Most $DAZL^{+ve}$ cells are distributed at 4 to 8 μm whilst $BOLL^{+ve}$ cells are at 8 to 12μm. No $DAZL^{+ve}$ germ cells had nuclei greater than 12μm, and no $BOLL^{+ve}$ cells has nuclei smaller than 4μm. Therefore, the data support that DAZL and BOLL are expressed in distinct groups of germ cells which are at different stages during development, with BOLL expressed by germ cells at a later stage of development than those expressing DAZL.

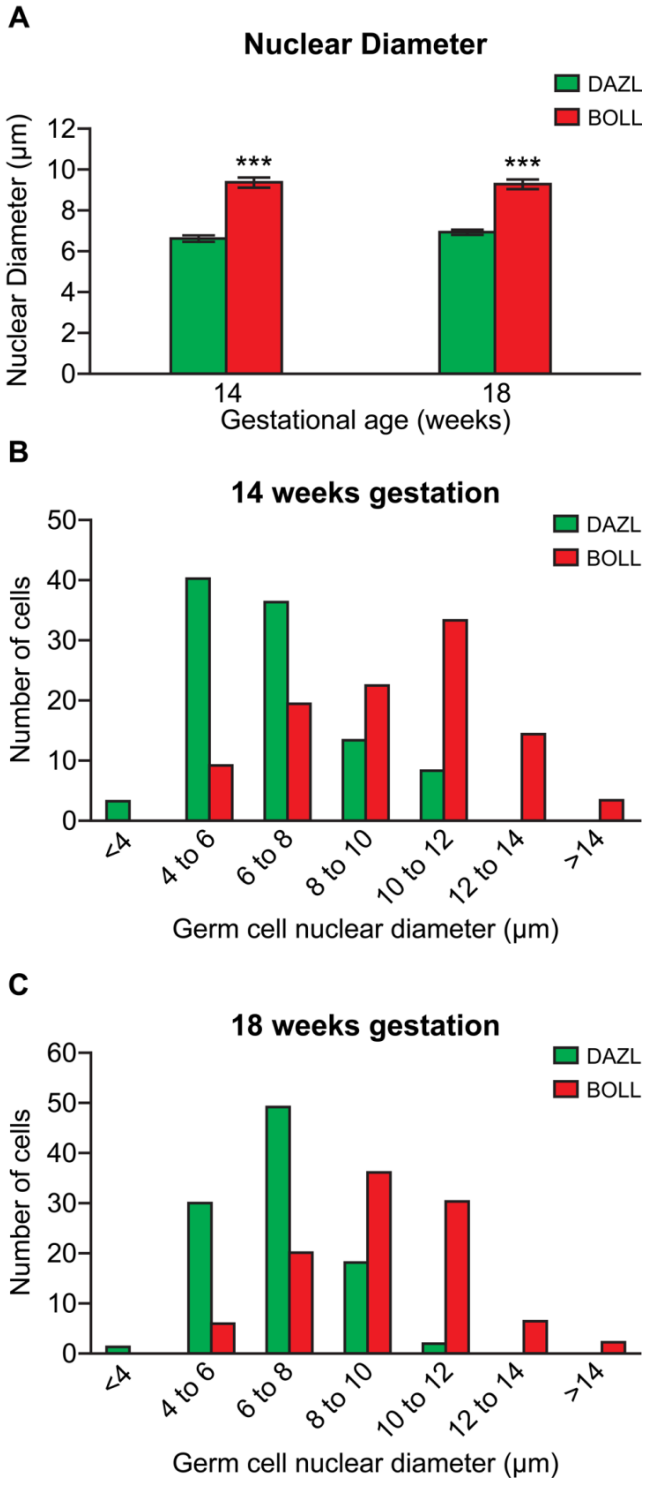

Figure 4. 6 Nuclear diameter of DAZL^{+ve} /BOLL^{+ve} cells (primordial follicles not included). **A)** BOLL^{+ve} cells have larger nuclei than DAZL^{+ve} cells at both 14 and 18 weeks gestation. **B) and C)** The nuclear diameter distribution of DAZL and BOLL^{+} cells at 14 and 18 weeks, respectively. DAZL^{+ve} cell nuclei are mainly distributed at 4-8µm, while BOLL^{+ve} cell nuclei are mainly 8-12µm in diameter. Only DAZL^{+ve} cells have nuclei smaller than 4 µm, and only BOLL $^{+ve}$ cells have nuclei larger than 12µm, and. (One sample for each gestation, cell number=108-191, ***p<0.001)

4.2.5 DAZL, but not BOLL, is expressed before meiosis

After investigating the expression patterns of DAZL and BOLL, we tried to determine how they were associated with germ cell development in the human fetal ovary, by looking at their co-localisation with stage-specific markers. In the following results, all the immunofluorescence was performed on the sections from at least 2 different individuals each gestation to make sure the results were robust.

LIN28 was identified as an early germ cell maker which is expressed in primordial and pre-meiotic germ cells in human fetal ovary (Childs *et al.*, 2011), thus we first performed triple immunofluorescence for DAZL, BOLL and LIN28 on second trimester human fetal ovary. We found that in these tissues, germ cells expressing the three proteins formed three layers. Tiled images of 15 weeks gestation tissue were taken to show the distribution. LIN28 is expressed at the periphery of the ovary, BOLL is expressed mainly in the more central area, whilst DAZL is expressed in germ cells distributed between the LIN28^{+ve} and BOLL^{+ve} cells; however, there are also several BOLL^{+ve} cells localised around the edge, along with some DAZL and/or LIN28^{+ve} cells localised in the central area (Figure 4.7A).

High resolution images were also taken to show the co-localisation between DAZL/LIN28 and BOLL/LIN28 (Figure 4.7B). DAZL and LIN28 are partially co-expressed in quite a few germ cells in both early (15 week, Figure 4.7B upper panels) and late second (18 week, Figure 4.7B lower panels) trimester tissues, especially in those cells which have nuclear DAZL expression. In contrast, although there appears to be a germ cell expressing very faint BOLL and LIN28 in the 15 week gestation tissue, no other germ cell was found expressing both BOLL and LIN28 in either 15 or 18 weeks gestation tissue (Figure 4.7B). No cell was found to express all three proteins (DAZL/BOLL/LIN28) either, although some DAZL/BOLL co-localisation was observed as described in previous sections (Figure 4.4 and 4.5). Therefore, the cell position and partial co-expression of DAZL and LIN28 suggest that in the second trimester, DAZL is expressed in primordial and pre-meiotic germ cells but not in very early LIN28^{+ve} primordial germ cells. The lack of LIN28 and BOLL co-expression demonstrates that BOLL is mostly expressed in germ cells at later stages of development, very likely after the initiation of meiosis. To conclude,

germ cells first express LIN28, then DAZL appears as LIN28 is down-regulated; DAZL expression then continues into meiosis, and is subsequently replaced by BOLL.

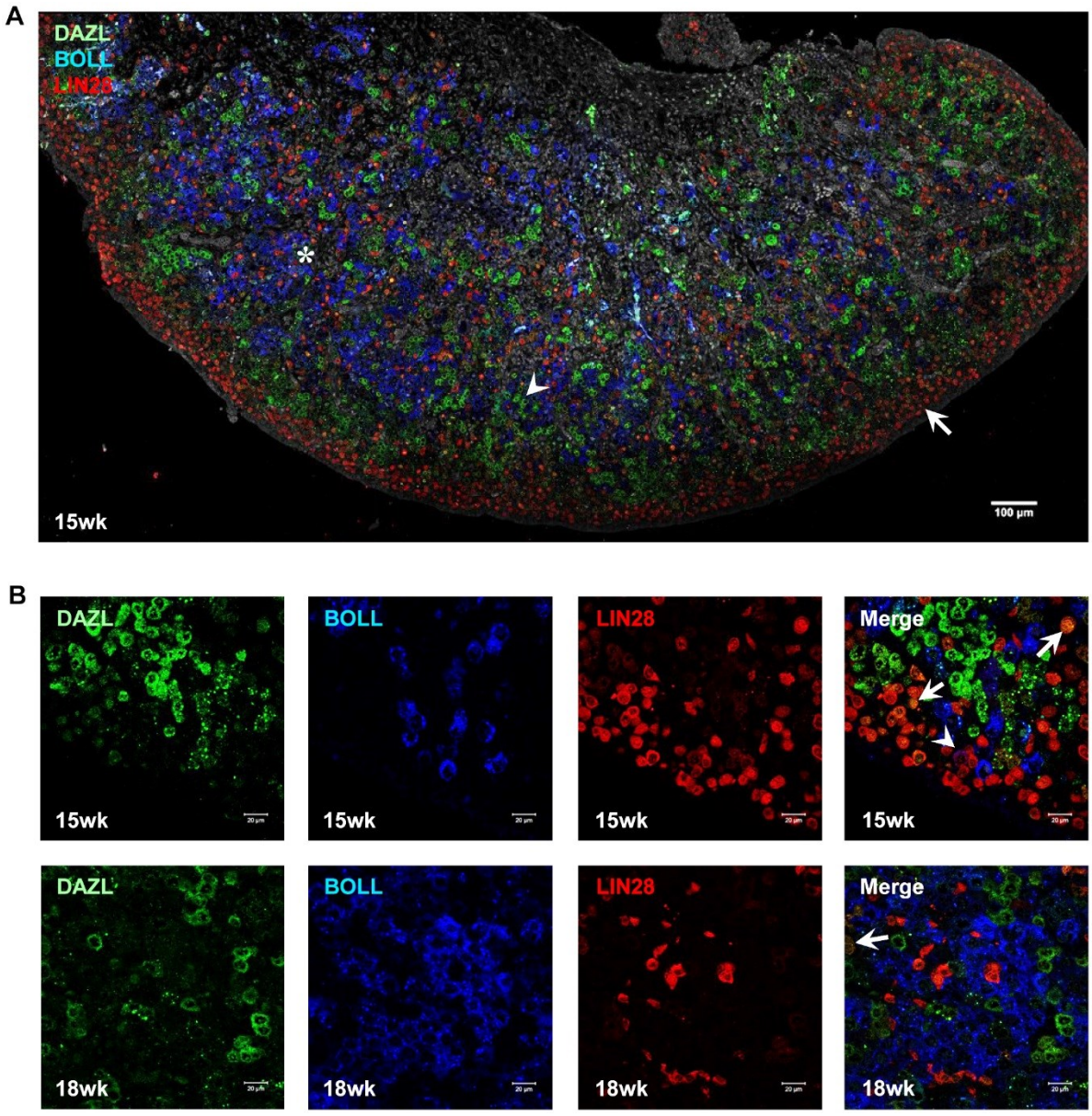

Figure 4. 7 DAZL but not BOLL is co-expressed with LIN28 in germ cells in the second trimester human fetal ovary.

A) Tiled image of 15 weeks gestation ovary to show the distribution of DAZL (Green), BOLL (Blue) or LIN28 (Red) positive cells. LIN28^{+ve} (arrow) cells are mainly located around the edge and BOLL^{+ve} cells (asterisk) are in the centre, while DAZL^{+ve} cells (arrowhead) are between them. **B)** In both 15 and 18 weeks gestation tissues, there are several cells are expressing both DAZL and LIN28 (arrows). Only one germ cell was found to express BOLL and LIN28 (arrowhead), and no cell was seen which expressed all three proteins. Scale bar **A)**=100µm, **B)**=20µm

4.2.6 DAZL and BOLL differentially associate with markers of meiosis

Given the fact that the DAZL expression persists to later stages of germ cell development (after which the pre-meiotic marker LIN28 is down-regulated), then the switch between DAZL and BOLL expression during human fetal oogenesis may occur during meiosis. To establish if this timing occurs at a specific stage of the meiosis prophase I, we first performed triple immunofluorescence analysis for DAZL, BOLL and the meiosis marker SYCP3. This is a component of synaptonemal complex which is expressed from pre-meiosis to diplotene in human fetal ovarian germ cells (Roig *et al.*, 2004). Again, we took tiled images of second trimester tissues to see the global distribution of DAZL, BOLL and SYCP3 (Figure 4.8). In both 15 and 17 weeks gestation tissues, SYCP3 is germ cell-specific and only distributed in the more central area of ovary (where $BOLL^{+ve}$ germ cells are mainly located). Most $SYCP3^{+ve}$ cells are also $BOLL^{+ve}$, but a few single $SYCP3^{+ve}$ cells and SYCP3/DAZL double-positive cells were found on these sections as well (Figure 4.9).

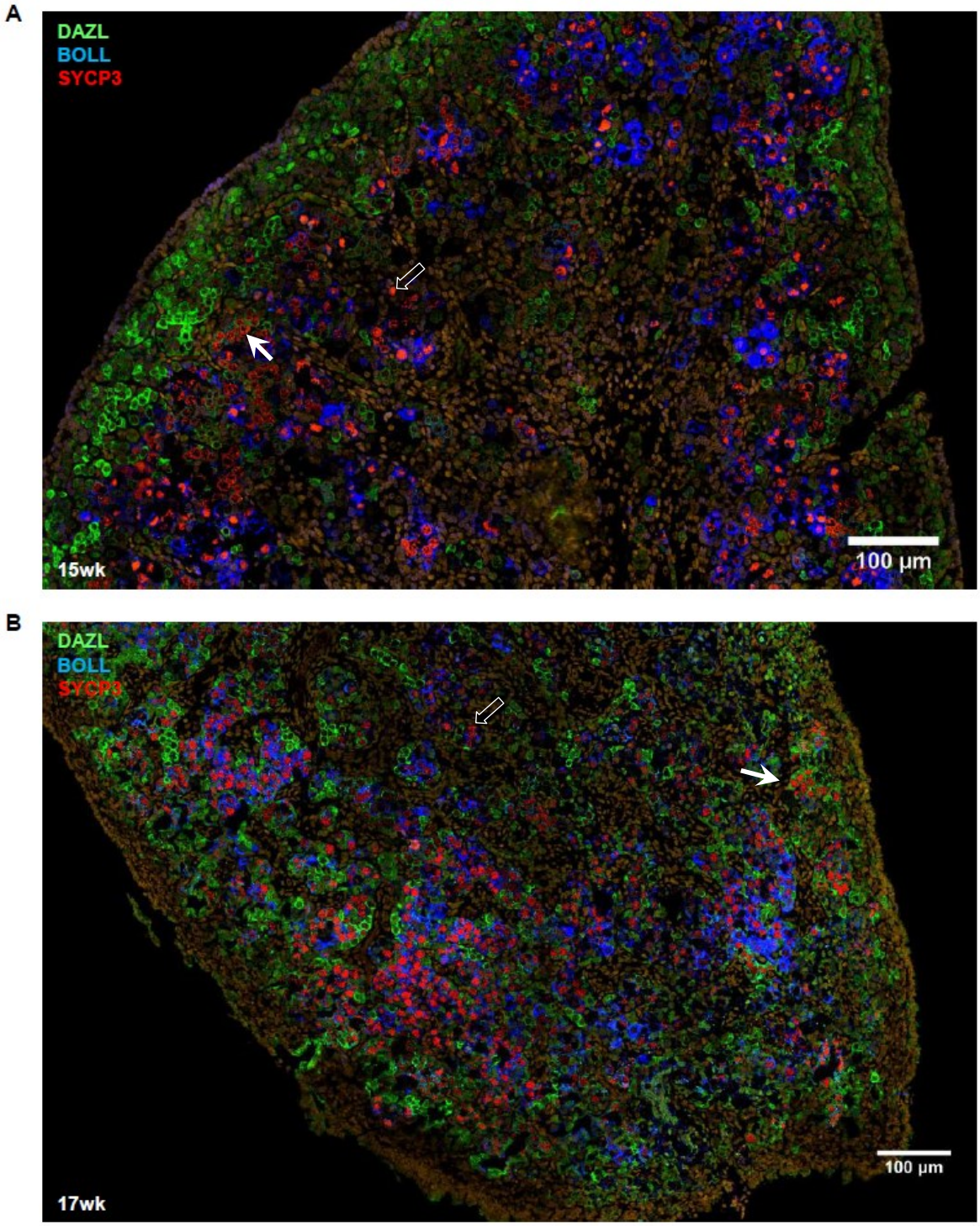

Figure 4. 8 BOLL is broadly co-expressed with SYCP3 in germ cells in the second trimester human fetal ovary.

A)&B) SYCP3 is expressed in germ cells of both 15 and 17 weeks gestation ovaries. Although most SYCP3^{+ve} cells are also BOLL^{+ve}, several cells express both SYCP3 and DAZL (arrows), and there are also some SYCP3 single-positive cells (unfilled arrows). Counter stained with DAPI (yellow), Scale bar=100µm

To make it clearer, we also took high resolution images of the triple staining. The images show that almost all BOLL^{+ve} germ cells are also SYCP3^{+ve}, and there are relatively few SYCP3^{+ve} germ cells that also express DAZL at 14, 15 and 17 weeks gestation (Figure 4.9A&B, sample of 15 weeks is not shown). Using randomly picked images from the tiled image, we calculated the ratios of all SYCP3 co-localisation patterns. This confirmed the extensive overlap of BOLL and SYCP3 expression (Figure 4.9C); nearly 70% SYCP3^{+ve} germ cells also expressed BOLL, a fraction significantly higher than the 14% of SYCP3 and DAZL double-positive germ cells, 11% of SYCP3^{+ve} germ cells which expressed both DAZL and BOLL, and the 6% of SYCP3^{+ve} germ cells that express neither DAZL or BOLL (SYCP3^{+ve} only; $p<0.001$, counted cell number=327-787, one sample from each gestation). Data was analysed using One-Way ANOVA with Tukey's multiple comparisons test. These data are also consistent with BOLL being expressed in germ cells that have reached a later stage of meiosis prophase I than those expressing DAZL.

We also compared the extent of co-expression of DAZL and BOLL with another meiosis marker, the phosphorylated isoform of the Ataxia Telangiectasia Mutated (phospho-ATM) protein, which is expressed by germ cells from pre-leptotene to pachytene of meiotic prophase I (Hamer *et al.* , 2004). The tiled images of DAZL or BOLL/phospho-ATM double immunofluorescence stained human fetal ovary at 16 weeks gestation show a pattern consistent with that of SYCP3. phospho-ATM is distributed in the nuclei of germ cells in the central area of ovary, and when co-stained with DAZL, most germ cells were found to be positive for either phospho-ATM or DAZL, with a few cells showing some co-expression of both markers (Figure 4.10A). In contrast, in the phospho-ATM/BOLL double stained tissue, almost all the phospho-ATM^{+ve} cells were also BOLL^{+ve}, with several BOLL single-positive cells and some very rare phospho-ATM single-positive cells (Figure 4.10B).

As we did with the SYCP3 co-localisation, high resolution images were also taken to show the details of co-localisation, and enable quantification of co-expression ratios were performed based on the tiled images. We found that the co-expression pattern was similar at 14and 16 weeks gestation, i.e. more phospho-ATM^{+ve} cells also

express BOLL compared to the number of DAZL/phospho-ATM double-positive cells (Figure 4.11A). This was further confirmed by quantification – the data show that a significantly greater proportion of phospho-ATM^{+ve} germ cells also express BOLL (78%) than express DAZL (37%; $p<0.05$) (Figure 4.11B). Data was analysed with unpaired t-test. As the sample number is too small and impossible for normality testing, it was assumed that both the data of SYCP3 and phospho-ATM were normally distributed and a parametric test was used.

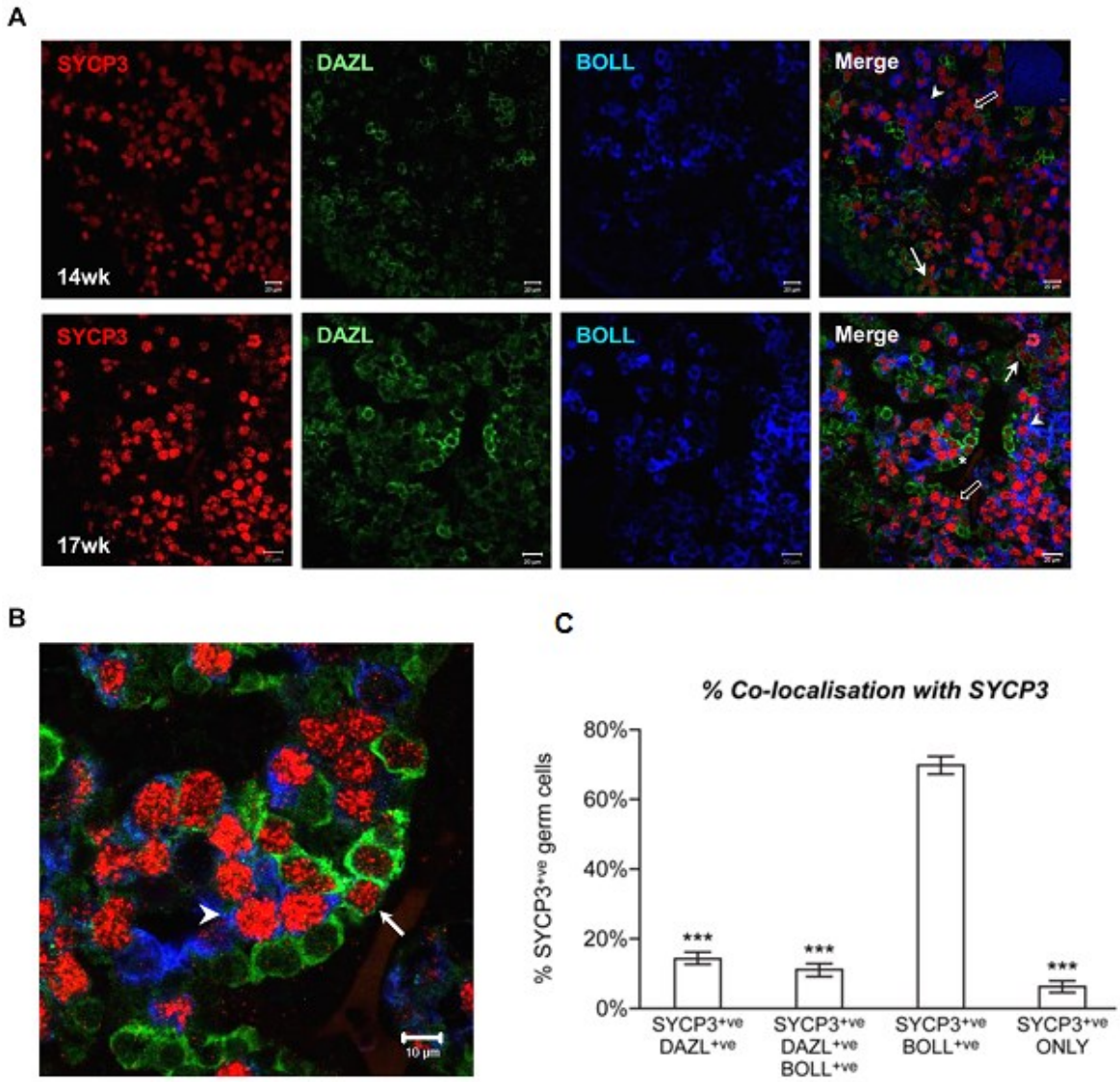

Figure 4. 9 BOLL displays greater co-localisation with the meiosis marker SYCP3 than DAZL.

A) Triple immunofluorescence analysis of DAZL (green), BOLL (blue) and SYCP3 (red) in 14 and 17 week ovaries. All BOLL^{+ve} germ cells also express SYCP3 (arrowheads), but only a few DAZL^{+ve} germ cell express SYCP3 (arrows). Unfilled arrows indicate the SYCP3^{+ve} cells that express neither DAZL nor BOLL. The asterisk indicates a germ cell nest containing BOLL/SYCP3^{+ve}, DAZL/SYCP3^{+ve} and DAZL single-positive germ cells in close proximity. **B)** Magnified image of germ cell nest marked with asterisk in A, showing neighbouring germ cells expressing different combinations of DAZL, BOLL and SYCP3 expression; arrow denotes a DAZL/SYCP3^{+ve} germ cell, arrowhead denotes a BOLL/SYCP^{+ve} germ cell. **C)** Quantification of DAZL, BOLL and SYCP3 co-expression. ~69% of SYCP3+ cells also express BOLL. This is significantly greater than the percentage of all the other co-expression patterns (value=mean±s.e.m., cell number=327-787, 14-17 week human fetal ovaries; one sample for each gestation, ***p<0.001). Scale bar **A)**=20µm, **B)**=10µm

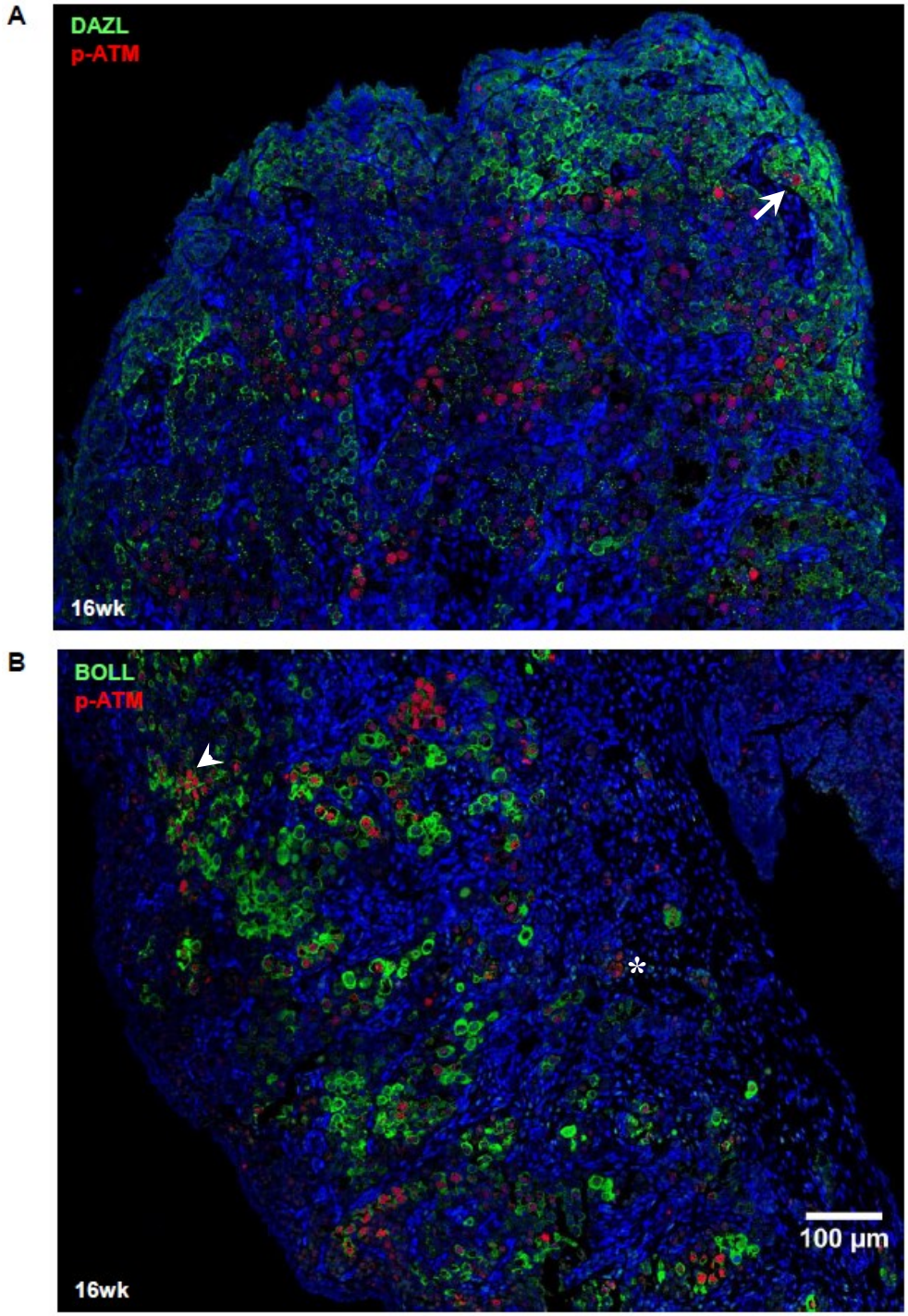

Figure 4. 10 BOLL is widely co-expressed with phospho-ATM in second trimester human fetal ovary.

A) The co-localisation of DAZL (green) and phospho-ATM (red) in 16 weeks gestation ovary. Very few phospho-ATM^{+ve} cells are also DAZL^{+ve} (arrow), and most cells express only DAZL or phospho-ATM. **B)** phospho-ATM (Red) is extensively co-expressed with BOLL (Green). Almost all the phospho-ATM germ cells also express BOLL (arrowhead), although some phospho-ATM single-positive cells can be seen (asterisk). Counter stained with DAPI (blue), Scale bar=100µm

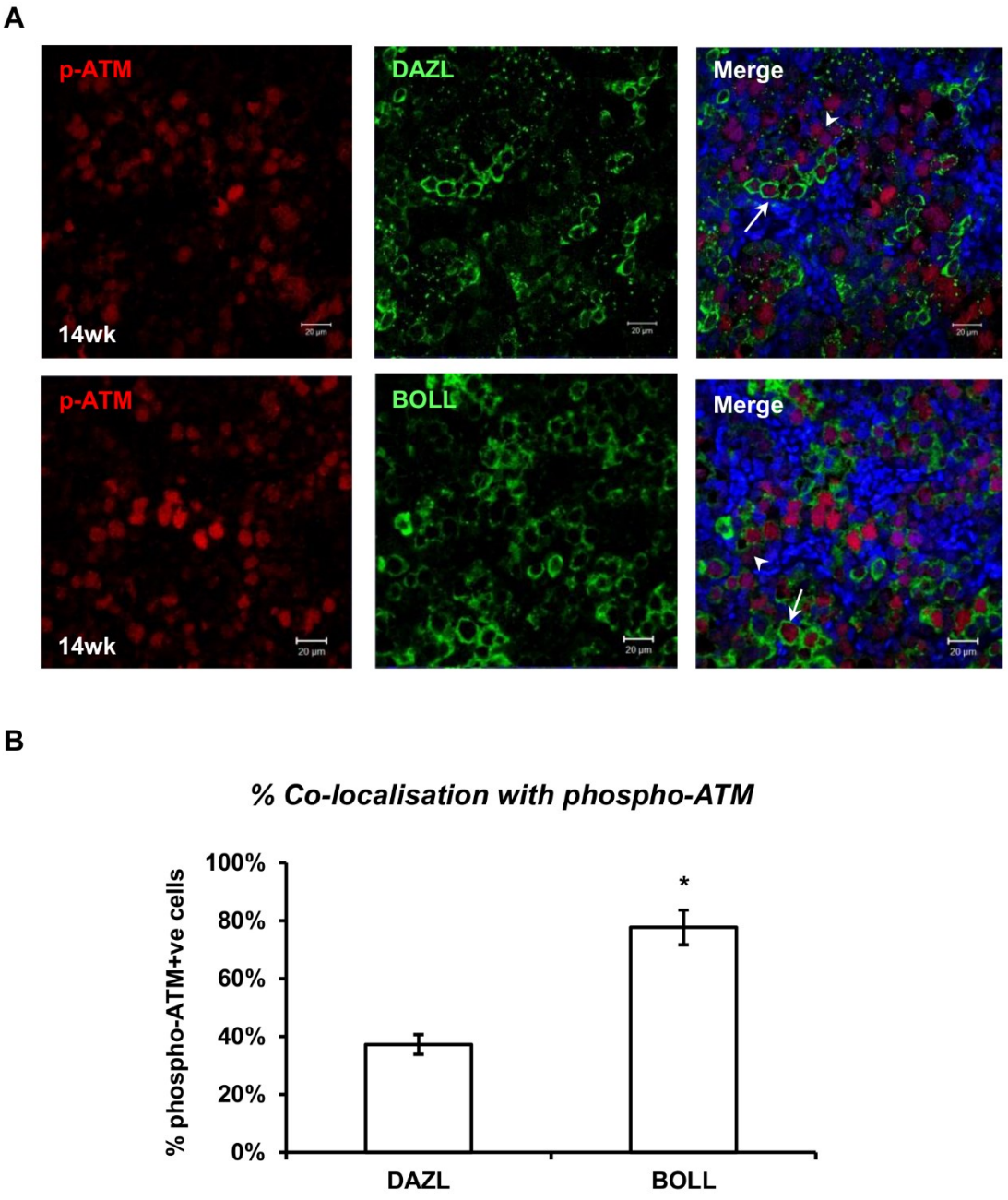

Figure 4. 11 Co-localisation of phospho-ATM with DAZL or BOLL.

A) Immunofluorescent co-localisation of phospho-ATM (red) with DAZL or BOLL (green) in the human fetal ovary (14 weeks gestation). DAZL shows limited co-expression with phospho-ATM, whereas almost all the phospho-ATM^{+ve} cells are also BOLL^{+ve}. Arrows indicate germ cells co-expressing phospho-ATM of DAZL/BOLL, and arrowheads indicate phospho-ATM single-positive germ cells. **B)** Quantification of phospho-ATM co-localisation with DAZL and BOLL. BOLL is expressed in ~80% of phospho-ATM^{+ve} cells, which is significantly higher than the proportion of DAZL/phospho-ATM double-positive cells (37%; value=mean±s.e.m., cell number=79-374, 14-16 week human fetal ovaries, one sample for each gestation, *$p<0.05$). Counterstained with DAPI (blue), Scale bar=20μm

4.2.7 Dazl and Boll show different expression patterns in mouse fetal ovary and adult testis

After confirming the specificity of the anti-Dazl and anti-Boll antibodies on mouse tissue in immunohistochemistry (see Section 3.2.2), we performed single immunofluorescence to detect either Dazl or Boll on fetal mouse ovaries at e13.5, e15.5, e18.5 and postnatal day 0 (P0). Experiments were performed on sections from 2 different individuals per development stage. Unlike the human, germ cell development is relatively synchronized in the fetal mouse ovary. Therefore, most of the germ cells in one section of a fetal mouse ovary are at the same approximate stage of development. The ages of the ovaries we used correspond to meiosis initiation (e13.5, Figure 4.1B, first panel), leptotene/zygotene (e15.5, Figure 4.1B, second panel), pachytene (e18.5) and diplotene/ follicle formation (P0, Figure 4.1B, third panel).

Consistent with previous studies, germ cells in the fetal mouse ovary expressed Dazl in the cytoplasm at all stages examined (Figure 4.12A). At e13.5 when meiosis has just started, small groups of $Dazl^{+ve}$ germ cells are readily detectable in the fetal mouse ovary. Their number subsequently increases and they become more homogeneously distributed throughout the ovary by e15.5. At e18.5, when most cells are entering into pachytene, $Dazl^{+ve}$ germ cells are clearly larger than at previous stages, but the number of cells appears to have decreased slightly, and they are predominantly localised towards the periphery of the ovary. At P0, Dazl is expressed in the primordial follicles and the cells maintain the peripheral distribution.

In contrast, no $Boll^{+ve}$ germ cells were detected at e13.5, 18.5 and P0, but Boll was extensively detectable in large numbers of germ cells at e15.5, with a distribution similar to that of Dazl (Figure 4.12A). The same experiments were also performed on adult mouse testis using same conditions as the positive control (Figure 4.12B). Consistent with the DAB staining, Dazl was mainly expressed in germ cells at earlier stages of development (from spermatogonia to pachytene) and Boll was only found in germ cells at later stages of meiosis (especially pachytene) suggesting that the fluorescence technique we used is as specific and effective as the DAB methods.

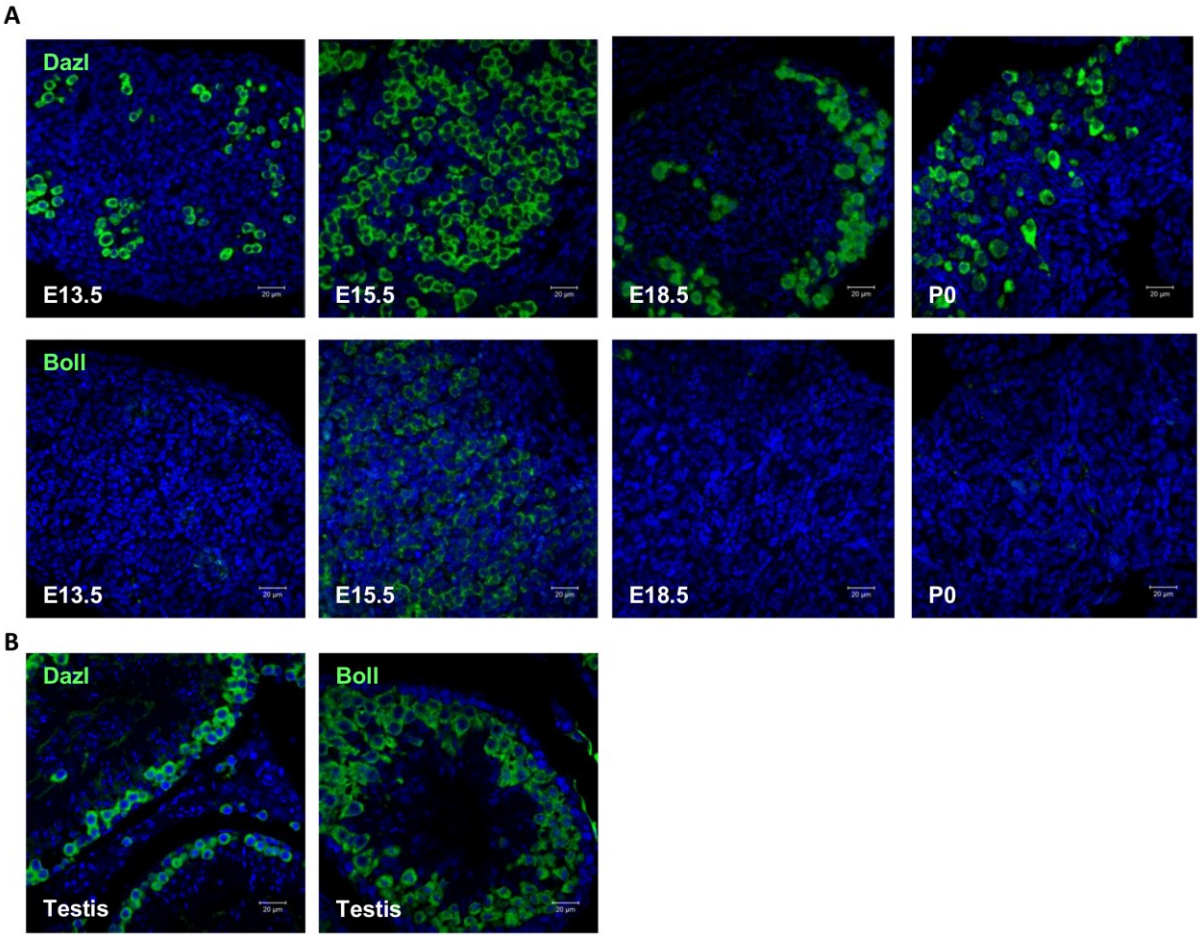

Figure 4. 12 Dazl and Boll proteins display distinct patterns of expression during mouse fetal ovary development.

A) Single immunostaining for Dazl or Boll (both green) in e13.5, e15.5, e18.5 and P0 mouse ovary. For different cell types in the ovary, see Figure 4.1B. Dazl is highly expressed in germ cells through all stages of development, whilst Boll is widely expressed in germ cells at e15.5 but not detectable at earlier or later gestations. **B)** Single immunostaining in adult mouse testis as positive control. The distribution of Dazl and Boll staining is similar to the DAB staining described in previous section and confirmed the effectiveness of the fluorescence methods. Counter stained with DAPI (blue), Scale bar=20μm

4.2.8 Dazl and Boll co-expression in mouse fetal ovary

The distribution of Dazl and Boll in the germ cells of the fetal mouse ovary at e15.5 suggests that Dazl and Boll may be extensively co-expressed in the same germ cells during fetal mouse oogenesis. We therefore performed double immunofluorescence to detect Dazl and Boll on sections of e15.5 fetal mouse ovaries (Figure 4.13A). The split channels of this image show that both Dazl and Boll are widely expressed in germ cells as detected by single staining. In contrast to our findings in the human fetal ovary, we confirmed that Dazl and Boll proteins are extensively co-expressed in the germ cells of the e15.5 fetal mouse ovary. Dual-immunofluorescence for both proteins was also performed on the adult mouse testis, in which both proteins are known to be expressed, revealing distinct but with some incomplete co-expression patterns of Dazl and Boll. Consistent with the single staining, Boll is expressed in germ cells at a later stage of development than those expressing Dazl (Figure 4.13B, VanGampel and Xu 2010; Xu *et al.*, 2001).

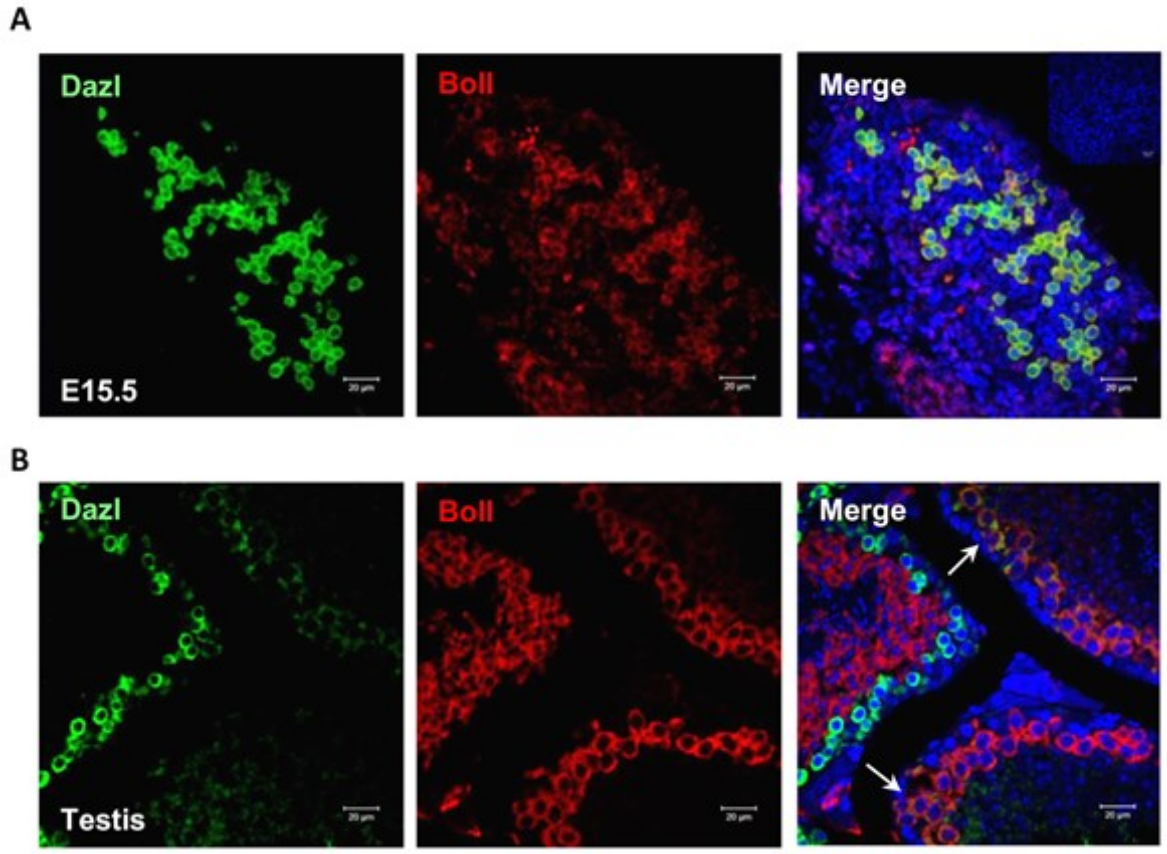

Figure 4. 13 Dazl and Boll are extensively co-expressed in fetal mouse ovary at e15.5. **A)** Double immunostaining for Dazl and Boll in e15.5 mouse fetal ovary: Dazl (green) and Boll (red) show extensive co-expression in germ cells at this gestation. **B)** Control showing mainly distinct expression and partial co-localisation of Dazl and Boll in germ cells in the adult mouse testis (arrows). Counter stained with DAPI (blue), Scale bar=20μm

4.3 Discussion

In this chapter, we investigated the expression and distribution of DAZL and BOLL during early oogenesis in the human and mouse ovary.

The difference in mRNA expression between *DAZL* and *BOLL* indicates that they may have different functions during germ cell development. The significantly increased levels of both mRNAs in the early second trimester suggest that these two genes may associate with meiosis. However the decrease in *BOLL* expression in late second trimester indicates that BOLL might be down regulated when germ cells become more mature and thus its expression is relatively transient when compared with *DAZL* in human fetal ovary. However, it is also necessary to recognise that the method used to calculate expression from the qRT-PCR data may be imperfect. The levels of *DAZL*/*BOLL* mRNAs were calculated relative to *RPL32* which is expressed by all cells in the sample, rather than just the germ cells. Therefore it is difficult to tell that whether the change in expression between gestations is caused by increased gene expression or changes in somatic or germ cell numbers. This could be corrected for by relating the values of *DAZL/BOLL* expression to a germ cell specific marker such as *VASA* instead of *RPL32*. This method has been utilised in another study (Bowles *et al.*, 2006) and therefore is accurate. Alternatively, expression could be calculated relative to counted germ cell numbers. Unfortunately, in this study, only the germ cell numbers in second trimester were counted (see Section 4.2.4), and data on first trimester numbers was unavailable. It was therefore impossible to correct the qRT-PCR results with this method. Modifications like this should be made if this experiment could be repeated and similar attention is necessary in the future studies.

Although both human *DAZL* and *BOLL* mRNA are expressed during the second trimester, their proteins are distributed in germ cells at different stages of development. DAZL expression is abundant after meiosis initiation in the early second trimester, but is mainly restricted to germ cells around the cortex of ovary, i.e. in the less mature germ cells. After that, it soon down-regulated and replaced by BOLL. Despite DAZL and BOLL possibly regulate some common mRNA targets, this pattern of sequential expression suggests that they may have distinct, non-overlapping functions. Indeed, this view is supported by Kee *et al.* (2009)'s

study, which suggests that DAZL is important for the differentiation of primordial germ cells whilst BOLL is promoting the later stages of meiosis. However, further investigation is still needed, potentially by isolating their specific mRNA targets.

BOLL expression begins at the second trimester, i.e. after meiosis has initiated in the human fetal ovary. Its expression increases with germ cell development and reaches a very high level in maturing germ cells in late second trimester before primordial follicle formation. The central localisation of BOLL-expressing germ cells also indicates that BOLL is only expressed in more mature germ cells. BOLL is then also down-regulated and DAZL is re-expressed when germ cells form primordial follicles.

Indeed, the small fraction of germ cells expressing DAZL and a meiosis marker and high ratio of BOLL/meiosis marker co-expressing germ cells, suggest that the DAZL expression persists from pre- to early stage of meiosis, and the switch between DAZL and BOLL expression happens during the early stage of meiosis prophase I. Thereafter, BOLL continues to be expressed during meiosis. DAZL is expressed before, and persists into, early meiotic prophase I, but is soon down-regulated around the leptotene/zygotene stage and replaced by BOLL. When meiosis arrests at diplotene and follicle formation is initiated, BOLL expression is extinguished and DAZL expression reactivated. This suggests a DAZL→BOLL→DAZL expression pattern during the development of a single germ cell in the human fetal ovary.

We then tried to find out whether the switch in expression from DAZL to BOLL that we observe during human fetal oogenesis also occurs during germ cell development in the fetal mouse ovary. However, in fetal mouse ovary, we found Dazl to be expressed at all the time points examined, from meiosis initiation to follicle formation. Boll is expressed in a limited window during meiosis prophase I (in human), and in mice we found Boll is also expressed in a narrow window around e15.5 (which corresponds with early meiosis at the leptotene/zygotene stages). Furthermore, we found Boll to be expressed in the same germ cells as Dazl in the fetal mouse ovary, in contrast to the pattern seen in the human. Moreover, the pattern in mouse fetal ovary is also different from adult mouse testis, in which the Boll starts to be expressed around the pachytene stage (VanGompel and Xu, 2010, 2011). Thus,

in the mouse there is continuous expression of Dazl throughout fetal germ cell development with coincident, brief, expression of Boll. This is in contrast to the two distinct windows of DAZL expression (separated by the expression of BOLL) and rare DAZL/BOLL co-expressing germ cells in the human fetal ovary. The relative timing of expression suggests there may be different functions for DAZL and BOLL proteins. The different expression patterns between human and mouse ovaries, or between mouse ovaries and testes imply the lack of conservation and therefore the mouse model might not perfectly represent Boll function in human.

Human ovarian development during the second trimester encompasses two key developmental stages; the formation of germ cell nests and entry into and progression through meiotic prophase I (approximately 12-16 weeks gestation) and the breakdown of germ cell nests and the assembly of individual oocytes into primordial follicles (approximately 17 weeks gestation onwards) (Hartshorne *et al.*, 2009). Consistent with the previous work from our laboratory which indicated that *DAZL* mRNA significantly increases between first and second trimester (Anderson *et al.*, 2007), our work more precisely positions this increase occurs between first and early second trimester. The increase of *DAZL* expression between first and second trimester is coincident with the onset of meiosis in the human fetal ovary (Anderson *et al.*, 2007). Lin *et al*. (2008) reported that mouse Dazl is necessary for the entry of meiosis together with retinoic acid, and that in *Dazl*$^{-/-}$ mice there is no initiation of meiosis, and the expression of *Stra8* RNA is nearly undetectable. Furthermore, Dazl also regulates the translation of some meiosis associated proteins such as Sycp3 in mouse (Reynolds *et al.*, 2007). In our study, we also tried STRA8 staining in human fetal ovary (data not shown) but the antibodies were not specific enough and we are not able to tell whether STRA8 is co-expressed with, and possibly regulated by, DAZL in the human fetal ovary. However, the significantly increased level of *DAZL* transcripts in pre-meiotic and early meiotic germ cells, and the protein translocation from nucleus (Figure 4.3) to cytoplasm, both support a conserved role for this protein in regulating the entry into meiosis in humans, consistent with the requirement for Dazl in fetal mouse ovarian germ cells to enable them to respond appropriately to the meiosis-inducing signal retinoic acid (Lin *et al.*, 2008).

In the human fetal ovary, we found that *BOLL* RNA is not detectable in first trimester, but is significantly up-regulated in early second trimester. The pattern of overlapping *DAZL* and *BOLL* expression, with the onset of *BOLL* expression occurring slightly later than that of *DAZL*, is comparable to that reported previously in the fetal sheep ovary (Mandon-Pepin *et al.*, 2003). In that model, although both *DAZL* and *BOLL* begin to express at 38 days post coitum (dpc), the level of DAZL RNA was found to be higher than that of BOLL at 49dpc (just prior of meiosis), and then they both dramatically increased at 56dpc (i.e. around the time of the initiation of meiosis). Interestingly, in our study, the level of *BOLL* slightly reduced (but not with statistical significance) at late second trimester in human fetal ovary. This may represent the down-regulation of BOLL during follicle formation, although this may also result from a dilution of *BOLL* mRNA due to the emergence of additional BOLL-negative germ cells at this stage.

Although the expression patterns of DAZL and BOLL mRNAs overlap in the second trimester, our immunohistochemistry data show that DAZL and BOLL protein are actually distributed in different groups of germ cells, with DAZL-expressing germ cells towards the periphery of the human fetal ovary, and BOLL-expressing germ cells towards the centre. The greater nuclear diameter of $BOLL^{+ve}$ cells compared to those of $DAZL^{+ve}$ cells suggests that BOLL is expressed in more mature germ cells (Fulton *et al.* , 2005). The co-localisation of the two proteins with meiosis-specific proteins further demonstrates that BOLL is expressed by germ cells at later stages of development, as both SYCP3 and phospho-ATM show a higher co-localisation ratio with BOLL than they do with DAZL. The expression pattern reveals different roles of DAZL and BOLL during germ cell development. The expression at pre-, early and arrested meiosis of DAZL suggests that DAZL is not only regulating the entry of meiosis, but also has some meiosis-independent functions such as germ cell differentiation. Indeed, this is supported by several studies which reported that the expression of pluripotency (e.g. *Oct4*) or germ cell markers (e.g. *Mvh*) were reduced in the germ cells of $Dazl^{-/-}$ mice on an inbred background at e14.5 (Lin and Page, 2005), and that Dazl might be necessary to maintain the number of pre-meiosis germ cells *in vivo* (Lin and Page, 2005) or the pluripotency of mouse primordial germ cells *in vitro* (Haston *et al.*, 2009). In contrast, BOLL has not been studied as extensively

as DAZL. Several studies suggest that the loss of Boll causes subfertility phenotypes across many species from flies, worms to mice, and it has been also reported to be associated with male subfertility phenotypes in human (Eberhart *et al.*, 1996; Karashima *et al.*, 2000; VanGompel and Xu, 2010; Kostova *et al.*, 2007). However, although the studies in model animals revealed that BOLL expression is associated with meiosis (Eberhart *et al.*, 1996, Karashima *et al.*, 2000), it is still unclear how BOLL is associated with oogenesis in humans. Our study indicates that in the human fetal ovary, BOLL is more tightly associated with meiosis than DAZL, and it is only expressed in a narrow window between meiosis initiation and meiosis arrest. The data presented here reveal a complex relationship between DAZL, BOLL and meiosis during human fetal ovarian development, and suggests that DAZL may have meiosis-dependent and meiosis-independent roles during human fetal germ cell development, the former being restricted to the fetal ovary and the latter shared with the germ cells of the human fetal testis.

In mice, deficiency of Boll causes subfertility phenotypes in males only (VanGompel and Xu, 2010), despite *Boll* mRNA being detectable in the mouse ovary from e10.5 to adult life (Shah *et al.*, 2010). We therefore studied the expression pattern of Dazl and Boll during mouse meiotic prophase I. To our surprise, Boll was only expressed at e15.5 (leptotene/zygotene) in fetal mouse ovary, and co-expressed in the same germ cells as Dazl; a very different pattern to that which we found in the human fetal ovary. This is not due to the synchronised germ cell development in fetal mouse ovary, as Boll-expressing germ cells are abundant at pachytene in both the human fetal ovary and mouse testis, whilst there is no Boll expression at e18.5 (pachytene) in fetal mouse ovary. This suggests that there is a genuine lack of conservation of the expression pattern of BOLL between human and mouse ovaries, and between female and male mouse meiosis.

The data presented here raise important questions about the validity of the *Boll*-knockout mouse as a model for understanding BOLL function during human female oogenesis. As RNA-binding proteins from the same family, the DAZ family proteins are highly conserved (Collier *et al.*, 2005) and may have partly overlapping targets such as *CDC25A* (Jiao *et al.*, 2002, Lin *et al.*, 2009). This is supported by

several studies, such as using *Xenopus dazl* to rescue the *Drosophila boule* phenotype (Houston *et al.*,1998), or using human *DAZ* to rescue the mouse *Dazl* knockout (Vogel *et al.*, 2002). Therefore, the complete co-expression of Dazl and Boll within the same germ cells in the fetal mouse ovary implies that Dazl may compensate for the loss of Boll in Boll-/- fetal ovarian germ cells, by binding and regulating some Boll target mRNAs. Because of the lack of overlap between DAZL and BOLL in the human fetal ovary (and to a less extent the adult mouse testis), such compensation is unlikely to happen. This probably explains the male-specific infertility phenotypes in Boll-/- mice, and also indicates that the Boll-/- mice may not accurately represent what happens during oogenesis in the fetal human ovary. Together, these data indicate that BOLL may have specific and important functions in regulating oogenesis in humans - distinct from those of DAZL - in contrast to its dispensability in mice.

Before concluding, it is still necessary to point out some weaknesses in the data. First, for all immunohistochemistry experiments, no peptide-block controls were applied. Only no-primary control (e.g. applying serum block without primary antibody) was used. To make sure the antibodies were specific, the peptides which were used to raise these antibodies should be applied together with the primary antibodies on the sections. However, since the peptides were not commercially available, this step was skipped. It also would be ideal to use isotype control, such as IgGs which are from the same species that the primary antibodies were raised against. And if no staining was observed, then it could be concluded that the staining on other sections was specific. And despite all the immunohistochemistry experiments being performed with no-primary control, some of them were only directly observed under microscope and images were not taken due to an underestimation of the importance of these controls. Failure to do the latter is a weakness of these studies and special attention to these is necessary in future work.

Another problem is that the sample size were quite small. For the datasets with this problem, the analysis of normal distribution was impossible and this could lead to type II error, which means the null hypothesis is not correctly rejected. Thus we could only assume that they were normally distributed and chose the corresponding

methods. The small sample size was caused by the limited resource of human tissue – the human tissue is very precious, and it is even more difficult to obtain the fetal ovary. Although all the immunohistochemistry was applied on sections from different individuals to make sure the results were convincing, the images showed here, and all the immunohistochemistry-dependent data collection and analyses were only based on one sample per gestation. This one sample basis was a big flaw and made the data less convincing than it should be. Unfortunately there was no time to redo all these work and increase the sample number, but it should be avoided in future work.

In conclusion, these data reveal that human DAZL and BOLL expression dynamically changes during fetal ovary development, and follows a DAZL→BOLL→DAZL pattern in a single germ cell. Further investigation strongly suggest that both proteins are associated with different stages of meiosis. The existence of a conserved and transient window of BOLL expression during fetal oogenesis in both humans and mice was observed, which probably corresponds to a specific stage of meiotic prophase I. However, the striking switch from DAZL expression to BOLL expression during germ cell maturation in the human fetal ovary does not occur in mice, suggest a non-conserved pattern of Dazl and Boll expression between human and mouse.

Chapter 5

Identification of Human mRNA Targets of DAZL and BOLL

Chapter 5. Identification of Human mRNA Targets of DAZL and BOLL

5.1 Introduction

DAZ family proteins bind mRNA targets and promote their translation (Collier *et al.*, 2005), and possibly enhance their stabilization (Takeda *et al.*, 2009, Wiszniak *et al.*, 2011). Although some target mRNAs have been reported in model animals, no definitive human DAZL targets have been identified so far.

It has been suggested that mouse Dazl recognises a U(2-10)G/CU(2-10) motif in the 3'-UTR of its mRNA targets (Reynolds *et al.*, 2005, Venables *et al.*, 2001), whilst zebrafish dazl binds to GUUC motifs (Maegawa *et al.*, 2002). Research on the crystal structure of DAZL RNA recognise motif (RRM) indicates that GUU might be sufficient for DAZL to bind, and suggests that BOLL may share some binding features with DAZL, but has its own binding motif (Jenkins *et al.*, 2011).

The putative dazl targets identified in zebrafish are *tdrd7*, *HuB* and *dazl* itself, and they are all protected by dazl protein from miRNA-mediated degradation, and possibly also show enhanced translation under this regulation; the stabilisation effect may play a role in germline-specific expression of these mRNA (Takeda *et al.*, 2009, Wiszniak *et al.*, 2011).

Most Dazl targets have been identified in mouse. Amongst these targets, *Mvh* and *Sycp3* are the only definitively proven ones (Reynolds *et al.*, 2007, Reynolds *et al.*, 2005). Putative Dazl binding sites are found in the 3'-UTR of both target mRNAs, and direct binding between Dazl and these two mRNA has been confirmed at the molecular level (Jenkins *et al.*, 2011). The activity of luciferase vectors conjugated with the *Mvh* or *Sycp3* 3'-UTRs could be stimulated by co-injecting *Dazl* into mouse oocytes (Reynolds *et al.*, 2007, Reynolds *et al.*, 2005). Moreover, the null-phenotypes of *Dazl* include reduced Mvh and Sycp3 protein levels in the testis, and the meiotic arrest phenotypes observed in *Dazl* or *Mvh*-null mutant mice are very similar (Reynolds *et al.*, 2007, Reynolds *et al.*, 2005). Some other targets have also been identified: Zeng *et al.* (2007, 2009) reported that Dazl could interact with *Tex19.1*, *Tssk1*, *2* and *4* (which all contain the DAZL binding sites in their 3'-UTRs),

and the translation of *Tex19.1* seems to be repressed by Dazl in single-cell zebrafish embryo. Research performed on mouse oocytes revealed similar RNA-protein interactions between Dazl and *Tpx2*, with the activity of luciferase conjugated to *Tpx2* 3'-UTR being down-regulated when Dazl is knocked down (Chen *et al.*, 2011). This work also confirmed that Dazl binds and promotes the translation of its own mRNA (Chen *et al.*, 2011).

The expression of a range of other mRNA targets has been reported to be affected by *Dazl* knockout, but their direct regulation by Dazl protein has not been proven yet. One of the most important candidates is *Stra8*, which is essential for the entry of meiosis, and which almost completely disappears in the *Dazl*$^{-/-}$ mouse fetal ovary, along with the several other meiosis-associated mRNA including *Dmc1*, *Spo11*, *Sycp3* and *Rec8* (Lin *et al.*, 2008). Like *Tex19.1*, Dazl also represses the translation of *Caspase 2*, *7* and *9* mRNAs (Chen *et al.*, 2014). A mouse Dazl variant which does not contain exon 8 seems be act as a repressor of its potential targets including *Mvh*, *Oct3/4* and *Sox2*, but again no evidence of direct binding has been reported (Xu *et al.*, 2013).

Some additional mRNAs have been reported to co-precipitate with Dazl but no further investigation has been performed so far. These include *Tpx1*, *Pam*, *Trf2*, *Grsf1*, *D2*, *Cappβ1*, *Pα7/C8*, *H47* (Jiao *et al.*, 2002), *Odc1*, *Tex14*, *Fthl17*, *Calm2* (Reynolds *et al.*, 2005), *Rap2c*, *Nbn*, *Ercc1*, *Spnr*, *Dnmt3l* and *Sox17* (Zeng *et al.*, 2008), which all co-precipitate with Dazl from mouse testis extracts. Using RNA immunoprecipitation (RIP) and microarray, several additional mRNA that directly bind with and repressed by Dazl has been identified, namely *Sox2*, *Sall4*, *Suz12*, *Zfp42* and *Zic3* (Chen *et al.*, 2014).

The only BOLL mRNA target identified so far is *twine*/*CDC25A* homologue. *twine* is expressed in *Drosophila*, and *twine* mutants show similar phenotypes to *boll* mutants (Eberhart *et al.*, 1996). Further investigation revealed that loss of one copy of *bol* in *twine* mutants increased the severity of the phenotype, from meiosis arrest to no entry into meiosis, and this could be rescued by *twine* expression that was independent of translation-regulation by bol (Maines and Wasserman, 1999). In humans, *CDC25A* is a strong putative BOLL target, as it is co-precipitated with

BOLL, through a 21-nucleotide sequence (AGGUGUAGGUGGGUUUUUCUU) on its 3'-UTR, the mutation of which (UUUUU to CCCCC) strongly reduces the strength of interaction (Lin *et al.*, 2009). Mouse *Cdc25a* has also been reported as a potential Dazl target, however only binding *in vitro* has been confirmed (Jiao *et al.*, 2002). Moreover, as DAZL and BOLL are from the same family and have highly conserved RNA-recognition motif (RRM) (Eberhart *et al.*, 1996), it is possible that they could recognise/bind to similar motifs in their mRNA targets, and cross-species rescue studies indicate that these proteins may regulate the same targets (Houston *et al.*, 1998). However, the investigation on the molecular structure of DAZL and BOLL proteins suggested that a crucial residue of amino acid in DAZL for the GUU triplet recognition is mutated in BOLL RRM, and it is not certain that BOLL could bind to GUU with the same way as DAZL (Jenkins *et al.*, 2011). Therefore, during further investigation we assumed that some of the DAZL targets listed in Table 5.1 may also be BOLL targets.

For human DAZL however, no definitive targets have been identified. One candidate is *SDAD1*, which is interacts with both DAZL and its co-factor PUM2 through its 3'-UTR in a yeast three-hybrid-assay (Fox *et al.*, 2005). Similarly, human *TSSK1*, *2*, *4* and *5* are also bound by DAZL (Zeng *et al.*, 2008). In addition, both expression of DAZL and BOLL seem to increase the percentage of VASA-GFP^{+ve} human ES cells, as well as the number of cells with SYCP3 protein loaded properly on chromosomes, suggesting that they may regulates these two proteins as well (Kee *et al.*, 2009).

To summarize, despite the identification of many potential targets of DAZL and BOLL, very few of them have been confirmed and most have only been investigated in a single respect – either direct binding or translation regulation. The known targets of human DAZL or BOLL are limited, and this has become a bottleneck to understanding the functions of DAZL and BOLL during germ cell development. This chapter will focus on identifying these mRNA targets and try to co-relate them to human oogenesis.

To identify putative DAZL targets, we searched on PubMed and established a list of potential mRNA targets identified previously in human or model animals. We

selected the human homologues of *Tex19*, *Tex14*, *Stk31* (Reynolds *et al.*, 2005), *Pam*, *Grdf1*, *Trf2* (Jiao *et al.*, 2002), *Tpx1*, *Ercc1*, *Tssk2*, *Spnr*, *Dnmt3l*, *Sox17* (Zeng *et al.*, 2008) to investigate further. By looking at the literature, we made Table 5.1 to show the expression and functions of each mRNA/protein, especially whether they were expressed in gonads and associated with infertility phenotypes. For the targets which only have been studied in non-human animals, we also found that all of them or their homologues were reported to be expressed in human. Almost all of the targets are related to subfertility/infertility phenotypes, but mostly only in mouse knockout models (Table 5.1). Based on the findings of this literature search, we selected *TEX19*, *TEX14*, *STK31*, *GRSF1*, *TRF2*, *TPX1*, *ERCC1*, *TSSK2*, *DNMT3L* and *SOX17* as the targets we investigated further.

Table 5. 1 Literature review of potential DAZL mRNA targets

The following aspects of these mRNA targets were checked: expression in human, whether they were expressed in germ cell/ovary/testis, their function and related infertility phenotype. X indicates detectable expression. The references are listed in the last column of the table.

Gene	Human	Germ cell	Ovary	Testis	Function/Phenotype	References
TEX19	X	X	mouse *Tex19.1*	X	Meiosis Impaired spermatogenesis (in mouse)	**Kuntz *et al.* (2008) Stem Cells;26(3):734-44** **Ollinger *et al.* (2008) PLoS Genet;4(9):e1000199.** **Tarabay *et al.* (2013) Hum Reprod.;28(8):2201-14**
STK31	X	X	mouse	X	Meiosis Dynamic change during mouse testis development Decreased in human testis of germ cell absent patients *	**Wang *et al.* (2001) Nat Genet.;27(4):422-6** **Olesen *et al.* (2007) Cell Tissue Res 328:207–221** **Bao *et al.* (2012) Histochem Cell Biol.;137(3):377-89**
TEX14	X	X	X	X	Meiosis Cell cycle Intercellular bridges absent, male infertility and oocyte decrease (in mouse)	**Wang *et al.* (2001) Nature Genet 2001;27:422-426** **Houmard *et al.* (2009) Biol Reprod.;81(2):438-43** **Greenbaum *et al.* (2009) Biol Reprod.;80:449–457** **Mondal *et al.* (2012) Mol Cell;45(5):680-95**
CRISP2	X	X	N	X	Sertoli/spermatogenic cells interaction Sperm-egg fusion Breakpoint may cause male infertility	**Olesen *et al.* (2001) Mol Hum Reprod.;7(1):11-20** **Maeda *et al.* (1998) Biochem Biophys Res Commun.;248(1):140-6** **Maeda *et al.* (1999) Dev Growth Differ;41(6):715-22.** **Nimlamool *et al.* (2013) Mol Reprod Dev;80(6):488-502**

PAM	X	?	X	X(basal cells in testicular seminiferous tubules)	Myc-related may be required in chromatin function	**Guo *et al.* (1998) Proc. Natl. Acad. Sci. USA;95:9172–9177** **Braas *et al.* (1992) Endocrinology;130(5):2778-88 abstract**
GRSF1	X	?	?	X(mouse)	5'-UTR mRNA-binding translational regulator Cleavage of primary mitochondrial RNA transcripts A target of the Wnt/β-catenin pathway which is necessary for mesoderm formation	**Sampath *et al.* (2008) Cell Stem Cell;2:448–460** **Lickert *et al.* (2005) Development;132:2599-2609** **Jourdain *et al.* (2013) Cell Metab.;17(3):399-410** **Antonicka *et al.* (2013) Cell Metab.;17(3):386-98**
TRF2	X	X	X(mouse)	X	Negative regulator of telomere length and keep telomere stable Defect in spermiogenesis (mouse)	**Smogorzewska *et al.* (2000) Mol Cell Biol.;20(5):1659-68** **Zhang *et al.* (2001) Science;292 (5519):1153-1155** **Xiao *et al.* (2006) Gene Expression Patterns;6:409–419**
ERCC1	X	X	X	X	Essential for nucleotide excision repair Infertility of both male and female mouse	**Hsia *et al.* (2003) Development;130:369-378** **Cheng *et al.* (1999) Cancer Epidemiol Biomarkers Prev.;8(9):801-7** **Koberle *et al.* (2010) Oncol Rep.;23(1):223-7**
TSSK2	X	X	N	X	Testis specific serine/threonine kinase Transformation of chromatoid body in elongating spermatids SNPs related to impaired human spermatogenesis	**Xu *et al.* (2008) Dev Biol.;319(2):211–222** **Zhang *et al.* (2010) J Androl.;31(4):388-92** **Hao *et al.* (2004) Mol Hum Reprod.;10(6):433-444** **Li *et al.* (2011b) Mol Hum Reprod.;17(1):42-56** **Shang *et al.* (2010) J Cell Sci.;123(Pt 3):331-9**

SPNR (STRBP)	X	X(mouse, post-meiotic germ cells)	X(mouse)	X	Spermatid perinuclear RNA binding protein Sperm defects in the flagellum (mouse)	**Pires-daSilva *et al.* (2001) Dev Biol.;233(2):319-28** **Schumacher *et al.* (1995) J Cell Biol. 1995;129(4):1023-32.** **Salemi *et al.* (2012) J Endocrinol Invest.;35(1):5-7**
DNMT3L	X	X	Low mRNA	X	Promote DNA methylation Required for imprints Variations associated with oligospermia.	**Aapola *et al.* (2000) Genomics;65(3):293-298** **Bourc'his *et al.* (2001) Science;294(5551):2536-9** **Kobayashi *et al.* (2009) Eur J Hum Genet;17(12):1582-9**
SOX17	X	X (early germ cell)	X	X	DNA-binding protein A transcriptional factor in premeiotic germ cells Promote germ cell differentiation	**Katoh (2002) Int J Mol Med;9(2):153-7 abstract** **de Jong *et al.* (2008b) J Pathol.;215(1):21-30** **Kanai *et al.* (1996) J Cell Biol. ;133(3):667-81** **Irie *et al.* (2015) Cell.;160(1-2):253-68**
CDC25A (twine)	X	X	X (low in adult mouse)	X	Regulate meiosis I-II transition and MII arrest in female mRNA level decreased in infertile human male	**Wickramasinghe *et al.* (1995) Development;121(7):2047-56.** **Solc *et al.* (2008) Dev Biol.;317(1):260-9** **Oh *et al.* (2013) J Cell Sci;126(Pt 5):1081-5** **Lin *et al.* (2006) Hum Reprod.;21(1):138-44**

Updated from Msc thesis, J. He 2010

In this study, we used HEK293 cells and TCam-2 cells as models to study DAZL function. TCam-2 cells was used as a germ cell model in this study. The studies on this cell line are very limited and it is very difficult to explain why it do not endogenously express DAZL or BOLL. However, the karyotype analysis indicates that TCam-2 cells seem to be tetraploid (Mizuno *et al.*, 1993). The gene expression analysis shows that it expresses several protein markers of primordial germ cells such as OCT4, NANOG and c-Kit (de Jong *et al.*, 2008; Eckert *et al.*, 2008). Together, these data imply that the TCam-2 cells are possibly similar to the differentiating primordial germ cells which has finished the pre-meiosis chromosome replication, but the meiosis is arrested, possibly because of carcinogenesis. Therefore the expression of DAZL and BOLL, which are potentially required for human primordial germ cell differentiation and/or meiosis (Kee *et al.*, 2009) might be stopped by the same cause of carcinogenesis.

As transfection of the germ cell tumor derived TCam-2 cells was difficult (see Section 3.2.5), HEK293 cells were used instead before this problem was solved.

We performed RT-PCR to find out the expression of potential DAZL targets in these two cell lines (MSc thesis, 2010). Figure 5.1 shows the expression of the putative mRNA targets of DAZL in 16 week gestation human fetal ovary, TCam-2 cells and HEK293 cells. All the targets are expressed in both fetal ovary and TCam-2 cells, although *STK31* and *TPX1* are very weak in TCam-2 cells.

HEK293 cells originate from human embryonic kidney and therefore are not an ideal model to study DAZL function in germ cells. Indeed, no bands of *DNMT3L*, *SOX17* or *TPX1* are detected in HEK293 cells and *STK31* is extremely weak as well. However, the remaining seven mRNA targets are all expressed at a relatively high levels in HEK293 cells. *RPL32* is also detected as positive control, suggesting that the PCR is effective. The expression of multiple potential DAZL/BOLL targets in HEK293 cells demonstrates that this cell line also could be used to study the effect of DAZL/BOLL on their endogenous mRNA targets.

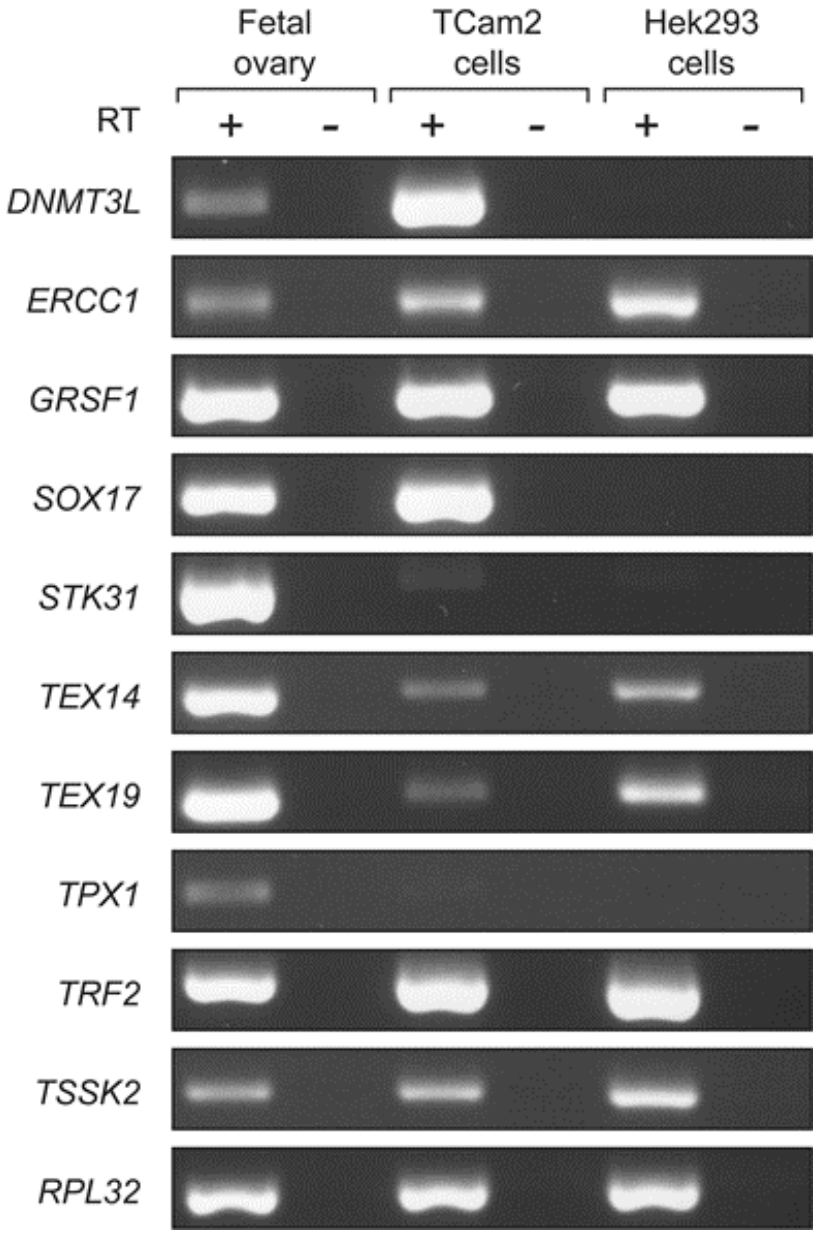

Figure 5. 1 Expression of potential DAZL targets/germ cell markers in 16 week gestation human fetal ovary, TCam-2 cells and HEK293 cells.

All the targets are expressed in fetal ovary and TCam-2 cells, although *STK31* and *TPX1* are very weak in TCam-2 cells. The non-germline cell line HEK293 also expresses most of the targets except *DNMT3L*, *SOX17* and *TPX1*, and *STK31* is very weak. The house keeping gene *RPL32* is also detected as positive control, and no band is seen in the –RT reactions, suggests that the PCR is effective and has no genomic DNA contamination.

MSc Thesis, J.He 2010

5.2 Results

5.2.1 Introducing DAZL or BOLL could increase the level of their potential mRNA targets in HEK293 cells

After successful transfection with *pCMV6-DAZL* or *pCMV6-BOLL* vectors in HEK293 cells was confirmed (see Section 3.2.3), mRNA was isolated from transfected cells, and expression of putative target mRNAs was analysed by qRT-PCR. Seven of the potential targets expressed in HEK293 cells, namely *TEX19*, *TEX14*, *CDC25A*, *TSSK2*, *GRSF1*, *ERCC1* and *TRF2* were previously tested between DAZL and Empty transfections (*MSc thesis, J He 2010*). The changes in mRNA levels were detected for *TEX19*, *TEX14* and *CDC25A*, therefore, these targets were selected for further investigation in *pCMV6-DAZL* or *pCMV6-BOLL* transfected cells (Figure 5.2). Each transfection contained one technical replicate during every experiment, and the experiment repeated for four times (four biological replicates). When doing the qRT-PCR, each sample is replicated for twice and the average Ct value was calculated for further analysis.

Since the samples were matched in each group, the data were analysed using (Repeated-measures) RM One-Way ANOVA with Geisser-Greenhouse's correction, followed by Tukey's multiple comparisons test. In *pCMV6-DAZL* transfected cells, the transcripts of *TEX19* and *TEX14* increased 1.68±0.09 (n=4) and 2.60±0.18 (n=4) fold relative to empty-vector transfected cells respectively (Figure 5.2, both $p<0.001$). The levels of these mRNAs also increased in *pCMV6-BOLL* transfected cells when compared to the empty vector transfections (both $p<0.05$), but were still significantly lower than those in DAZL expressing cells ($p<0.005$ for *TEX19* and $p<0.001$ for *TEX14*).

Besides *TEX19* and *TEX14*, *CDC25A* expression was also analysed as it has been reported to be a potential target of both DAZL and BOLL (Lin *et al.*, 2009, Pan *et al.*, 2009). *CDC25A* expression only increased very slightly in *pCMV6-DAZL* transfections (but not significant) and showed almost no change in *pCMV6-BOLL* transfection. Cadherin-associated protein beta 1 (beta-catenin) (*CTNNB1*) was chosen as the non-DAZL target control because it is highly expressed in HEK293 cells and no evidence so far demonstrates that it could be bound directly by DAZL,

although its 3'-UTR does contain some potential DAZL recognition sites. Results showed that the levels of *CTNNB1* remained unchanged in all transfections (Figure 5.2).

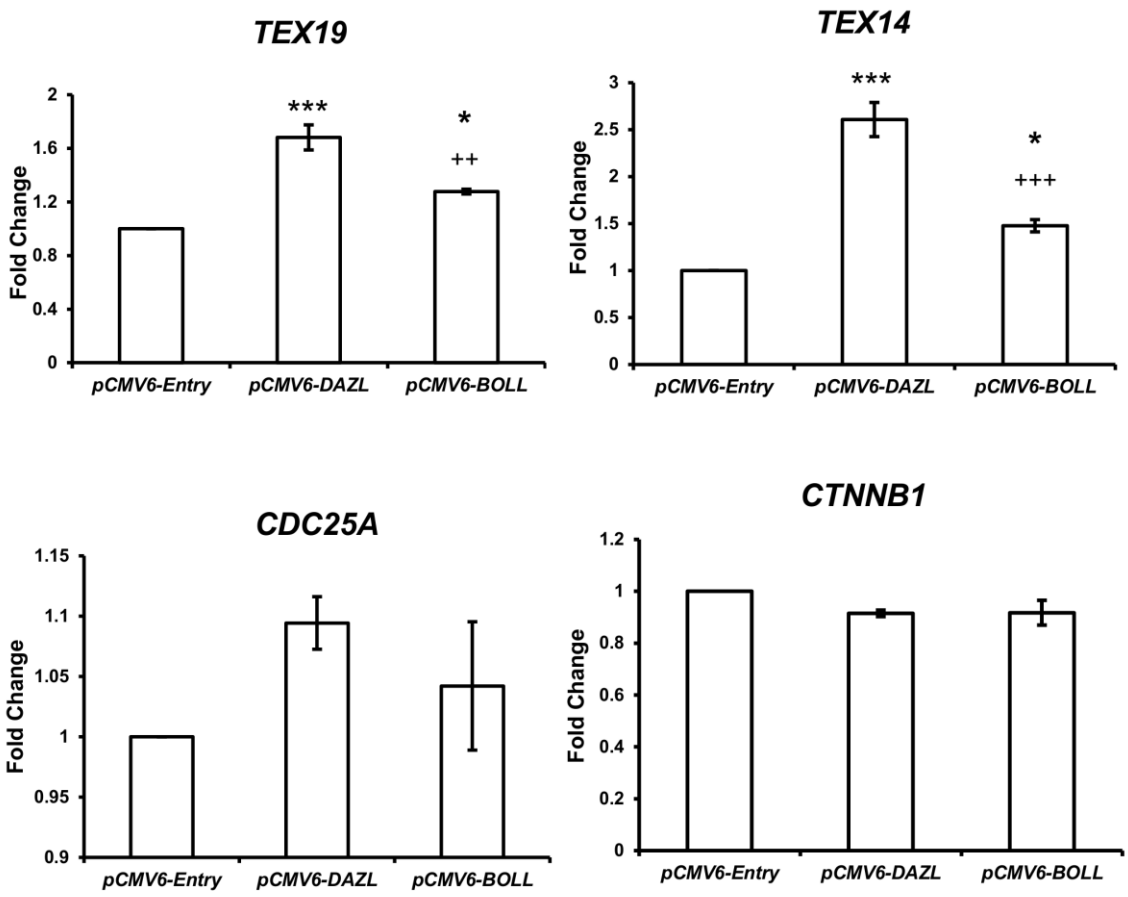

Figure 5. 2 qRT-PCR for potential DAZL targets after expressing DAZL/BOLL in HEK293 cells.

TEX19 increases 1.68±0.09 fold and *TEX14* increases 2.60±0.18 fold after *pCMV6-DAZL* transfection. Introducing BOLL also has some effects on both the targets (1.28±0.02 fold for *TEX19* and 1.47±0.07 fold for *TEX14*) but the increases are still significantly lower than those with DAZL. *CDC25A* increases 1.09±0.02 fold in DAZL expressing cells but not significant, and BOLL has no effect on this mRNA. No significant change was detected in non-DAZL/BOLL target *CTNNB1*. n=4 per group, * relative to Control, +relative to DAZL, ***p<0.001, **p<0.01, *p<0.05, value=mean±s.e.m.

5.2.2 The increase in *TEX19* and *TEX14* mRNA levels may be due to DAZL-mediated mRNA stability

We already found that *TEX19* and *TEX14* mRNA levels increased after *pCMV6-DAZL* transfection. This could arise from increased transcription or increased mRNA stability. As RNA-binding proteins, DAZL and BOLL cannot promote the transcription of *TEX14* and *TEX19* directly, but are more likely to regulate their mRNA targets at a post-transcriptional level.

To find out whether overexpression of DAZL increased target mRNA stability *in vitro*, we transfected HEK293 cells with *pCMV6-DAZL* or empty vector, followed by 5μg/ml Actinomycin D (ActD) treatment to block transcription. This dose and treatment time was based on previously published studies (Basu *et al.* , 2010, Ren *et al.* , 2005). Each treatment contained one sample and 5 groups of treatment were carried out on different passages of cells in total. After 24h ActD treatment, levels of *TEX19* and *TEX14* mRNA decreased to 7.69±1.52% (n=5) and 90.06±11.11% (n=5) of their Time 0 levels in empty-vector transfected cells, respectively. In contrast, 21.40±2.64% of *TEX19* mRNA remained after 24h in *pCMV6-DAZL* transfected cells and *TEX14* slightly increased to 104±10.35% when compare to time 0 level (Figure 5.3), both of which were significantly higher than the levels in empty-vector transfected cells after treatment ($p<0.005$). The non-DAZL target *CTNNB1* was investigated as a negative control but its level did not decline over the time window examined in empty-vector transfected cells.

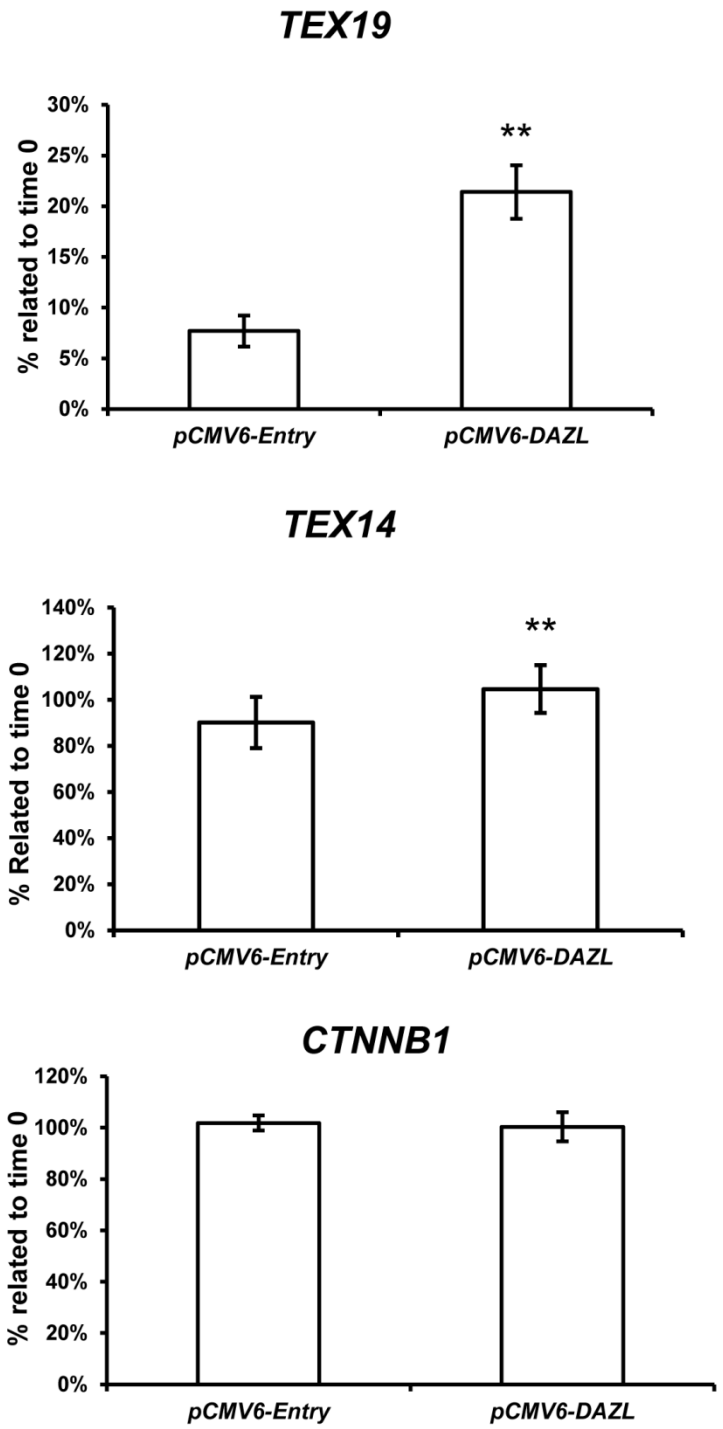

Figure 5. 3 The mRNA levels of *TEX19* and *TEX14* in *pCMV6-DAZL* transfected HEK293 cells are rescued after 24h ActD treatment (transcription blocking)

7.69±1.52% *TEX19* mRNA and 90.06±11.11% *TEX14* mRNA is left in the control transfected cells 24h after ActD treatment. In contrast, 21.40±2.64% *TEX19* mRNA survived in DAZL expressing cells and *TEX14 mRNA* levels increase to 104±10.35% when compare to time 0. No change was observed in non-DAZL/BOLL target *CTNNB1*. n=5 cultures per group, **p<0.01, value=mean±s.e.m.

5.2.3 Quantification of DAZL and BOLL protein expression in HEK293 cells at different time point after transfection

The differential increases in the level of target mRNAs between DAZL and BOLL-transfected cells may be due to the selective binding of the mRNA targets, but also could be caused by different levels of DAZL or BOLL protein expression at the same time point when the mRNA was isolated (i.e. variation in efficiency of transfection or kinetics of protein production). Therefore, to find out when the peak of DAZL and BOLL protein expression occurred after transfection and to compare their levels at the same time point, we transfected HEK293 cells with *pCMV6-DAZL* or *-BOLL* vectors, harvested the cells and extracted the protein every 12h from 0h to 72h after transfection. Western blotting was performed to quantify the amount of DAZL or BOLL protein, relative to the loading control α-tubulin (Figure 5.4).

By Western blotting, both the anti-FLAG and α-tubulin antibodies detected corresponding bands at the right size (DAZL-FLAG=~37kDa, BOLL-FLAG=~35kDa, α-tubulin=~50kDa) in the lanes of 12 to 72h transfected samples. Only α-tubulin (no or very faint DAZL/BOLL bands) was detected in the lanes of 0h or untransfected cells, suggesting that the FLAG-tagged DAZL or BOLL bands were specific (Figure 5.4A). Quantification (Figure 5.4B) based on Western blotting was performed, using the LiCor Odyssey system to calculate the colour intensity of each band, and demonstrated that almost no FLAG-tagged DAZL or BOLL protein was expressed at time 0, but after 12h both proteins appeared. It then took 36h for DAZL protein to reach its peak amount, whilst for BOLL the peak was at 48h. After these time points the amount of both proteins began to reduce slightly, but still remained easily detectable until 72h. The average relative expression levels of FLAG-tagged DAZL protein were higher than BOLL at all the tested time points include 48h, but not significantly so (n=4).

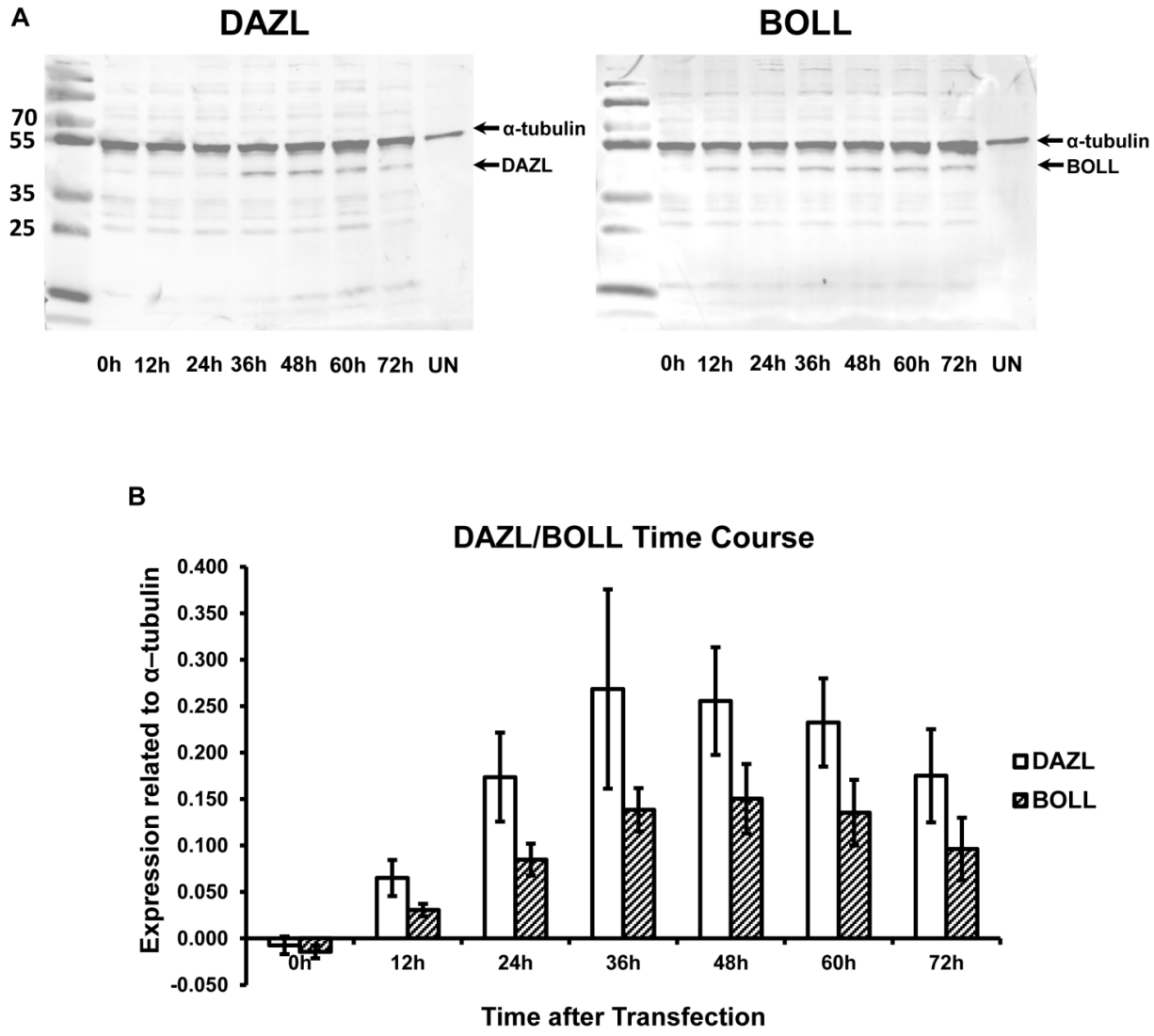

Figure 5. 4 Time course of DAZL or BOLL protein in transfected HEK293 cells.

A) Western blotting for *pCMV6-DAZL* or *-BOLL* transfected HEK293 cells at different time points. The left set of samples were transfected with *pCMV6-DAZL* vector whilst the right set were transfected with *pCMV6-BOLL* vector, and both were detected using FLAG and α-tubulin primary antibodies. DAZL and BOLL bands appear in all the lanes except very faint DAZL or BOLL bands are detected in the lanes of 0h transfection and no band in the untransfected samples. α -tubulin is detected in all the lanes. **B)** Quantification of DAZL and BOLL proteins in the transfected HEK293 cells at different time point, relative to α -tubulin. Both the proteins begin to express at 12h and the levels of DAZL are higher than BOLL at all the time points but not significant. The peak of DAZL expression appears at 36h (0.27±0.11 relative to α-tubulin, whilst the peak of BOLL is at 48h (0.15±0.04 relative to α-tubulin). n=4, value=mean±s.e.m., UN=untransfected cells

5.2.4 The levels of putative DAZL mRNA targets change significantly in GFP-sorted, *pCMV-DAZL* transfected TCam-2 cells

The *pCMV6* vectors could be transcripted in TCam-2 cells and the stable transfected cells lines were generated, however no protein was translated (see Section 3.2.5). Moreover, the TCam-2 cells have an extremely low transfection ratio. To solve the problem of these non-working vectors on TCam-2 cells and the low transfection ratio, a co-transfection/FACS system was established (see Section 3.2.6-3.2.7), and used this to look at how DAZL expression affected the expression of its mRNA targets in TCam-2 cells by qRT-PCR (Figure 5.5). Each treatment contained one sample, and 5 groups were generated in total. For qRT-PCR, every sample was repeated once and the average of Ct value was calculated.

We compared the levels of putative mRNA targets of DAZL between the GFP^{+ve} ($DAZL^{+ve}$) and GFP^{-ve} ($DAZL^{-ve}$) cells. Both *SYCP3* ($p<0.005$) and *TEX14* ($p<0.05$) mRNA levels increased significantly in GFP^{+ve} cells, 2.05±0.22 (n=5) and 1.37±0.14 (n=5) fold respectively relative to GFP^{-ve} cells. Surprisingly, the mRNA levels of *DNMT3L* ($p<0.05$) and *SOX17* ($p<0.005$) both significantly decreased in the GFP^{+ve} cells; *DNMT3L* to 58±0.05% (n=5) and *SOX17* to 57±0.04% (n=5) compared to their levels in GFP^{-ve} cells, indicating that the DAZL protein may have a novel repression effect on some mRNA targets in human. A 1.44±0.19 fold increase of the mRNA level of *VASA* in GFP^{+ve} cells was not significant (although VASA protein levels increased when DAZL overexpressed in human ES cells, and thus is a potential DAZL target in human (Kee *et al.*, 2009)) The mRNA level of another putative DAZL target *TRF2* remained unchanged (1.01±0.02 (n=5) fold relative to levels in GFP^{-ve} cells).

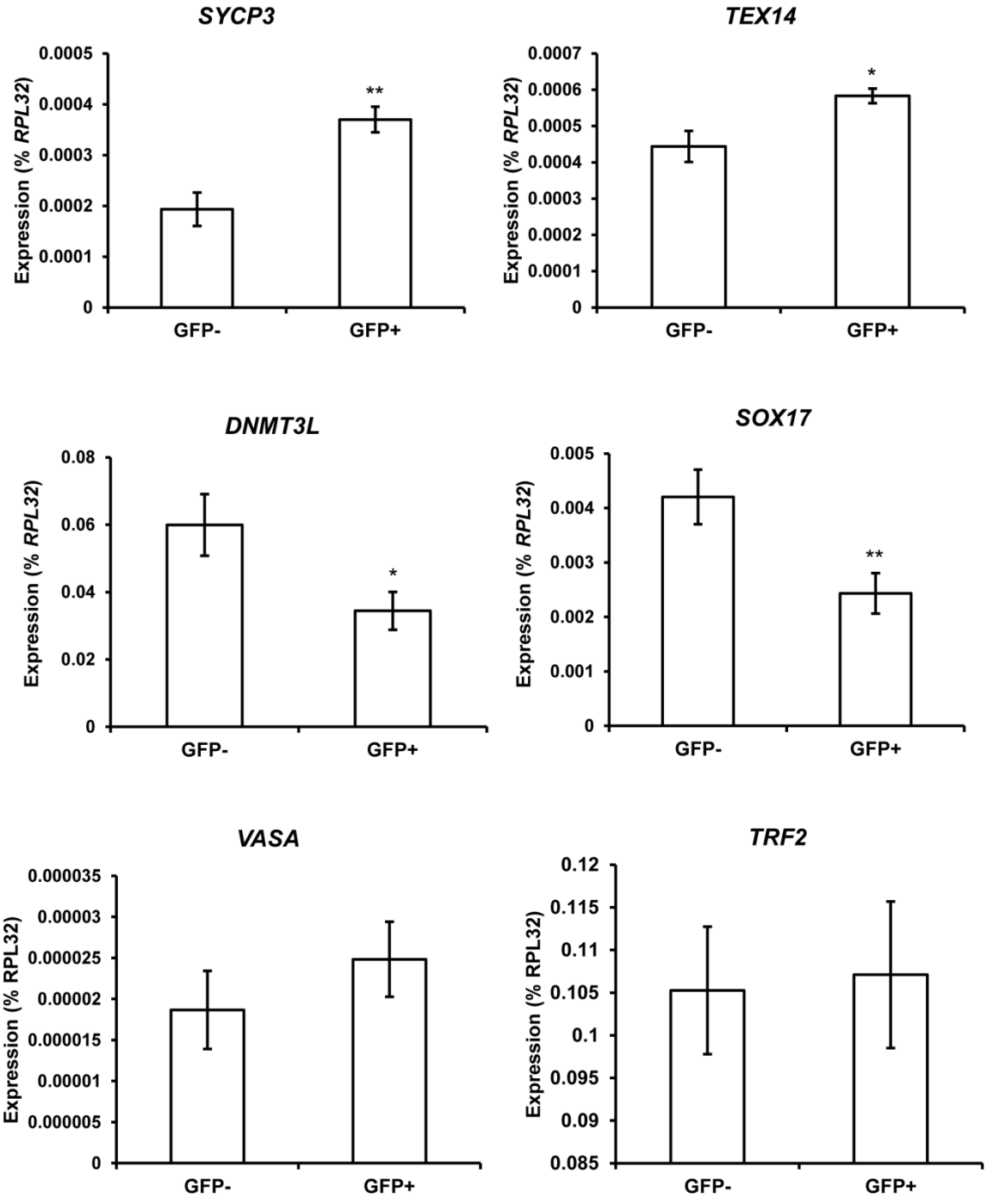

Figure 5. 5 The mRNA levels of potential DAZL targets show significant difference after *DAZL/GFP* co-transfection and GFP sorting.

SYCP3 and *TEX14* mRNA levels both significantly increase in $GFP^{+ve}/DAZL^{+ve}$ TCam-2 cells (2.05±0.22 fold for *SYCP3* and 1.37±0.14 fold for *TEX14*) relative to $GFP^{-ve}/DAZL^{-ve}$ cells. *DNMT3L* and *SOX17* mRNA levels were significantly reduced to ~57% of their levels in the $GFP^{-ve}/DAZL^{-ve}$ cells. The human DAZL target *VASA* also slightly increased in $GFP^{+ve}/DAZL^{+ve}$ cells (1.44±0.19 fold) but not significant, and another putative DAZL target *TRF2* did not show any change (1.01±0.02 fold). n=5, *p<0.05, **p<0.01, value=mean±s.e.m.

5.2.5 DAZL promotes the translation of *Luciferase* mRNA conjugated with *TEX14*-3'UTR in HEK293 cells

After identifying the effect on the mRNA levels of putative DAZL mRNA targets, we next sought to investigate whether DAZL regulates the protein levels of these mRNAs. For this purpose, a 3'-UTR luciferase assay was designed. As DAZL usually functions by binding to the 3'-UTR of its mRNA targets (Collier *et al.*, 2005), optimized *Renilla Luciferase* vectors with either no 3'-UTR, or conjugated to the human *GAPDH* 3'-UTR or *TEX14* 3'-UTR were used as the reporter and co-transfected with *pCMV6-Entry* (empty) or *pCMV6-DAZL* vectors into HEK293 cells for 48h (Table 5.2). If DAZL promotes the translation of these mRNAs through their 3'UTRs, then the translation of luciferase will be enhanced and thus the luminescence will be stronger (Figure 5.6). The *Luciferase* vectors with no 3'-UTR or *GAPDH* 3'-UTR cannot be regulated by DAZL and are therefore used as control and also for normalisation. Each experiment contained 3 technical replicates, and the experiment was performed 4 times on different passages of cells. After transfection, cell lysis and the luminesce reaction were both triggered by adding the assay solution which contained the specific substrate of *Renilla* luciferase directly to the wells. After 30min incubation, the luminescence values which represented the activity and thus the protein level of luciferase were read by FLUOstar OPTIMA. The average reading was calculated for the 3 replicates in each round of the experiment and the original data were normalised following the manufacture's protocol (see Section 2.10.2).

Table 5. 1 The combination of vectors in the *TEX14* 3'-UTR luciferase assay

pCMV6-Entry vec+ Luc-no 3'-UTR	***pCMV6-Entry vec+ Luc-GAPDH 3'-UTR***	***pCMV6-Entry vec+ Luc-TEX14 3'-UTR***
pCMV6-DAZL vec+ Luc-no 3'-UTR	***pCMV6-DAZL vec+ Luc-GAPDH 3'-UTR***	***pCMV6-DAZL vec+ Luc-TEX14 3'-UTR***

After normalisation following manufacturer's protocol, the data were analysed using paired t-tests as the treatment was matched in each experiment. We found that the

activity of luciferase with *TEX14* 3'-UTR was significantly ($p<0.05$) increased about 1.92±0.18 fold (n=4) in the *DAZL* co-transfected cells, when compared to the empty vector co-transfected cells (Figure 5.6).

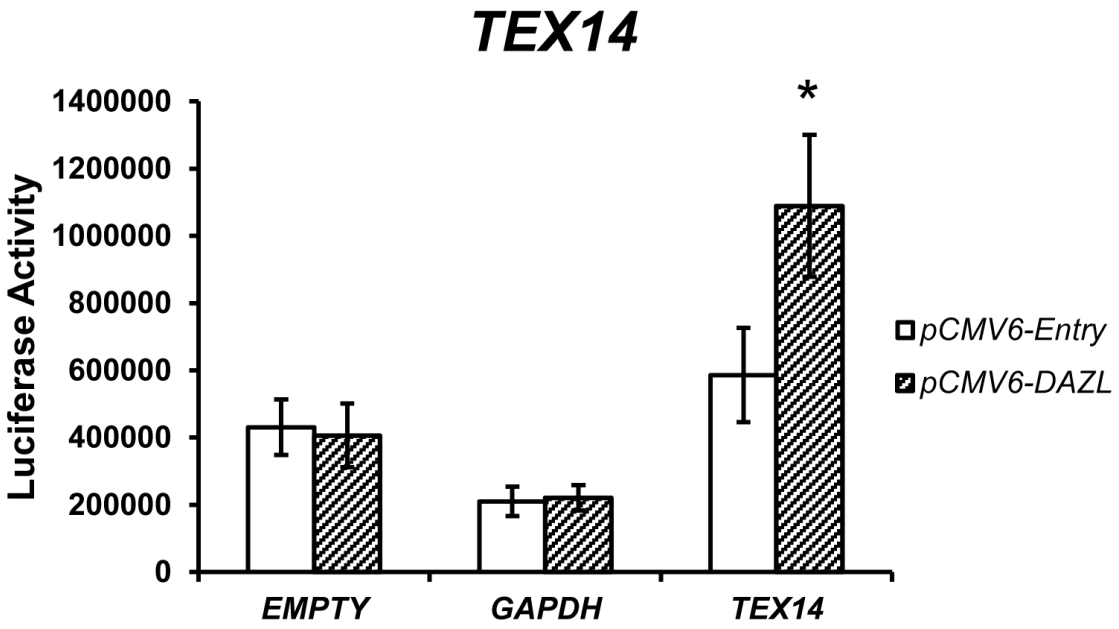

Figure 5. 6 Luciferase activity increases in *pCMV6-DAZL/Luc-TEX14* 3'-UTR co-transfected HEK293 cells.

HEK293 cells were transfected with either *pCMV6-Entry* (empty) or *pCMV6-DAZL* vectors combined with *Luciferase* vectors which were conjugated with no 3'-UTR, *GAPDH* 3'-UTR or *TEX14* 3'-UTR. Whilst no difference was detected in no UTR or *GAPDH* 3'-UTR co-transfections, the activity of luciferase increased in *pCMV6-DAZL* and *Luc-TEX14* 3'-UTR co-transfected cells when compared to the empty vector transfection. n=4, *$p<0.05$, value=mean±s.e.m.

5.2.6 DAZL represses the translation of *Luciferase* mRNA conjugated to *SOX17*-3'UTR in TCam-2 cells

A similar approach was applied to testing the regulation of the *SOX17* 3'-UTR regulation by DAZL, but 3 replicates of experiments on different passages of cells were carried out. The experimental design was similar to the one of the *TEX14* 3'-UTR (see Table 5.3 for the combination of vectors), but using the *pCMV-DAZL* vector instead of the *pCMV6-DAZL* vector and TCam-2 cells were used as the *in vitro* model, because the HEK293 cells might lack some key factors which involved in regulating *SOX17*.

Table 5. 2 The combination of vectors in the *TEX14* 3'-UTR luciferase assay

pCMV6-Entry vec+ Luc-no 3'-UTR	***pCMV6-Entry vec+ Luc-GAPDH 3'-UTR***	***pCMV6-Entry vec+ Luc-SOX17 3'-UTR***
pCMV-DAZL vec+ Luc-no 3'-UTR	***pCMV-DAZL vec+ Luc-GAPDH 3'-UTR***	***pCMV-DAZL vec+ Luc-SOX17 3'-UTR***

These data were also analysed using a paired t-test. The activity of *SOX17* 3'-UTR significantly ($p<0.01$) decreased in the pCMV-*DAZL* co-transfected TCam-2 cells (Figure 5.7), to about 68.81±0.04% (n=3) when compared to the cells co-transfected with empty vector.

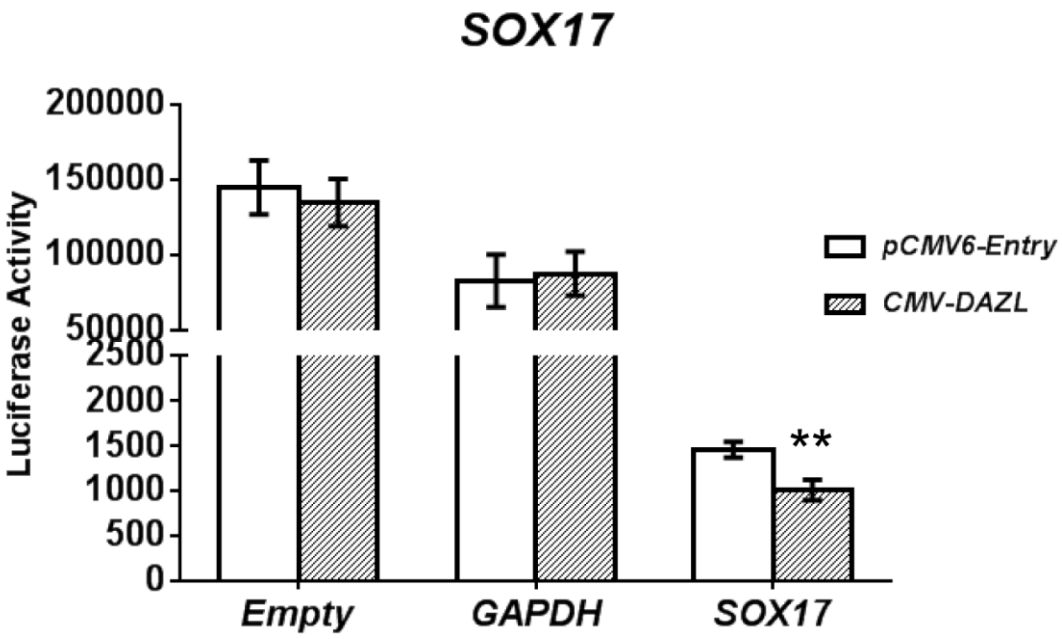

Figure 5. 7 *SOX17* Luciferase activity decreases in *pCMV-DAZL*/*Luc-SOX17-3*'UTR co-transfected TCam-2 cells.

Similar transfections were applied on TCam-2 as listed in Figure 5.6 but with the *pCMV-DAZL* vector, and Luciferase vector is conjugated with *SOX17* 3'-UTR. Whilst no difference was detected in non- or *GAPDH* 3'-UTR co-transfections, the activity of luciferase decreased to 68.81±0.04% in *pCMV-DAZL* and *SOX17* 3'-UTR co-transfected cells when compare to the empty vector transfection. n=3, **p<0.01, value=mean±s.e.m.

5.2.7 *Luciferase* mRNA with *TEX14* 3'-UTR co-precipitates with human DAZL protein

Once the immunoprecipitation of human DAZL after co-transfection was successfully confirmed (see Section 3.2.8), we performed RNA extraction and RT-PCR to isolate and detect the luciferase mRNA co-precipitated with DAZL. The methods of transfection, RIP and combination of vectors were the same as those described in previous section (see Section 5.2.5 and 5.2.6). After RIP, the RNA of both INPUT and RIP samples were isolated and converted to cDNA, and then end-point PCR was performed to detect the *luciferase* mRNA using the primers designed against the sequence of *luciferase* gene provided by manufacturer (not relative to the sequence of 3'-UTR).

Agarose electrophoresis for the PCR product (Figure 5.8) showed that the luciferase mRNA was appropriately expressed in all the INPUT samples whether they contained *GAPDH* or *TEX14* 3'-UTR, or were co-transfected with empty or *DAZL* vectors. After RIP, there was no detectable *luciferase* mRNA in the lanes of empty vector or *DAZL/GAPDH* 3'-UTR co-transfected samples, and the only band was seen in the lane of *DAZL/TEX*14 3'-UTR co-transfected cells. The electrophoresis for –RT was clear without any band, suggested that the bands in +RT reactions were not primer-dimer or because of any contamination. This experiment was repeated twice more with the same results.

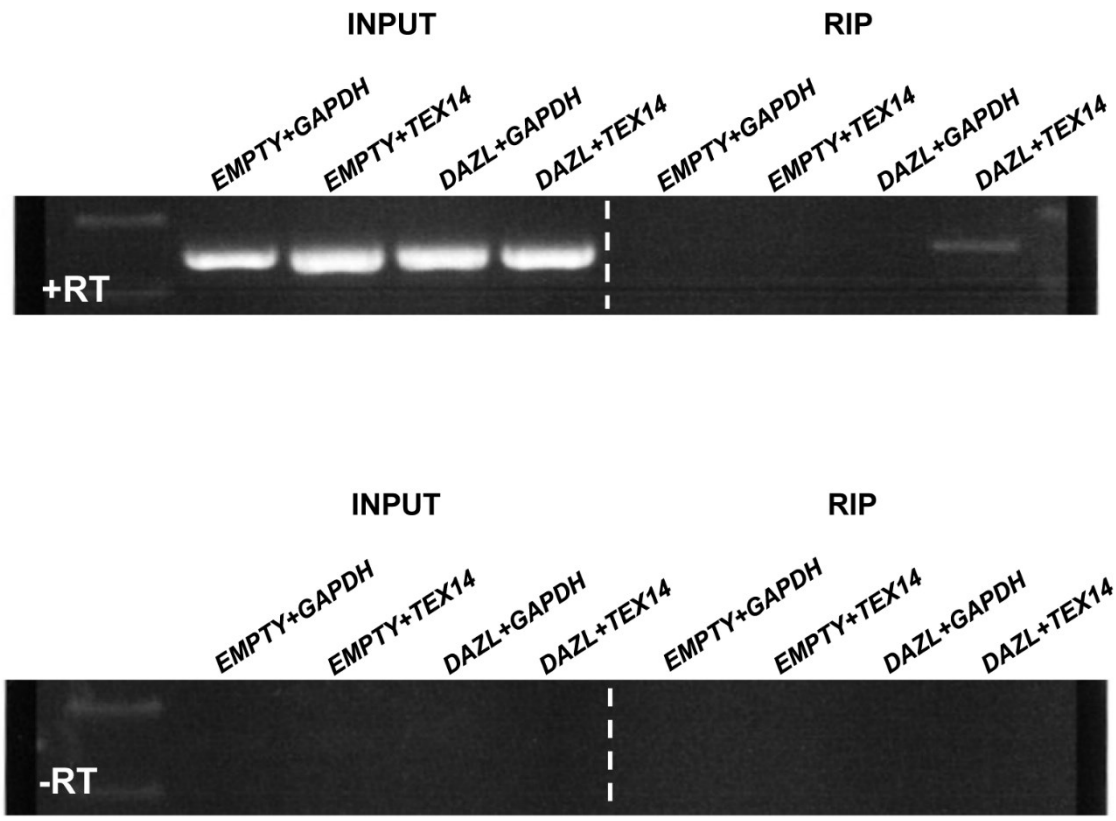

Figure 5. 8 *Luciferase mRNA* is co-precipitated with DAZL protein in only *pCMV6-DAZL/Luc-TEX14* 3'-UTR co-transfected HEK293 cells.

The samples of INPUT and RIP were separated by the white dashed line. The bands of *Luciferase* mRNA were detected in all the INPUT lanes, suggesting that it was expressed normally in all the co-transfections before RIP. However after RIP, the mRNA was only detected in *pCMV6-DAZL/Luc-TEX14* 3'-UTR co-transfected cells. No bands were seen in –RT samples, indicating there was no contamination in the PCR system.

5.2.8 The level of *Luciferase* mRNA is significantly higher in *pCMV6-DAZL/Luc-TEX14* 3'-UTR co-transfected HEK293 cells after RIP

To further test the results obtained from RIP, *luciferase* mRNA was quantified using qRT-PCR to find out the enrichment of *luciferase* mRNA. Three sets of transfections was performed on different passages of cells. Since a huge amount of input RNA is necessary for RIP, each treatment contained 3 3×10cm dishes of cells that were mixed together once the cells were lysed. For qRT-PCR, each sample was repeated once and the average Ct value was calculated for further analysis. As it could not guarantee that the level of housekeeping gene was stable after the RIP for normalisation, the amount of *luciferase* mRNA was determined relative to the concentration of isolated mRNA from corresponding INPUT samples, and then calculated as fold change between INPUT and RIP. The data seemed to show a skewed distribution after RIP (1.97 vs 26.43 for *GAPDH* and 140.88 vs 780.88 for *TEX14*), but due to the small sample size the normalisation test could not be performed. Therefore the results were assumed not normally distributed and were logged before analysis. Significance was analysed using a paired t-test and the results are shown in Figure 5.9.

The data suggest that in the INPUT samples before RIP, the levels of *luciferase* mRNA conjugated with *GAPDH* or *TEX14* 3'-UTR did not show any significant difference in *DAZL* co-transfection samples when compare to *pCVM6-Entry* vector transfections (1.09±0.18 fold for *GAPDH* and 1.09±0.24 fold for *TEX14*). After RIP, there was a low level of *GAPDH* 3'-UTR *luciferase* mRNA still remaining in the samples, with no significant difference between *pCVM6-Entry* and *DAZL* transfected samples (10.24±8 fold in *DAZL* transfections). In contrast, the *Luc-TEX14* 3'-UTR mRNA significantly increased in the *pCMV6-DAZL* co-transfected samples ($p<0.01$), by about 359±210 fold (n=3) compared to the level of *pCVM6-Entry* co-transfected mRNA.

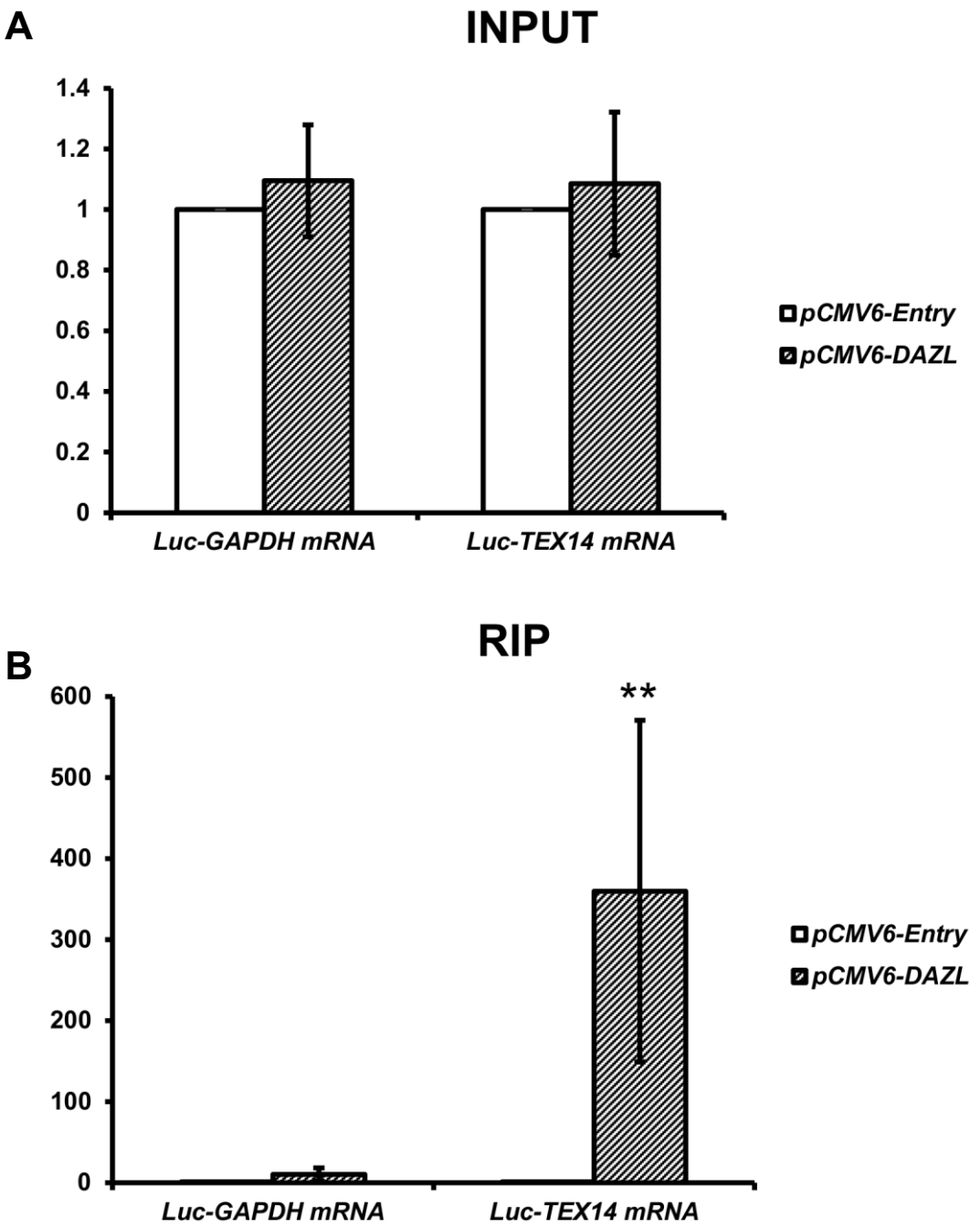

Figure 5. 9 *TEX14* 3'-UTR conjugated *Luciferase* mRNA significantly enriches in *DAZL* co-transfected samples after RIP.

A) The levels of both *GAPDH* and *TEX14* 3'-UTR conjugated *luciferase* mRNA did not show any significant difference between empty and *pCMV6-DAZL* transfections before RIP. **B)** In contrast, *luciferase* mRNA enriched 359±210 fold in *pCMV6-DAZL/Luc-TEX14* 3'-UTR co-transfections when compared to the *pCMV6-Entry/Luc-TEX14* 3'-UTR transfected sample after RIP. No significant difference is detected between the *Luc-GAPDH* transfections, indicating direct binding between DAZL and *TEX14* 3'-UTR. n=3 groups, **p<0.01, value=mean±s.e.m.

5.2.9 Human DAZL directly binds to its endogenous potential mRNA target in TCam-2 cells

Although the above experiments demonstrate that DAZL can bind to the 3'-UTR of *TEX14* and regulate the translation of a luciferase vector conjugated to this 3'-UTR, this was based on transfections of HEK293 cells, which was not an ideal model to study germ cells, and the *luciferase* mRNA was also artificial (exogenous vector rather than an endogenously-expressed transcript). Hence, it was still unclear that whether the same regulatory relationship also exists in germ cells, between DAZL and endogenous mRNAs. In order to determine whether DAZL can also bind to its endogenous mRNA targets in human germ cells, we again performed RIP on TCam-2 cells. The cells were transfected with *pCMV6-Entry* (empty) or *pCMV-DAZL* vectors and no luciferase or other vectors were added. The rest of methods were the same as the ones we applied on HEK293 cells and 3 sets of experiments were performed. To perform RIP requires large amount of input RNA, therefore, considering the transfection ratio and extremely low yield of transfected cells after FACS, the co-transfection/FACS system was not applied.

After RIP, RT-PCR was utilised to detect the precipitated potential DAZL targets. In previous co-transfection/FACS experiments on TCam-2 cells (see Section 5.2.4) *TEX19*, *TEX14*, *SYCP3*, *DNMT3L* and *SOX17* had been investigated as potential human DAZL targets and the binding between *TEX14* 3'-UTR and DAZL had been already confirmed, so primers against these genes were used to detect the presence of their mRNA in both the INPUT and RIP products. The non-DAZL target *GAPDH* was also examined to identify the specificity of RIP, and besides the ±RT, another reaction for each gene using dH_2O as the blank template was set up as a negative control (Figure 5.10, (1)&(2)).

Although some primer-dimers formed, no major bands were detected in the –RT or dH_2O samples, demonstrating that the bands in +RT reactions were not produced by non-specific reactions. As anticipated, all tested mRNAs were expressed endogenously in the INPUT samples before RIP, and the strength of bands did not show major differences between empty vector and DAZL transfected samples (Figure 5.10, (1)&(2)). After RIP, the bands for *GAPDH*, *DNMT3L*, *SOX17* and

SYCP3 were still detectable in both empty vector and DAZL-transfected samples. *GAPDH* did not show any difference between the two samples. The bands for*DNMT3L* and *SYCP3* were very weak, and only slightly brighter in the *pCMV-DAZL* transfections than in the empty vector samples. In contrast, the band for *SOX17* mRNA in the RIP sample from DAZL-expressing TCam-2 cells was much stronger than that for empty vector transfected cells, and *TEX19* was only detectable in the RIP from *pCMV-DAZL* transfected cells. Together, the data suggest that *SOX17* and *TEX19* mRNA are directly bound by DAZL protein, and *DNMT3L* and *SYCP3* were likely to be co-precipitated as well. The similar levels of *GAPDH* between *pCMV-DAZL* and empty vector transfections indicate that the DAZL binding was specific.

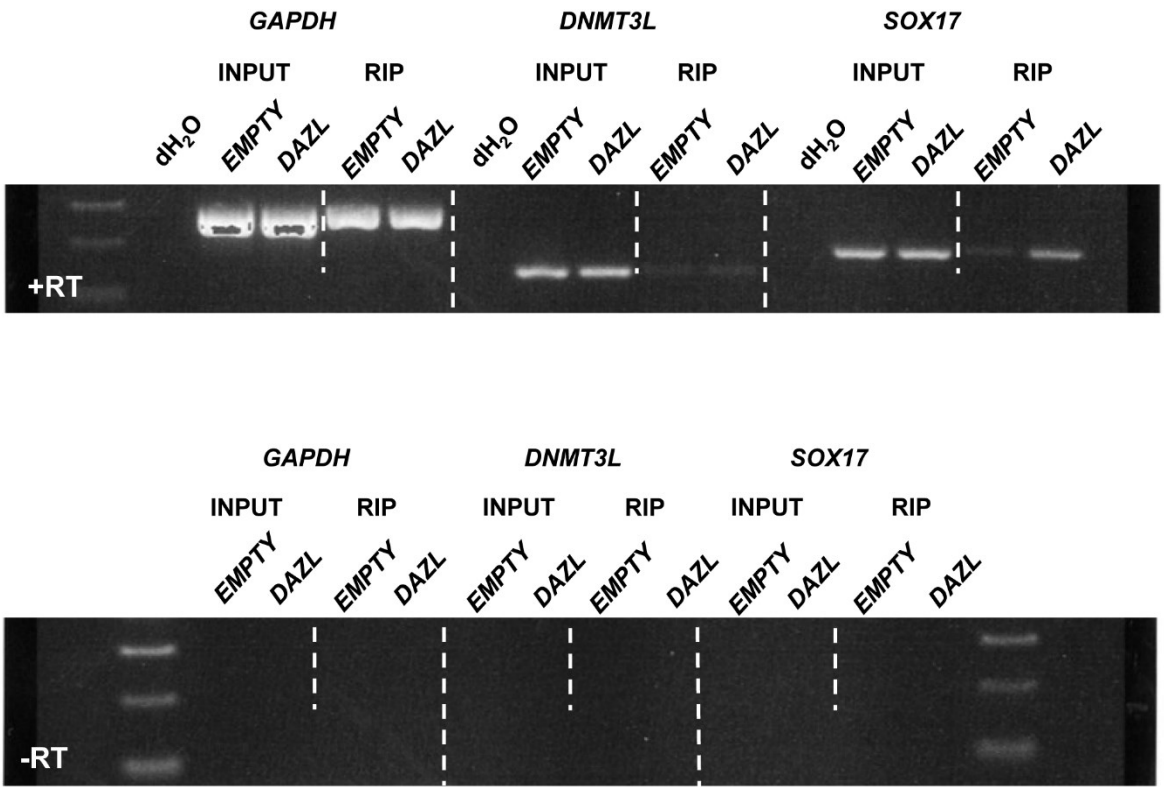

Figure 5. 10 (1/2) RT-PCR for the endogenous potential DAZL targets before/after RIP in TCam-2 cells.

Blots are sorted by gene names with long dashed lines, and also by INPUT/RIP with short dashed lines. *GAPDH*, *DNMT3L* and *SOX17* are expressed normally in both *pCMV-DAZL* and empty vector transfections before RIP. After the RIP, *SOX17* shows a stronger band in DAZL expressing samples, whilst *DNMT3L* is only very slightly stronger and *GAPDH* is similar. Although some primer-dimer formed, no similar band as in the +RT is detected in –RT or dH_2O template negative controls, suggests that the bands in +RT are specific.

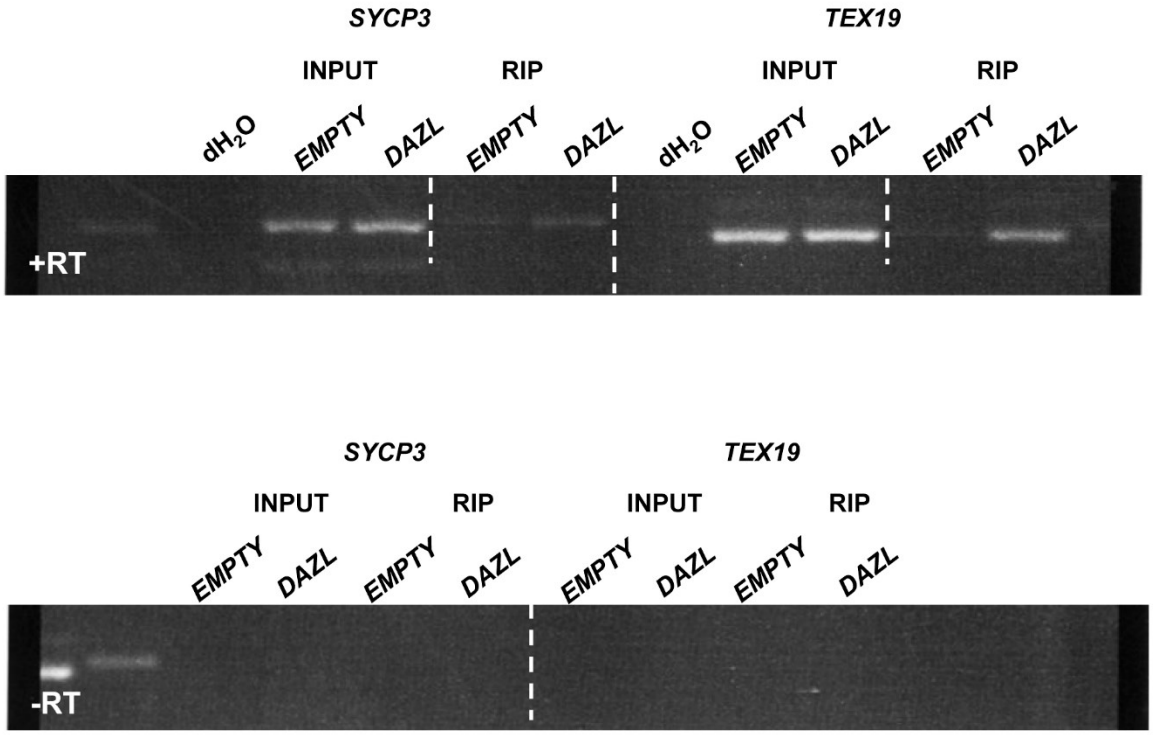

Figure 5.10 (2/2) RT-PCR for the endogenous potential DAZL targets before/after RIP in TCam-2 cells.

Blots are sorted by gene names with long dashed lines, and also by INPUT/RIP with short dashed lines. *SYCP3* and *TEX19* are also expressed normally in the INPUT samples before the RIP. After the RIP, although still detectable in the empty vector transfection, *SYCP3* shows a slightly stronger band in the *pCMV-DAZL* transfection, whilst *TEX19* only appears in the DAZL expressing sample. The –RT and dH_2O negative controls were also clean, indicating contamination was avoided in the PCR system.

5.2.10 Quantification of DAZL co-precipitated endogenous mRNA targets

After RIP in TCam-2 cells for endogenous DAZL targets, these experiments were repeated to quantify the amounts of target mRNA isolated from both INPUT and RIP samples by qRT-PCR. The significance of data was analysed using paired t-test as only two kinds of treatments (i.e. transfected with *DAZL* or empty vector) were performed and they were matched in each experiments.

In Figure 5.11, in all of the INPUT samples, almost no difference was detected between the empty and *pCMV-DAZL* transfected samples. This was unexpected, as previous experiments had demonstrated that *DAZL* transfection could affect the level of its mRNA targets, but may be explained by the very low transfection ratio of TCam-2 cells – any change in a small percentage of cells might be masked by the presence of many untransfected cells. In the RIP samples, *TEX19*, *TEX14* and *SOX17* all showed a significantly higher amount of mRNA in the DAZL transfected cells. To specify, *TEX19* was 7.11±1.65 (n=3) fold ($p<0.05$) higher and *TEX14* ($p<0.01$) had 2.7 fold enrichment in one set of samples (but its overall fold change was unable to be calculated as it was undetectable in two other sets of empty vector transfected samples after RIP). *SOX17* was 22.84±4.51 (n=3) fold ($p<0.01$) higher when compared to the empty vector transfected cells. *DNMT3L* also showed enrichment (2.48±0.85 (n=3) fold on average) in the *pCMV-DAZL* transfections after RIP in every experiment we performed but this difference was not significant. Although *GAPDH* was also slightly enriched in the *pCMV-DAZL* transfections (1.48±0.61 (n=3) fold on average), it was very variable in the RIP and not statistically significant. To conclude, *TEX19*, *TEX14* and *SOX17* are all significantly enriched in DAZL RIP suggesting that they can be directly bound by to DAZL protein in human germ cells. The validity of *DNMT3L* as a possible DAZL target is still unclear, and the variable but not consistently changed level of the non-DAZL target *GAPDH* confirms that the binding between DAZL and its mRNA targets are specific.

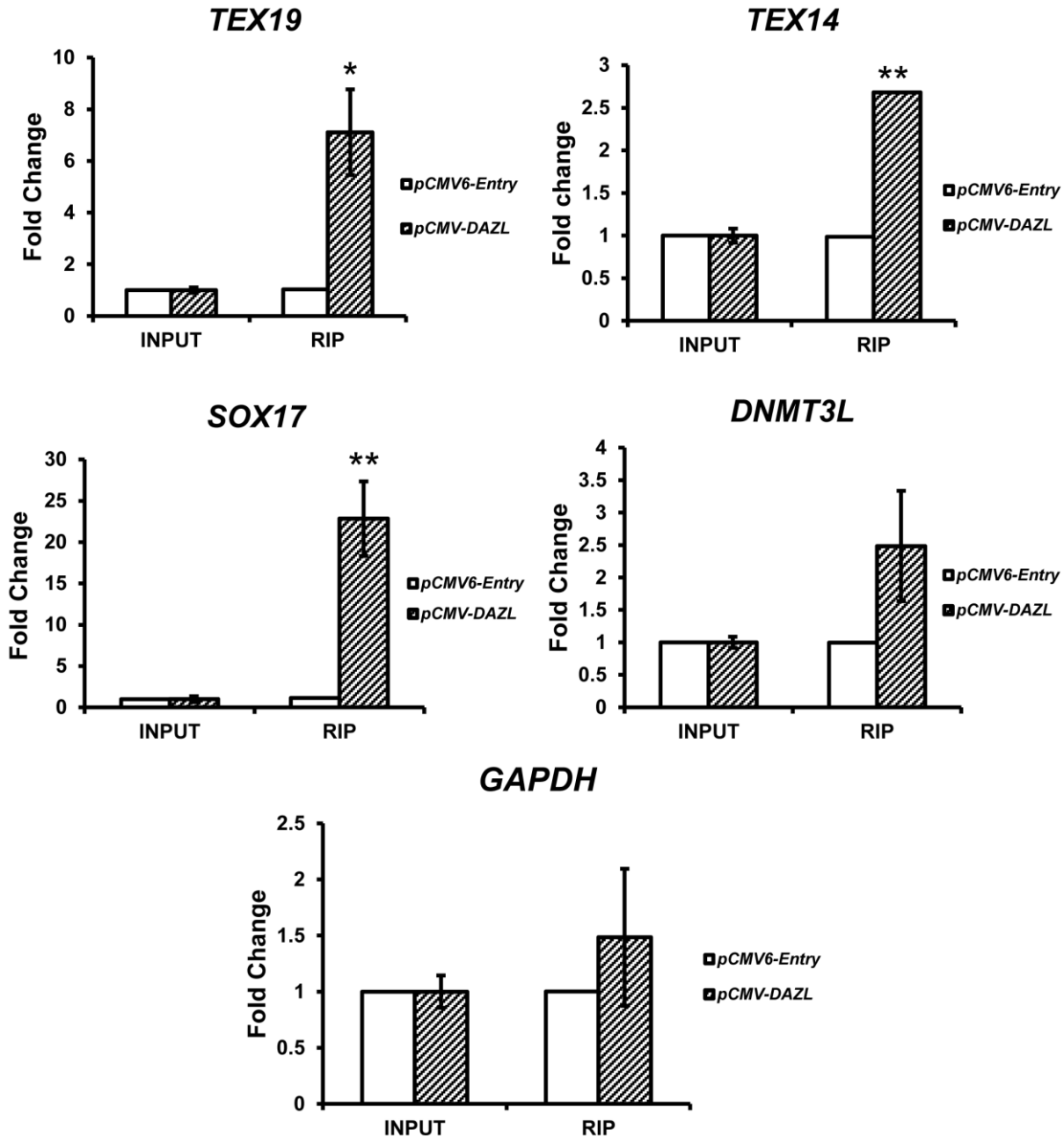

Figure 5. 11 The putative mRNA targets of DAZL enrich in *pCMV-DAZL* transfected TCam-2 cells after RIP.

None of the mRNAs we examined showed significant change between *pCMV-DAZL* and empty vector transfections in the INPUT samples. After the RIP, *TEX19, TEX14* and *SOX17* were significantly enriched in DAZL expressing cells when compare to the empty vector transfected cells. Since *TEX14* was undetectable after RIP in two empty vector transfected samples, the fold change of it after RIP in the figure was calculated based on only one sample and the significance was analysed based on the raw PCR data rather than fold change. *DNMT3L* was also enriched but not significant, and *GAPDH* remained unchanged between *pCMV-DAZL* or empty transfections. n=3, *p<0.05, **p<0.01, value=mean±s.e.m.

5.3 Discussion

In this chapter, we identified several putative human DAZL targets, namely *TEX19*, *TEX14*, *CDC25A*, *SOX17*, *SYCP3* and *DNMT3L*, and the interactions between DAZL and *TEX14*/*SOX17* mRNAs were studied in detail.

Although several mRNA targets of mouse Dazl have been identified (Chen *et al.*, 2014, Chen *et al.*, 2011, Jiao *et al.*, 2002, Reynolds *et al.*, 2007, Reynolds *et al.*, 2005, Zeng *et al.*, 2008, Zeng *et al.*, 2009), and DAZL silencing/overexpression can affect the expression or distribution of some proteins in human ES cells (Kee *et al.*, 2009), the only mRNA target that has been proven to interact with human DAZL is *SDAD1,* and this was only shown using a yeast three-hybrid-assay *in vitro* (Fox *et al.*, 2005) so may not represent a physiological interaction. In our research, we not only showed that human DAZL could regulate some putative targets at mRNA and/or corresponding protein levels, but also confirmed that this regulation is due to the direct binding between DAZL and 3'-UTR of these targets.

Significantly increased levels of endogenously-expressed mRNAs were seen in HEK293 cells after DAZL or BOLL was introduced, suggesting that *TEX19*, *TEX14* and *CDC25A* could be potential DAZL/BOLL targets. That there was no significant change in *CTNNB1* expression indicates that that the effect on theses transcripts is specific, and not caused by a global increase in mRNA levels in response to DAZL/BOLL expression. The time course analysis of DAZL and BOLL protein expression suggests that *pCMV6-DAZL* vector reached peak production of DAZL protein at 24h (when the mRNA was isolated at 24h) in contrast to the *pCMV6-BOLL* vector (which peaked later at 36h), this difference might not be the most important factor to explain the stronger effect on target mRNA levels caused by DAZL than by BOLL. The different regulation effect may be due to the different binding capacity and/or recognise motif between DAZL and BOLL, because a substitution of a crucial amino acid residue was found on the RRM of BOLL when compare with DAZL (Jenkins *et al.*, 2011). In addition, despite both DAZL and BOLL share some similar co-factors such as PABPs (Collier *et al.*, 2005) and PUM2 (Urano *et al.*, 2005), the binding mechanisms can be different and their protein complexes indeed recognise different mRNA targets (Urano *et al.*, 2005). However, no further investigation of the

BOLL regulation on *TEX19* and *TEX14* has been performed and therefore it is still difficult to tell whether these mRNAs are directly modulated by BOLL, or how effective the regulation is.

After that, our experiments using TCam-2 cells added *SYCP3*, *SOX17* and *DNMT3L* as potential DAZL targets. They had been originally identified as potential Dazl targets by previous research in mouse (Reynolds *et al.*, 2007, Reynolds *et al.*, 2005, Zeng *et al.*, 2008, Zeng *et al.*, 2009), although this is the first time they have been demonstrated to be targets of human DAZL. The luciferase assay demonstrates that the translation of a luciferase reported conjugated to the *TEX14* or SOX17 3'UTR of DAZL target mRNAs is specifically promoted by DAZL (relative to control 3'UTRs), and therefore DAZL may regulate the translation of these targets in germ cells via this mechanism. Furthermore, by RIP, it was shown that only the *luciferase* mRNA conjugated with *TEX14* 3'-UTR could be co-precipitated with DAZL protein, indicating that there is direct binding between DAZL and the *TEX14* 3'-UTR. Furthermore, the RIP performed on TCam-2 cells also demonstrated direct binding between DAZL protein and its targets, i.e. *TEX14*, *TEX19*, *SOX17* and potentially *DNMT3L*.

Although the mouse Dazl homologue targets *Tex19.1* and *Sycp3* have been investigated in detail (Reynolds *et al.*, 2007, Zeng *et al.*, 2009), no previous studies have described how Dazl regulates these targets at mRNA level. In addition, *Tex14*, *Sox17* and *Dnmt3l* mRNA in mouse were only co-precipitated with Dazl protein and no further effect of regulation was described in these studies. The data presented here is therefore the first demonstration of DAZL regulation of these targets, and of the regulation of target mRNA levels by DAZL.

Mouse has two *Tex19* homologues, *Tex19.1* and *Tex19.2*, of which *Tex19.1* is more conserved with the one human *TEX19* gene (Kuntz *et al.*, 2008). In our experiments, human *TEX19* mRNA levels increased in both HEK293 and TCam-2 cells after DAZL transfection. In addition, endogenous *TEX19* mRNA in TCam-2 cells could be co-precipitated with DAZL protein, which confirms a direct binding of human DAZL to *TEX19* mRNA, as occurs in mice. However, previous research suggests that the

translation of a luciferase vector conjugated to 3'UTR of mouse *Tex19.1* is down-regulated when co-transfected with mouse *Dazl* into zebrafish oocytes (Zeng *et al.*, 2009), which is in conflict with our experiments. This may be due to the presence of different Dazl co-factors between zebrafish and mammals, and thus the zebrafish model may not represent the Dazl regulation of *Tex19.1 in vivo* accurately. Another possibility is that mouse has two *Tex19* genes whilst humans have only one *TEX19* homologue (Kuntz *et al.*, 2008), and therefore their functions – and regulation - may not be exactly conserved.

Tex14 mRNA can be co-precipitated with Dazl from testis extracts (Reynolds *et al.*, 2005). Here we have shown that *TEX14* mRNA levels increase after DAZL transfection in both HEK293 and TCam-2 cells, the activity of luciferase conjugated with *TEX14* 3'-UTR increases when it is co-transfected with *DAZL*, and we have demonstrated direct binding between DAZL and the *TEX14* 3'-UTR. This provides very strong evidence that *TEX14* is an mRNA target of human DAZL. Although human studies are lacking, mouse *Tex14*, which is 64% conserved with its human homologue (Wu *et al.* , 2003) has been investigated in detail, especially during germ cell development. In mouse, *Tex14* is essential for the formation of germ cell intercellular bridges (Greenbaum *et al.*, 2006), and male *Tex14*$^{-/-}$ mice display meiosis arrest and sterility. Females are fertile, but have fewer follicles and significantly smaller litter sizes (Greenbaum *et al.*, 2009, Greenbaum *et al.*, 2006). Tex14 protein is expressed by spermatogonia and spermatocytes in testis (Greenbaum *et al.*, 2006), and is therefore at least partly co-expressed with Dazl, meaning that this regulation might occur *in vivo* as well. The expression pattern of TEX14 is therefore likely to be conserved between human and mouse, and suggests that *TEX14* mRNA could interact with DAZL protein during human fetal oogenesis *in vivo*.

Another target we identified is *SOX17*. Although the functions of SOX17 and its relationship with DAZL during germ cell development remains unknown, its expression pattern in gonads is studied across several species such as human, mouse and fish (de Jong *et al.*, 2008b, Kanai *et al.*, 1996, Navarro-Martin *et al.* , 2009). A study in human male suggests that SOX17 is expressed in the germ cells of fetal

testis, and in spermatogonia, secondary spermatocytes and spermatids (but not in primary spermatocytes) in adult testis (de Jong *et al.*, 2008b). In mouse testis, *Sox17* mRNA has two isoforms and the functional one is also mainly expressed in spermatogonia but is low from early pachytene (Kanai *et al.*, 1996). This is supported by our *in vitro* studies in which both the endogenous *SOX17* mRNA level and the translation of a luciferase reporter with *SOX17* 3'-UTR are decreased in TCam-2 cells after DAZL transfection, and this is due to the direct binding between DAZL and *SOX17* 3'-UTR. Similar binding also happens between mouse Dazl and *Sox17* (Zeng *et al.*, 2008). Together, our results suggest *SOX17* as a human DAZL target, and they reveal a novel repression function of human DAZL as well.

SYCP3 is a component of the synaptonemal complex (SC) and is necessary for synapsis during meiosis (Yuan *et al.*, 2000). *Sycp3* has been identified as a definitive Dazl target in mouse (Reynolds *et al.*, 2007). In humans, the mRNA expression of *SYCP3* increases in human fetal ovary around the time of the entry of the first germ cells into meiosis (Houmard *et al.*, 2009), which is coincident with the increased *DAZL* expression at the same period. Our study on TCam-2 cells shows that the human *SYCP3* mRNA increases after DAZL transfection, and it is co-precipitated with DAZL protein. Furthermore, its protein is partly co-localised with DAZL in human fetal ovary (see Chapter 4). Therefore, *SYCP3* is likely to be a conserved mRNA target of DAZL in mouse and human.

We also investigated *DNMT3L*, which is significantly decreased in DAZL transfected TCam-2 cells, although we could not definitely demonstrate that DAZL directly binds to DNTML3L mRNA. The repression of expression of *DNMT3L* mRNA by DAZL *in vitro* is consistent with the patterns of expression seen in *in vivo*. A previous study suggested that Dazl could bind mouse *Dnmt3l* mRNA (Zeng *et al.*, 2008), however the human *DNMT3L* has an extremely short 3'-UTR (58bp) compared to that of the mouse (273bp), and therefore this protein-mRNA interaction might not be conserved between human and mouse. It is possible that DAZL represses *DNMT3L* expression, however our experiments has not provided enough evidence to prove whether this is through direct or indirect pathway yet.

Previous research indicates that *CDC25A* could be a common target of both DAZL and BOLL (Jiao *et al.*, 2002, Lin *et al.*, 2009). Our *in vitro* experiments using HEK293 cells however, indicate that DAZL, but not BOLL, could possibly promote the stability of *CDC25A*, as the mRNA level of *CDC25A* in HEK293 cells slightly increased after introducing DAZL, although this change was not significant and further evidence is needed.

VASA (*Mvh*) is another DAZL mRNA target which has been demonstrated in mouse (Reynolds *et al.*, 2005), and suggested to be a target in humans based on increased numbers of VASA-GFP^{+ve} human XX ES cell when DAZL or BOLL is overexpressed (Kee *et al.*, 2009). It is co-expressed with DAZL in human fetal ovary and increases at meiosis initiation *in vivo* as well, although a similar increase is also found in the human fetal testis suggesting this might not be a meiosis-specific effect (Anderson *et al.*, 2007). However we had difficulty investigating this mRNA as it is not expressed in HEK293 cells and has very extremely low mRNA level in TCam-2 cells, and no detectable protein expression. Slightly, but not significantly, increased *VASA* mRNA level was observed in DAZL transfected TCam-2 cells. As its protein expression increased in human ES cell when DAZL was overexpressed (Kee *et al.*, 2009) but no significant change of mRNA level was observed in our experiments, it is possible that the human DAZL only promote the *VASA* translation, rather than both translation and mRNA stability.

Our study also indicates that DAZL may stabilise its targets in human. Previous research (Takeda *et al.*, 2009) demonstrated that zebrafish Dazl could stabilise the mRNA by preventing miRNA-mediated deadenylation. However other research (Wiszniak *et al.*, 2011) which reported a similar phenomenon suggested that other pathways such as interaction with other germ cell-specific RNA-binding proteins may also contribute to the stabilisation of target mRNAs. By ActD treatment (transcription blocking), our study indicated that the increase might be due to the protection of mRNA from degradation, rather than up-regulated transcription. Our results also indicate a repression function of DAZL on its target at both mRNA and protein level; for detailed discussion see Chapter 7. Although we know these effects are due to post-transactional regulation, it is still unclear whether this occurs due to

prevented/promoted deadenylation or polyadenylation, or through other pathways and this remains to be investigated.

The work described in this chapter has some weaknesses, and improvements could be made if they were to be repeated/extended in future. The first problem is as discussed in previous chapter, which is the small sample size. Each experiment was repeated 3-5 times and thus it was not possible to test whether the data obtained were normally distributed or not. Because of the small sample size, we had to use only non-parametric methods for the data analysis. Another similar problem is the few transfection replicates of the DAZL/BOLL transfection experiments on HEK293 cells. Although the experiments were repeated for several times, each time one transfection only contained one sample. This could not guarantee that every time the transfection was performed properly as there was no sample to compare with. Although fortunately it seemed that the data were not extremely dispersed in this study, more replicates for every experiment and each treatment should be performed in future work.

The next problem was the selection of controls. Although ActD treatment was supposed to stop transcription, the level of *CTNNB1* mRNA showed almost no change after 24h. This indicates that either the transcription of this mRNA was still ongoing, or it might be protected by other mechanisms. The former indicates that further optimization of the ActD treatment may be required, to ensure that transcriptional arrest is complete. The latter suggests that other parameters which may affect the DAZL targets also need to be considered. And in either way, the *CTNNB1* might not be the ideal control and seeking a new control mRNA would be necessary for future work.

It will also be necessary to use PCR controls in in future RIP experiments. Although the –RT reactions were performed to make sure the no unspecific reactions occurred in +RT samples, it was not clear whether the PCR was worked properly, especially when no bands appeared in the +RT RIP samples. Therefore, the PCR positive controls are necessary. These could be performed using samples which contained the target mRNA (for example, cDNA of human fetal ovary) and with the corresponding primers.

Finally, for the luciferase assay, it would be necessary to standardise the cell numbers used between each experiment. Currently no standardisation was performed. Although the methods (volume of cell suspension added to the wells) were optimised beforehand to make sure the ideal cell density was achieved after plating and the wells were observed under microscope, the cells were no longer counted in following experiments. To count the cells before each plating to make sure same numbers of cells were plated is a possible solution, or this could be corrected by isolating the mRNA and performing qRT-PCR to compare the levels of a housekeeping gene. It was also not ideal to use the *pCMV6*-Entry vector as a control for the *pCMV-DAZL* vector. The best control should be an empty vector with the *pCMV* promoter, however it was unavailable. Since the unexpected problem of using *pCMV6* vectors in TCam-2 cells (see Section 3.2.5), this could not be solved during this study. But with hindsight, if performing the same experiments again, the vectors from a same series would be a much better choice.

In conclusion, we have identified several putative human DAZL/BOLL targets, and have found that *TEX14* and *SOX17* are likely to be definitive mRNA targets of human DAZL. Regulation of *TEX19* and *TEX14* by BOLL was also observed, but needs further investigation. The expression levels of other DAZL targets including *TEX19*, *DNMT3L*, *SYCP3* and potentially *CDC25A*, all changed after *DAZL* transfection *in vitro*, suggesting these too may be DAZL targets in humans. The increased expression of *TEX19* and *SYCP3* is coincident with increased DAZL expression in the human fetal ovary, and we demonstrated direct binding of DAZL to these mRNAs as well. We also found that DAZL may regulate the stability of its targets at post-transcription level, although the pathway remains unclear. Overall, our study not only identified potential DAZL/BOLL targets, but also co-related them with DAZL expression during human oogenesis; this will be further discussed in Chapter 7.

Chapter 6

Investigating the Expression of Putative DAZL Targets in Human Fetal Ovary

Chapter 6. Investigating the Expression of Putative DAZL Targets in Human Fetal Ovary

6.1 Introduction

In the previous chapter, several potential DAZL mRNA targets, namely *TEX14*, *TEX19*, *CDC25A*, *SOX17*, *SYCP3* and *DNMT3L* were identified. However, the work in the previous chapter was all based on the *in vitro* study. This does not always represent what actually happens *in vivo* and therefore it still cannot be concluded that the mRNAs identified are real human DAZL targets.

For RNA-binding protein, it is essential to be co-localised with its targets in the same cells to regulate them. Several methods can be used to answer this question, including establishment of the protein expression profile of these targets in human fetal ovary and co-localising them with DAZL.

Due to the commercial availability of antibodies, this chapter will focus on the expression of SOX17 and DNMT3L protein. Among all the other targets, the co-localisation of DAZL and SYCP3 has already been confirmed in Chapter 4. TEX14 protein is widely expressed in intercellular bridges between germ cells (Greenbaum *et al.*, 2007), therefore it is very likely to be co-expressed with DAZL.

TEX19 expression in human is not very clear. In mouse, Kuntz *et al.* (2008) reported that in fetal ovary, *Tex19.1* mRNA expression increases at meiosis, then transiently decreases at e15.5 but recovered at e16.5. Other research suggested that its expression may extend to birth in female (Celebi *et al.* , 2012). In male mouse however, its protein seems to decrease at meiosis (Ollinger *et al.*, 2008). According to these studies, *Tex19.1* expression seems to be associated with meiosis and is very likely to be co-expressed with mouse Dazl as well.

CDC25A expression has been investigated in human. In female ovary, its mRNA is known to be expressed in GV stage oocytes and increases during the growth of oocyte (Assou *et al.* , 2006) but it is not clear at earlier stages. DAZL is found in human GV oocytes as well (Chen *et al.*, 2011) so their co-expression is possible. In males, its protein is most abundant at pachytene, co-localised with BOLL (Lin *et al.*,

2009, Luetjens *et al.*, 2004) but is also found in spermatogonia (Lin *et al.*, 2009) and possibly co-expressed with DAZL at this stage as well.

Mouse *Dnmt3l* is believed to be present in growing oocytes of adults (Bourc'his *et al.*, 2001). Some studies claim that it is not expressed in germ cells of early stages in fetal ovary (reviewed by Schaefer *et al.*, 2007), however this seems to be based on one study (La Salle *et al.* , 2004) which only investigated e13.5 and later. In testis, *Dnmt3l* cannot be found in non-dividing pro-spermatogonia or spermatogonia, but is highly expressed in differentiating spermatogonia at day 2 after birth (Bourc'his and Bestor, 2004) then soon becomes undetectable after day 6 (Bourc'his and Bestor, 2004, La Salle *et al.*, 2004). Notably, it also declines in e13.5 male germ cells when meiosis is induced by RA treatment (Ohta *et al.* , 2010).

For *Sox17*, one of its functional variants in mouse is expressed in pre-meiotic cells (Kanai *et al.*, 1996). In human, its expression pattern remains unknown in the ovary, but its protein is detected in testis in spermatogonia, secondary spermatocytes and spermatids (de Jong *et al.*, 2008b).

In previous work (MSc thesis, *J He* 2010), I have already tried to find out whether their expression changes *in vivo*, especially around the initiation of meiosis because DAZL is necessary for this process (Lin *et al.*, 2008). qRT-PCR was applied to mRNA extracted from human fetal ovary to detect these targets during three stages which represent the periods of key events of development, i.e. before meiosis (8-9 week), after meiosis initiation (14-16 week) and the beginning of follicle formation (17-20 week). Each group contained 5-6 individuals, and the samples were assayed in duplicate by qRT-PCR. Due to the small sample size, it was not possible to determine the normality. Data were then analysed by One-Way ANOVA, followed by Tukey's multiple comparisons test.

At 14-16 week gestation, i.e. at meiosis initiation, both *TEX19* and *TEX14* increased significantly ($p<0.005$, $n=5-6$) compared to 8-9 week gestation. The increased expression of *TEX14* is consistent with other research which indicated that *TEX14* sharply increased at 10-12 week and maintains this level afterwards, whilst in testis its level is relative stable (Houmard *et al.*, 2009). Expression of both was slightly

higher at 17-20 week but not significantly so when compared to the 14-16 week gestation (Figure 6.1). The expression of *SYCP3* mRNA has been previously investigated and found to increase when meiosis started, with high expression remaining at later gestations (Houmard *et al.*, 2009). In contrast, *DNMT3L* mRNA showed a trend of slightly reduced expression during development but not significantly so. *SOX17* declined to less than 50% of its level at 8-9 week gestation after meiosis initiation and this change was significant ($p<0.05$, n=5-6). This reduction seemed to be transient, because while expression at 17-20 week was lower than at 8-9 week gestation, this was not significant.

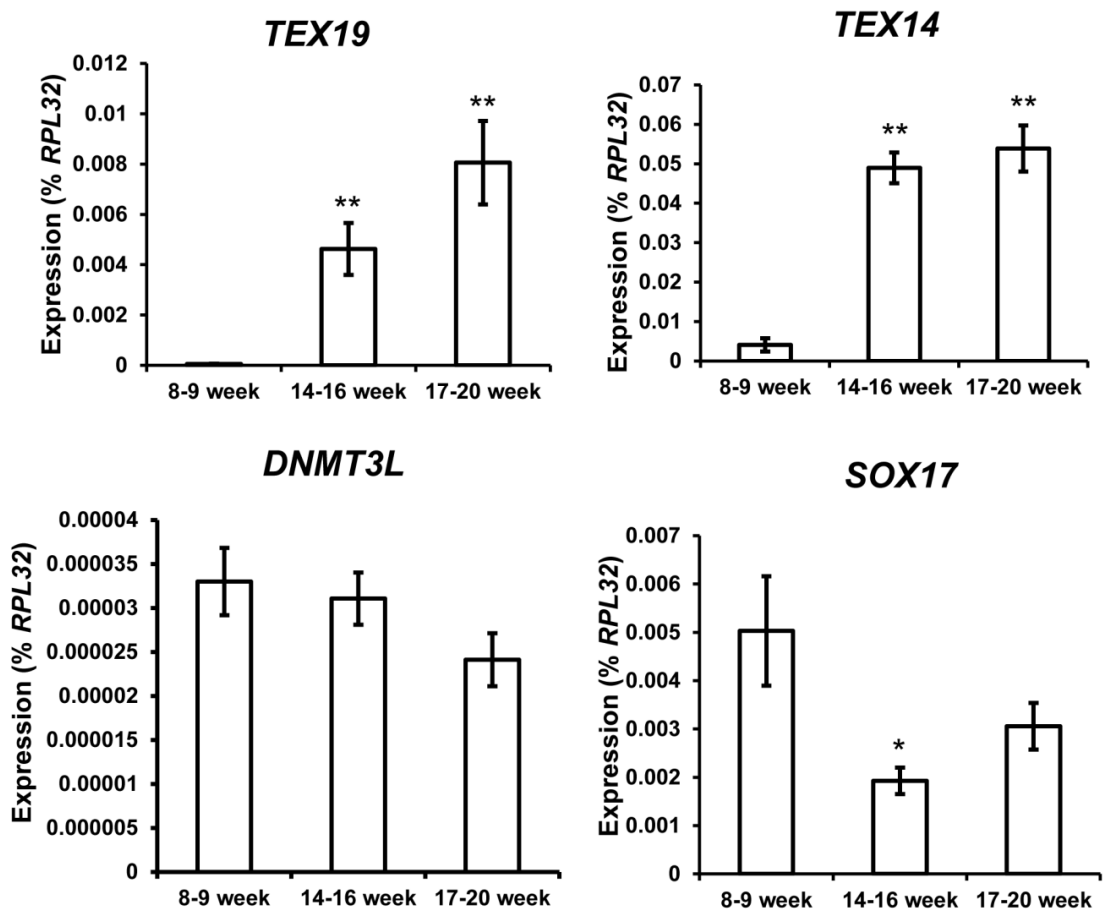

Figure 6. 1 The mRNA expression in human fetal ovary of putative DAZL targets.
Almost no *TEX19* is expressed before meiosis at 8-9 week gestation ($4.93\pm1.36\times10^{-5}$ relative to *RPL32*), then its level dramatically increases after the meiosis initiation ($4.63\pm1.03\times10^{-3}$ relative to *RPL32*) becoming higher during later development ($8.06\pm1.66\times10^{-3}$ relative to *RPL32*). The level of *TEX14* is also significantly higher when meiosis starts ($4.90\pm0.39\times10^{-2}$ vs $4.08\pm1.69\times10^{-3}$, both relative to *RPL32*) and remains at a high level when the primordial follicles begin to form. *DNMT3L* shows a trend of declining expression through the three key stages of human ovary development but the change is not significant. At 14-16 week gestation, *SOX17* decreases to only 38% ($1.93\pm0.27\times10^{-3}$ relative to *RPL32*) of its level in 8-9 week gestation ($5.03\pm1.13\times10^{-3}$ relative to *RPL32*) and it soon recovers to about 60% ($3.06\pm0.49\times10^{-3}$ relative to *RPL32*) at 17-20 week. n=5-6, *p<0.05, **p<0.01, value=mean±s.e.m.

MSc Thesis, J.He 2010

6.2 Results

6.2.1 DNMT3L is expressed in less mature germ cells in human fetal ovary

We next examined the protein expression of the potential DAZL targets in human fetal ovary. As there were no good commercial antibodies for other targets and SYCP3 expression had already been investigated in my previous studies (see Chapter 4), we focused on the expression of DNMT3L and SOX17. In the following results, all the experiments were performed on at least 2 sections from 2 different individuals to make sure the results were robust.

Although *DNMT3L* was not significantly enriched in DAZL RIP, its mRNA level decreased after the DAZL transfection (see Chapter 5). Because the sample size of the DAZL RIP was small (n=3), which could lead to a type II error (did not correctly reject the null hypothesis), the possibility remained that *DNMT3L* could directly bind with DAZL.

Single immunofluorescence was first applied on human fetal ovaries at different gestations to show the expression pattern of DNMT3L (Figure 6.2). At 63 or 65 days (9-10 week) gestation, DNMT3L is widely expressed in the nuclei of germ cells. Later at 14 weeks gestation after meiosis started, DNMT3L was still germ cell specific but with fewer cells expressing it in their nucleus; most of these were less mature germ cells distributed around the edge of ovary (Figure 6.2B). Toward the central area, most germ cells were DNMT3L^{-ve} with some still having positive staining. At 18 week gestation when germ cells began to form primordial follicles, the distribution of DNMT3L^{+ve} cells was similar to that at 14 week gestation – some germ cells with DNMT3L staining around the peripheral area and no or few positive cells occurred in the central area.

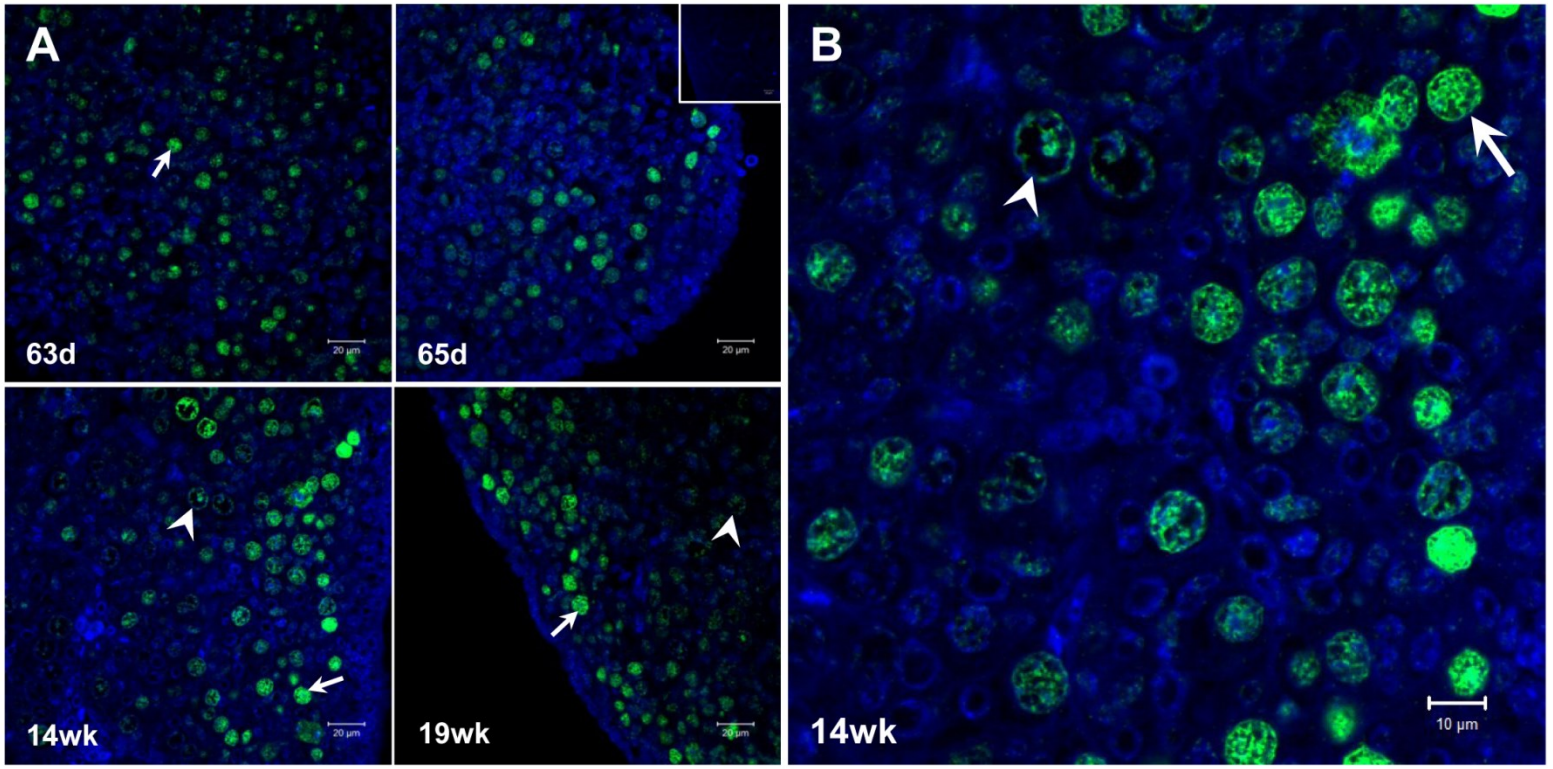

Figure 6. 2 The protein expression of DNMT3L in human fetal ovary.

A) At 63 and 65 day gestation, DNMT3L (green) was widely expressed in the nucleus of germ cells with round pattern (arrow). This pattern also existed in the ovaries at later stages of development (14 and 19 week gestation) but most cells were less mature and distributed around the edge of the ovary (arrows). Some more mature germ cells with bigger nucleus in the central area of the ovary were also DNMT3L^{+ve} (arrowheads) but most were negative, suggesting that the protein level of DNMT3L decreased during germ cell development. **B)** Higher power image of the 14 week section. Arrow indicates the cell with abundant nuclear DNMT3L in the edge, and arrowhead points a more mature germ cell with staining in the central area. Counter stained with DAPI (blue), Scale bar=20µm

6.2.2 DNMT3L is partly co-expressed with DAZL in human fetal ovary

After investigating the expression pattern of DNMT3L protein in human fetal ovary, the next question we raised was whether its protein translation could be regulated by DAZL *in vivo*. This included whether they co-express and whether any suggestion that DAZL was repressing DNMT3L could be detected in germ cells, as seen in the previous *in vitro* experiments.

We applied dual-fluorescence immunohistochemistry for DAZL and DNMT3L in the human fetal ovary at these three key developmental stages (Figure 6.3). As previously shown, both DAZL and DNMT3L were specifically expressed in germ cells. In all the specimens investigated at different gestations, three kinds of germ cell type were identified – only $DAZL^{+ve}$, only $DNMT3L^{+ve}$ and $DAZL^{+ve}DNMT3L^{+ve}$ co-expressing cells. At 65d (9-10 week) gestation, most $DNMT3L^{+ve}$ germ cells were also $DAZL^{+ve}$, whilst some $DAZL^{+ve}$ cells, especially in the central area did not show DNMT3L expression (Figure 6.3A, upper panels). At 14 week gestation, there were a lot of $DNMT3L^{+ve}$ cells identified which did not express DAZL, and most of positive ones were around the edge of the ovary. From the edge toward the central area, DAZL and DNMT3L showed an extensive co-expression pattern, however when the germ cells were more mature, had bigger nuclei and abundant DAZL staining, the DNMT3L staining seemed to be disappearing (Figure 6.3A, middle panels; Figure 6.3B, upper panel). At 16 week gestation, the expression and distribution pattern of DNMT3L and DAZL was similar to that at 14 week, however there were fewer germ cells co-expressing both proteins (Figure 6.3A, lower panels; Figure 6.3B, lower panel).

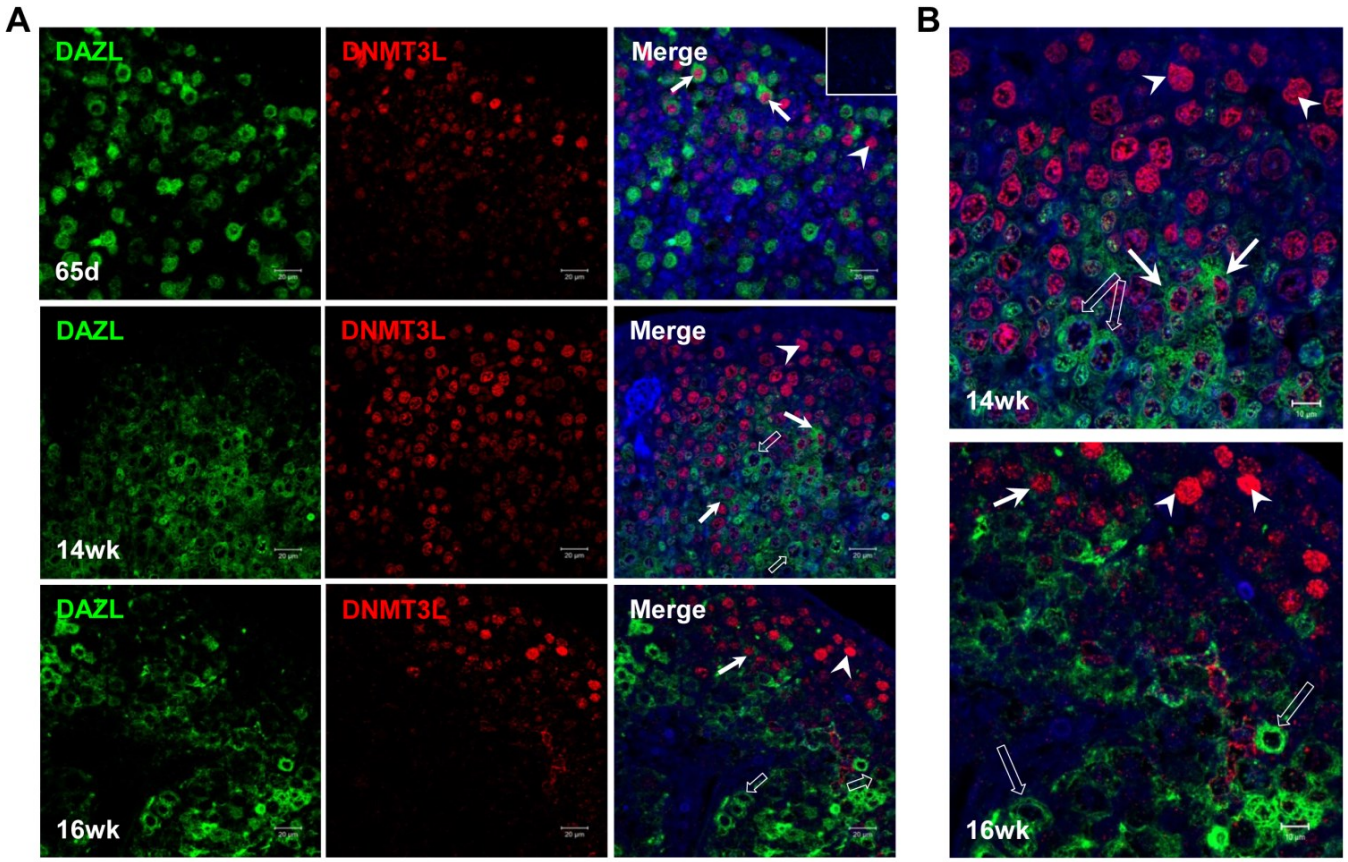

Figure 6. 3 The co-expression of DAZL and DNMT3L proteins in human fetal ovary.
Both DAZL (green) and DNMT3L (red) were expressed in all the specimens we examined. **A)** At 65 day gestation, DNMT3L was partly co-expressed with DAZL (arrows) but some cells were DNMT3L single positive (arrowhead). At 14 and 16 week gestation, most DNMT3L^{+ve} cells were in the peripheral area and did not express DAZL (arrowheads), whilst some more mature DNMT3L+ve cells were also DAZL^{+ve}. But in some more mature cells with bigger nucleus, the DNMT3L almost disappeared (unfilled arrows). In 16 week, the DNMT3L/DAZL double positive cells were not so extensively distributed as the ones at 14 week. **B)** High power images for the 14 and 16 week gestation specimens. As in Figure 6.3A, arrows indicated DNMT3L/DAZL co-expression, arrowheads and unfilled arrows indicated DNMT3L and DAZL single positive cells, respectively. Counter stained with DAPI (blue), Scale bar=20μm

6.2.3 Does DNMT3L re-express when DAZL expression decreases?

Because the DAZL expression is transiently replaced by BOLL during germ cell development in the human fetal ovary (see Chapter 4), the repression effect on DNMT3L by DAZL could be relieved when the DAZL expression is reduced. Alternatively BOLL may also have a regulatory function on DNMT3L.

To examine this hypothesis, we applied dual-fluorescence immunohistochemistry for DNMT3L and BOLL to see their co-expression pattern (Figure 6.4). The $BOLL^{+ve}$ germ cells represented the more mature germ cells with lower or no DAZL expression. As BOLL was not expressed before meiosis, only ovary sections at 14 and 16 weeks gestation were used. Although the images of Figure 6.4 were taken from central area of the sections where mostly more mature germ cells were settled in, both specimens still contained DNMT3L single positive cells. In the section at 14 week gestation (Figure 6.4, upper panels), although a lot of cells were $BOLL^{+ve}$, only one cell was found had DNMT3L/BOLL co-expression. In contrast, the ovary at 16 week gestation showed a higher ratio of co-expression with DNMT3L among the $BOLL^{+ve}$ cell group (Figure 6.4, lower panels, about 50% in this image).

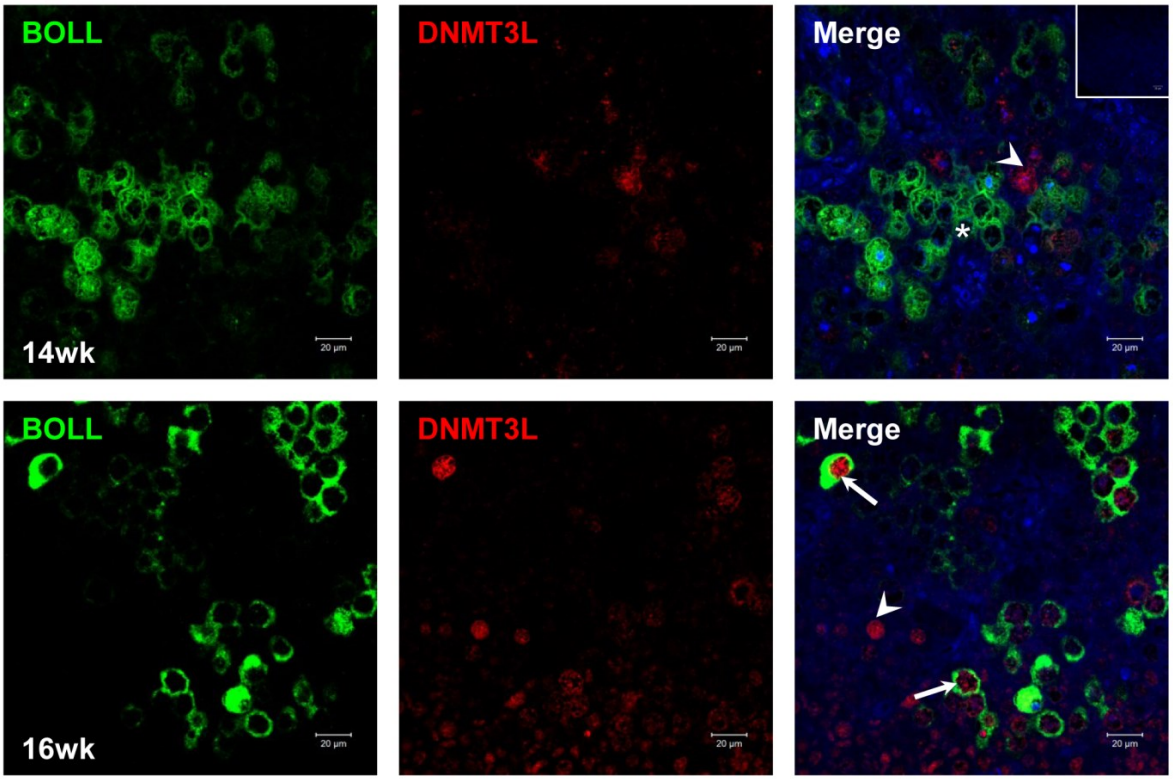

Figure 6. 4 The DNMT3L and BOLL protein co-expression in human fetal ovary.

At 14 week gestation, almost no BOLL^{+ve} (green) germ cells were also expressing DNMT3L (red, asterisk). Although most BOLL^{+ve} germ cells were distributed in the centre of the ovary, there were still some DNMT3L single positive germ cells in this area (arrowhead). Later at 16 week gestation however, more DNMT3L/BOLL double positive germ cells were seen (arrows), with some DNMT3L^{+ve} cells were still BOLL^{-ve} (arrowhead). Counter stained with DAPI (blue), Scale bar=20μm

6.2.4 SOX17 is partly co-expressed with DAZL in human fetal ovary

As the level of *SOX17* transcripts was also repressed by DAZL transfection in TCam-2 cells (see Section 5.2.4), we performed dual-fluorescence immunohistochemistry for SOX17 and DAZL on human fetal ovary at three different developmental stages to determine their expression pattern (Figure 6.5).

At 65d (9-10 week) gestation when most germ cells were still undifferentiated, SOX17 was expressed in germ cells and many of these cells were also $DAZL^{+ve}$ (Figure 6.5A, upper panels). Later at 14 week gestation after meiosis initiation, SOX17 was also mostly expressed in the less mature germ cells across the edge but still partly co-expressed with DAZL (Figure 6.5A, middle panels; Figure 6.5B, upper panel). Similar images were also obtained from 16 week specimens (data not shown). Another image (Figure 6.5A, lower panels; Figure 6.5B, lower panel) shows a lot of peripheral cells that had both SOX17 and DAZL proteins (Figure 6.5B, arrows), but the more mature $DAZL^{+ve}$ germ cells distributed in the central area were still mostly $SOX17^{-ve}$ (Figure 6.5B, unfilled arrows). Since the section still showed the trend of decreasing SOX17 in maturing $DAZL^{+ve}$ germ cells, the unusual large number of SOX17 and DAZL positive cells here might not be a new cell type, but more mature germ cells at the transient period just before SOX17 protein began to decrease.

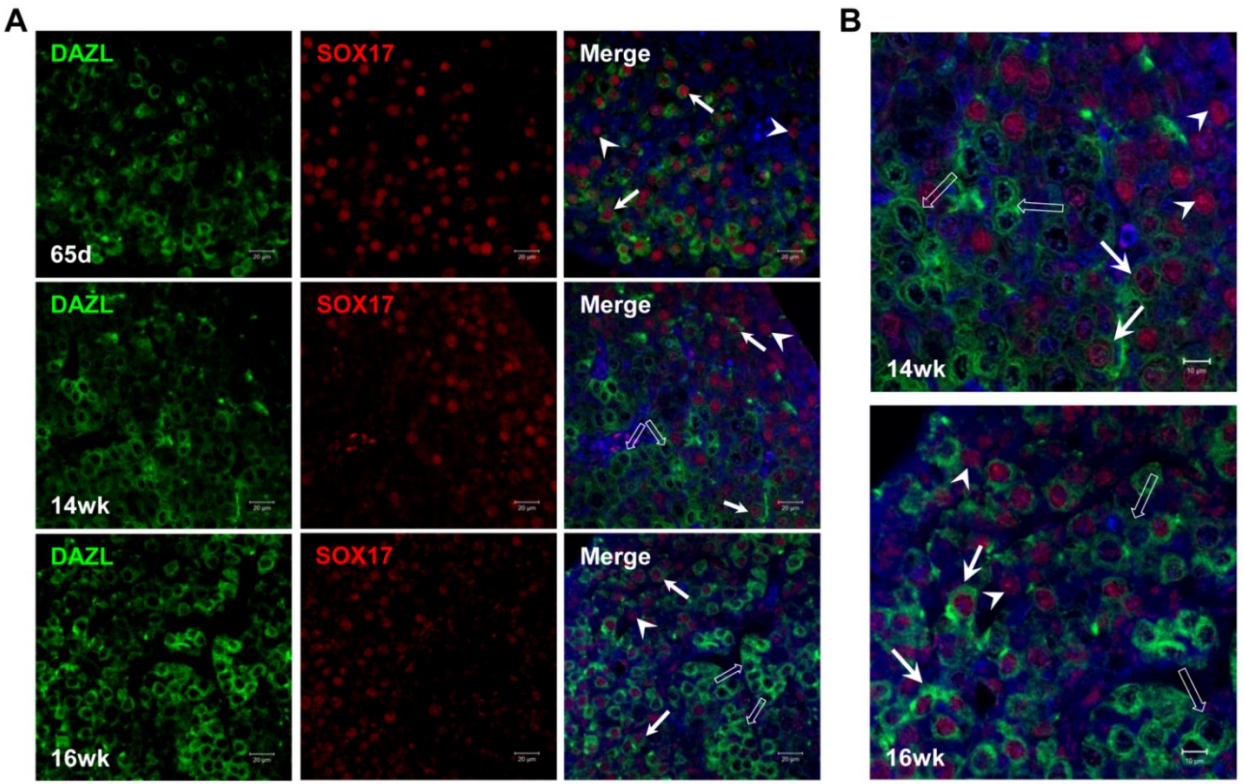

Figure 6. 5 SOX17 and DAZL protein co-localisation in human fetal ovary.
A) At 65 day gestation, SOX17 (red) was expressed across the whole section of ovary and mostly co-expressed with DAZL (green, arrows), but some cells were still SOX17 single positive (arrowheads). After meiosis initiation at 14 week gestation, SOX17 was mostly expressed in the less mature DAZL^{-ve} germ cells around the edge (arrowhead), with limited co-expression with DAZL (arrows). However, more mature DAZL^{+ve} cells with larger nuclei did not express SOX17 (unfilled arrows). At 16 week gestation, the staining in some sections was similar to the 14 week gestation (data not shown), but in this section, although most SOX17^{+ve} cells were still around the edge, almost no cells are SOX17 single positive (arrowhead), and most SOX17^{+ve} cells were also DAZL^{+ve} (arrows). However, the more mature DAZL^{+ve} were still SOX17^{-ve} (unfilled arrows). **B)** High power images for 14 and 16 week gestation sections. Arrowheads and unfilled arrows indicated SOX17 and DAZL single positive cells, respectively, whilst arrows pointed SOX17/DAZL double positive cells. Counter stained with DAPI (blue), Scale bar=20μm

6.3 Discussion

DNMT3L and SOX17 were identified as potential human DAZL targets in Chapter 5. In this chapter, to explore whether the regulation also happens *in vivo*, the expression pattern of their protein and their co-localisation with DAZL was investigated in human fetal ovary.

In human fetal ovary, the decreasing trend of mRNA level of *SOX17* and *DNMT3L* was consistent with the repression by DAZL on their mRNA in *in vitro* experiments. For other targets, the increased mRNA level of *TEX19* and *TEX14* was also consistent with *in vitro* results, most likely by increasing their stabilization by DAZL.

The expression pattern through the three stages of fetal ovarian development suggested that DNMT3L protein was mainly expressed in less mature germ cells and its level decreased during germ cell development, which was consistent with the dynamic change of its mRNA level in human fetal ovary. In second trimester, the DNMT3L was mainly expressed in early germ cells, especially in $DAZL^{-ve}$ cells but still partly co-expressed with DAZL. This was therefore evidence for the hypothesis that DAZL is repressing the translation of DNMT3L protein. Co-staining with BOLL suggested that DNMT3L did not immediately re-express when the level of DAZL protein decreased, but possibly appeared after a short delay whilst BOLL protein still existed, providing further evidence of a potential repression function of DAZL on DNMT3L *in vivo*.

DNMT3L expression in human fetal ovary had not been investigated so far and most research has focused on its function in *de novo* methylation, which occurs in adults at ovulation (reviewed by Schaefer *et al.*, 2007). In mouse, it was believed that the *Dnmt3l* is absent in early germ cells in females, however the original research only investigated e13.5 and later (La Salle *et al.*, 2004). Therefore, its germ cell expression before meiosis remains unknown in both human and mouse ovary. This research raises the possibility that human DNMT3L is actually expressed in pre-meiotic germ cells in the female and decreases later, which is conserved with its transient expression in mouse testis in differentiating spermatogonia (Bourc'his and Bestor, 2004). The loss of mouse *Dnmt3l* can cause failure of meiosis in testis, but is

lethal to female fetuses (Bourc'his and Bestor, 2004) thus its function in fetal ovary is still not very clear. However, the conservation of its transient expression between human female and mouse male may imply that it has the similar functions in human, i.e. involved in a genome scanning for *de novo* methylation before meiosis (Bourc'his and Bestor, 2004).

The expression and function of SOX17, however, has not been so extensively investigated as DNMT3L. In human, its protein expresses in spermatogonia, secondary spermatocytes and spermatids (de Jong *et al.*, 2008b) but the expression in female remains unclear. In this study, SOX17 was found to be expressed in early germ cells in human fetal ovary, potentially in pre-meiotic ones. The loss of SOX17 protein expression in ovarian meiotic cells was consistent with its expression pattern in human testis (not detected in spermatocytes) as well as the level change of its mRNA. The co-staining of SOX17 and DAZL showed that SOX17 was reduced in $DAZL^{+ve}$ cells and therefore it could also be down-regulated by DAZL *in vivo*. Notably, unlike the results from DNMT3L co-staining which suggested continuing DNMT3L expression when DAZL was present, most $DAZL^{+ve}$ cells at early second trimester were already completely $SOX17^{-ve}$, likely indicating a more rapid reduction of SOX17 protein in these cells.

The function of SOX17 during early germ cell development remains unclear, although a recent study suggests that it is necessary for promoting the differentiation from iESC to PGC-like cells (Irie *et al.* , 2015). It is possible that SOX17 is not required for development after PGC differentiation and then it is repressed by DAZL at meiosis initiation. Indeed, the absence of SOX17 in human primary spermatocytes (de Jong *et al.*, 2008b) may support this point of view, but further investigation is still needed.

However, it is also necessary to point out that the co-localisation between DAZL and the translated protein of its mRNA targets does not directly confirm the regulation. Although not very likely, the protein of these targets can be translated in $DAZL^{-ve}$ cells and transported to $DAZL^{+ve}$ cells, leading to false positive results. Therefore the best way is to co-localise DAZL with the target mRNA, however this was not possible in this study (as discussed in Chapter 7). Another possible improvement is

that the expression level of target proteins can be semi-quantified and statistically analysed based on the immunohistochemistry images. The expression of both DNMT3L and SOX17 seemed to be gradually decreasing in $DAZL^{+ve}$ cells, but without the proper quantification, it cannot be concluded whether this is true. If it is, it can be strong evidence of the repression function of DAZL on these two targets.

In summary, this chapter extended the *in vitro* study to *in vivo* investigation, further proved the findings in previous chapter. DNMT3L and SOX17 protein were both expressed in germ cells and decreased when DAZL expression was observed, supporting a novel repression function of DAZL on these two targets in human fetal ovary. The expression patterns of these two proteins were consistent with the changes in their mRNA levels and were conserved between species and/or sexes, providing some clue to explain their functions during germ cell development.

Chapter 7

General Discussion and Future Work

Chapter 7. General Discussion and Future Work

7.1 Introduction

In this study, we investigated the expression and potential targets of human DAZL and BOLL. In Chapter 4, we examined DAZL and BOLL expression patterns in human fetal ovary in first and second trimester, further related their expression timing with different stages of meiosis prophase I, and compared it with that of mouse fetal ovary. In Chapter 5 and 6, we identified several potential mRNA targets of human DAZL and BOLL using a range of methods, and co-localised the protein of two potential targets with DAZL in human fetal ovary.

In Chapter 1, two hypotheses were proposed for this PhD project:

3. DAZL and BOLL show different expression patterns during human oogenesis, and these expression patterns may reflect distinct roles for these proteins in regulating this process.
4. DAZL plays a critical role in regulating human oogenesis by controlling the translation of mRNAs encoding key proteins involved in germ cell development.

For the first hypothesis, this research found that DAZL and BOLL are both expressed in human fetal ovary prior to the arrest of meiosis I, however they are distributed in germ cells of different developmental stages – DAZL is expressed in germ cells before pachytene and also in primordial follicles, whilst BOLL expression is transient and mainly associated with pachytene. Interestingly, this distribution pattern is not conserved in the ovary between human and mouse.

Corresponding to hypothesis 2, further research isolated several potential mRNA targets of human DAZL, including *TEX19*, *TEX14*, *CDC25A*, *SOX17*, *SYCP3* and *DNMT3L*. Genetic manipulation of all these targets is associated with reproductive phenotypes, especially with disordered meiosis, and therefore provided support to the hypothesis that human DAZL is very likely to be essential for germ cell development as in mouse. It is also the first time repression function at translational level of

human DAZL has been reported. Unfortunately, due to the lack of a functional *BOLL* vector, the work on BOLL targets and function was limited.

Most previous studies on DAZL and/or BOLL either focus on animal experiments, or simply relate human reproductive phenotypes with DAZL/BOLL expression deficiencies but lack any insight into the molecular mechanisms. An overall comparison of DAZL/BOLL expression and function between human and model animals is also limited. The research of this thesis therefore for the first time focused on DAZL and BOLL functions during human oogenesis at a molecular level, and contributed to our understanding of their different expression/functions between human and model animals. It provided some clues about that how meiosis prophase I, and potentially how the general process of germ cell development, is regulated in humans, expanded our understanding of the causes of human reproductive dysfunction.

7.2 Establishment of human DAZL and BOLL expression profile

In hypothesis 1, we proposed that BOLL is likely to be expressed during early stages of meiosis prophase I in human fetal ovary, and aimed to find out the relationship between DAZL/BOLL expression and germ cell development.

Using qRT-PCR, we found that both *DAZL* and *BOLL* mRNA levels increase around the time of the entry of meiosis in human fetal ovary, and they show different timing of protein expression which is very different from that of mouse (Figure 7.1). This suggests that the two proteins may associate with different stages of meiosis during oogenesis. This result is consistent with the previous speculation that DAZL and BOLL show distinct expression patterns during human fetal ovary development. However, it was unexpected that this expression pattern appears to be non-conserved with that in mouse fetal ovary.

The possibility that BOLL plays a more important role for germ cell development in human than in mouse was discussed in Chapter 4. However, it is also worth considering that whether different BOLL expression patterns between these two species is caused by the compressed germ cell development period in mouse. Human has a much longer pregnancy period than mouse. In human, meiosis arrest and primordial follicle formation begins at approx. 18 week gestation (De Pol *et al.*, 1997), whilst it begins in neonatal mouse just after 20.5 days (about 3 weeks) development (Borum, 1961). This implies that the human early germ cell development could be much more similar to mouse than it appears to be, if it is also compressed in such a short period. Furthermore, in our study, the complete co-expression of mouse Dazl and Boll was observed at e15.5 (leptotene/zygotene) whereas Boll disappears at e18.5 (pachytene), thus we assumed that the Boll disappears just after e15.5. However, samples at the period between e15.5 and 18.5 were not examined and it cannot be excluded that Boll expression actually extended to e16.5 or further.

In human fetal ovary, Boll expression was mainly distributed in pachytene cells. This study already demonstrated that mouse Boll expresses at e15.5 and disappears after e18.5. In mouse, pachytene occurs from e15.5 to e19.5 (Borum, 1961). If the

minimal-co-expression of Dazl and Boll is similar that in human, then Boll single positive germ cells may exist and occur in mouse fetal ovary at e16.5 and/or e17.5. If that were to be the case, then it is possible that mouse Boll is equally importantly associated with the later stages of meiosis I as in human, although this is not supported by the phenotype of the *Boll* deficient mouse.

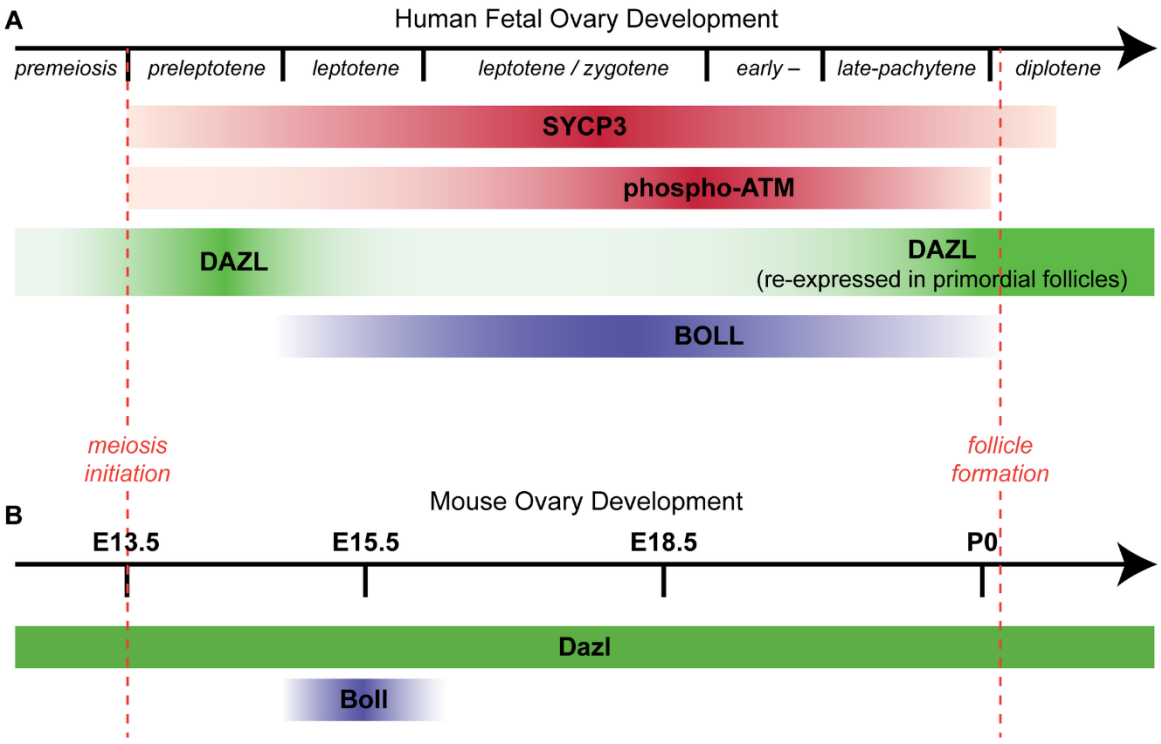

Figure 7. 1 Comparison of human and mouse DAZL/BOLL expression patterns during meiosis.

A) DAZL and BOLL show distinct spatio-temporal distributions during human fetal oogenesis. DAZL is expressed before and at meiosis initiation but down-regulated afterwards; BOLL is transiently expressed at later stages of meiosis with minimal co-expression with DAZL. DAZL is re-expressed in oocytes within primordial follicles. B) Expression of Dazl and Boll during meiosis from e13.5 to neonatal mouse ovary. Dazl expression persists during meiosis, whereas Boll is only transiently expressed around E15.5.

adapted from He *et al.* (2013)

However, it is also worth pointing out that our study suggests in human fetal ovary, the BOLL expression persists to a very late stage of meiosis prophase I, very likely until late pachytene or early diplotene just before meiosis arrest. In contrast, in mouse ovary, Boll expression has already completely ceased at e18.5, at which time point most germ cells are still at late pachytene and some reach early diplotene (Borum, 1961). In addition, if mouse Boll expression extends beyond e15.5, the present data suggest it stops at e16.5 or e17.5, which is much earlier than in human. Therefore, with the limitation of this study, it is very difficult to affirm that the DAZL/BOLL expression pattern in fetal ovary is largely conserved between human and mouse, but it remains as an additional possibility to be considered.

Whether the minimal co-expression pattern is conserved between human and mouse or not, the mechanism behind this phenomenon remains unknown. *DAZL* is known to self-promoting the production of its own protein (Chen *et al.*, 2011; Maegawa *et al.*, 2002), and CPEB1 can also increase the translation of *DAZL* (Chen *et al.*, 2011). CPEB1 is essential for both maintaining the number of germ cells and meiosis (Tay and Richter, 2001), the latter function is possibly partly achieved by indirectly regulating Sycp3 expression in mouse, by regulating the expression of Dazl (Reynolds *et al.*, 2007). Interestingly, CPEB1 is also known as a translation repressor (de Moor and Richter, 1999), although it is not known to be involved in DAZL regulation. Therefore, a possible pathway of DAZL regulation, for both the translation activation and repression could be through CPEB1. And although no previous study has investigated the regulation of BOLL, both the DAZL and CPEB1 recognition motif ($UU_{2\text{-}5}$[C/G]$UU_{2\text{-}5}$ for DAZL and UUUU[A/AA]U for CPEB1) can be found on its 3'-UTR, implies that it could be a target of both DAZL and CPEB1, and temporarily increased/repressed by these two protein. Finally, it is also worth noting that even in fish, dazl mRNA expression does not overlap with *boll* (Li *et al.*, 2011a; Xu *et al.*, 2009; for detailed description see Section 1.4.3.2). Therefore, this expression pattern could be very critical to maintain normal germ cell development in vertebrates and further investigation is necessary.

7.3 The roles of DAZL and BOLL during germ cell development

In hypothesis 2, we speculated that human DAZL and BOLL translationally regulate some mRNA targets which are important for the germ cell development, and some of the targets may be the homologue of those in model organisms, especially those in mouse.

To further understand the predicted human DAZL and BOLL functions, we tried to find out their potential mRNA targets using both *in vitro* and *in vivo* methods. In Chapter 6, *TEX14*, *SOX17*, *TEX19*, *SYCP3*, *DNMT3L* and *CDC25A* were identified as putative DAZL and/or BOLL targets in human. Among these targets, the translation of *TEX14* and *SOX17* were confirmed to be directly regulated by DAZL through their 3'-UTR, whilst *TEX19*, *SYCP3* and potentially *DNMT3L* showed mRNA-protein interaction with DAZL. Unfortunately, although there was some evidence that BOLL also had some effect on the regulation of *TEX14* and *TEX19*, due to the lack of a functional *BOLL* vector in TCam-2 cells, further experiments were not performed. Our investigation on potential human targets is summarised in Table 7.1.

Table 7. 1 Summary of our investigation of potential human DAZL targets

Targets	HEK293 mRNA	TCam-2 mRNA	HEK293 Luciferase	TCam-2 Luciferase	HEK293 RIP	TCam-2 RIP	Change in HF Ovary	Ovary co-DAZL
TEX19	↑	↑ (ns)	unknown	unknown	unknown	+	↑	unknown
TEX14	↑	↑	↑	unknown	+	+	↑	unknown
DNMT3L	no expression	↓	unknown	unknown	unknown	+ (?)	↓ (ns)	+
SOX17	no expression	↓	unknown	↓	unknown	+	↓	+
SYCP3	no expression	↑	unknown	unknown	unknown	+	↑*	+
CDC25A	↑	unknown	unknown	unknown	unknown	unknown	↔	unknown
VASA	no expression	↑ (ns)	unknown	unknown	unknown	unknown	↑**	+**

** Previously investigated by Anderson *et al.* (2007)
* Previously investigated by Houmard *et al.* (2009)
↑, increased; ↓, decreased; ↔, no change; +, positively detected; ns, not significant.

All the mRNA targets identified in this project are associated with different stages of germ cell development. These targets could be sorted by their functions – *TEX14*, *TEX19*, *SYCP3* and *CDC25A* are related to germ cell development and/or meiosis, *SOX17* and *TEX19* are involved in pluripotency whilst *DNMT3L* is necessary during *de novo* methylation, especially for the establishment of maternal imprints. We also found that DAZL could regulate its mRNA targets at the post-transcriptional level, which has only previously been reported in zebrafish (Takeda *et al.*, 2009, Wiszniak *et al.*, 2011), and it also shows a novel repression function on its potential target *SOX17*, which has never been reported before in human.

Therefore, part of the hypothesis was not fully tested - the targets of BOLL still remain unclear, though *TEX14* and *TEX19* were identified as potential targets. On the other hand however, part of the aims were robustly achieved. Several mRNA targets of human DAZL were identified as we expected, mostly the homologue of mouse. And through them, it is possible to associate DAZL with defects in human reproduction. An unexpected novel repression function of human DAZL was also discovered, which enlarges current understanding of its roles.

Our study demonstrated that human DAZL function is tightly associated with meiosis. A potential common target of both DAZL and BOLL we identified is *TEX19*. Our study reveals that in human, its mRNA expression increases at the entry of meiosis, and this is consistent with mouse *Tex19.1* in females, which increases at meiosis initiation as well, but shows a transient decrease at e15.5 and then recovers at e16.5 (Kuntz *et al.*, 2008). The dynamic change of Tex19.1, as well as of human *TEX19*, does strongly imply that it is associated with meiosis. Previous studies already demonstrated that Tex19.1 plays an important role during germ cell differentiation, synapsis and recombination, by helping to stabilise the genome and reducing DNA damage (Ollinger *et al.*, 2008, Tarabay *et al.*, 2013). In our study, human *TEX19* could be regulated by DAZL and potentially by BOLL; and if the function of human TEX19 is conserved with that of mouse Tex19.1, DAZL could act to indirectly promote germ cell derivation and stabilise the genome at recombination by regulating TEX19 protein expression. Both *Tex19.1* and *Tex14*-deficient male mice show a phenotype of meiotic arrest at pachytene. Given that BOLL expression

appears to be the abundant DAZ family member in germ cells in the human fetal ovary at this stage, this suggests that BOLL may be involved in the regulation of *TEX19*. It is noteworthy that the dramatic decrease in *Tex19.1* at e15.5 in mouse fetal ovary completely overlaps with the transient Boll expression, and therefore it is possible that mouse Boll may contribute to the repression of *Tex19.1*. This is supported by the reports of repression function of Dazl on *Tex19.1* (Zeng *et al.*, 2009).

It seems likely that DAZL is regulating/promoting the progress of synapsis/recombination, as another DAZL target we identified, *SYCP3*, is one of the very few confirmed mouse Dazl target (Reynolds *et al.*, 2007) and is essential for synapsis. In our study, both DAZL and BOLL were co-localised with SYCP3 protein, but BOLL shows a higher co-localisation ratio. Sycp3 expression seems to be critical in male mouse at zygotene stage, and our study suggests that during human oogenesis it is the period at which DAZL is down-regulated and BOLL begins to be extensively expressed; therefore it is possible that the translation of SYCP3 is first promoted by DAZL, then maintained by BOLL to regulate synapsis. The regulation of *SYCP3* by BOLL is supported by Kee *et al.* (2009), who demonstrated that both DAZL and BOLL could promote the correct assembly of SYCP3 on chromosomes. But some *SYCP3* expression without the presence of either DAZL or BOLL was also found in human fetal ovary, which implies that DAZL or BOLL could up-regulate SYCP3 expression to a required threshold and help it to load on chromosomes, to maintain normal synapsis and the formation of chiasmata, but are perhaps not essential for late stages of SYCP3 expression.

Beside the progression of meiosis, DAZL is also known to be necessary for entry into meiosis (Lin *et al.*, 2008). Unfortunately we were not able to test if *STRA8,* which is also required for meiotic initiation, is regulated by human DAZL due to the limitations of the *in vitro* model used (no *STRA8* expression in our cell lines) and the lack of an antibody to study it *in vivo*. Instead we investigated *CDC25A*, the human homologue of *Drosophila twine*. *twine* was originally identified as a target of fly bol (Maines and Wasserman, 1999) and is required for meiosis initiation in male, and meiosis maintenance in female (Alphey *et al.* , 1992, Courtot *et al.* , 1992). However,

in our study, BOLL seemed to have no effect on *CDC25A* mRNA expression, whilst DAZL slightly increased its expression level, but not significantly. This is consistent with (Lin *et al.*, 2009)'s report, which demonstrated that human BOLL could bind to and promote the translation of *CDC25A*, but cannot stabilise it. This mRNA does not show significant change during human ovary development (see Figure 6.1), so it is difficult to conclude whether it is regulated by DAZL and/or BOLL *in vivo*. Human CDC25A protein is found in spermatogonia, but is most abundant in pachytene spermatocytes and spermatids (Lin *et al.*, 2009). If it is a target of DAZL and BOLL, then the regulation of *CDC25A* may be divided into two stages – by DAZL in spermatogonia, then by BOLL at pachytene and later.

To conclude, by regulating *TEX19*, *SYCP3* and possibly *CDC25A*, DAZL and potentially BOLL act to maintain the normal progression of meiosis, especially synapsis and recombination. This also helps to explain the severe meiotic phenotypes in DAZL deficient mouse. And in human, the *DAZL* mRNA expression is much lower (albeit not statistically significantly) in azoospermia patients with maturation arrest, who have meiotic spermatocytes (Lin *et al.*, 2001). If DAZL is involved in meiosis, then it is possible that insufficient DAZL expression caused this phenotype. However very limited information is available about the relevant human phenotypes (both male and female), thus it is difficult to made a detailed assessment of how the data presented here match with the known human information.

The functions of TEX14 have been described in Section 1.2.3. It is an essential component of intercellular bridges. This connection allows germ cells to exchange cell organelles/components, contributes to synchronised development inside the cysts and helps some germ cells "nurse" others (Ruby *et al.*, 1969, Zamboni and Gondos, 1968). In our study, the mRNA level of *TEX14* increased in early second trimester, implying that is likely to be co-expressed in germ cells with DAZL and is may be associated with meiosis. Indeed, another study suggests that *Tex14* mRNA expression in mouse testis begins at the spermatogonia stage and peaks in pachytene, diplotene and in meiotically dividing spermatocytes (Wu *et al.*, 2003), implying a possible requirement of this protein during meiosis. Our other experiments also strongly suggest that DAZL promotes the translation of *TEX14* through direct binding of

3'-UTR, and therefore it might be an important pathway to regulate meiosis by DAZL. An interesting finding is that the female *Tex14* deficient mouse is fertile but has reduced follicle numbers; if TEX14 function is conserved between human and mouse, and its expression is promoted by DAZL, then it may contribute to the phenotypes of premature ovarian failure/early menopause in human with DAZL SNPs (Tung *et al.*, 2006b).

Notably, the mRNA level of *TEX14* also increased in BOLL-transfected HEK293 cells, raising a possibility that it is a common target of both DAZL and BOLL; indeed, according to the pachytene arrest *Tex14* phenotype in mouse and the strong BOLL expression around pachytene in human, it is very likely that BOLL is regulating human TEX14 during oogenesis.

A novel repression function of DAZL was found regarding the regulation of *SOX17*. It is well known that during embryo development, disrupted interaction between OCT4 and SOX2 by SOX17 seems to be necessary for promoting the differentiation of endoderm (Stefanovic *et al.* , 2009), but the role of SOX17 during germ cell development remained unclear, until recently a study suggested that human SOX17 is critical for the differentiation of iESCs to PGC-like cells by regulating BLIMP1, which is not conserved with this progression in mouse (Irie *et al.*, 2015). It is also known that in human PGCs, SOX17 replaces SOX2, a factor which maintains pluripotency together with OCT4 (de Jong *et al.*, 2008b). In mouse testis, a functional form of *Sox17* variant (DNA-binding active) is mainly expressed in pre-meiotic germ cells (Kanai *et al.*, 1996).

In our study, qRT-PCR suggests that *SOX17* expression significantly decreased when meiosis starts in human fetal ovary, and this is further demonstrated by double fluorescence immunohistochemistry which shows that SOX17 protein is decreases in in the nuclei of differentiating germ cells, and it is partly co-expressed in some germ cells with DAZL. SOX17 expression then slightly increases again at later stages, which is coincident with the re-expression of OCT4 in primordial follicles. Thus the pattern of low SOX17 expression in early meiotic germ cells appears to be conserved between human male and female gametogenesis. Together these data suggest that besides promoting the differentiation of PGC, SOX17 with its co-factor OCT4 in

germ cells may also act to maintain the pluripotent state of PGC or prevent apoptosis in germ cells. If this is true, then by down-regulating *SOX17*, DAZL is further driving both the germ cell fate and entry of meiosis. This is consistent with DAZL limiting pluripotency and promoting germ cell differentiation from both human and mouse ES cells (Chen *et al.*, 2014, Haston *et al.*, 2009, Kee *et al.*, 2009).

The final, and uncertain putative DAZL target we identified is *DNMT3L*. Despite it being down-regulated after *DAZL* transfection in TCam-2 cells, *DNMT3L* was only slightly enriched in DAZL pull-downs; therefore their direct interaction is not clear. DNMT3L functions to promote DNA methylation, and during germ cell development, it is necessary for the *de novo* methylation and establishment of maternal imprint (Bourc'his *et al.*, 2001, Ooi *et al.* , 2007). During meiosis in mouse fetal ovary at e17.5, the methylation of several imprinted gene remains at a low level, in contrast to the higher methylation level in fetal testis (Li *et al.* , 2004), and this may be associated with repression of methylation factors. Indeed, the *DNMT3L* mRNA level slightly decreased through gestation in human fetal ovary, and this could be regulated by DAZL according to our immunohistochemistry analysis. However, this still needs to be confirmed.

Overall, by analysing the functions of putative DAZL/BOLL mRNA targets we identified, it could be concluded that during germ cell development, the roles of DAZL and BOLL are largely involved in, but not limited to, meiosis. These data suggest that DAZL promotes germ cell differentiation and meiotic fate, and helps to stabilise the synaptonemal complex and genome by modulating the expression of its targets. BOLL is mainly involved in the later meiosis, possibly being necessary for meiosis progress beyond pachytene but before primordial follicle formation. Although there are several questions which remain to be answered, those potential targets we have identified contribute to our understanding of DAZL/BOLL function during human oogenesis.

7.4 Limitations and possible improvements to this project

Despite this project extended the understanding of human DAZL/BOLL function and the progress of germ cell development, some improvement could still be made.

The major limitations of this project were caused by the unexpected dysfunctional *pCMV6* vectors in TCam-2 cells, which worked well in HEK293 cells. It is very difficult to give the reasons why *pCMV6* did not express the protein in TCam-2 cells as no further experiments was performed. But since the transcription of these vectors in TCam-2 cells was shown (see Section 3.2.5), it is very likely that it is the stage of translation that was blocked.

Due to this limitation, the first problem was that human BOLL function was not able to be as sufficiently investigated as DAZL, as planned in hypothesis 2. Furthermore, considerable expenditure of time in solving this problem made the project much more complicated than it would be.

Misled by the positive transfection results in HEK293 cells, the cause of undetectable target protein levels in transient transfected TCam-2 cells was mistakenly thought as the low transfection ratio rather than the vectors themselves. To solve this, the effort of establishment of a stable transfected cell line was also in vain. To establish a stable transfected cell line, a single clone of transfected cells should be picked, which was not achieved in this project either. This was because no protein was detected in the polyclonal colonies and therefore this experiment was halted before the single clones could be made.

Another subsequence was that although a replacement *pCMV-DAZL* vector was found, using *pCMV6-Entry* vector as a negative control was not a perfect combination. And if the *pCMV-DAZL* vector contains an antibiotic resistance maker, that would provide a potentially easier route to making a stable line with it rather than using the FACS system to separate the transfected/un-transfected cells.

Therefore, a very critical improvement of this project could be made by the better selection and utilising of vectors. Another series of vectors containing empty, *DAZL*

and *BOLL* encoding sequences and antibiotic resistance loci, and most importantly, is translatable in TCam-2 cells would allow significant progress.

Another problem was that, despite the direct interaction of DAZL and its potential mRNA targets being confirmed by the *in vitro* experiments, it is still unclear whether they really interact *in vivo*. This is a challenge if we want to find the real biological significance of the experimental data.

One solutions would be to perform immunoprecipitation with human ovary tissue instead of the transfected cells. But more importantly, confirmation of the DAZL-targets co-expression is necessary. In this project, SYCP3 protein was co-localised with both DAZL and BOLL in human fetal ovary and thus provided essential precondition of the regulation, however the co-expression of other targets with DAZL/BOLL remains unknown. Part of the reason is the limited supply of commercial available antibodies against these targets.

Alternatively, co-localisation of DAZL and its mRNA targets using fluorescent immunohistochemistry plus *in situ* hybridisation is also theoretically possible. This is even more advanced than the protein-protein co-localisation as it would aim to investigate the protein-mRNA interaction. Unfortunately, this technique is not easy to perform and may require a lot of time for optimisation, as well as the fetal ovarian tissue itself being in limited supply. Furthermore, most of the ovary tissues in our lab are fixed with Bouin's fluid, which better maintains the morphology of human fetal ovary than other kinds of fixatives. However previous investigation already demonstrated that this fixation is not suitable for *in situ* hybridisation (McAllister and Rock, 1985). This makes it even more impossible to co-localise DAZL and its mRNA targets under the current experimental condition in our lab. Nonetheless, this step is still essential for finding out the *in vivo* targets of DAZL/BOLL and could be a future work.

It is important to consider whether those findings which are statistically significant are also likely to have biological significance. For example, *CDC25A*, which is reported to be a BOLL-regulated mRNA target, only increased 1.09 fold after *DAZL* transfection and showed almost no change in *BOLL* transfected cells. However, it is

the only known BOLL target in human (Lin *et al.*, 2009). Our finding is consistent with the fact that BOLL does not affect the *CDC25A* at mRNA level (Lin *et al.*, 2009), but leads to important questions as to whether some of the transcripts studied (such as *VASA* and *TRF2*) may still be human DAZL/BOLL targets despite not showing significant changes at mRNA level in response to DAZL/BOLL transfection in this study. Considering that the best-known regulating function of DAZL is on translation, rather than on target mRNA levels, it is possible that these targets are regulated by DAZL and/or BOLL but only at translational level. This could be investigated further by examining whether DAZL/BOLL affect the translation of these targets in a luciferase assay, which was not possible in this project in the time available.

Furthermore, the magnitude of the changes seen in target mRNA also needs to be carefully assessed. *TEX14* increased 2.6 fold in *DAZL* transfected HEK293 cells and the activity of its 3'-UTR conjugated luciferase increased 1.92 fold after *DAZL* transfection, and this consistency between mRNA and protein changes strongly indicates that regulation of *TEX14* by DAZL may indeed have some significance *in vivo*. But in contrast, *TEX19* only increased 1.68 fold in HEK293 cells, and it is unclear as to whether this represents a sufficiently large change in expression to affect cell function or development. Transfection can stress cells to produce a large amount of target protein, which is not what usually happens *in vivo*. There may also be confounding factors provided by proteins expressed in the host cell line. For example, although the changes in *SOX17* mRNA levels (decreased to 57% of control) and luciferase activity (decreased to 68.8% of control) moved in the same direction in response to *DAZL* transfection, the absolute value of the *SOX17*-3'UTR reporter luciferase activity was extremely low when compare to that of the control vectors (2,000 vs 150,000). This may imply that the translation of *SOX17* had already been largely repressed through its 3'-UTR in TCam-2 cells, by a factor other than DAZL. In both the case of *TEX19* and *SOX17*, even if the regulation by DAZL is real, it is difficult to tell that whether this change will have any significance during germ cell development. Examining the expression of these factors in DAZL-deficient germ cells *in vivo* may provide insight into this.

As discussed in previous chapters, the small sample size was a major problem in this study. This was partly caused by the difficulty of obtaining human tissues, which made it difficult to analyse the distribution of data and I could only assume that they were normally distributed for further analysis. Therefore there was a risk of choosing improper methods. And if the standard deviation of distribution is higher than the difference of means, then even the data were statistically significant, it might still have no biological significance. But the small sample size made it very difficult to evaluate which one was true.

In conclusion, this study provided some brand-new clues on the functions of human DAZL/BOLL during fetal oogenesis, although there are several flaws including selection of materials, chosen of methods, sample size and data analysis which made the results less convincing. Some of these defects were potentially avoidable and improvements should be made in future work.

7.5 Conclusions

In this study, we found that human DAZL and BOLL are expressed at, and potentially associated with different stages of germ cell development in fetal ovary. Furthermore, a novel repression function of human DAZL is also reported.

The major findings of this project are summarised in Figure 7.2. Although no definitive BOLL targets were found in this project, some of its novel putative targets were raised, as well as several almost definitive human DAZL targets being found. This investigation further revealed their roles in oogenesis and helps to explain their phenotypes in humans. BOLL is more strictly related with the later stages of meiosis prophase I but may also contribute to the interaction between germ cells. In contrast, functions of DAZL widely cover various aspects of germ cell development including early differentiation, epigenetic regulation, but still most importantly, with meiosis. And finally, by sharing some putative similar targets, DAZL may initially promote their expression whilst BOLL maintains it. Together, these findings contribute to the understanding of human oogenesis and possibly, the associated subfertility phenotypes.

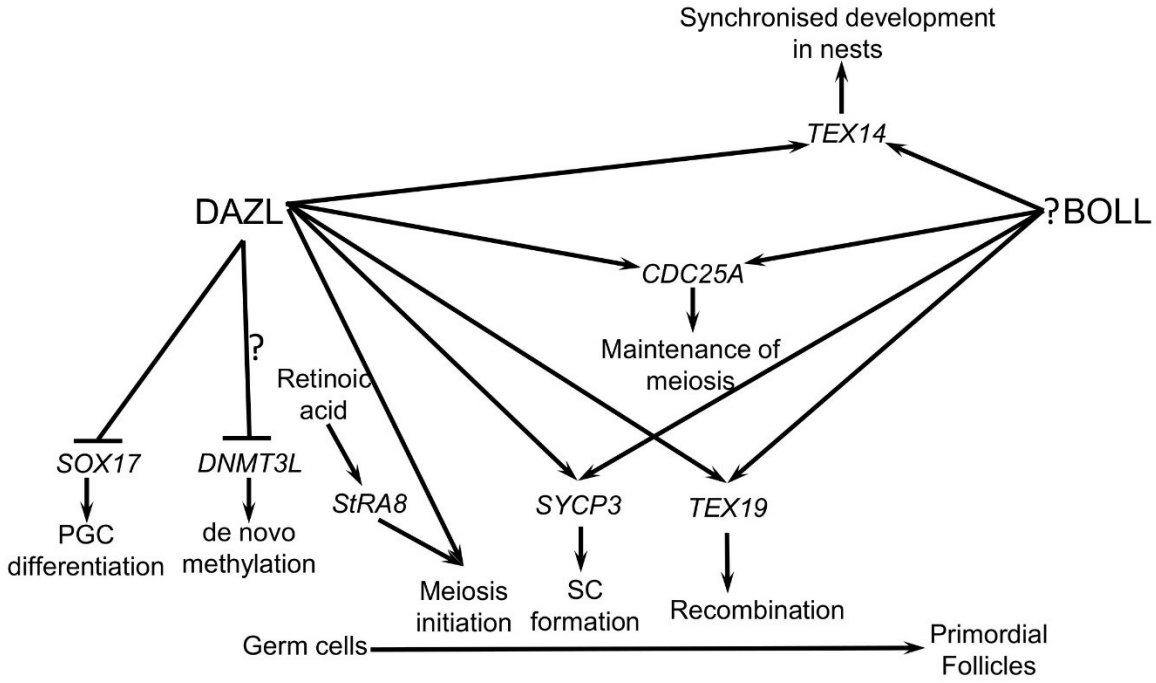

Table 7. 2 Predicted roles of DAZL and BOLL during germ cell development in human fetal ovary

DAZL is expressed in germ cells prior to and at early meiosis prophase I, whilst BOLL is associated with later stages, especially pachytene. However, DAZL is re-expressed in primordial follicles which do not express BOLL (not shown).

According to the mRNA targets identified in this project, DAZL may contribute to the modulation of differentiation and methylation in early germ cells by a novel repressing function on both *SOX17* and *DNMT3L*. Unfortunately its role together with retinoic acid/StRA8 during meiosis initiation is not proved in this study, but it is indeed essential for the development afterwards such as SC formation and recombination, by regulating *SYCP3*, *TEX19* and *CDC25A*. And by promoting *TEX14* expression, DAZL may also be involved in communication between germ cells in nests. No definitive targets of BOLL were identified. However, it potentially shares *TEX14* and all meiotic-associated targets we identified with DAZL, and may help to maintain their expression when DAZL is transiently down-regulated in germ cells.

7.6 Future work

Our study mainly investigated the expression pattern and potential mRNA targets of human DAZL and BOLL, especially focusing on their roles during oogenesis in fetal ovary. However, several questions extended from our research, and are yet to be answered.

The investigation of BOLL is still far from sufficient; the BOLL targets we identified are only based on the *BOLL*-transfected HEK293 cells. To further investigate these targets, it is necessary to confirm the direct binding between BOLL and these targets, and how their translation are regulated; for this propose, it is also essential to identify the recognition motif of BOLL – although its ability to stimulating translation has been known for a long time, surprisingly no study has focused on this.

Additionally, the 3'-UTR interaction was only confirmed between DAZL and *TEX14*/*SOX17*. Although the direct protein-mRNA interaction was proved possible for *TEX19*, *SYCP3* and *DNMT3L*, whether they are regulated through the 3'-UTR is unknown and therefore similar luciferase assays are required. As mentioned in Section 7.4, RIP and/or co-localisation should be performed for both DAZL and BOLL targets as well using human tissue, to find out whether they can interact with their targets *in vivo*. Another task is to determine how DAZL regulates the expression of STRA8 and meiosis entry; the co-localisation of DAZL and STRA8 has never been investigated in human fetal ovary, neither are their interactions.

Moreover, although several *in vitro* studies suggest that DAZL could promote germ cell differentiation from ES cells, its expression at PGC formation, or whether it regulates this process *in vivo* remains unknown so far. And for BOLL expression, we still do not know whether it is necessary for meiosis II in fertilised oocytes, which is similar to DAZL. The roles of DAZL in pre-implantation embryos are quite interesting as well, as its functions are potentially not restricted to germ cells.

And finally, the novel repression functions of DAZL also need to be investigated in depth. Although there are several possible explanations, the underlying mechanism is still far from clear. This investigation could also extend to the other two members of the DAZ family, how they are regulated, and species other than human and mouse, to

give an in-depth look of the evolution of this gene family which is central to fertility across a wide range of species.

References

Aapola U, Kawasaki K, Scott HS, Ollila J, Vihinen M, Heino M, Shintani A, Kawasaki K, Minoshima S, Krohn K *et al.* Isolation and initial characterization of a novel zinc finger gene, DNMT3L, on 21q22.3, related to the cytosine-5-methyltransferase 3 gene family. Genomics. 2000;**65**:293-8.

Adhikari D, Liu K. Molecular mechanisms underlying the activation of mammalian primordial follicles. Endocr Rev. 2009;**30**:438-64.

Agar W. Memoirs: The Spermatogenesis of Lepidosiren Paradoxa. Quarterly Journal of Microscopical Science. 1911;**2**:1-44.

Alphey L, Jimenez J, White-Cooper H, Dawson I, Nurse P, Glover DM. twine, a cdc25 homolog that functions in the male and female germline of Drosophila. Cell. 1992;**69**:977-88.

Andegeko Y, Moyal L, Mittelman L, Tsarfaty I, Shiloh Y, Rotman G. Nuclear retention of ATM at sites of DNA double strand breaks. J Biol Chem. 2001;**276**:38224-30.

Anderson EL, Baltus AE, Roepers-Gajadien HL, Hassold TJ, de Rooij DG, van Pelt AM, Page DC. Stra8 and its inducer, retinoic acid, regulate meiotic initiation in both spermatogenesis and oogenesis in mice. Proc Natl Acad Sci U S A. 2008;**105**:14976-80.

Anderson R, Copeland TK, Scholer H, Heasman J, Wylie C. The onset of germ cell migration in the mouse embryo. Mech Dev. 2000;**91**:61-8.

Anderson RA, Fulton N, Cowan G, Coutts S, Saunders PT. Conserved and divergent patterns of expression of DAZL, VASA and OCT4 in the germ cells of the human fetal ovary and testis. BMC Dev Biol. 2007;**7**:136.

Antonicka H, Sasarman F, Nishimura T, Paupe V, Shoubridge EA. The mitochondrial RNA-binding protein GRSF1 localizes to RNA granules and is required for posttranscriptional mitochondrial gene expression. Cell metabolism. 2013;**17**:386-98.

Assou S, Anahory T, Pantesco V, Le Carrour T, Pellestor F, Klein B, Reyftmann L, Dechaud H, De Vos J, Hamamah S. The human cumulus--oocyte complex gene-expression profile. Hum Reprod. 2006;**21**:1705-19.

Baillet A, Mandon-Pepin B. Mammalian ovary differentiation - a focus on female meiosis. Mol Cell Endocrinol. 2012;**356**:13-23.

Baker TG. A Quantitative and Cytological Study of Germ Cells in Human Ovaries. Proc R Soc Lond B Biol Sci. 1963;**158**:417-33.

Bakkenist CJ, Kastan MB. DNA damage activates ATM through intermolecular autophosphorylation and dimer dissociation. Nature. 2003;**421**:499-506.

Baltus AE, Menke DB, Hu YC, Goodheart ML, Carpenter AE, de Rooij DG, Page DC. In germ cells of mouse embryonic ovaries, the decision to enter meiosis precedes premeiotic DNA replication. Nat Genet. 2006;**38**:1430-4.

Bao J, Wang L, Lei J, Hu Y, Liu Y, Shen H, Yan W, Xu C. STK31(TDRD8) is dynamically regulated throughout mouse spermatogenesis and interacts with MIWI protein. Histochemistry and cell biology. 2012;**137**:377-89.

Barchi M, Mahadevaiah S, Di Giacomo M, Baudat F, de Rooij DG, Burgoyne PS, Jasin M, Keeney S. Surveillance of different recombination defects in mouse spermatocytes yields distinct responses despite elimination at an identical developmental stage. Molecular and cellular biology. 2005;**25**:7203-15.

Basu A, Datta D, Zurakowski D, Pal S. Altered VEGF mRNA stability following treatments with immunosuppressive agents: implications for cancer development. J Biol Chem. 2010;**285**:25196-202.

Baxter A, Farley J. Mendel and Meiosis. J Hist Biol. 1979;**12**:137-73.

Beaumont HM, Mandl AM. A quantitative and cytological study of oogonia and oocytes in the foetal and neonatal rat. Proceedings of the Royal Society of London Series B, Biological Sciences. 1962;**155**:557-79.

Bendel-Stenzel MR, Gomperts M, Anderson R, Heasman J, Wylie C. The role of cadherins during primordial germ cell migration and early gonad formation in the mouse. Mech Dev. 2000;**91**:143-52.

Blandau RJ, White BJ, Rumery RE. Observations on the Movements of the Living Primordial Germ Cells in the Mouse. Fertil Steril. 1963;**14**:482-9.

Blobel G. A protein of molecular weight 78,000 bound to the polyadenylate region of eukaryotic messenger RNAs. Proc Natl Acad Sci U S A. 1973;**70**:924-8.

Bolor H, Mori T, Nishiyama S, Ito Y, Hosoba E, Inagaki H, Kogo H, Ohye T, Tsutsumi M, Kato T *et al.* Mutations of the SYCP3 gene in women with recurrent pregnancy loss. Am J Hum Genet. 2009;**84**:14-20.

Bonner WA, Hulett HR, Sweet RG, Herzenberg LA. Fluorescence activated cell sorting. Rev Sci Instrum. 1972;**43**:404-9.

Borum K. Oogenesis in the mouse. A study of the meiotic prophase. Exp Cell Res. 1961;**24**:495-507.

Bouillet P, Oulad-Abdelghani M, Vicaire S, Garnier JM, Schuhbaur B, Dolle P, Chambon P. Efficient cloning of cDNAs of retinoic acid-responsive genes in P19 embryonal carcinoma cells and characterization of a novel mouse gene, Stra1 (mouse LERK-2/Eplg2). Dev Biol. 1995;**170**:420-33.

Bourc'his D, Bestor TH. Meiotic catastrophe and retrotransposon reactivation in male germ cells lacking Dnmt3L. Nature. 2004;**431**:96-9.

Bourc'his D, Xu GL, Lin CS, Bollman B, Bestor TH. Dnmt3L and the establishment of maternal genomic imprints. Science. 2001;**294**:2536-9.

Bowles J, Knight D, Smith C, Wilhelm D, Richman J, Mamiya S, Yashiro K, Chawengsaksophak K, Wilson MJ, Rossant J *et al.* Retinoid signaling determines germ cell fate in mice. Science. 2006;**312**:596-600.

Bowles J, Koopman P. Retinoic acid, meiosis and germ cell fate in mammals. Development. 2007;**134**:3401-11.

Braas KM, Harakall SA, Ouafik L, Eipper BA, May V. Expression of peptidylglycine alpha-amidating monooxygenase: an in situ hybridization and immunocytochemical study. Endocrinology. 1992;**130**:2778-88.

Bristol-Gould SK, Kreeger PK, Selkirk CG, Kilen SM, Cook RW, Kipp JL, Shea LD, Mayo KE, Woodruff TK. Postnatal regulation of germ cells by activin: the establishment of the initial follicle pool. Dev Biol. 2006;**298**:132-48.

Brook M, Smith JW, Gray NK. The DAZL and PABP families: RNA-binding proteins with interrelated roles in translational control in oocytes. Reproduction. 2009;**137**:595-617.

Buehr M, McLaren A, Bartley A, Darling S. Proliferation and migration of primordial germ cells in We/We mouse embryos. Dev Dyn. 1993;**198**:182-9.

Burma S, Chen BP, Murphy M, Kurimasa A, Chen DJ. ATM phosphorylates histone H2AX in response to DNA double-strand breaks. J Biol Chem. 2001;**276**:42462-7.

Castrillon DH, Gonczy P, Alexander S, Rawson R, Eberhart CG, Viswanathan S, DiNardo S, Wasserman SA. Toward a molecular genetic analysis of spermatogenesis in Drosophila melanogaster: characterization of male-sterile mutants generated by single P element mutagenesis. Genetics. 1993;**135**:489-505.

Cauffman G, Van de Velde H, Liebaers I, Van Steirteghem A. DAZL expression in human oocytes, preimplantation embryos and embryonic stem cells. Mol Hum Reprod. 2005;**11**:405-11.

Celebi C, van Montfoort A, Skory V, Kieffer E, Kuntz S, Mark M, Viville S. Tex 19 paralogs exhibit a gonad and placenta-specific expression in the mouse. J Reprod Dev. 2012;**58**:360-5.

Celeste A, Petersen S, Romanienko PJ, Fernandez-Capetillo O, Chen HT, Sedelnikova OA, Reina-San-Martin B, Coppola V, Meffre E, Difilippantonio MJ *et al.* Genomic instability in mice lacking histone H2AX. Science. 2002;**296**:922-7.

Chang H, Matzuk MM. Smad5 is required for mouse primordial germ cell development. Mech Dev. 2001;**104**:61-7.

Chawengsaksophak K, Svingen T, Ng ET, Epp T, Spiller CM, Clark C, Cooper H, Koopman P. Loss of Wnt5a disrupts primordial germ cell migration and male sexual development in mice. Biol Reprod. 2012;**86**:1-12.

Chen H-H, Welling M, Bloch Donald B, Muñoz J, Mientjes E, Chen X, Tramp C, Wu J, Yabuuchi A, Chou Y-F *et al.* DAZL Limits Pluripotency, Differentiation, and Apoptosis in Developing Primordial Germ Cells. Stem Cell Reports. 2014.

Chen J, Melton C, Suh N, Oh JS, Horner K, Xie F, Sette C, Blelloch R, Conti M. Genome-wide analysis of translation reveals a critical role for deleted in azoospermia-like (Dazl) at the oocyte-to-zygote transition. Genes Dev. 2011;**25**:755-66.

Cheng L, Guan Y, Li L, Legerski RJ, Einspahr J, Bangert J, Alberts DS, Wei Q. Expression in normal human tissues of five nucleotide excision repair genes measured simultaneously by multiplex reverse transcription-polymerase chain reaction. Cancer epidemiology, biomarkers & prevention : a publication of the American Association for Cancer Research, cosponsored by the American Society of Preventive Oncology. 1999;**8**:801-7.

Childs AJ, Anderson RA. Activin A selectively represses expression of the membrane-bound isoform of Kit ligand in human fetal ovary. Fertil Steril. 2009;**92**:1416-9.

Childs AJ, Cowan G, Kinnell HL, Anderson RA, Saunders PT. Retinoic Acid signalling and the control of meiotic entry in the human fetal gonad. PLoS One. 2011;**6**:e20249.

Chiquoine AD. The identification, origin, and migration of the primordial germ cells in the mouse embryo. Anat Rec. 1954;**118**:135-46.

Clark AT, Bodnar MS, Fox M, Rodriquez RT, Abeyta MJ, Firpo MT, Pera RAR. Spontaneous differentiation of germ cells from human embryonic stem cells in vitro. Human molecular genetics. 2004;**13**:727-39.

Collier B, Gorgoni B, Loveridge C, Cooke HJ, Gray NK. The DAZL family proteins are PABP-binding proteins that regulate translation in germ cells. EMBO J. 2005;**24**:2656-66.

Conrad S, Azizi H, Hatami M, Kubista M, Bonin M, Hennenlotter J, Renninger M, Skutella T. Differential gene expression profiling of enriched human spermatogonia after short- and long-term culture. Biomed Res Int. 2014;**2014**:138350.

Cooke HJ, Lee M, Kerr S, Ruggiu M. A murine homologue of the human DAZ gene is autosomal and expressed only in male and female gonads. Hum Mol Genet. 1996;**5**:513-6.

Courtot C, Fankhauser C, Simanis V, Lehner CF. The Drosophila cdc25 homolog twine is required for meiosis. Development. 1992;**116**:405-16.

Coutts SM, Childs AJ, Fulton N, Collins C, Bayne RA, McNeilly AS, Anderson RA. Activin signals via SMAD2/3 between germ and somatic cells in the human fetal ovary and regulates kit ligand expression. Dev Biol. 2008;**314**:189-99.

Dai T, Vera Y, Salido EC, Yen PH. Characterization of the mouse Dazap1 gene encoding an RNA-binding protein that interacts with infertility factors DAZ and DAZL. BMC Genomics. 2001;**2**:6.

de Jong J, Stoop H, Gillis AJ, Hersmus R, van Gurp RJ, van de Geijn GJ, van Drunen E, Beverloo HB, Schneider DT, Sherlock JK *et al.* Further characterization of the first seminoma cell line TCam-2. Genes Chromosomes Cancer. 2008a;**47**:185-96.

de Jong J, Stoop H, Gillis AJ, van Gurp RJ, van de Geijn GJ, Boer M, Hersmus R, Saunders PT, Anderson RA, Oosterhuis JW *et al.* Differential expression of SOX17

and SOX2 in germ cells and stem cells has biological and clinical implications. J Pathol. 2008b;**215**:21-30.

de Moor CH, Richter JD. Cytoplasmic polyadenylation elements mediate masking and unmasking of cyclin B1 mRNA. EMBO J. 1999;**18**:2294-303.

De Pol A, Vaccina F, Forabosco A, Cavazzuti E, Marzona L. Apoptosis of germ cells during human prenatal oogenesis. Hum Reprod. 1997;**12**:2235-41.

Dobson MJ, Pearlman RE, Karaiskakis A, Spyropoulos B, Moens PB. Synaptonemal complex proteins: occurrence, epitope mapping and chromosome disjunction. J Cell Sci. 1994;**107 (Pt 10)**:2749-60.

Donovan PJ, Stott D, Cairns LA, Heasman J, Wylie CC. Migratory and postmigratory mouse primordial germ cells behave differently in culture. Cell. 1986;**44**:831-8.

Dorfman DM, Genest DR, Reijo Pera RA. Human DAZL1 encodes a candidate fertility factor in women that localizes to the prenatal and postnatal germ cells. Hum Reprod. 1999;**14**:2531-6.

Dumont JN. Oogenesis in Xenopus laevis (Daudin). I. Stages of oocyte development in laboratory maintained animals. J Morphol. 1972;**136**:153-79.

Dym M, Fawcett DW. Further observations on the numbers of spermatogonia, spermatocytes, and spermatids connected by intercellular bridges in the mammalian testis. Biol Reprod. 1971;**4**:195-215.

Eberhart CG, Maines JZ, Wasserman SA. Meiotic cell cycle requirement for a fly homologue of human Deleted in Azoospermia. Nature. 1996;**381**:783-5.

Eckert D, Nettersheim D, Heukamp LC, Kitazawa S, Biermann K, Schorle H. TCam-2 but not JKT-1 cells resemble seminoma in cell culture. Cell Tissue Res. 2008;**331**:529-38.

Farmer JB, Moore J. Memoirs: On the Maiotic Phase (Reduction Divisions) in Animals and Plants. Quarterly Journal of Microscopical Science. 1905;**2**:489-558.

Felix W. The development of the urogenital organs. Manual of human embryology. 1912;**2**:752-979.

Fox M, Urano J, Reijo Pera RA. Identification and characterization of RNA sequences to which human PUMILIO-2 (PUM2) and deleted in Azoospermia-like (DAZL) bind. Genomics. 2005;**85**:92-105.

Fulton N, Martins da Silva SJ, Bayne RA, Anderson RA. Germ cell proliferation and apoptosis in the developing human ovary. J Clin Endocrinol Metab. 2005;**90**:4664-70.

Garcia-Cruz R, Brieno MA, Roig I, Grossmann M, Velilla E, Pujol A, Cabero L, Pessarrodona A, Barbero JL, Garcia Caldes M. Dynamics of cohesin proteins REC8, STAG3, SMC1 beta and SMC3 are consistent with a role in sister chromatid cohesion during meiosis in human oocytes. Hum Reprod. 2010;**25**:2316-27.

Gilbert C, Kristjuhan A, Winkler GS, Svejstrup JQ. Elongator interactions with nascent mRNA revealed by RNA immunoprecipitation. Mol Cell. 2004;**14**:457-64.

Gill ME, Hu YC, Lin Y, Page DC. Licensing of gametogenesis, dependent on RNA binding protein DAZL, as a gateway to sexual differentiation of fetal germ cells. Proc Natl Acad Sci U S A. 2011;**108**:7443-8.

Ginsburg M, Snow MH, McLaren A. Primordial germ cells in the mouse embryo during gastrulation. Development. 1990;**110**:521-8.

Godin I, Wylie CC. TGF beta 1 inhibits proliferation and has a chemotropic effect on mouse primordial germ cells in culture. Development. 1991;**113**:1451-7.

Gokul G, Gautami B, Malathi S, Sowjanya AP, Poli UR, Jain M, Ramakrishna G, Khosla S. DNA methylation profile at the DNMT3L promoter: a potential biomarker for cervical cancer. Epigenetics : official journal of the DNA Methylation Society. 2007;**2**:80-5.

Gomperts M, Garcia-Castro M, Wylie C, Heasman J. Interactions between primordial germ cells play a role in their migration in mouse embryos. Development. 1994;**120**:135-41.

Gondos B. Comparative studies of normal and neoplastic ovarian germ cells: 1. Ultrastructure of oogonia and intercellular bridges in the fetal ovary. Int J Gynecol Pathol. 1987;**6**:114-23.

Gondos B, Westergaard L, Byskov AG. Initiation of oogenesis in the human fetal ovary: ultrastructural and squash preparation study. Am J Obstet Gynecol. 1986;**155**:189-95.

Greenbaum MP, Iwamori N, Agno JE, Matzuk MM. Mouse TEX14 is required for embryonic germ cell intercellular bridges but not female fertility. Biol Reprod. 2009;**80**:449-57.

Greenbaum MP, Iwamori T, Buchold GM, Matzuk MM. Germ cell intercellular bridges. Cold Spring Harb Perspect Biol. 2011;**3**:a005850.

Greenbaum MP, Ma L, Matzuk MM. Conversion of midbodies into germ cell intercellular bridges. Dev Biol. 2007;**305**:389-96.

Greenbaum MP, Yan W, Wu MH, Lin YN, Agno JE, Sharma M, Braun RE, Rajkovic A, Matzuk MM. TEX14 is essential for intercellular bridges and fertility in male mice. Proc Natl Acad Sci U S A. 2006;**103**:4982-7.

Gu Y, Runyan C, Shoemaker A, Surani A, Wylie C. Steel factor controls primordial germ cell survival and motility from the time of their specification in the allantois, and provides a continuous niche throughout their migration. Development. 2009;**136**:1295-303.

Guo Q, Xie J, Dang CV, Liu ET, Bishop JM. Identification of a large Myc-binding protein that contains RCC1-like repeats. Proc Natl Acad Sci U S A. 1998;**95**:9172-7.

Haag ES. Rolling back to BOULE. Proc Natl Acad Sci U S A. 2001;**98**:6983-5.

Hamer G, Kal HB, Westphal CH, Ashley T, de Rooij DG. Ataxia telangiectasia mutated expression and activation in the testis. Biol Reprod. 2004;**70**:1206-12.

Hamer G, Roepers-Gajadien HL, van Duyn-Goedhart A, Gademan IS, Kal HB, van Buul PP, de Rooij DG. DNA double-strand breaks and gamma-H2AX signaling in the testis. Biol Reprod. 2003;**68**:628-34.

Hao Z, Jha KN, Kim YH, Vemuganti S, Westbrook VA, Chertihin O, Markgraf K, Flickinger CJ, Coppola M, Herr JC *et al.* Expression analysis of the human testis-specific serine/threonine kinase (TSSK) homologues. A TSSK member is present in the equatorial segment of human sperm. Mol Hum Reprod. 2004;**10**:433-44.

Hartley PS, Bayne RA, Robinson LL, Fulton N, Anderson RA. Developmental changes in expression of myeloid cell leukemia-1 in human germ cells during oogenesis and early folliculogenesis. J Clin Endocrinol Metab. 2002;**87**:3417-27.

Hartshorne GM, Lyrakou S, Hamoda H, Oloto E, Ghafari F. Oogenesis and cell death in human prenatal ovaries: what are the criteria for oocyte selection? Mol Hum Reprod. 2009;**15**:805-19.

Hasegawa E, Karashima T, Sumiyoshi E, Yamamoto M. C. elegans CPB-3 interacts with DAZ-1 and functions in multiple steps of germline development. Dev Biol. 2006;**295**:689-99.

Haston KM, Tung JY, Reijo Pera RA. Dazl functions in maintenance of pluripotency and genetic and epigenetic programs of differentiation in mouse primordial germ cells in vivo and in vitro. PLoS One. 2009;**4**:e5654.

He J, Stewart K, Kinnell HL, Anderson RA, Childs AJ. A Developmental Stage-Specific Switch from DAZL to BOLL Occurs during Fetal Oogenesis in Humans, but Not Mice. PLoS ONE. 2013;**8**:e73996.

Higuchi R, Dollinger G, Walsh PS, Griffith R. Simultaneous amplification and detection of specific DNA sequences. Biotechnology (N Y). 1992;**10**:413-7.

Hilscher B, Hilscher W, Bulthoff-Ohnolz B, Kramer U, Birke A, Pelzer H, Gauss G. Kinetics of gametogenesis. I. Comparative histological and autoradiographic studies of oocytes and transitional prospermatogonia during oogenesis and prespermatogenesis. Cell Tissue Res. 1974;**154**:443-70.

Hoopfer ED, Penton A, Watts RJ, Luo L. Genomic analysis of Drosophila neuronal remodeling: a role for the RNA-binding protein Boule as a negative regulator of axon pruning. J Neurosci. 2008;**28**:6092-103.

Houmard B, Small C, Yang L, Naluai-Cecchini T, Cheng E, Hassold T, Griswold M. Global gene expression in the human fetal testis and ovary. Biol Reprod. 2009;**81**:438-43.

Houston DW, King ML. A critical role for Xdazl, a germ plasm-localized RNA, in the differentiation of primordial germ cells in Xenopus. Development. 2000;**127**:447-56.

Houston DW, Zhang J, Maines JZ, Wasserman SA, King ML. A Xenopus DAZ-like gene encodes an RNA component of germ plasm and is a functional homologue of Drosophila boule. Development. 1998;**125**:171-80.

Hreinsson JG, Scott JE, Rasmussen C, Swahn ML, Hsueh AJ, Hovatta O. Growth differentiation factor-9 promotes the growth, development, and survival of human ovarian follicles in organ culture. J Clin Endocrinol Metab. 2002;**87**:316-21.

Hsia KT, Millar MR, King S, Selfridge J, Redhead NJ, Melton DW, Saunders PT. DNA repair gene Ercc1 is essential for normal spermatogenesis and oogenesis and for functional integrity of germ cell DNA in the mouse. Development. 2003;**130**:369-78.

Huynh JR, St Johnston D. The origin of asymmetry: early polarisation of the Drosophila germline cyst and oocyte. Curr Biol. 2004;**14**:R438-49.

Irie N, Weinberger L, Tang WW, Kobayashi T, Viukov S, Manor YS, Dietmann S, Hanna JH, Surani MA. SOX17 is a critical specifier of human primordial germ cell fate. Cell. 2015;**160**:253-68.

Jenkins HT, Malkova B, Edwards TA. Kinked beta-strands mediate high-affinity recognition of mRNA targets by the germ-cell regulator DAZL. Proc Natl Acad Sci U S A. 2011;**108**:18266-71.

Jiao X, Trifillis P, Kiledjian M. Identification of target messenger RNA substrates for the murine deleted in azoospermia-like RNA-binding protein. Biol Reprod. 2002;**66**:475-85.

Jourdain AA, Koppen M, Wydro M, Rodley CD, Lightowlers RN, Chrzanowska-Lightowlers ZM, Martinou JC. GRSF1 regulates RNA processing in mitochondrial RNA granules. Cell metabolism. 2013;**17**:399-410.

Kahvejian A, Roy G, Sonenberg N. The mRNA closed-loop model: the function of PABP and PABP-interacting proteins in mRNA translation. Cold Spring Harb Symp Quant Biol. 2001;**66**:293-300.

Kanai Y, Kanai-Azuma M, Noce T, Saido TC, Shiroishi T, Hayashi Y, Yazaki K. Identification of two Sox17 messenger RNA isoforms, with and without the high mobility group box region, and their differential expression in mouse spermatogenesis. J Cell Biol. 1996;**133**:667-81.

Karashima T, Sugimoto A, Yamamoto M. Caenorhabditis elegans homologue of the human azoospermia factor DAZ is required for oogenesis but not for spermatogenesis. Development. 2000;**127**:1069-79.

Katoh M. Molecular cloning and characterization of human SOX17. International journal of molecular medicine. 2002;**9**:153-7.

Kee K, Angeles VT, Flores M, Nguyen HN, Reijo Pera RA. Human DAZL, DAZ and BOULE genes modulate primordial germ-cell and haploid gamete formation. Nature. 2009;**462**:222-5.

Keegan KS, Holtzman DA, Plug AW, Christenson ER, Brainerd EE, Flaggs G, Bentley NJ, Taylor EM, Meyn MS, Moss SB *et al.* The Atr and Atm protein kinases associate with different sites along meiotically pairing chromosomes. Genes Dev. 1996;**10**:2423-37.

Keshet E, Lyman SD, Williams DE, Anderson DM, Jenkins NA, Copeland NG, Parada LF. Embryonic RNA expression patterns of the c-kit receptor and its cognate ligand suggest multiple functional roles in mouse development. EMBO J. 1991;**10**:2425-35.

Kim B, Cooke HJ, Rhee K. DAZL is essential for stress granule formation implicated in germ cell survival upon heat stress. Development. 2012;**139**:568-78.

Kleiman SE, Lehavi O, Hauser R, Botchan A, Paz G, Yavetz H, Yogev L. CDY1 and BOULE transcripts assessed in the same biopsy as predictive markers for successful testicular sperm retrieval. Fertil Steril. 2011;**95**:2297-302, 302 e1.

Kobayashi H, Hiura H, John RM, Sato A, Otsu E, Kobayashi N, Suzuki R, Suzuki F, Hayashi C, Utsunomiya T *et al.* DNA methylation errors at imprinted loci after assisted conception originate in the parental sperm. European journal of human genetics : EJHG. 2009;**17**:1582-91.

Koberle B, Brenner W, Albers A, Usanova S, Thuroff JW, Kaina B. ERCC1 and XPF expression in human testicular germ cell tumors. Oncology reports. 2010;**23**:223-7.

Kosaka K, Kawakami K, Sakamoto H, Inoue K. Spatiotemporal localization of germ plasm RNAs during zebrafish oogenesis. Mech Dev. 2007;**124**:279-89.

Kostova E, Yeung CH, Luetjens CM, Brune M, Nieschlag E, Gromoll J. Association of three isoforms of the meiotic BOULE gene with spermatogenic failure in infertile men. Mol Hum Reprod. 2007;**13**:85-93.

Koubova J, Menke DB, Zhou Q, Capel B, Griswold MD, Page DC. Retinoic acid regulates sex-specific timing of meiotic initiation in mice. Proc Natl Acad Sci U S A. 2006;**103**:2474-9.

Kozopas KM, Yang T, Buchan HL, Zhou P, Craig RW. MCL1, a gene expressed in programmed myeloid cell differentiation, has sequence similarity to BCL2. Proc Natl Acad Sci U S A. 1993;**90**:3516-20.

Kretzschmar M, Liu F, Hata A, Doody J, Massague J. The TGF-beta family mediator Smad1 is phosphorylated directly and activated functionally by the BMP receptor kinase. Genes Dev. 1997;**11**:984-95.

Kuales G, De Mulder K, Glashauser J, Salvenmoser W, Takashima S, Hartenstein V, Berezikov E, Salzburger W, Ladurner P. Boule-like genes regulate male and female gametogenesis in the flatworm Macrostomum lignano. Dev Biol. 2011;**357**:117-32.

Kumar S, Chatzi C, Brade T, Cunningham TJ, Zhao X, Duester G. Sex-specific timing of meiotic initiation is regulated by Cyp26b1 independent of retinoic acid signalling. Nature communications. 2011;**2**:151.

Kuntz S, Kieffer E, Bianchetti L, Lamoureux N, Fuhrmann G, Viville S. Tex19, a mammalian-specific protein with a restricted expression in pluripotent stem cells and germ line. Stem Cells. 2008;**26**:734-44.

Kuo LJ, Yang LX. Gamma-H2AX - a novel biomarker for DNA double-strand breaks. In vivo. 2008;**22**:305-9.

La Salle S, Mertineit C, Taketo T, Moens PB, Bestor TH, Trasler JM. Windows for sex-specific methylation marked by DNA methyltransferase expression profiles in mouse germ cells. Dev Biol. 2004;**268**:403-15.

Lammers JH, Offenberg HH, van Aalderen M, Vink AC, Dietrich AJ, Heyting C. The gene encoding a major component of the lateral elements of synaptonemal complexes of the rat is related to X-linked lymphocyte-regulated genes. Molecular and cellular biology. 1994;**14**:1137-46.

Lawson KA, Dunn NR, Roelen BA, Zeinstra LM, Davis AM, Wright CV, Korving JP, Hogan BL. Bmp4 is required for the generation of primordial germ cells in the mouse embryo. Genes Dev. 1999;**13**:424-36.

Le Bouffant R, Guerquin MJ, Duquenne C, Frydman N, Coffigny H, Rouiller-Fabre V, Frydman R, Habert R, Livera G. Meiosis initiation in the human ovary requires intrinsic retinoic acid synthesis. Hum Reprod. 2010;**25**:2579-90.

Le Bouffant R, Souquet B, Duval N, Duquenne C, Herve R, Frydman N, Robert B, Habert R, Livera G. Msx1 and Msx2 promote meiosis initiation. Development. 2011;**138**:5393-402.

Lee KH, Lee S, Kim B, Chang S, Kim SW, Paick JS, Rhee K. Dazl can bind to dynein motor complex and may play a role in transport of specific mRNAs. EMBO J. 2006;**25**:4263-70.

Li B, Li JB, Xiao XF, Ma YF, Wang J, Liang XX, Zhao HX, Jiang F, Yao YQ, Wang XH. Altered DNA methylation patterns of the H19 differentially methylated region and the DAZL gene promoter are associated with defective human sperm. PLoS One. 2013a;**8**:e71215.

Li JY, Lees-Murdock DJ, Xu GL, Walsh CP. Timing of establishment of paternal methylation imprints in the mouse. Genomics. 2004;**84**:952-60.

Li M, Liu C, Zhu H, Sun J, Yu M, Niu Z, Liu W, Peng S, Hua J. Expression pattern of Boule in dairy goat testis and its function in promoting the meiosis in male germline stem cells (mGSCs). J Cell Biochem. 2013b;**114**:294-302.

Li M, Shen Q, Xu H, Wong FM, Cui J, Li Z, Hong N, Wang L, Zhao H, Ma B *et al.* Differential conservation and divergence of fertility genes boule and dazl in the rainbow trout. PLoS One. 2011a;**6**:e15910.

Li Y, Sosnik J, Brassard L, Reese M, Spiridonov NA, Bates TC, Johnson GR, Anguita J, Visconti PE, Salicioni AM. Expression and localization of five members of the testis-specific serine kinase (Tssk) family in mouse and human sperm and testis. Mol Hum Reprod. 2011b;**17**:42-56.

Lickert H, Cox B, Wehrle C, Taketo MM, Kemler R, Rossant J. Dissecting Wnt/beta-catenin signaling during gastrulation using RNA interference in mouse embryos. Development. 2005;**132**:2599-609.

Lin Y, Gill ME, Koubova J, Page DC. Germ cell-intrinsic and -extrinsic factors govern meiotic initiation in mouse embryos. Science. 2008;**322**:1685-7.

Lin Y, Page DC. Dazl deficiency leads to embryonic arrest of germ cell development in XY C57BL/6 mice. Dev Biol. 2005;**288**:309-16.

Lin YM, Chen CW, Sun HS, Tsai SJ, Hsu CC, Teng YN, Lin JS, Kuo PL. Expression patterns and transcript concentrations of the autosomal DAZL gene in testes of azoospermic men. Mol Hum Reprod. 2001;**7**:1015-22.

Lin YM, Chung CL, Cheng YS. Posttranscriptional regulation of CDC25A by BOLL is a conserved fertility mechanism essential for human spermatogenesis. J Clin Endocrinol Metab. 2009;**94**:2650-7.

Lin YM, Kuo PL, Lin YH, Teng YN, Nan Lin JS. Messenger RNA transcripts of the meiotic regulator BOULE in the testis of azoospermic men and their application in predicting the success of sperm retrieval. Hum Reprod. 2005;**20**:782-8.

Lin YM, Teng YN, Chung CL, Tsai WC, Lin YH, Lin JS, Kuo PL. Decreased mRNA transcripts of M-phase promoting factor and its regulators in the testes of infertile men. Hum Reprod. 2006;**21**:138-44.

Linher K, Cheung Q, Baker P, Bedecarrats G, Shiota K, Li J. An epigenetic mechanism regulates germ cell-specific expression of the porcine Deleted in Azoospermia-Like (DAZL) gene. Differentiation. 2009;**77**:335-49.

Liu K, Rajareddy S, Liu L, Jagarlamudi K, Boman K, Selstam G, Reddy P. Control of mammalian oocyte growth and early follicular development by the oocyte PI3 kinase pathway: new roles for an old timer. Dev Biol. 2006;**299**:1-11.

Livera G, Rouiller-Fabre V, Valla J, Habert R. Effects of retinoids on the meiosis in the fetal rat ovary in culture. Mol Cell Endocrinol. 2000;**165**:225-31.

Loveland KL, Schlatt S. Stem cell factor and c-kit in the mammalian testis: lessons originating from Mother Nature's gene knockouts. J Endocrinol. 1997;**153**:337-44.

Luetjens CM, Xu EY, Rejo Pera RA, Kamischke A, Nieschlag E, Gromoll J. Association of meiotic arrest with lack of BOULE protein expression in infertile men. J Clin Endocrinol Metab. 2004;**89**:1926-33.

MacLean G, Li H, Metzger D, Chambon P, Petkovich M. Apoptotic extinction of germ cells in testes of Cyp26b1 knockout mice. Endocrinology. 2007;**148**:4560-7.

Madabhushi M, Lacy E. Anterior visceral endoderm directs ventral morphogenesis and placement of head and heart via BMP2 expression. Dev Cell. 2011;**21**:907-19.

Maeda T, Nishida J, Nakanishi Y. Expression pattern, subcellular localization and structure--function relationship of rat Tpx-1, a spermatogenic cell adhesion molecule responsible for association with Sertoli cells. Development, growth & differentiation. 1999;**41**:715-22.

Maeda T, Sakashita M, Ohba Y, Nakanishi Y. Molecular cloning of the rat Tpx-1 responsible for the interaction between spermatogenic and Sertoli cells. Biochem Biophys Res Commun. 1998;**248**:140-6.

Maegawa S, Yamashita M, Yasuda K, Inoue K. Zebrafish DAZ-like protein controls translation via the sequence 'GUUC'. Genes to cells : devoted to molecular & cellular mechanisms. 2002;**7**:971-84.

Maegawa S, Yasuda K, Inoue K. Maternal mRNA localization of zebrafish DAZ-like gene. Mech Dev. 1999;**81**:223-6.

Mahadevaiah SK, Turner JM, Baudat F, Rogakou EP, de Boer P, Blanco-Rodriguez J, Jasin M, Keeney S, Bonner WM, Burgoyne PS. Recombinational DNA double-strand breaks in mice precede synapsis. Nat Genet. 2001;**27**:271-6.

Maheshwari A, Fowler PA. Primordial follicular assembly in humans--revisited. Zygote. 2008;**16**:285-96.

Maines JZ, Wasserman SA. Post-transcriptional regulation of the meiotic Cdc25 protein Twine by the Dazl orthologue Boule. Nat Cell Biol. 1999;**1**:171-4.

Mandon-Pepin B, Oustry-Vaiman A, Vigier B, Piumi F, Cribiu E, Cotinot C. Expression profiles and chromosomal localization of genes controlling meiosis and follicular development in the sheep ovary. Biol Reprod. 2003;**68**:985-95.

Manton I. Evidence on Spiral Structure and Chromosome Pairing in Osmunda regalis L. Philosophical Transactions of the Royal Society of London Series B, Biological Sciences. 1939;**230**:179-215.

Maratou K, Forster T, Costa Y, Taggart M, Speed RM, Ireland J, Teague P, Roy D, Cooke HJ. Expression profiling of the developing testis in wild-type and Dazl knockout mice. Mol Reprod Dev. 2004;**67**:26-54.

Mark M, Jacobs H, Oulad-Abdelghani M, Dennefeld C, Feret B, Vernet N, Codreanu CA, Chambon P, Ghyselinck NB. STRA8-deficient spermatocytes initiate, but fail to complete, meiosis and undergo premature chromosome condensation. J Cell Sci. 2008;**121**:3233-42.

Martins da Silva SJ, Bayne RA, Cambray N, Hartley PS, McNeilly AS, Anderson RA. Expression of activin subunits and receptors in the developing human ovary: activin A promotes germ cell survival and proliferation before primordial follicle formation. Dev Biol. 2004;**266**:334-45.

McAllister HA, Rock DL. Comparative usefulness of tissue fixatives for in situ viral nucleic acid hybridization. J Histochem Cytochem. 1985;**33**:1026-32.

McGee EA, Hsueh AJ. Initial and cyclic recruitment of ovarian follicles. Endocr Rev. 2000;**21**:200-14.

McLaren A, Southee D. Entry of mouse embryonic germ cells into meiosis. Dev Biol. 1997;**187**:107-13.

McNeilly JR, Saunders PT, Taggart M, Cranfield M, Cooke HJ, McNeilly AS. Loss of oocytes in Dazl knockout mice results in maintained ovarian steroidogenic

function but altered gonadotropin secretion in adult animals. Endocrinology. 2000;**141**:4284-94.

McNeilly JR, Watson EA, White YA, Murray AA, Spears N, McNeilly AS. Decreased oocyte DAZL expression in mice results in increased litter size by modulating follicle-stimulating hormone-induced follicular growth. Biol Reprod. 2011;**85**:584-93.

Medrano JV, Ramathal C, Nguyen HN, Simon C, Reijo Pera RA. Divergent RNA-binding proteins, DAZL and VASA, induce meiotic progression in human germ cells derived in vitro. Stem Cells. 2012;**30**:441-51.

Menke DB, Koubova J, Page DC. Sexual differentiation of germ cells in XX mouse gonads occurs in an anterior-to-posterior wave. Dev Biol. 2003;**262**:303-12.

Michaelis C, Ciosk R, Nasmyth K. Cohesins: chromosomal proteins that prevent premature separation of sister chromatids. Cell. 1997;**91**:35-45.

Mishima M, Kaitna S, Glotzer M. Central spindle assembly and cytokinesis require a kinesin-like protein/RhoGAP complex with microtubule bundling activity. Dev Cell. 2002;**2**:41-54.

Mishima Y, Giraldez AJ, Takeda Y, Fujiwara T, Sakamoto H, Schier AF, Inoue K. Differential regulation of germline mRNAs in soma and germ cells by zebrafish miR-430. Curr Biol. 2006;**16**:2135-42.

Mita K, Yamashita M. Expression of Xenopus Daz-like protein during gametogenesis and embryogenesis. Mech Dev. 2000;**94**:251-5.

Miyamoto T, Hasuike S, Yogev L, Maduro MR, Ishikawa M, Westphal H, Lamb DJ. Azoospermia in patients heterozygous for a mutation in SYCP3. Lancet. 2003;**362**:1714-9.

Mizuno Y, Gotoh A, Kamidono S, Kitazawa S. Establishment and characterization of a new human testicular germ cell tumor cell line (TCam-2). Nihon Hinyokika Gakkai Zasshi. 1993;**84**:1211-8.

Modi DN, Sane S, Bhartiya D. Accelerated germ cell apoptosis in sex chromosome aneuploid fetal human gonads. Mol Hum Reprod. 2003;**9**:219-25.

Molyneaux KA, Stallock J, Schaible K, Wylie C. Time-lapse analysis of living mouse germ cell migration. Dev Biol. 2001;**240**:488-98.

Molyneaux KA, Zinszner H, Kunwar PS, Schaible K, Stebler J, Sunshine MJ, O'Brien W, Raz E, Littman D, Wylie C *et al.* The chemokine SDF1/CXCL12 and its receptor CXCR4 regulate mouse germ cell migration and survival. Development. 2003;**130**:4279-86.

Mondal G, Ohashi A, Yang L, Rowley M, Couch FJ. Tex14, a Plk1-regulated protein, is required for kinetochore-microtubule attachment and regulation of the spindle assembly checkpoint. Mol Cell. 2012;**45**:680-95.

Monk M, McLaren A. X-chromosome activity in foetal germ cells of the mouse. J Embryol Exp Morphol. 1981;**63**:75-84.

Moore FL, Jaruzelska J, Fox MS, Urano J, Firpo MT, Turek PJ, Dorfman DM, Pera RA. Human Pumilio-2 is expressed in embryonic stem cells and germ cells and interacts with DAZ (Deleted in AZoospermia) and DAZ-like proteins. Proc Natl Acad Sci U S A. 2003;**100**:538-43.

Moore J. On the essential similarity of the process of chromosome reduction in animals and plants. Annals of Botany. 1895:431-9.

Morita Y, Tilly JL. Oocyte apoptosis: like sand through an hourglass. Dev Biol. 1999;**213**:1-17.

Morton S, Yang HT, Moleleki N, Campbell DG, Cohen P, Rousseau S. Phosphorylation of the ARE-binding protein DAZAP1 by ERK2 induces its dissociation from DAZ. Biochem J. 2006;**399**:265-73.

Moses MJ. The relation between the axial complex of meiotic prophase chromosomes and chromosome pairing in a salamander (Plethodon cinereus). The Journal of biophysical and biochemical cytology. 1958;**4**:633-8.

Motro B, van der Kooy D, Rossant J, Reith A, Bernstein A. Contiguous patterns of c-kit and steel expression: analysis of mutations at the W and Sl loci. Development. 1991;**113**:1207-21.

Mullis KB, Faloona FA. Specific synthesis of DNA in vitro via a polymerase-catalyzed chain reaction. Methods Enzymol. 1987;**155**:335-50.

Navarro-Costa P, Nogueira P, Carvalho M, Leal F, Cordeiro I, Calhaz-Jorge C, Goncalves J, Plancha CE. Incorrect DNA methylation of the DAZL promoter CpG island associates with defective human sperm. Hum Reprod. 2010;**25**:2647-54.

Navarro-Martin L, Galay-Burgos M, Sweeney G, Piferrer F. Different sox17 transcripts during sex differentiation in sea bass, Dicentrarchus labrax. Mol Cell Endocrinol. 2009;**299**:240-51.

Nettersheim D, Gillis AJ, Looijenga LH, Schorle H. TGF-beta1, EGF and FGF4 synergistically induce differentiation of the seminoma cell line TCam-2 into a cell type resembling mixed non-seminoma. Int J Androl. 2011;**34**:e189-203.

Nicholas CR, Xu EY, Banani SF, Hammer RE, Hamra FK, Reijo Pera RA. Characterization of a Dazl-GFP germ cell-specific reporter. Genesis. 2009;**47**:74-84.

Nimlamool W, Bean BS, Lowe-Krentz LJ. Human sperm CRISP2 is released from the acrosome during the acrosome reaction and re-associates at the equatorial segment. Mol Reprod Dev. 2013;**80**:488-502.

Oh JS, Susor A, Schindler K, Schultz RM, Conti M. Cdc25A activity is required for the metaphase II arrest in mouse oocytes. J Cell Sci. 2013;**126**:1081-5.

Ohinata Y, Payer B, O'Carroll D, Ancelin K, Ono Y, Sano M, Barton SC, Obukhanych T, Nussenzweig M, Tarakhovsky A *et al.* Blimp1 is a critical determinant of the germ cell lineage in mice. Nature. 2005;**436**:207-13.

Ohta K, Lin Y, Hogg N, Yamamoto M, Yamazaki Y. Direct effects of retinoic acid on entry of fetal male germ cells into meiosis in mice. Biol Reprod. 2010;**83**:1056-63.

Olesen C, Hansen C, Bendsen E, Byskov AG, Schwinger E, Lopez-Pajares I, Jensen PK, Kristoffersson U, Schubert R, Van Assche E *et al.* Identification of human candidate genes for male infertility by digital differential display. Mol Hum Reprod. 2001;**7**:11-20.

Olesen C, Nyeng P, Kalisz M, Jensen TH, Moller M, Tommerup N, Byskov AG. Global gene expression analysis in fetal mouse ovaries with and without meiosis and comparison of selected genes with meiosis in the testis. Cell Tissue Res. 2007;**328**:207-21.

Ollinger R, Childs AJ, Burgess HM, Speed RM, Lundegaard PR, Reynolds N, Gray NK, Cooke HJ, Adams IR. Deletion of the pluripotency-associated Tex19.1 gene causes activation of endogenous retroviruses and defective spermatogenesis in mice. PLoS Genet. 2008;**4**:e1000199.

Oltvai ZN, Milliman CL, Korsmeyer SJ. Bcl-2 heterodimerizes in vivo with a conserved homolog, Bax, that accelerates programmed cell death. Cell. 1993;**74**:609-19.

Ooi SK, Qiu C, Bernstein E, Li K, Jia D, Yang Z, Erdjument-Bromage H, Tempst P, Lin SP, Allis CD *et al.* DNMT3L connects unmethylated lysine 4 of histone H3 to de novo methylation of DNA. Nature. 2007;**448**:714-7.

Oulad-Abdelghani M, Bouillet P, Decimo D, Gansmuller A, Heyberger S, Dolle P, Bronner S, Lutz Y, Chambon P. Characterization of a premeiotic germ cell-specific cytoplasmic protein encoded by Stra8, a novel retinoic acid-responsive gene. J Cell Biol. 1996;**135**:469-77.

Pan HA, Lee YC, Teng YN, Tsai SJ, Lin YM, Kuo PL. CDC25 protein expression and interaction with DAZL in human corpus luteum. Fertil Steril. 2009;**92**:1997-2003.

Pan HA, Liao RW, Chung CL, Teng YN, Lin YM, Kuo PL. DAZL protein expression in mouse preimplantation embryo. Fertil Steril. 2008;**89**:1324-7.

Paredes A, Garcia-Rudaz C, Kerr B, Tapia V, Dissen GA, Costa ME, Cornea A, Ojeda SR. Loss of synaptonemal complex protein-1, a synaptonemal complex protein, contributes to the initiation of follicular assembly in the developing rat ovary. Endocrinology. 2005;**146**:5267-77.

Pellegrini M, Grimaldi P, Rossi P, Geremia R, Dolci S. Developmental expression of BMP4/ALK3/SMAD5 signaling pathway in the mouse testis: a potential role of BMP4 in spermatogonia differentiation. J Cell Sci. 2003;**116**:3363-72.

Peng JX, Xie JL, Zhou L, Hong YH, Gui JF. Evolutionary conservation of Dazl genomic organization and its continuous and dynamic distribution throughout germline development in gynogenetic gibel carp. J Exp Zool B Mol Dev Evol. 2009;**312**:855-71.

Pepling ME, Spradling AC. Female mouse germ cells form synchronously dividing cysts. Development. 1998;**125**:3323-8.

Perez GI, Robles R, Knudson CM, Flaws JA, Korsmeyer SJ, Tilly JL. Prolongation of ovarian lifespan into advanced chronological age by Bax-deficiency. Nat Genet. 1999;**21**:200-3.

Perez GI, Trbovich AM, Gosden RG, Tilly JL. Mitochondria and the death of oocytes. Nature. 2000;**403**:500-1.

Pesce M, Wang X, Wolgemuth DJ, Scholer H. Differential expression of the Oct-4 transcription factor during mouse germ cell differentiation. Mech Dev. 1998;**71**:89-98.

Pires-daSilva A, Nayernia K, Engel W, Torres M, Stoykova A, Chowdhury K, Gruss P. Mice deficient for spermatid perinuclear RNA-binding protein show neurologic, spermatogenic, and sperm morphological abnormalities. Dev Biol. 2001;**233**:319-28.

Rajkovic A, Pangas SA, Ballow D, Suzumori N, Matzuk MM. NOBOX deficiency disrupts early folliculogenesis and oocyte-specific gene expression. Science. 2004;**305**:1157-9.

Reddy P, Liu L, Adhikari D, Jagarlamudi K, Rajareddy S, Shen Y, Du C, Tang W, Hamalainen T, Peng SL *et al.* Oocyte-specific deletion of Pten causes premature activation of the primordial follicle pool. Science. 2008;**319**:611-3.

Reijo R, Lee TY, Salo P, Alagappan R, Brown LG, Rosenberg M, Rozen S, Jaffe T, Straus D, Hovatta O *et al.* Diverse spermatogenic defects in humans caused by Y chromosome deletions encompassing a novel RNA-binding protein gene. Nat Genet. 1995;**10**:383-93.

Reijo R, Seligman J, Dinulos MB, Jaffe T, Brown LG, Disteche CM, Page DC. Mouse autosomal homolog of DAZ, a candidate male sterility gene in humans, is expressed in male germ cells before and after puberty. Genomics. 1996;**35**:346-52.

Reijo RA, Dorfman DM, Slee R, Renshaw AA, Loughlin KR, Cooke H, Page DC. DAZ family proteins exist throughout male germ cell development and transit from nucleus to cytoplasm at meiosis in humans and mice. Biol Reprod. 2000;**63**:1490-6.

Ren S, Xin C, Beck KF, Saleem MA, Mathieson P, Pavenstädt H, Pfeilschifter J, Huwiler A. PPARalpha activation upregulates nephrin expression in human embryonic kidney epithelial cells and podocytes by a dual mechanism. Biochem Biophys Res Commun. 2005;**338**:1818-24.

Reynolds N, Collier B, Bingham V, Gray NK, Cooke HJ. Translation of the synaptonemal complex component Sycp3 is enhanced in vivo by the germ cell specific regulator Dazl. RNA. 2007;**13**:974-81.

Reynolds N, Collier B, Maratou K, Bingham V, Speed RM, Taggart M, Semple CA, Gray NK, Cooke HJ. Dazl binds in vivo to specific transcripts and can regulate the pre-meiotic translation of Mvh in germ cells. Hum Mol Genet. 2005;**14**:3899-909.

Ririe KM, Rasmussen RP, Wittwer CT. Product differentiation by analysis of DNA melting curves during the polymerase chain reaction. Anal Biochem. 1997;**245**:154-60.

Rocchietti-March M, Weinbauer GF, Page DC, Nieschlag E, Gromoll J. Dazl protein expression in adult rat testis is up-regulated at meiosis and not hormonally regulated. Int J Androl. 2000;**23**:51-6.

Rogakou EP, Pilch DR, Orr AH, Ivanova VS, Bonner WM. DNA double-stranded breaks induce histone H2AX phosphorylation on serine 139. J Biol Chem. 1998;**273**:5858-68.

Roig I, Liebe B, Egozcue J, Cabero L, Garcia M, Scherthan H. Female-specific features of recombinational double-stranded DNA repair in relation to synapsis and telomere dynamics in human oocytes. Chromosoma. 2004;**113**:22-33.

Ruby JR, Dyer RF, Skalko RG. The occurrence of intercellular bridges during oogenesis in the mouse. J Morphol. 1969;**127**:307-39.

Ruggiu M, Saunders PT, Cooke HJ. Dynamic subcellular distribution of the DAZL protein is confined to primate male germ cells. J Androl. 2000;**21**:470-7.

Ruggiu M, Speed R, Taggart M, McKay SJ, Kilanowski F, Saunders P, Dorin J, Cooke HJ. The mouse Dazla gene encodes a cytoplasmic protein essential for gametogenesis. Nature. 1997;**389**:73-7.

Runyan C, Schaible K, Molyneaux K, Wang Z, Levin L, Wylie C. Steel factor controls midline cell death of primordial germ cells and is essential for their normal proliferation and migration. Development. 2006;**133**:4861-9.

Saba R, Wu Q, Saga Y. CYP26B1 promotes male germ cell differentiation by suppressing STRA8-dependent meiotic and STRA8-independent mitotic pathways. Dev Biol. 2014;**389**:173-81.

Saitou M, Barton SC, Surani MA. A molecular programme for the specification of germ cell fate in mice. Nature. 2002;**418**:293-300.

Salemi M, La Vignera S, Castiglione R, Condorelli RA, Cimino L, Bosco P, Romano C, Romano C, Calogero AE. Expression of STRBP mRNA in patients with

cryptorchidism and Down's syndrome. Journal of endocrinological investigation. 2012;**35**:5-7.

Sampath P, Pritchard DK, Pabon L, Reinecke H, Schwartz SM, Morris DR, Murry CE. A hierarchical network controls protein translation during murine embryonic stem cell self-renewal and differentiation. Cell stem cell. 2008;**2**:448-60.

Saunders PT, Turner JM, Ruggiu M, Taggart M, Burgoyne PS, Elliott D, Cooke HJ. Absence of mDazl produces a final block on germ cell development at meiosis. Reproduction. 2003;**126**:589-97.

Saxena R, Brown LG, Hawkins T, Alagappan RK, Skaletsky H, Reeve MP, Reijo R, Rozen S, Dinulos MB, Disteche CM *et al.* The DAZ gene cluster on the human Y chromosome arose from an autosomal gene that was transposed, repeatedly amplified and pruned. Nat Genet. 1996;**14**:292-9.

Schaefer CB, Ooi SK, Bestor TH, Bourc'his D. Epigenetic decisions in mammalian germ cells. Science. 2007;**316**:398-9.

Schrans-Stassen BH, Saunders PT, Cooke HJ, de Rooij DG. Nature of the spermatogenic arrest in Dazl -/- mice. Biol Reprod. 2001;**65**:771-6.

Schumacher JM, Lee K, Edelhoff S, Braun RE. Spnr, a murine RNA-binding protein that is localized to cytoplasmic microtubules. J Cell Biol. 1995;**129**:1023-32.

Seligman J, Page DC. The Dazh gene is expressed in male and female embryonic gonads before germ cell sex differentiation. Biochem Biophys Res Commun. 1998;**245**:878-82.

Selman K, Wallace RA, Sarka A, Qi X. Stages of oocyte development in the zebrafish, Brachydanio rerio. Journal of Morphology. 1993;**218**:203-24.

Shah C, Vangompel MJ, Naeem V, Chen Y, Lee T, Angeloni N, Wang Y, Xu EY. Widespread presence of human BOULE homologs among animals and conservation of their ancient reproductive function. PLoS Genet. 2010;**6**:e1001022.

Shang P, Baarends WM, Hoogerbrugge J, Ooms MP, van Cappellen WA, de Jong AA, Dohle GR, van Eenennaam H, Gossen JA, Grootegoed JA. Functional transformation of the chromatoid body in mouse spermatids requires testis-specific serine/threonine kinases. J Cell Sci. 2010;**123**:331-9.

Slee R, Grimes B, Speed RM, Taggart M, Maguire SM, Ross A, McGill NI, Saunders PT, Cooke HJ. A human DAZ transgene confers partial rescue of the mouse Dazl null phenotype. Proc Natl Acad Sci U S A. 1999;**96**:8040-5.

Smogorzewska A, van Steensel B, Bianchi A, Oelmann S, Schaefer MR, Schnapp G, de Lange T. Control of human telomere length by TRF1 and TRF2. Molecular and cellular biology. 2000;**20**:1659-68.

Solc P, Saskova A, Baran V, Kubelka M, Schultz RM, Motlik J. CDC25A phosphatase controls meiosis I progression in mouse oocytes. Dev Biol. 2008;**317**:260-9.

Soyal SM, Amleh A, Dean J. FIGalpha, a germ cell-specific transcription factor required for ovarian follicle formation. Development. 2000;**127**:4645-54.

Stefanovic S, Abboud N, Desilets S, Nury D, Cowan C, Puceat M. Interplay of Oct4 with Sox2 and Sox17: a molecular switch from stem cell pluripotency to specifying a cardiac fate. J Cell Biol. 2009;**186**:665-73.

Stoop H, Honecker F, Cools M, de Krijger R, Bokemeyer C, Looijenga LH. Differentiation and development of human female germ cells during prenatal gonadogenesis: an immunohistochemical study. Hum Reprod. 2005;**20**:1466-76.

Susa T, Kato T, Kato Y. Reproducible transfection in the presence of carrier DNA using FuGENE6 and Lipofectamine2000. Mol Biol Rep. 2008;**35**:313-9.

Takeda Y, Mishima Y, Fujiwara T, Sakamoto H, Inoue K. DAZL relieves miRNA-mediated repression of germline mRNAs by controlling poly(A) tail length in zebrafish. PLoS One. 2009;**4**:e7513.

Tam PP, Zhou SX. The allocation of epiblast cells to ectodermal and germ-line lineages is influenced by the position of the cells in the gastrulating mouse embryo. Dev Biol. 1996;**178**:124-32.

Tarabay Y, Kieffer E, Teletin M, Celebi C, Van Montfoort A, Zamudio N, Achour M, El Ramy R, Gazdag E, Tropel P *et al.* The mammalian-specific Tex19.1 gene plays an essential role in spermatogenesis and placenta-supported development. Hum Reprod. 2013;**28**:2201-14.

Tay J, Richter JD. Germ cell differentiation and synaptonemal complex formation are disrupted in CPEB knockout mice. Dev Cell. 2001;**1**:201-13.

Teng YN, Chang YP, Tseng JT, Kuo PH, Lee IW, Lee MS, Kuo PL. A single-nucleotide polymorphism of the DAZL gene promoter confers susceptibility to spermatogenic failure in the Taiwanese Han. Hum Reprod. 2012;**27**:2857-65.

Tilly JL. Commuting the death sentence: how oocytes strive to survive. Nat Rev Mol Cell Biol. 2001;**2**:838-48.

Tingen C, Kim A, Woodruff TK. The primordial pool of follicles and nest breakdown in mammalian ovaries. Mol Hum Reprod. 2009;**15**:795-803.

Towbin H, Staehelin T, Gordon J. Electrophoretic transfer of proteins from polyacrylamide gels to nitrocellulose sheets: procedure and some applications. Proc Natl Acad Sci U S A. 1979;**76**:4350-4.

Trautmann E, Guerquin MJ, Duquenne C, Lahaye JB, Habert R, Livera G. Retinoic acid prevents germ cell mitotic arrest in mouse fetal testes. Cell Cycle. 2008;**7**:656-64.

Tremblay KD, Dunn NR, Robertson EJ. Mouse embryos lacking Smad1 signals display defects in extra-embryonic tissues and germ cell formation. Development. 2001;**128**:3609-21.

Tsuda M, Sasaoka Y, Kiso M, Abe K, Haraguchi S, Kobayashi S, Saga Y. Conserved role of nanos proteins in germ cell development. Science. 2003;**301**:1239-41.

Tsui S, Dai T, Roettger S, Schempp W, Salido EC, Yen PH. Identification of two novel proteins that interact with germ-cell-specific RNA-binding proteins DAZ and DAZL1. Genomics. 2000a;**65**:266-73.

Tsui S, Dai T, Warren ST, Salido EC, Yen PH. Association of the mouse infertility factor DAZL1 with actively translating polyribosomes. Biol Reprod. 2000b;**62**:1655-60.

Tung JY, Luetjens CM, Wistuba J, Xu EY, Reijo Pera RA, Gromoll J. Evolutionary comparison of the reproductive genes, DAZL and BOULE, in primates with and without DAZ. Dev Genes Evol. 2006a;**216**:158-68.

Tung JY, Rosen MP, Nelson LM, Turek PJ, Witte JS, Cramer DW, Cedars MI, Pera RA. Variants in Deleted in AZoospermia-Like (DAZL) are correlated with reproductive parameters in men and women. Hum Genet. 2006b;**118**:730-40.

Tung JY, Rosen MP, Nelson LM, Turek PJ, Witte JS, Cramer DW, Cedars MI, Reijo-Pera RA. Novel missense mutations of the Deleted-in-AZoospermia-Like (DAZL) gene in infertile women and men. Reprod Biol Endocrinol. 2006c;**4**:40.

Urano J, Fox MS, Reijo Pera RA. Interaction of the conserved meiotic regulators, BOULE (BOL) and PUMILIO-2 (PUM2). Mol Reprod Dev. 2005;**71**:290-8.

VanGompel MJ, Xu EY. A novel requirement in mammalian spermatid differentiation for the DAZ-family protein Boule. Hum Mol Genet. 2010;**19**:2360-9.

Vangompel MJ, Xu EY. The roles of the DAZ family in spermatogenesis: More than just translation? Spermatogenesis. 2011;**1**:36-46.

Venables JP, Ruggiu M, Cooke HJ. The RNA-binding specificity of the mouse Dazl protein. Nucleic Acids Res. 2001;**29**:2479-83.

Vogel T, Speed RM, Ross A, Cooke HJ. Partial rescue of the Dazl knockout mouse by the human DAZL gene. Mol Hum Reprod. 2002;**8**:797-804.

Wandji SA, Srsen V, Voss AK, Eppig JJ, Fortune JE. Initiation in vitro of growth of bovine primordial follicles. Biol Reprod. 1996;**55**:942-8.

Wang C, Roy SK. Expression of growth differentiation factor 9 in the oocytes is essential for the development of primordial follicles in the hamster ovary. Endocrinology. 2006;**147**:1725-34.

Wang PJ, McCarrey JR, Yang F, Page DC. An abundance of X-linked genes expressed in spermatogonia. Nat Genet. 2001;**27**:422-6.

Weber JE, Russell LD. A study of intercellular bridges during spermatogenesis in the rat. Am J Anat. 1987;**180**:1-24.

Wells SE, Hillner PE, Vale RD, Sachs AB. Circularization of mRNA by eukaryotic translation initiation factors. Mol Cell. 1998;**2**:135-40.

White JA, Ramshaw H, Taimi M, Stangle W, Zhang A, Everingham S, Creighton S, Tam SP, Jones G, Petkovich M. Identification of the human cytochrome P450, P450RAI-2, which is predominantly expressed in the adult cerebellum and is responsible for all-trans-retinoic acid metabolism. Proc Natl Acad Sci U S A. 2000;**97**:6403-8.

White YA, Woods DC, Takai Y, Ishihara O, Seki H, Tilly JL. Oocyte formation by mitotically active germ cells purified from ovaries of reproductive-age women. Nat Med. 2012;**18**:413-21.

Wickramasinghe D, Becker S, Ernst MK, Resnick JL, Centanni JM, Tessarollo L, Grabel LB, Donovan PJ. Two CDC25 homologues are differentially expressed during mouse development. Development. 1995;**121**:2047-56.

Wieser R, Wrana JL, Massague J. GS domain mutations that constitutively activate T beta R-I, the downstream signaling component in the TGF-beta receptor complex. EMBO J. 1995;**14**:2199-208.

Wiszniak SE, Dredge BK, Jensen KB. HuB (elavl2) mRNA is restricted to the germ cells by post-transcriptional mechanisms including stabilisation of the message by DAZL. PLoS One. 2011;**6**:e20773.

Witschi E. Migration of the germ cells of human embryos from the yolk sac to the primitive gonadal folds. Contrib Embryol. 1948;**32**:67-80.

Wreden C, Verrotti AC, Schisa JA, Lieberfarb ME, Strickland S. Nanos and pumilio establish embryonic polarity in Drosophila by promoting posterior deadenylation of hunchback mRNA. Development. 1997;**124**:3015-23.

Wu MH, Rajkovic A, Burns KH, Yan W, Lin YN, Matzuk MM. Sequence and expression of testis-expressed gene 14 (Tex14): a gene encoding a protein kinase preferentially expressed during spermatogenesis. Gene Expr Patterns. 2003;**3**:231-6.

Xiao L, Kim M, DeJong J. Developmental and cell type-specific regulation of core promoter transcription factors in germ cells of frogs and mice. Gene Expr Patterns. 2006;**6**:409-19.

Xu B, Hao Z, Jha KN, Zhang Z, Urekar C, Digilio L, Pulido S, Strauss JF, 3rd, Flickinger CJ, Herr JC. Targeted deletion of Tssk1 and 2 causes male infertility due to haploinsufficiency. Dev Biol. 2008;**319**:211-22.

Xu EY, Lee DF, Klebes A, Turek PJ, Kornberg TB, Reijo Pera RA. Human BOULE gene rescues meiotic defects in infertile flies. Hum Mol Genet. 2003;**12**:169-75.

Xu EY, Moore FL, Pera RA. A gene family required for human germ cell development evolved from an ancient meiotic gene conserved in metazoans. Proc Natl Acad Sci U S A. 2001;**98**:7414-9.

Xu H, Li M, Gui J, Hong Y. Cloning and expression of medaka dazl during embryogenesis and gametogenesis. Gene Expr Patterns. 2007;**7**:332-8.

Xu H, Li Z, Li M, Wang L, Hong Y. Boule is present in fish and bisexually expressed in adult and embryonic germ cells of medaka. PLoS One. 2009;**4**:e6097.

Xu X, Tan X, Lin Q, Schmidt B, Engel W, Pantakani DV. Mouse Dazl and its novel splice variant functions in translational repression of target mRNAs in embryonic stem cells. Biochim Biophys Acta. 2013;**1829**:425-35.

Xu Y, Ashley T, Brainerd EE, Bronson RT, Meyn MS, Baltimore D. Targeted disruption of ATM leads to growth retardation, chromosomal fragmentation during meiosis, immune defects, and thymic lymphoma. Genes Dev. 1996;**10**:2411-22.

Yamaguchi S, Kimura H, Tada M, Nakatsuji N, Tada T. Nanog expression in mouse germ cell development. Gene Expr Patterns. 2005;**5**:639-46.

Yang E, Zha J, Jockel J, Boise LH, Thompson CB, Korsmeyer SJ. Bad, a heterodimeric partner for Bcl-XL and Bcl-2, displaces Bax and promotes cell death. Cell. 1995;**80**:285-91.

Ying Y, Liu XM, Marble A, Lawson KA, Zhao GQ. Requirement of Bmp8b for the generation of primordial germ cells in the mouse. Mol Endocrinol. 2000;**14**:1053-63.

Ying Y, Zhao GQ. Cooperation of endoderm-derived BMP2 and extraembryonic ectoderm-derived BMP4 in primordial germ cell generation in the mouse. Dev Biol. 2001;**232**:484-92.

Yuan L, Liu JG, Hoja MR, Wilbertz J, Nordqvist K, Hoog C. Female germ cell aneuploidy and embryo death in mice lacking the meiosis-specific protein SCP3. Science. 2002;**296**:1115-8.

Yuan L, Liu JG, Zhao J, Brundell E, Daneholt B, Hoog C. The murine SCP3 gene is required for synaptonemal complex assembly, chromosome synapsis, and male fertility. Mol Cell. 2000;**5**:73-83.

Yuan L, Pelttari J, Brundell E, Bjorkroth B, Zhao J, Liu JG, Brismar H, Daneholt B, Hoog C. The synaptonemal complex protein SCP3 can form multistranded, cross-striated fibers in vivo. J Cell Biol. 1998;**142**:331-9.

Zamboni L, Gondos B. Intercellular bridges and synchronization of germ cell differentiation during oogenesis in the rabbit. J Cell Biol. 1968;**36**:276-82.

Zamore PD, Williamson JR, Lehmann R. The Pumilio protein binds RNA through a conserved domain that defines a new class of RNA-binding proteins. RNA. 1997;**3**:1421-33.

Zeng M, Deng W, Wang X, Qiu W, Liu Y, Sun H, Tao D, Zhang S, Ma Y. DAZL binds to the transcripts of several Tssk genes in germ cells. BMB Rep. 2008;**41**:300-4.

Zeng M, Lu Y, Liao X, Li D, Sun H, Liang S, Zhang S, Ma Y, Yang Z. DAZL binds to 3'UTR of Tex19.1 mRNAs and regulates Tex19.1 expression. Mol Biol Rep. 2009;**36**:2399-403.

Zhang D, Penttila TL, Morris PL, Teichmann M, Roeder RG. Spermiogenesis deficiency in mice lacking the Trf2 gene. Science. 2001;**292**:1153-5.

Zhang H, Su D, Yang Y, Zhang W, Liu Y, Bai G, Ma M, Ma Y, Zhang S. Some single-nucleotide polymorphisms of the TSSK2 gene may be associated with human spermatogenesis impairment. J Androl. 2010;**31**:388-92.

Zhang Q, Li J, Li Q, Li X, Liu Z, Song D, Xie Z. Cloning and characterization of the gene encoding the bovine BOULE protein. Mol Genet Genomics. 2009;**281**:67-75.

Zhou Q, Li Y, Nie R, Friel P, Mitchell D, Evanoff RM, Pouchnik D, Banasik B, McCarrey JR, Small C *et al.* Expression of stimulated by retinoic acid gene 8 (Stra8) and maturation of murine gonocytes and spermatogonia induced by retinoic acid in vitro. Biol Reprod. 2008;**78**:537-45.

Corrections:

November 14, 2013

As a result of mistakes in the typesetting process, there were errors in the Figure 4 legend in the PDF. A correct version of the legend is available below.

Figure 4. BOLL displays greater co-localisation with the meiosis marker SYCP3 than DAZL.

A) Triple immunofluorescence analysis of DAZL (green), BOLL (blue) and SYCP3 (red) in 14 and 17 week ovary. All BOLL+ germ cells also express SYCP3 (arrowheads), but only a few DAZL+ germ cell express SYCP3 (arrows). Unfilled arrows indicate the SYCP3-positive cells that express neither DAZL nor BOLL. The asterisk indicates a germ cell nest containing BOLL+SYCP3+, DAZL+SYCP3+ and DAZL+SYCP- germ cells in close proximity. Scale bars: 20μm. B) magnified image of germ cell nest marked with asterisk in A, showing neighboring germ cells expressing different combinations of DAZL, BOLL and SYCP3 expression; arrow denotes DAZL+SYCP3+ germ cell, arrowhead denotes BOLL+SYCP+ germ cell. C) Quantification of DAZL, BOLL and SYCP3 co-expression. ~69% of SYCP3+ cells also express BOLL+. This is significantly greater than the percentage of all the other co-expression patterns (n=3 14-17 week human fetal ovaries; ***$p<0.001$).

August 13, 2015

In the Funding section, the name of the first funder is incorrect. The correct name is: Medical Research Scotland. The correct funding information is: This work was supported by Medical Research Scotland [grant 354FRG to AJC] and the Medical Research Council [grant G1100357 to RAA]. J.H. is supported by a University of Edinburgh Darwin Scholarship and K.S. is the recipient of a Society for Reproduction and Fertility Summer Vacation Scholarship. The funders had no role in study design, data collection and analysis, decision to publish, or preparation of the manuscript.